GA-A15171
UC-77

PCRV STRUCTURAL RESPONSE VERIFICATION

by

K. C. CHEUNG

Prepared Under
Contract EY-76-C-03-0167
Project Agreement No. 65
for the San Francisco Operations Office
Department of Energy

GENERAL ATOMIC PROJECT 6432
DATE PUBLISHED: FEBRUARY 1979

GENERAL ATOMIC COMPANY

ABSTRACT

This report covers the tasks undertaken to obtain, reduce, and analyze tendon loads, strain, and deflection data for the purpose of validating structural analysis computer codes by comparison of observed vessel behavior with predicted PCRV structural response at Fort St. Vrain. On the basis of test data obtained during reactor rise to 70% power, the following observations on the overall structural response of the PCRV are made:

1. The structural response of the vessel to pressure changes is essentially linear. Concrete strains and PCRV deflections are in general agreement with those predicted by the elastic finite element analysis.

2. The consistency exhibited in the concrete strain and deflection data obtained from the initial proof pressure and start-up tests indicates that no significant change in the PCRV structural stiffness has occurred during this period.

3. The long-term tendon loads have been conservatively estimated in the PCRV design, and observed prestress losses are well within the design limits.

4. Good correlations between analytical results and measured data verify the adequacy of the two-dimensional creep analysis code used to predict the time-dependent structural response of the FSV PCRV.

CONTENTS

FIGURES

TABLES

1. INTRODUCTION

The Fort St. Vrain (FSV) prestressed concrete reactor vessel (PCRV) offers the unique vehicle which experiences all the appropriate environmental effects of a high temperature gas-cooled reactor (HTGR). To take advantage of the opportunity provided by the scheduled start-up tests, a program was initiated in FY-76 to collect data from PCRV embedded sensors, tendon load cells, and deflection measurements for the purpose of verifying the capability of structural analysis computer codes to predict short-term and time-dependent PCRV response. Data from sensors installed in the PCRV have been collected on a noninterference basis.

Instrumentation was incorporated in the FSV PCRV to obtain data for validating the design and construction and to monitor the structural response of the PCRV during its design life. The sensors include load cells on selected tendons, strain gages embedded in concrete, strain gages on steel liner, and thermocouples embedded in the PCRV. All sensors are monitored in a 600-channel digital data acquisition system (DAS). The DAS is capable of continually or intermittently monitoring the PCRV structural response. The output from the DAS appears on a digital voltmeter for local readout, printed paper tape for record purpose, and punched paper tape for computer processing.

In 1971, the structural response of the PCRV subjected to initial proof test pressure (IPTP) was evaluated utilizing the data provided by the installed sensors. In addition, optical PCRV deflection measurements were performed. The proof pressure test demonstrated that the PCRV was soundly constructed and that the overall structural response of the PCRV was essentially linear up to IPTP of 970 psig (6.69 MPa). The test results were in general agreement with those predicted by the elastic finite element analysis (Ref. 1). The analytical and test data obtained for the IPTP tests were used as the basis for verifying PCRV structural response in subsequent pressurizations during the rise to power.

2. SHORT-TERM PCRV RESPONSE

The behavior of the Fort St. Vrain PCRV has been assessed during the reactor start-up tests. The short-term PCRV response to reactor rise to 70% power level was evaluated from measurements of tendon loads, concrete strains, PCRV deflection, and concrete temperatures.

2.1. PCRV RESPONSE TO PRESSURIZATIONS

The PCRV sensor data collected during reactor rise to power were analyzed. The maximum internal pressure reached during the start-up tests was 650 psi (4.48 MPa), corresponding to approximately 90% of the normal working pressure (NWP). Test results of recent pressurizations at 50%, 60%, and 70% reactor power including all tendon load cell readings, concrete strains, and thermocouples at representative locations of the PCRV are presented in Table 1. Locations of tendon load cells are shown in Fig. 1. The structural response of the PCRV to pressurizations was evaluated by comparing the tendon load changes and concrete strains with the anticipated values which were established based on the analysis of the IPTP test results. The start-up test data were found acceptable.

Figures 2 through 6 show the development of concrete strain with internal pressure generated by the control strain gages located at critical sections of the PCRV. The recorded strains were in general agreement with predicted values obtained from elastic three-dimensional finite element analysis of the PCRV under pressurization. Measured strains recorded in the initial proof pressure test by the same strain gages are included on the figures for comparison. Consistent overall responses exhibited in both the initial pressure and the start-up tests not only verify the essentially elastic response of the PCRV to pressure changes but also establish the reliability of strain gages embedded in the concrete. The deviations of

TABLE 1
REPRESENTATIVE TEST RESULTS

SUT[a] BO Sequence		--	46	--	53	61
Reactor Power (%)		0	50	0	60	70
Pressure (psia/MPa)		0	620/4.27	8/0.06	637/4.39	650/4.48
Channel	Load Cell	Load (kips/MN)				
2	VM-3	1288.6/5.73	1278.6/5.69	1279.6/5.69	1272.6/5.66	1309.7/5.83
1	VI-10	1264.5/5.62	1253.9/5.58	1249.8/5.56	1245.7/5.54	1273.4/5.66
0	VM-17	1320.7/5.87	1316.7/5.86	1312.6/5.84	1302.4/5.79	1334.0/5.93
3	VI-24	1304.8/5.80	1292.7/5.75	1293.7/5.75	1288.7/5.73	1313.9/5.84
4	VM-31	1276.6/5.68	1262.5/5.62	1266.5/5.63	1256.4/5.59	1287.8/5.73
100	VI-38	1240.7/5.51	1232.6/5.48	1231.6/5.48	1230.5/5.47	1258.0/5.60
101	TOR-U2	1277.3/5.68	1259.5/5.60	1260.5/5.61	1256.3/5.59	1283.6/5.71
102	TIR-M1	1152.2/5.12	1122.9/4.99	1131.3/5.03	1116.3/4.97	1138.6/5.06
103	BOR-L4	1281.3/5.70	1262.5/5.62	1261.5/5.61	1254.2/5.58	1283.4/5.71
104	BIR-M4	1230.0/5.47	1218.4/5.42	1215.2/5.41	1205.7/5.36	1235.3/5.49
200	CO-1.6	1259.5/5.60	1237.6/5.50	1241.8/5.52	1230.3/5.47	1257.4/5.59
201	CI-1.4	1269.0/5.64	1250.0/5.56	1251.0/5.56	1241.5/5.52	1269.0/5.64
202	CO-2.2	1285.2/5.72	1282.1/5.70	1269.6/5.65	1270.7/5.65	1297.6/5.77
203	CO-2.1	1236.2/5.50	1227.9/5.46	1221.6/5.43	1221.6/5.43	1248.7/5.55
204	CO-3.2	1358.2/6.04	1345.8/5.97	1341.6/5.97	1338.5/5.95	1365.4/6.07
300	CO-3.1	1201.2/5.34	1187.7/5.28	1186.6/5.28	1181.4/5.25	1210.6/5.38
301	CI-7.4	1078.5/4.80	1075.4/4.78	1059.6/4.70	1063.8/4.73	1094.4/4.87
302	CO-8.3	1134.9/5.05	1124.4/5.00	1119.1/4.98	1119.1/4.98	1146.4/5.10
303	CI-10.1	1093.6/4.86	1090.4/4.85	1078.7/4.80	1084.0/4.82	1114.9/4.96
304	CO-11.2	1089.5/4.85	1093.7/4.86	1079.1/4.80	1081.2/4.81	1110.3/4.94
400	CI-15.3	1134.9/5.05	1121.2/4.99	1123.4/5.00	1113.9/4.95	1142.3/5.08
401	CO-17.6	1180.7/5.25	1166.1/5.10	1171.3/5.21	1163.0/5.17	1190.1/5.29
402	CO-17.5	1211.4/5.39	1199.7/5.34	1200.8/5.34	1187.0/5.28	1217.7/5.42
403	CO-17.4	1278.4/5.69	1262.0/5.61	1269.2/5.65	1258.0/5.60	1285.6/5.72
404	CO-17.3	1214.1/5.40	1204.8/5.36	1203.8/5.35	1195.6/5.32	1224.4/5.45
500	CI-18.5	1317.1/5.86	1198.5/5.33	1200.6/5.34	1195.4/5.32	1222.3/5.44
501	CO-19.6	1356.4/6.03	1341.9/5.97	1340.9/5.96	1331.7/5.92	1357.4/6.03

TABLE 1 (Continued)

SUT[a] BO SEQUENCE		--	46	--	53	61
Reactor Power (%)		0	50	0	60	70
Pressure (psia/MPa)			620/4.27	8/0.06	637/4.39	650/4.48
Channel	Strain Gage	Strain ($x10^{-6}$)				
150	YE-1170-43	562	665	580	648	652
458	YE-1170-58	-358	-51	-380	-55	-46
247	YE-1170-74	-153	38	-170	38	43
262	YE-1170-65	-81	-4	-193	86	1
366	YE-11205-16	-82	-76	-94	-83	-67
Channel	Thermocouple	Temperature (°F/°C)				
144	TE-1170-28	106/41	102/39	97/36	102/39	105/41
535	TE-1170-17	105/41	105/41	96/36	105/41	107/42
432	TE-1170-46	105/41	102/39	95/35	101/38	103/39
444	TE-1170-47	102/39	98/37	93/34	96/36	96/36
445	TE-1170-48	96/36	94/34	90/32	94/34	95/35
414	TE-1170-65	104/40	101/38	96/36	101/38	100/38
416	TE-1170-54	104/40	99/37	96/36	99/37	99/37
418	TE-1170-56	104/40	101/38	95/35	102/39	102/39
423	TE-1170-78	107/42	107/42	96/36	107/42	109/43
506	TE-1170-72	105/41	103/39	96/36	103/39	106/41
031	TE-1170-127	107/42	101/38	97/36	102/39	103/39
128	TE-1170-96	107/42	109/43	95/35	110/43	116/47
325	TE-1170-130	107/42	102/39	95/35	103/39	105/41
235	TE-1170-110	108/42	105/41	97/36	105/41	112/44
030	TE-1170-109	106/41	115/46	97/36	115/46	118/48
343	TE-1170-111	104/40	104/40	94/34	106/41	105/41
331	TE-1170-114	103/39	98/37	96/36	97/36	97/36
335	TE-1170-107	105/41	99/37	97/36	96/36	98/37

[a] SUT = start-up test.

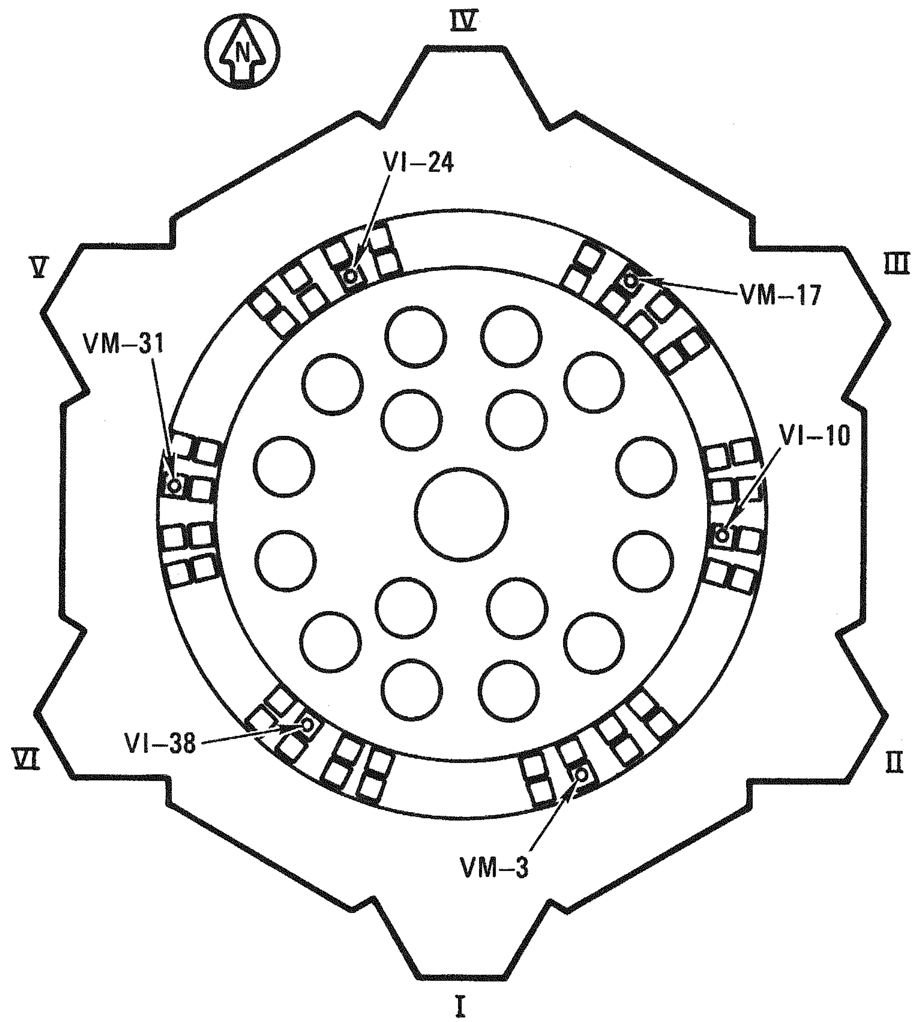

Fig. 1(a). Load cell locations on vertical tendons

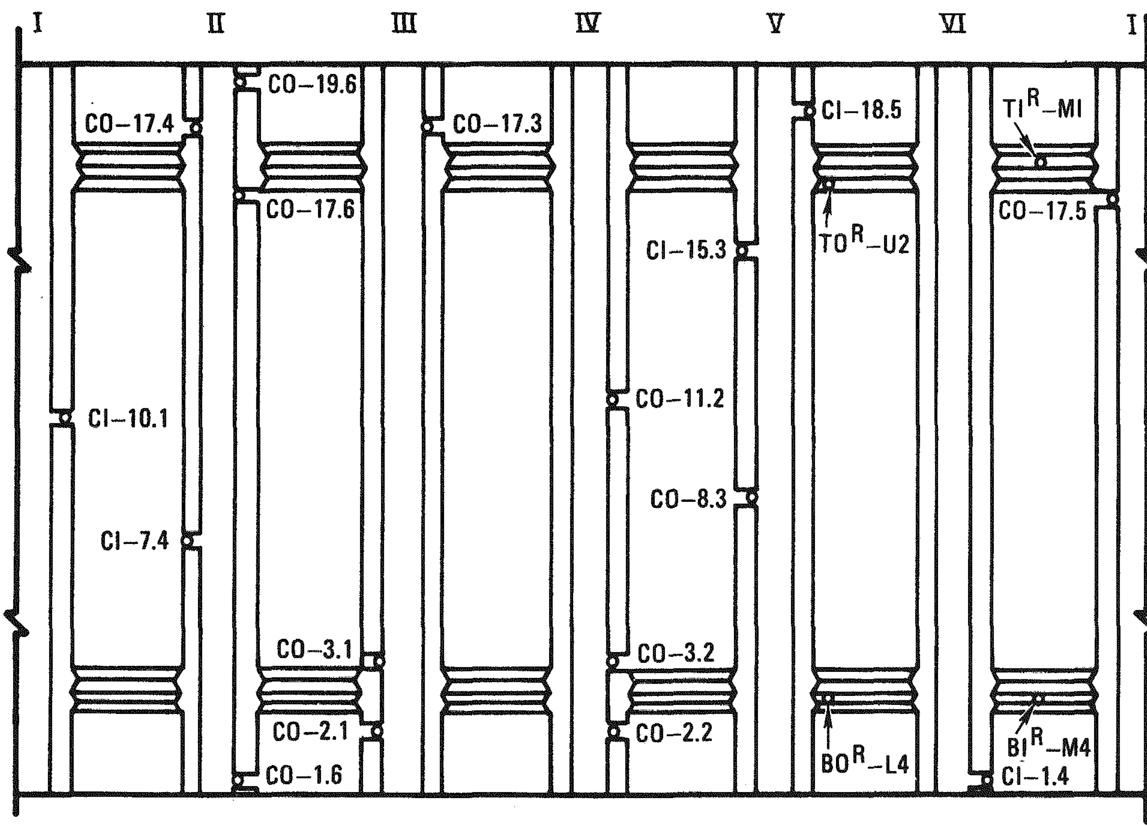

Fig. 1(b). Load cell locations on circumferential and cross-head tendons

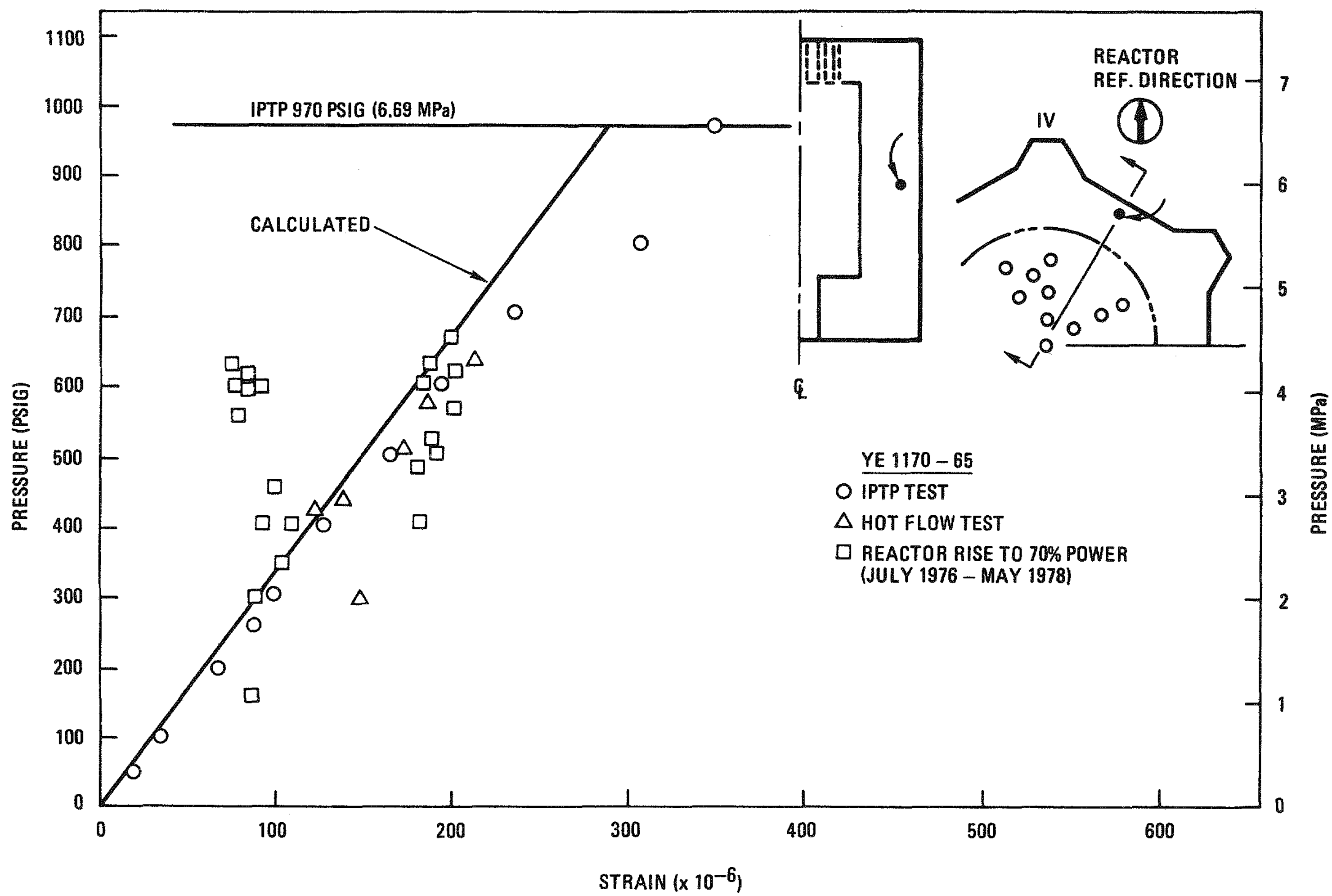

Fig. 2. Circumferential concrete strain at outer wall midheight

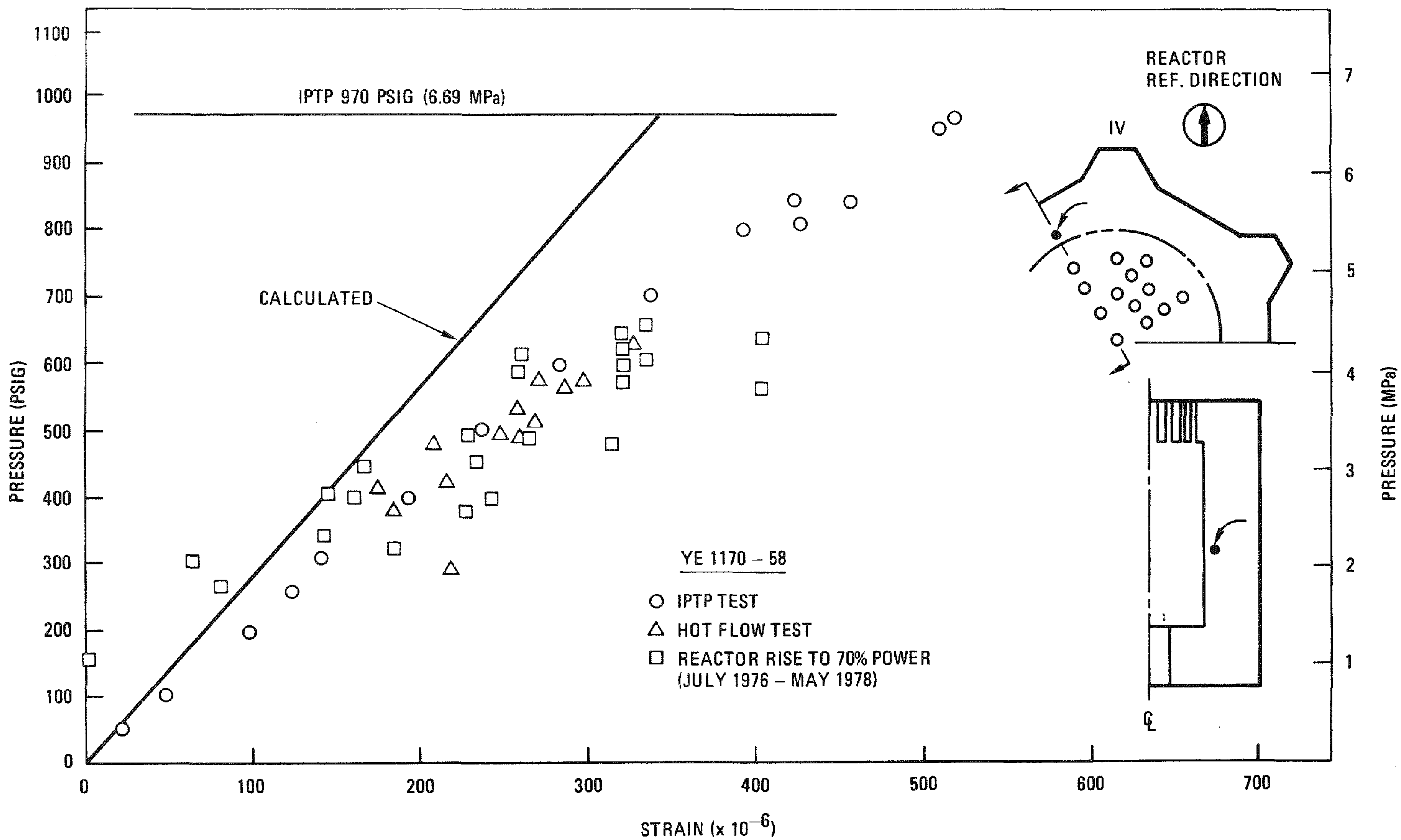

Fig. 3. Circumferential concrete strain at inner wall midheight

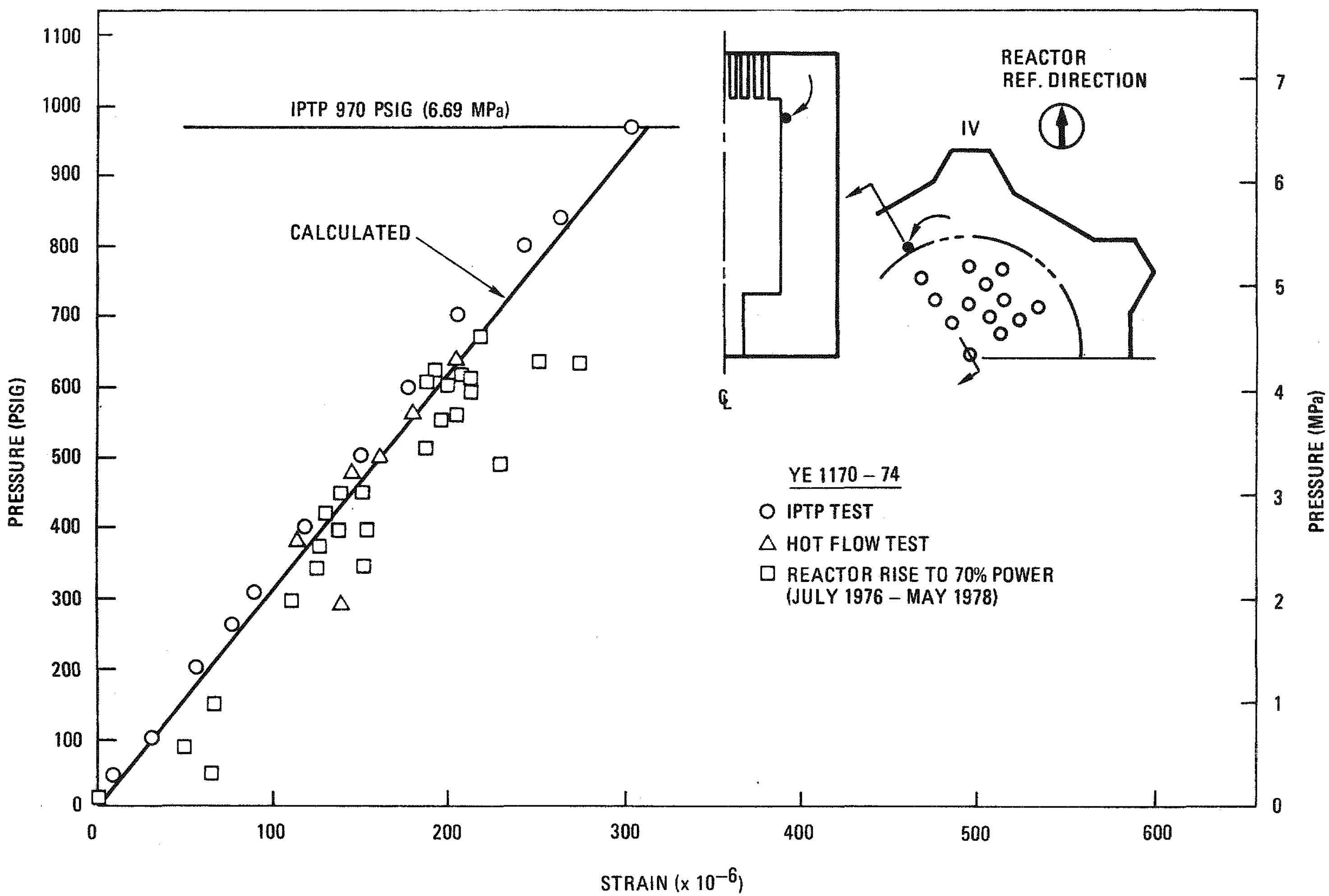

Fig. 4. Circumferential concrete strain at inner wall 13 ft. 0 in. from top haunch

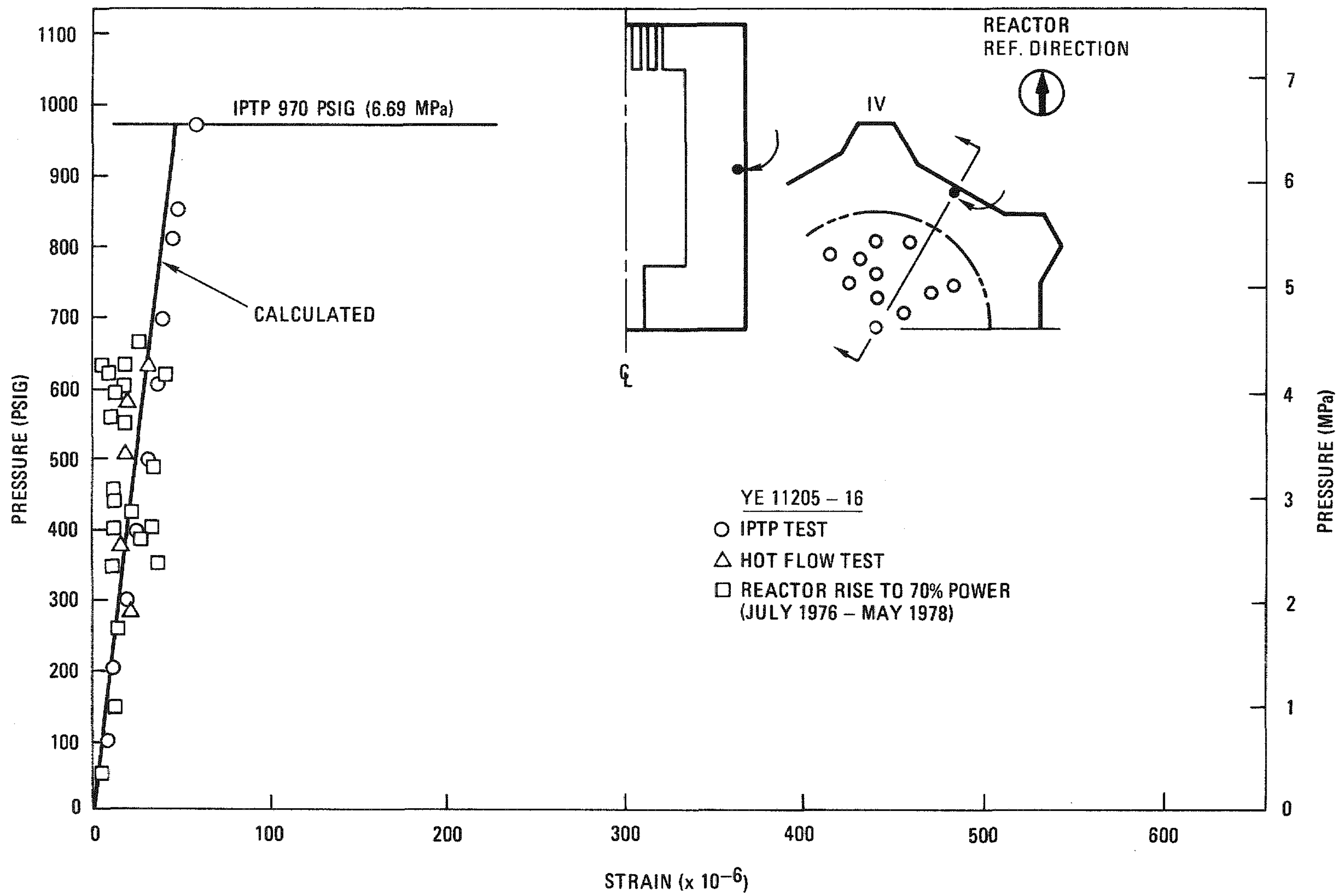

Fig. 5. Axial concrete strain at outer wall midheight

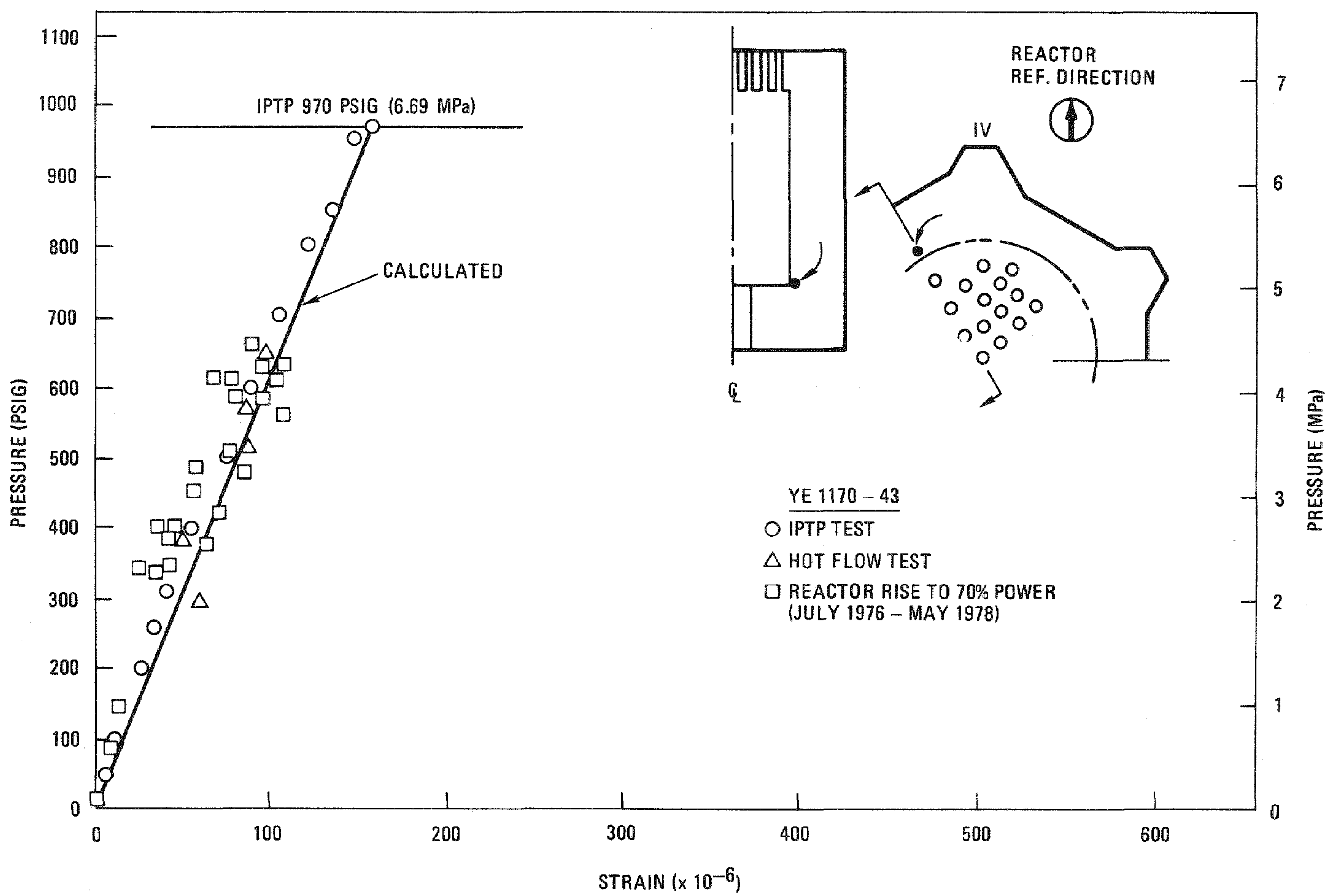

Fig. 6. Axial concrete strain at wall near bottom haunch

the test results from the analytically predicted values are within the limits established in the initial proof pressure test.

2.2. PCRV DEFLECTION

PCRV radial deflections along two diametrically opposite pilasters and the vertical deflection of the center of the top head were measured using precision alignment techniques. Remountable high-power telescopes (45X magnification) and see-through targets were employed to meet specification accuracy requirements of ±0.005 in. (±0.127 mm). A copy of the PCRV deflection measuring system specification is included in Appendix A.

The PCRV optical deflection measurements were performed prior to reactor start-up tests and after the first year of reactor operation. Pressure versus deflection curves for the PCRV wall midheight and the center of the top head are shown on Figs. 7 and 8. Deflection data are given relative to the outer edge corners of the PCRV. The measured deflections were compared with analytical results and found acceptable. The acceptance criteria are based on calculated deflections from elastic stress analysis with error bands for both calculational and measurement inaccuracies as established for the IPTP tests. The deflections obtained from IPTP tests are plotted on the same figures. No creep effects were considered in the finite element elastic stress analysis. The effect of creep on the measured deflections of the PCRV top head resulting from the elapsed time of 31 days between the measurements for vessel pressures of 375 psig (2.59 MPa) and 600 psig (4.14 MPa) is apparent on Fig. 8. The magnitude of creep was consistent with that observed during the IPTP tests. Comparison of deflection measurements performed during the IPTP and reactor start-up tests indicates no significant change in the structural stiffness of the PCRV.

2.3. CONCRETE TEMPERATURES

Representative concrete temperatures up to 70% power level are given in Table 1. No unanticipated increase in concrete temperature was

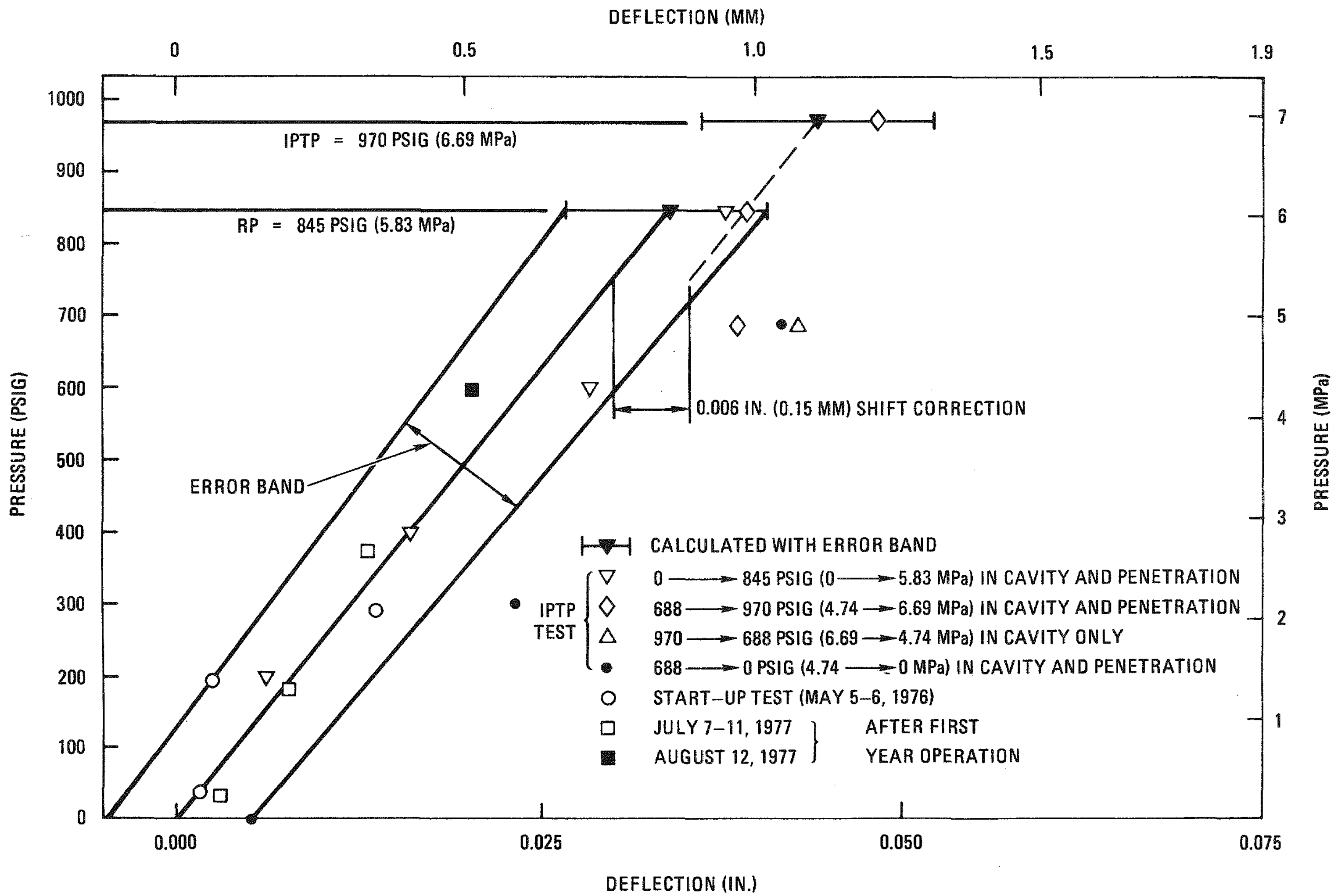

Fig. 7. Average radial deflection at wall midheight through pilaster section (relative to outer edge corners of PCRV)

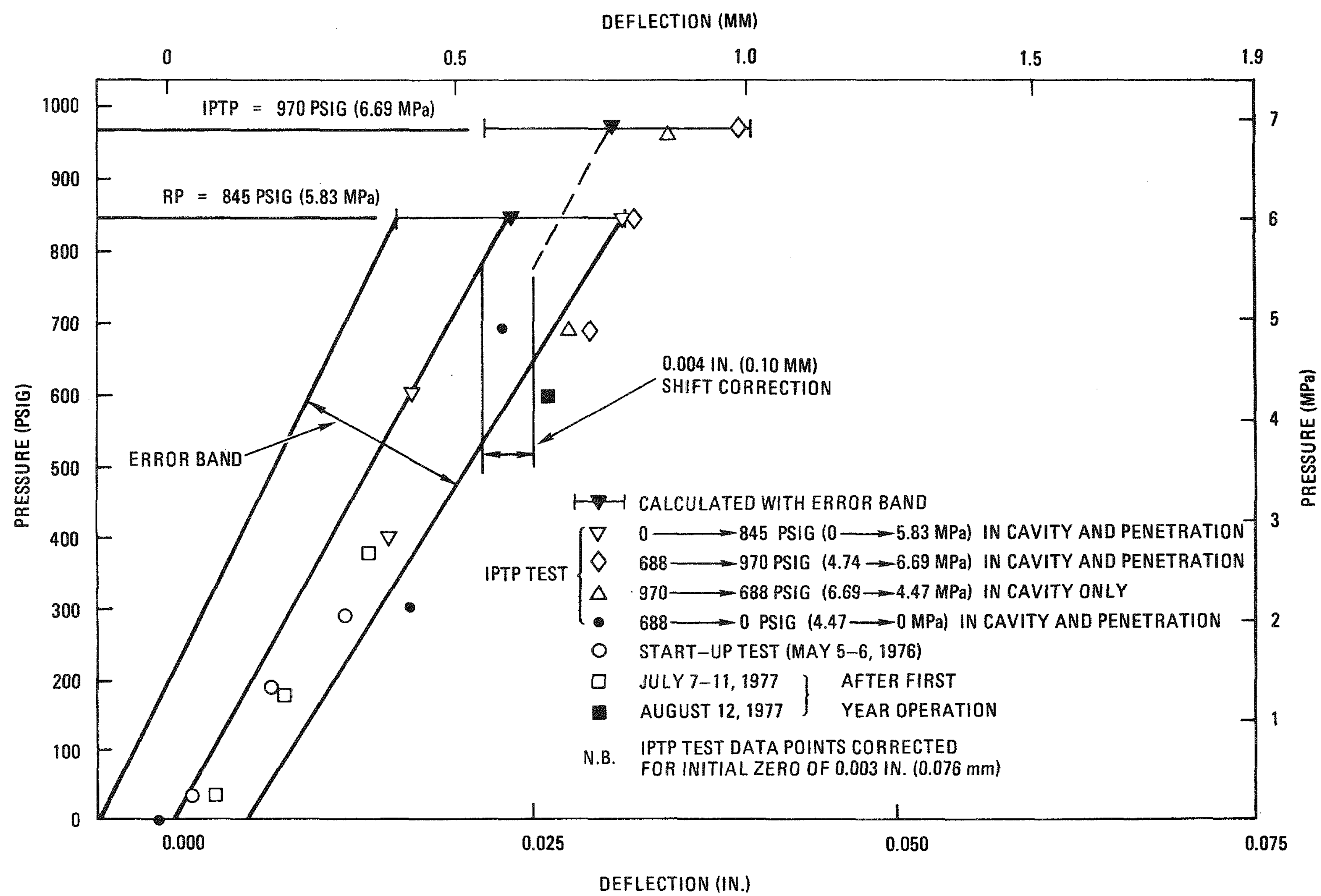

Fig. 8. Vertical deflection at center of top head (relative to outer edge corners of PCRV)

indicated by the embedded thermocouples during reactor rise to power. Concrete temperature profiles between refueling penetrations in the PCRV top head are shown in Fig. 9. Concrete/liner interface temperatures at the bottom of the top head are presented in Fig. 10. A comparison of the top head concrete temperatures with those recorded during earlier start-up tests at corresponding power levels showed an average temperature drop of 5°F (3°C) to 10°F (6°C) reflecting the lowering of inlet cooling water temperature for top head penetration subheaders.

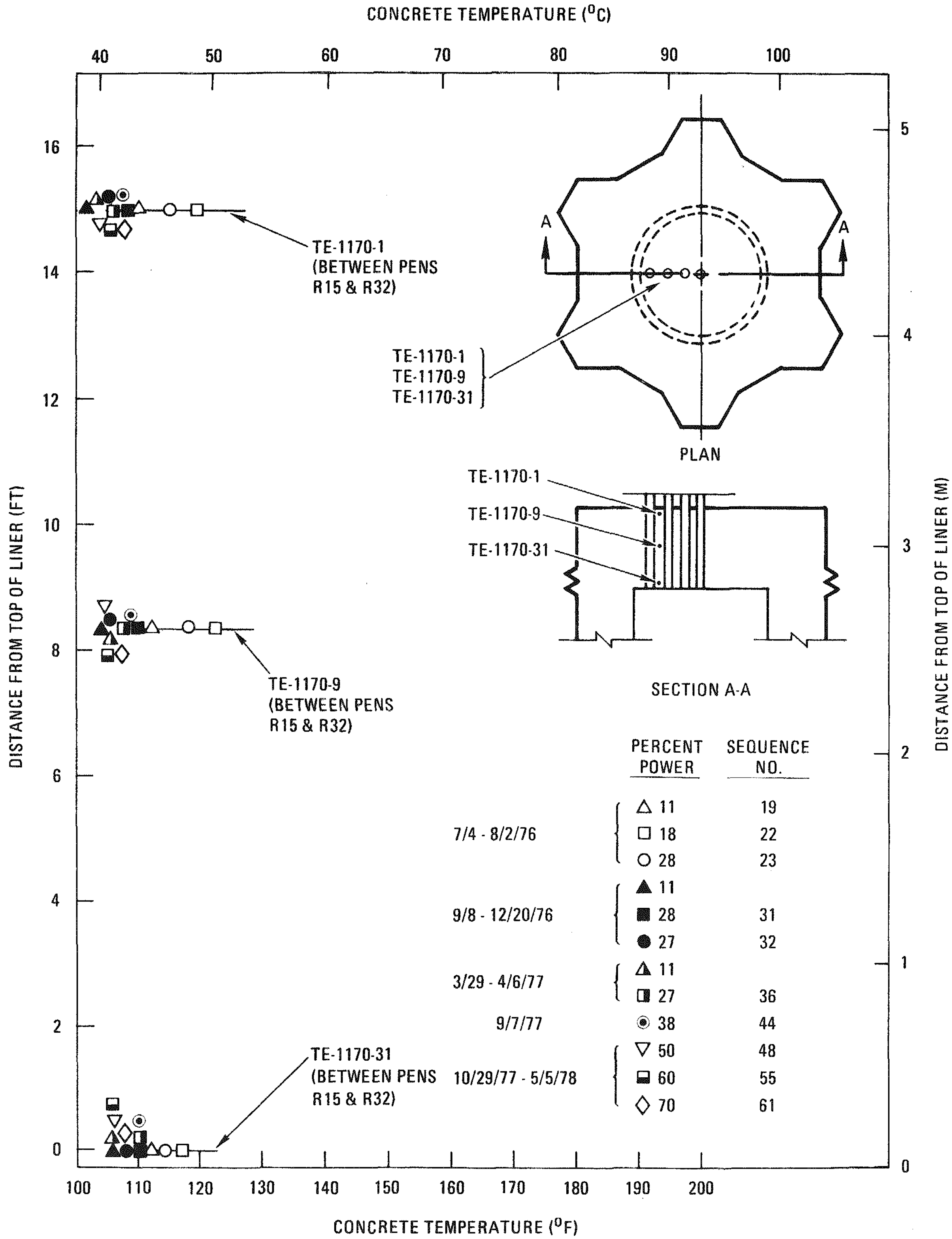

Fig. 9. Concrete temperature profile in top head

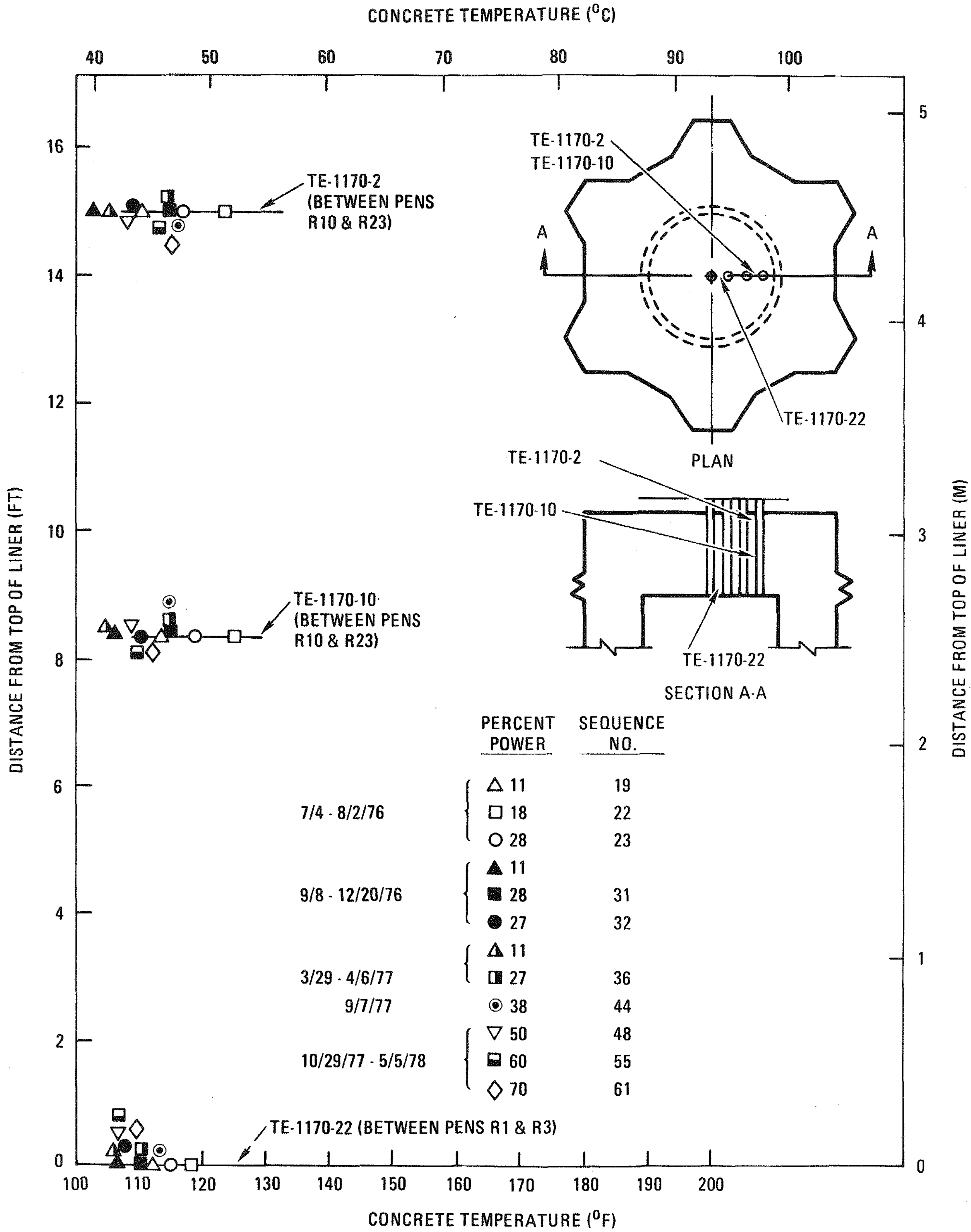

Fig. 9. Concrete temperature profile in top head (continued)

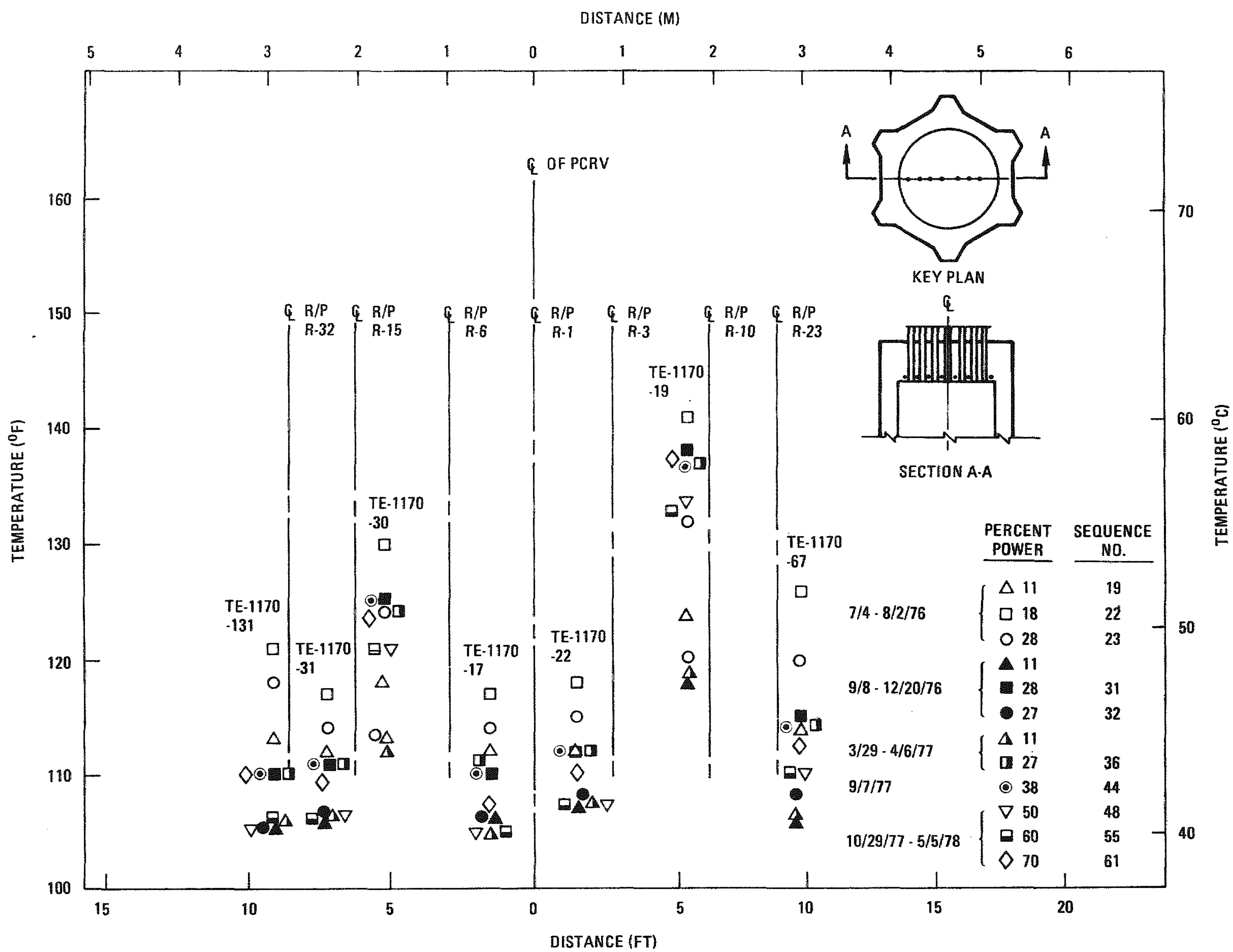

Fig. 10. Concrete temperature profile at concrete-liner interface: section A-A

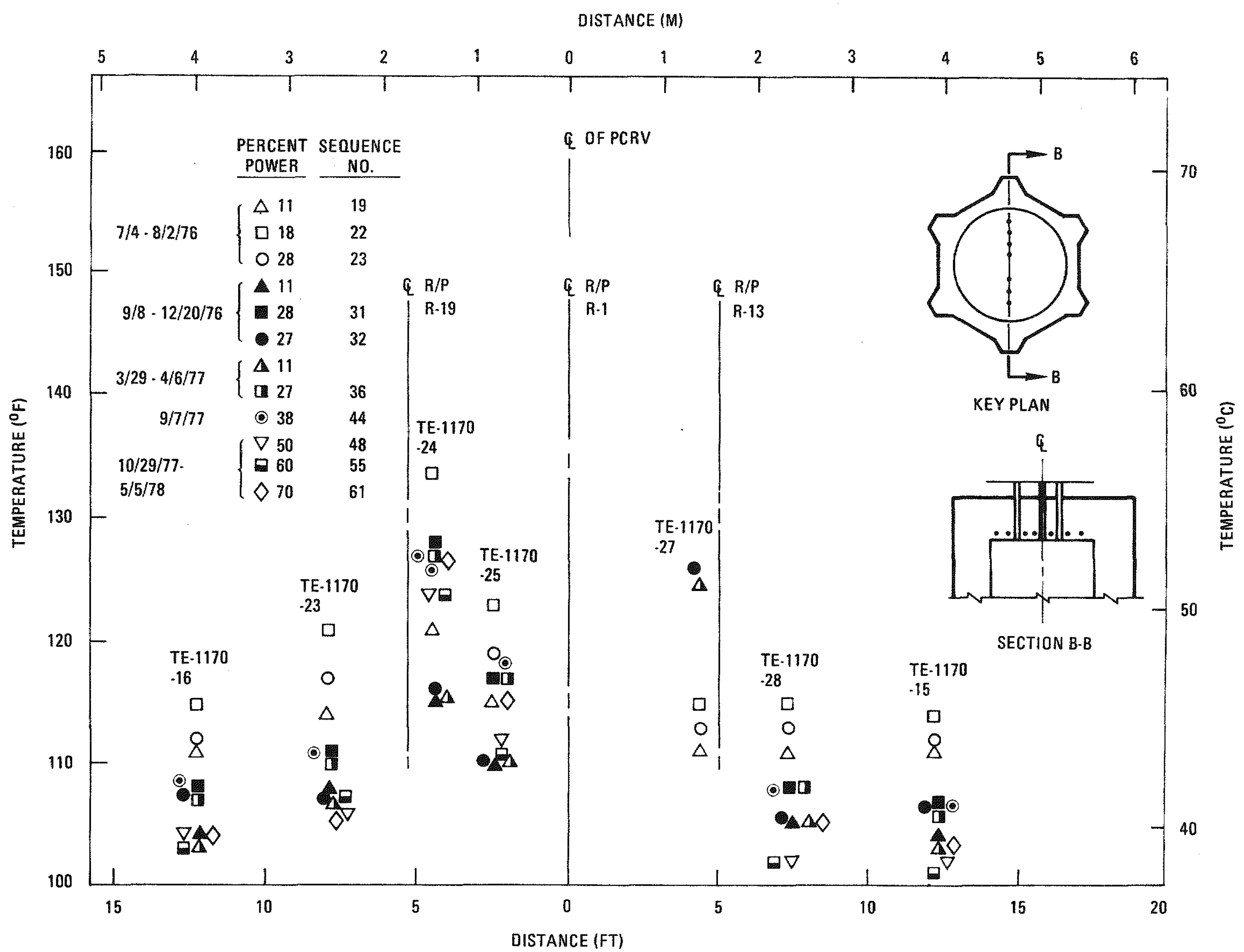

Fig. 10. Concrete temperature profile at concrete-liner interface (continued): section B-B

3. TIME-DEPENDENT PCRV RESPONSE

As part of the data updating effort, sensor data collected since FSV PCRV construction via the data acquisition system have been collated on one magnetic tape in a manner that permits the use of computer plotting routines. The data plots generated on a log-time scale provide an overall picture of the time-dependent responses of the PCRV. Computer plots of representative data from vibrating wire strain gages, Carlson strain gages, tendon load cells, and thermocouples collected up to the end of August 1978 are included in Appendix B. Figures 11 and 12 show the time-dependent responses of typical vertical and circumferential tendons as predicted for PCRV design with their corresponding load cell data. As can be seen, the actual prestress losses are well within the design limits.

3.1. CORRELATION OF ANALYTICAL RESULTS WITH PCRV SENSOR DATA

Time-dependent structural response of the PCRV was estimated initially on the basis of a projected time-load history. To properly account for the observed vessel behavior, creep analyses were performed using the actual FSV loading history for correlation of analytical results with measured data. The finite element model used in the axisymmetric creep analysis was similar to that reported in Appendix E of the FSV Final Safety Analysis Report. The correlation of analytical creep results with measured PCRV data was carried out in two stages. The time-load history covering the period from PCRV initial prestressing to the initial proof pressure test was considered in the first stage of the creep analysis. Various refinements in material assumptions and analytical procedures were investigated to provide better correlation for subsequent analyses. In the second stage, the PCRV creep analysis was extended to cover the period from initial prestressing to recent pressurizations during reactor rise to

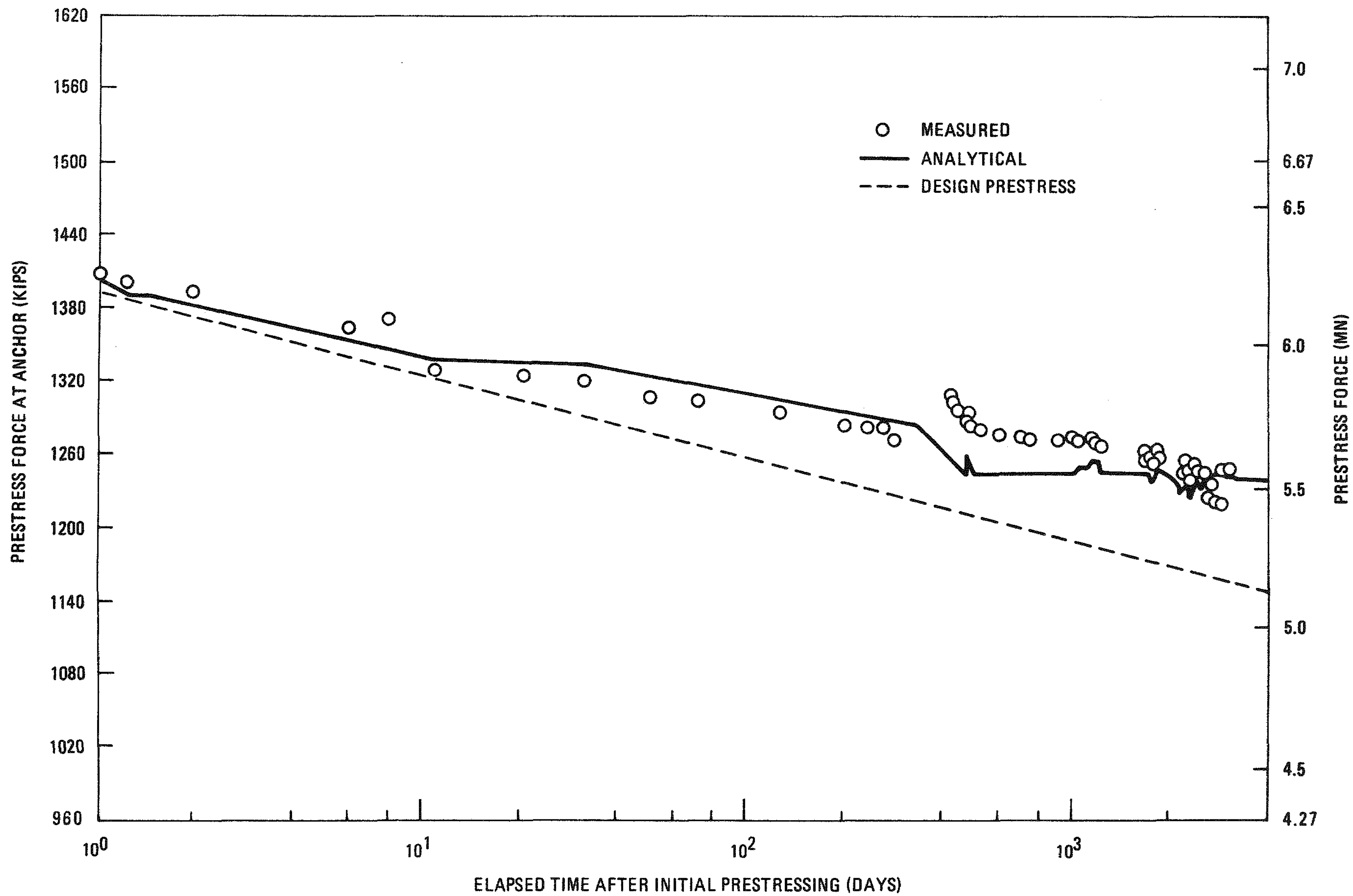

Fig. 11. Typical vertical tendon force versus time

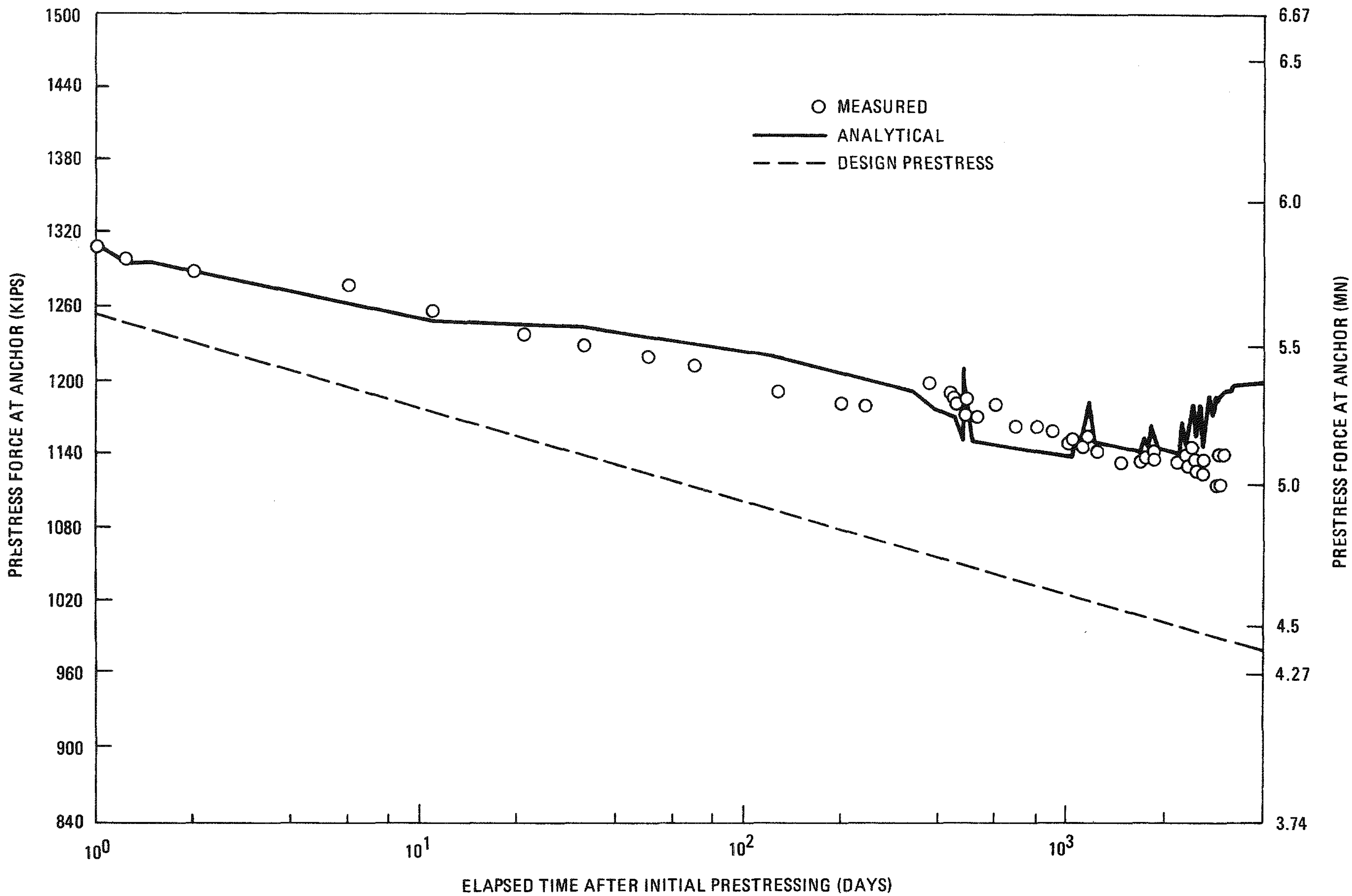

Fig. 12. Typical circumferential tendon force at barrel midheight versus time

power. An axisymmetric creep analysis was performed using the SAFE-CRACK code (Ref. 2).

3.1.1. Analytical Model

The finite element idealization of the top half of the PCRV is shown in Fig. 13. The pilasters of the PCRV were modeled by axisymmetric triangular elements with no stiffness in the hoop direction. The longitudinal stiffness of the pilasters was varied to account for the geometry of the pilasters. The refueling region of the top head was modeled with solid elements with reduced elastic modulus. Cavity liners were treated as plate elements, whereas reinforcement and prestressing tendons were modeled by one-dimensional bar elements. The vertical and circumferential prestressing loads were simulated by inducing thermal strains in the prestressing elements.

3.1.2. Time-Load History

The time-load history for final creep analysis derived from the sensor data log of the FSV PCRV is presented in Table 2. The actual time-load history of the PCRV (April 10, 1970, to August 11, 1978) from initial prestressing to start-up test including major events leading to 70% reactor power level was represented in 56 time steps. Temperature input was based on representative concrete temperatures as indicated by the embedded thermocouples in the PCRV. The initial prestressing loads were taken from the anchor loads recorded by the tendon load cells. The prestress tendon steel relaxation was taken into account by incorporating a series of relaxation factors in terms of initial prestress corresponding to the time steps.

3.1.3. Results and Evaluation

Based on results of the preliminary analysis, an iterative approach to approximate the elastic shortening in the concrete caused by prestress

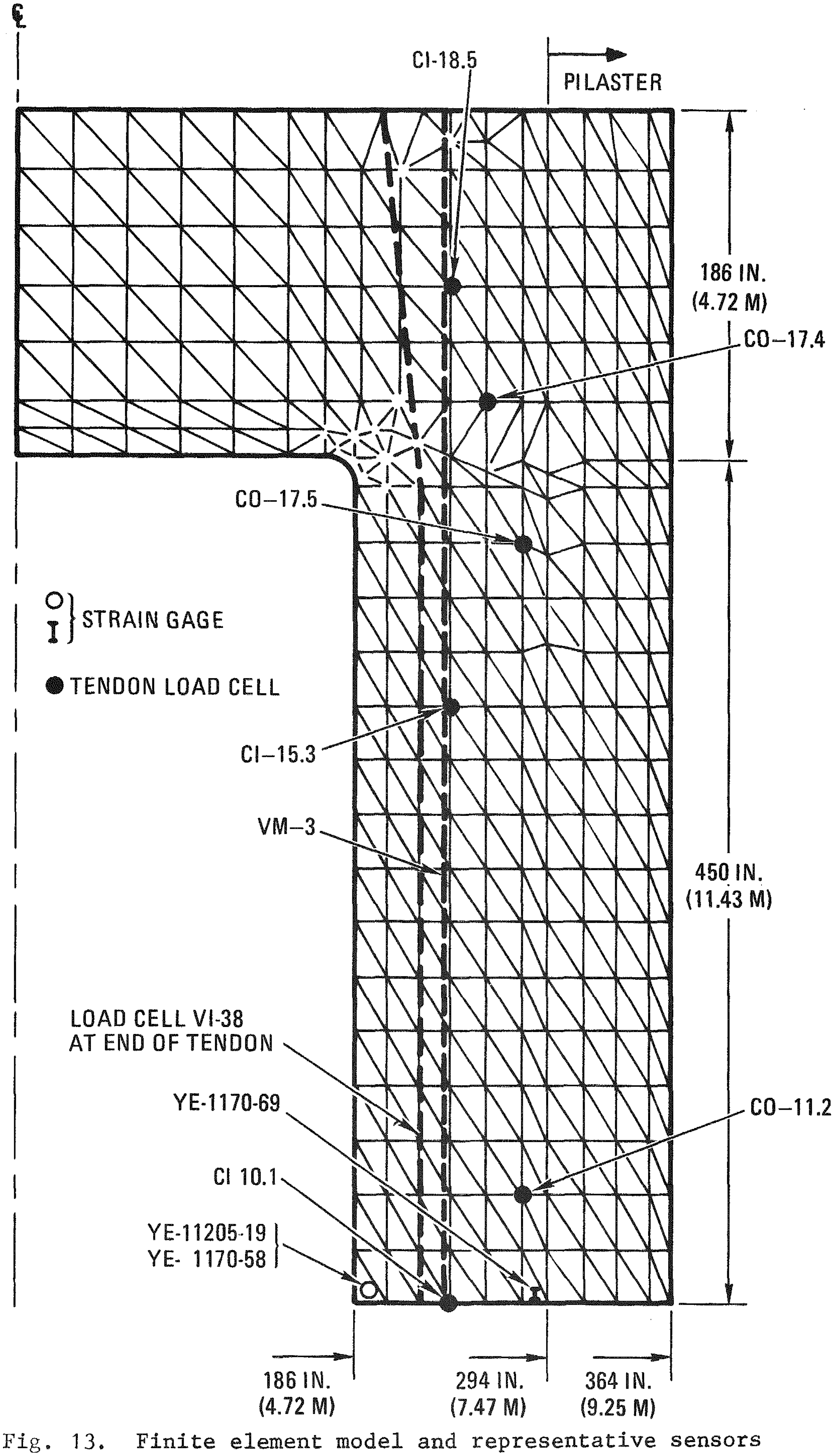

Fig. 13. Finite element model and representative sensors

TABLE 2
TIME-LOAD HISTORY

Days		Relaxation Factor	Temperature (°F/°C)	Pressure (psi/MPa)
1	0	1.00	58/14	0
2	0.25	0.99	58/14	0
3	0.50	0.99	58/14	0
4	5	0.97	58/14	0
5	10	0.96	58/14	0
6	31	0.96	58/14	0
7	126	0.95	74/23	0
8	335	0.94	71/22	0
9	371	0.94	84/29	0
10	446	0.94	115/46	0
11	475	0.94	118/48	0
12	479	0.94	118/48	400/2.76
13	483	0.94	119/48	970/6.69
14	492	0.94	117/47	500/3.45
15	495	0.94	117/47	0
16	500	0.94	117/47	0
17	1025	0.94	100/38	0
18	1053	0.94	100/38	155/1.07
19	1130	0.94	100/38	163/1.12
20	1165	0.94	105/41	623/4.30
21	1197	0.94	107/42	480/3.31
22	1225	0.94	103/39	0
23	1711	0.94	98/37	0
24	1752	0.94	110/43	190/1.31
25	1758	0.94	120/49	249/1.72
26	1819	0.94	112/44	125/0.86
27	1831	0.94	112/44	365/2.52
28	1861	0.94	104/40	389/2.68
29	1897	0.94	101/38	0
30	2194	0.94	114/46	0

TABLE 2 (Continued)

Days		Relaxation Factor	Temperature (°F/°C)	Pressure (psi/MPa)
31	2225	0.93	101/38	207/1.43
32	2305	0.93	110/43	634/4.37
33	2315	0.93	115/46	50/0.34
34	2326	0.93	106/41	0
35	2390	0.93	102/39	401/2.76
36	2439	0.93	103/39	588/4.05
37	2460	0.93	104/40	635/4.38
38	2473	0.93	104/40	629/4.34
39	2531	0.93	104/40	12/0.08
40	2552	0.93	103/39	606/4.18
41	2597	0.93	102/39	585/4.03
42	2603	0.93	101/38	283/1.95
43	2630	0.93	102/39	18/0.12
44	2677	0.93	106/41	603/4.16
45	2700	0.93	102/39	338/2.33
46	2706	0.93	104/40	607/4.19
47	2742	0.93	103/39	608/4.19
48	2774	0.93	100/38	646/4.45
49	2789	0.93	101/38	636/4.39
50	2830	0.93	104/40	395/2.72
51	2838	0.93	103/39	627/4.32
52	2844	0.93	103/39	637/4.39
53	2865	0.93	100/38	342/2.35
54	2880	0.93	101/38	485/3.34
55	2922	0.93	104/40	644/4.44
56	3035	0.93	103/39	651/4.49
57	3186	0.93	110/43	670/4.62
58	3190	0.93	120/49	688/4.74
59	4900	0.93	120/49	688/4.74
60	7500	0.93	120/49	688/4.74

TABLE 2 (Continued)

Days		Relaxation Factor	Temperature (°F/°C)	Pressure (psi/MPa)
61	10000	0.92	120/49	688/4.74
62	12600	0.92	120/49	688/4.74
63	12605	0.92	120/49	688/4.74

application was utilized in the final creep analysis to obtain better correlation between the analytical initial tendon loads and the load cell values. The concrete elastic modulus of $E_c = 5.0 \times 10^6$ psi (34.5×10^3 MPa) was assumed. This value was verified in the proof pressure test to be close to the actual elastic modulus of the PCRV concrete. The analytical results show the predicted time-dependent structural response in general agreement with the available PCRV sensor data. The locations of representative tendon load cells and strain gages selected for data comparisons are given in Fig. 13. Figures 14 and 15 compare the time-dependent responses of vertical tendons with the load cell readings. Analytical results versus load cell data for the circumferential tendons at midheight of the PCRV barrel are shown in Figs. 16 and 17. Similar comparisons for circumferential tendons at the top head and upper barrel are presented in Figs. 18 through 21, inclusive. The assessment of tendon responses indicates that the creep analysis overestimated creep recovery resulting from pressurizations. The inclusions of additional time steps to better represent vessel pressurizations during reactor rise to power did not show significant improvement in the analytical predictions. Figure 22 shows the comparison of predicted concrete circumferential strain response with measured strains indicated by two embedded concrete gages at the midheight of the inner PCRV wall. Comparisons of predicted and measured vertical concrete strains at the outer PCRV wall are given in Fig. 23.

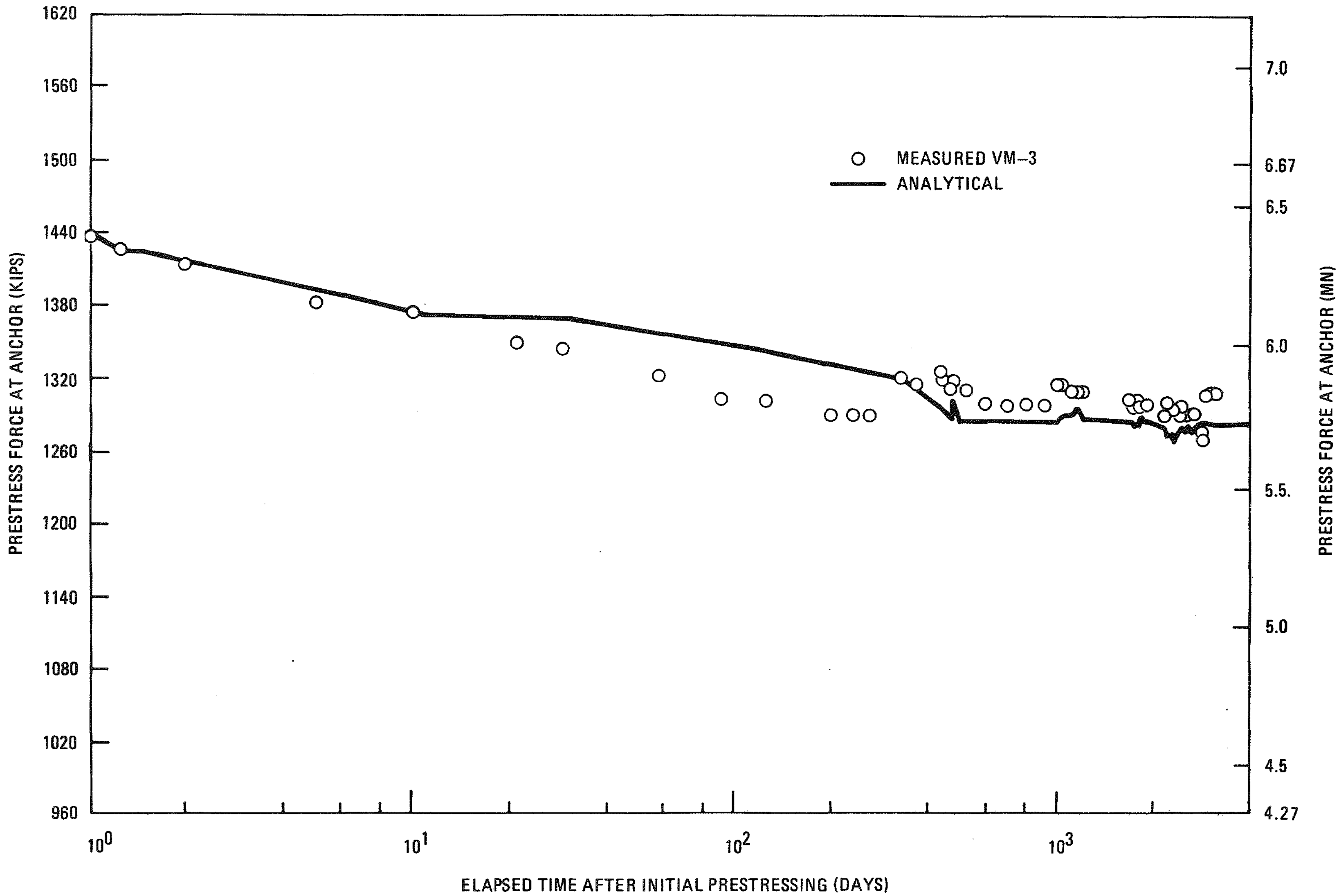

Fig. 14. Vertical tendon force (load cell VM-3) versus time

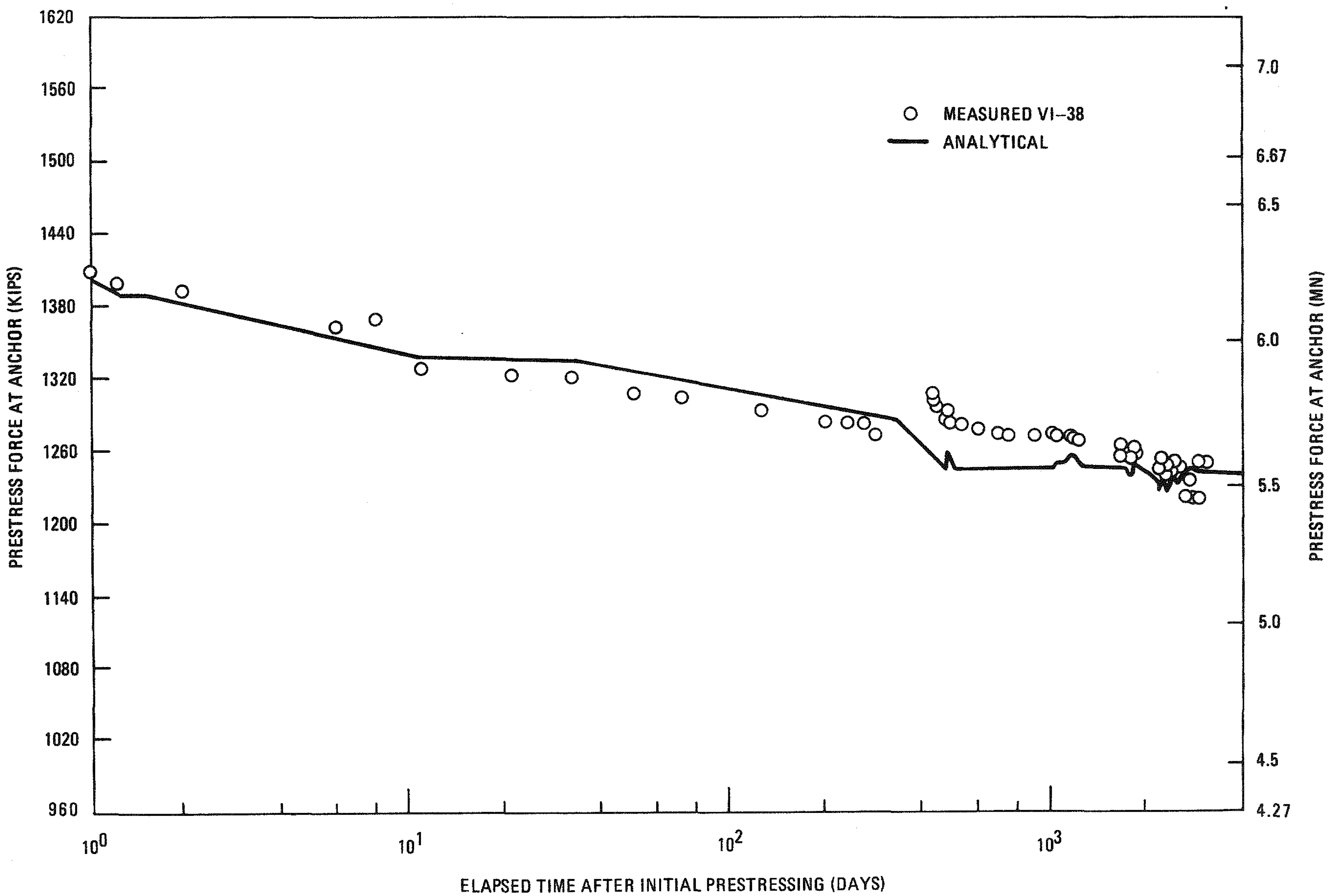

Fig. 15. Vertical tendon force (load cell VI-38) versus time

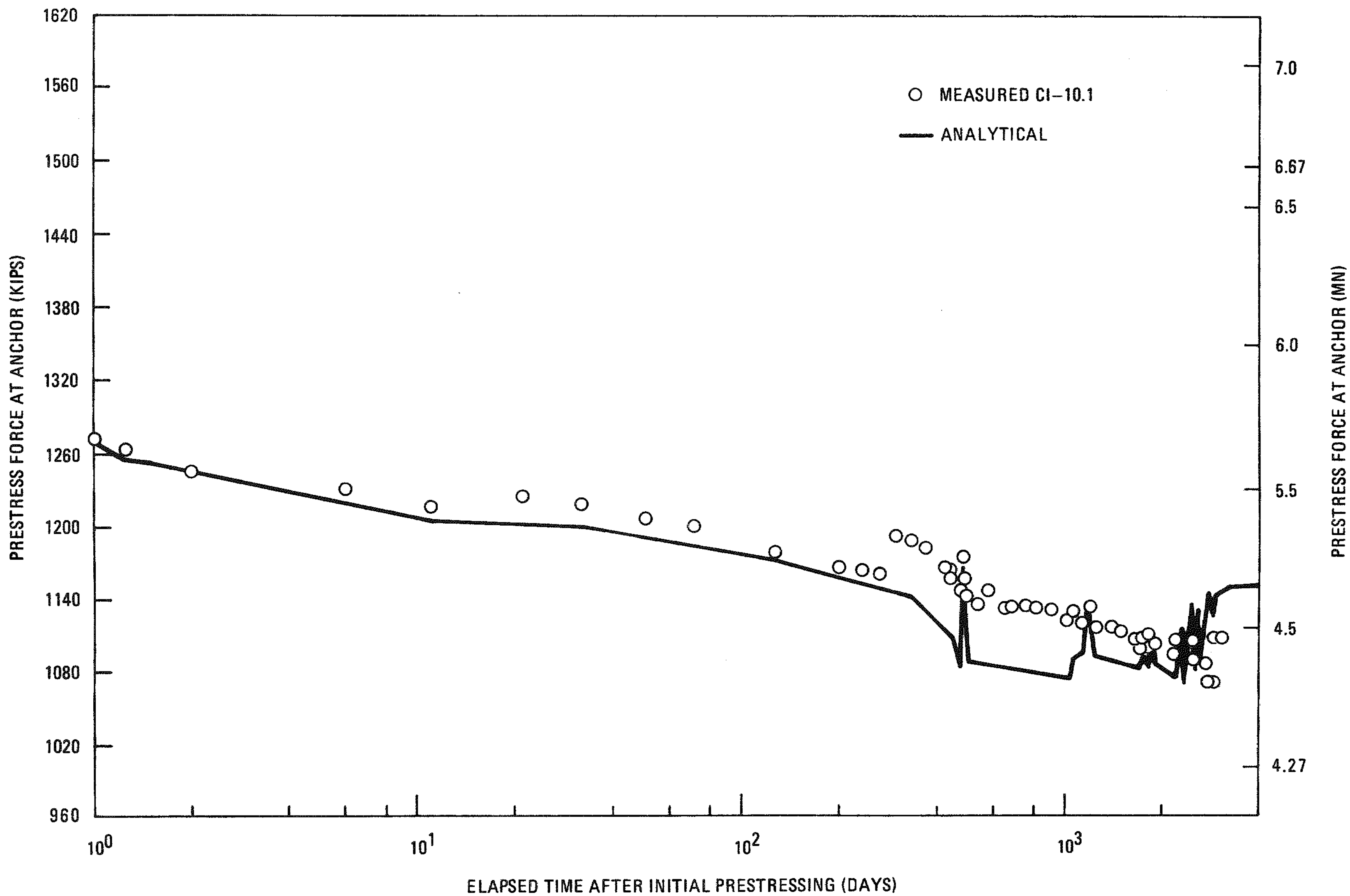

Fig. 16. Circumferential tendon force (load cell CI-10.1) at barrel midheight versus time

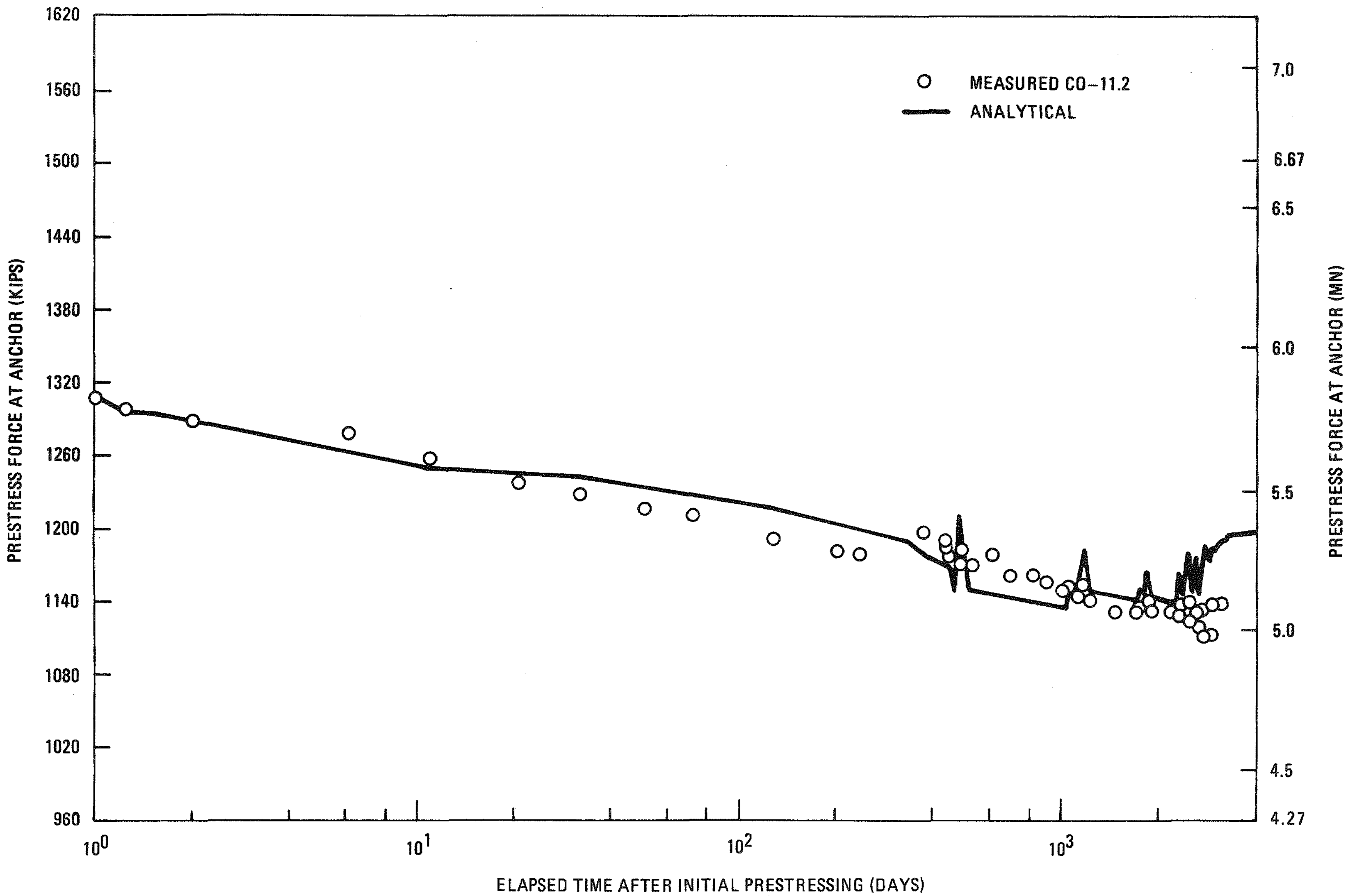

Fig. 17. Circumferential tendon force (load cell CO-11.2) at barrel midheight versus time

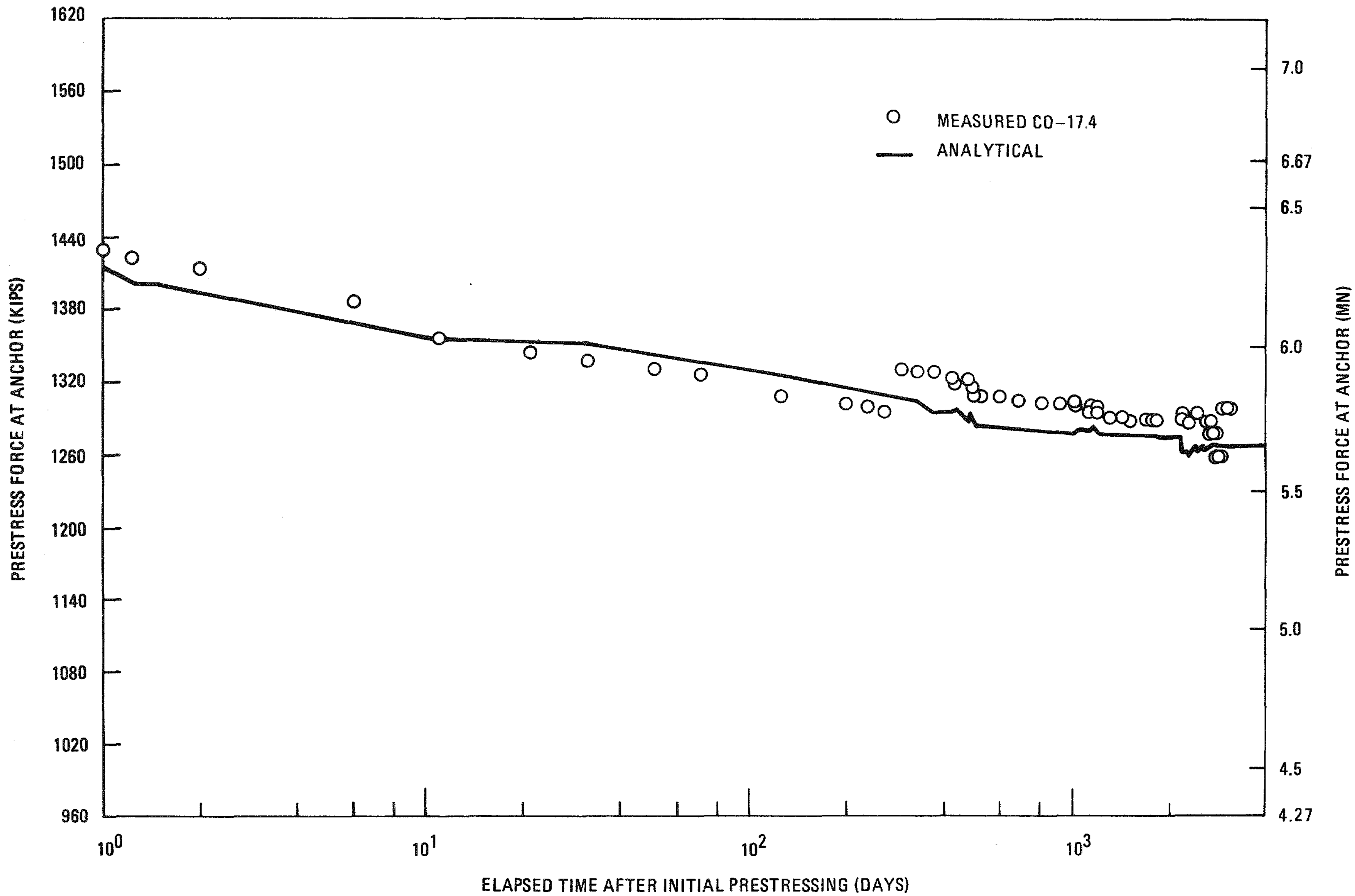

Fig. 18. Circumferential tendon force (load cell CO-17.4) at top head versus time

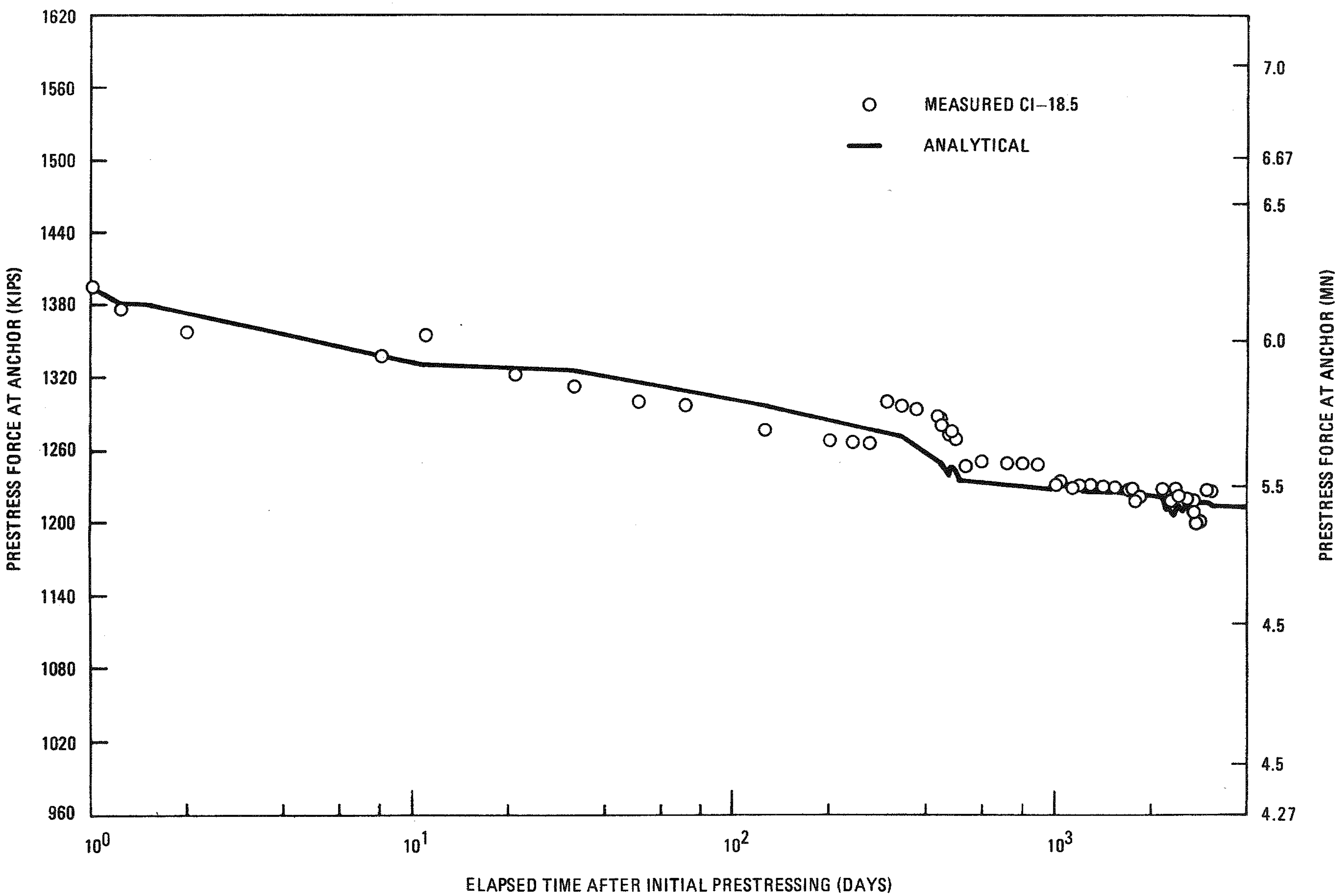

Fig. 19. Circumferential tendon force (load cell CI-18.5) at top head versus time

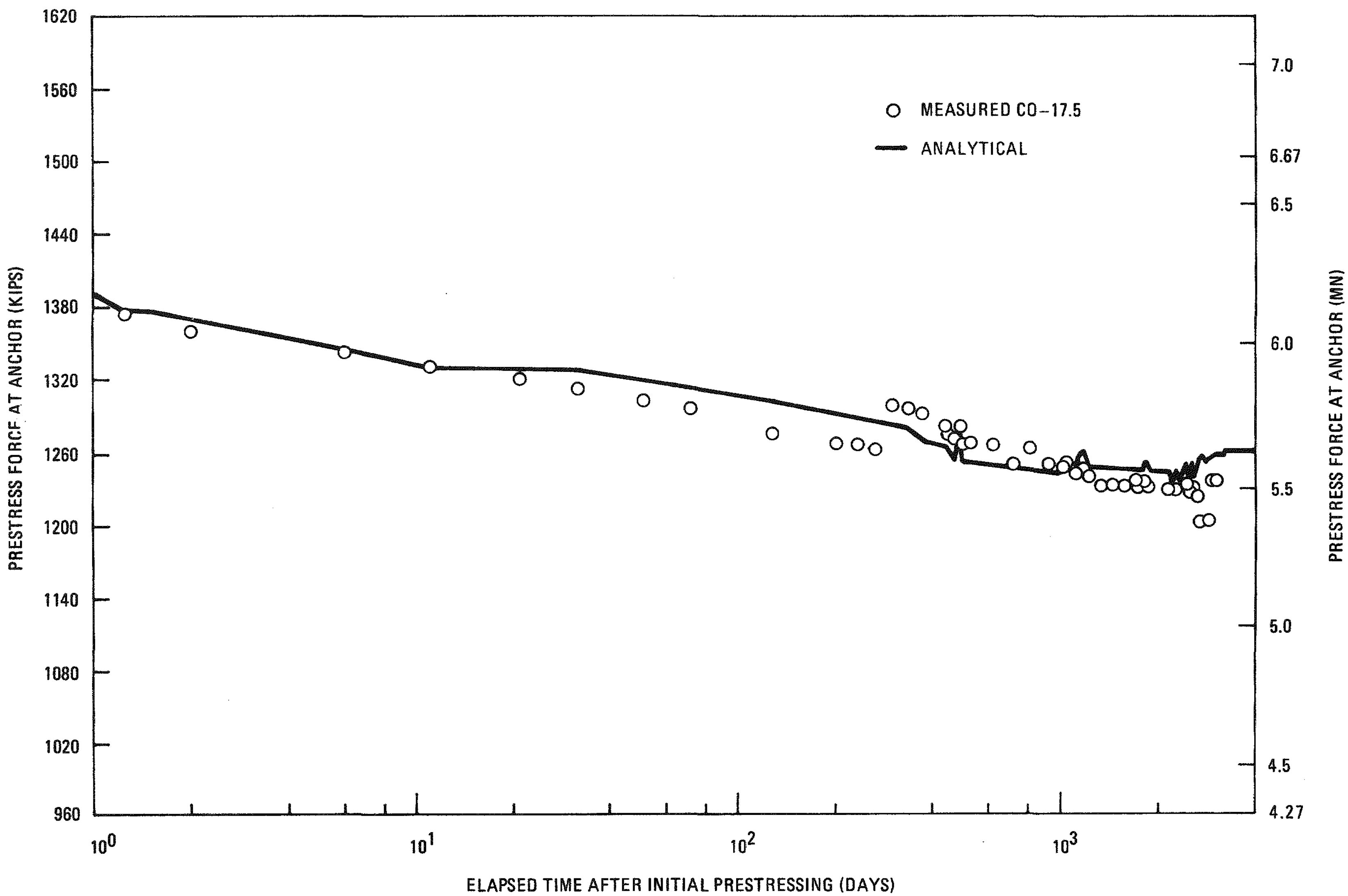

Fig. 20. Circumferential tendon force (load cell CO-17.5) at upper barrel versus time

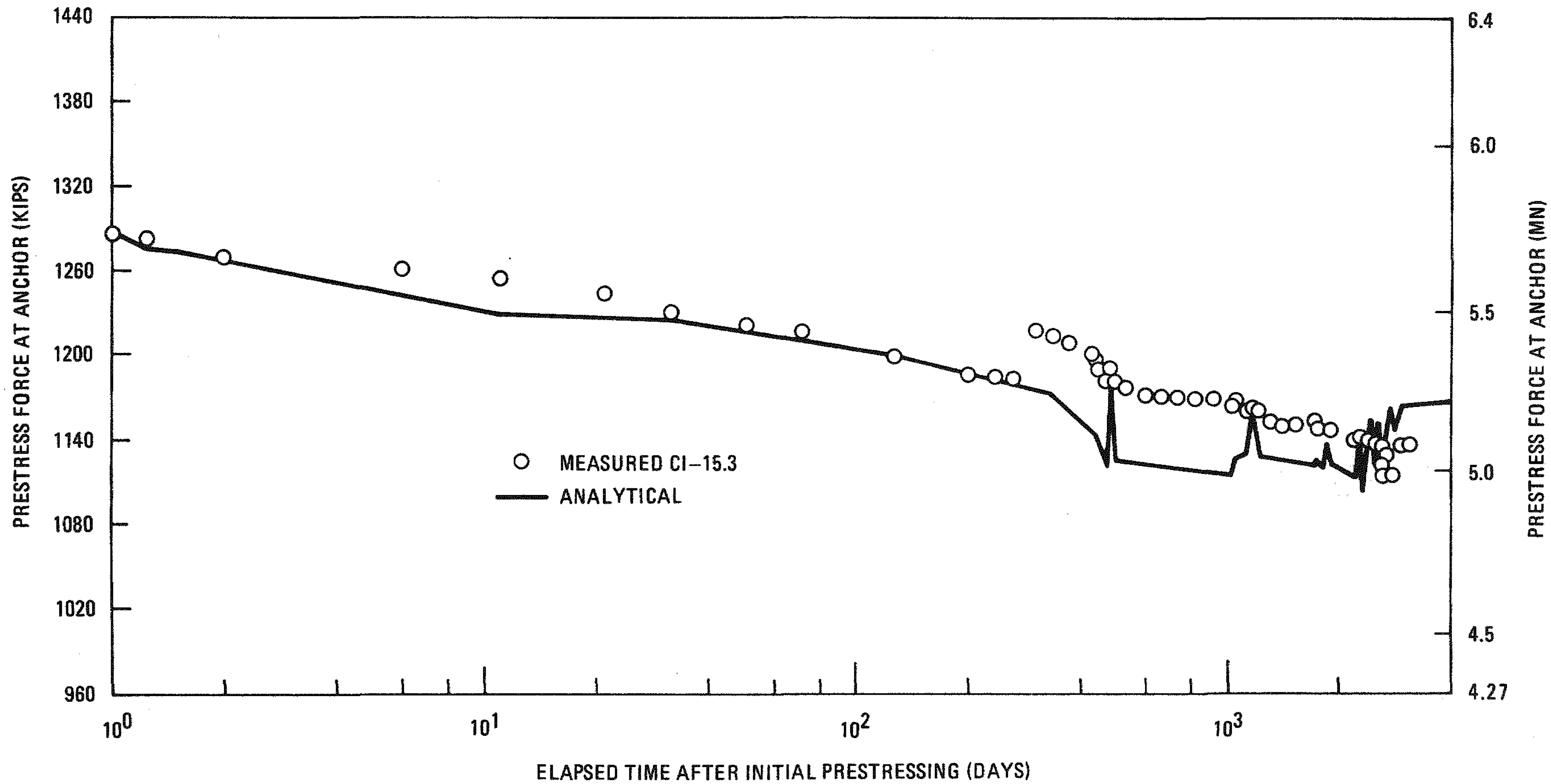

Fig. 21. Circumferential tendon force (load cell CI-15.3) at upper barrel versus time

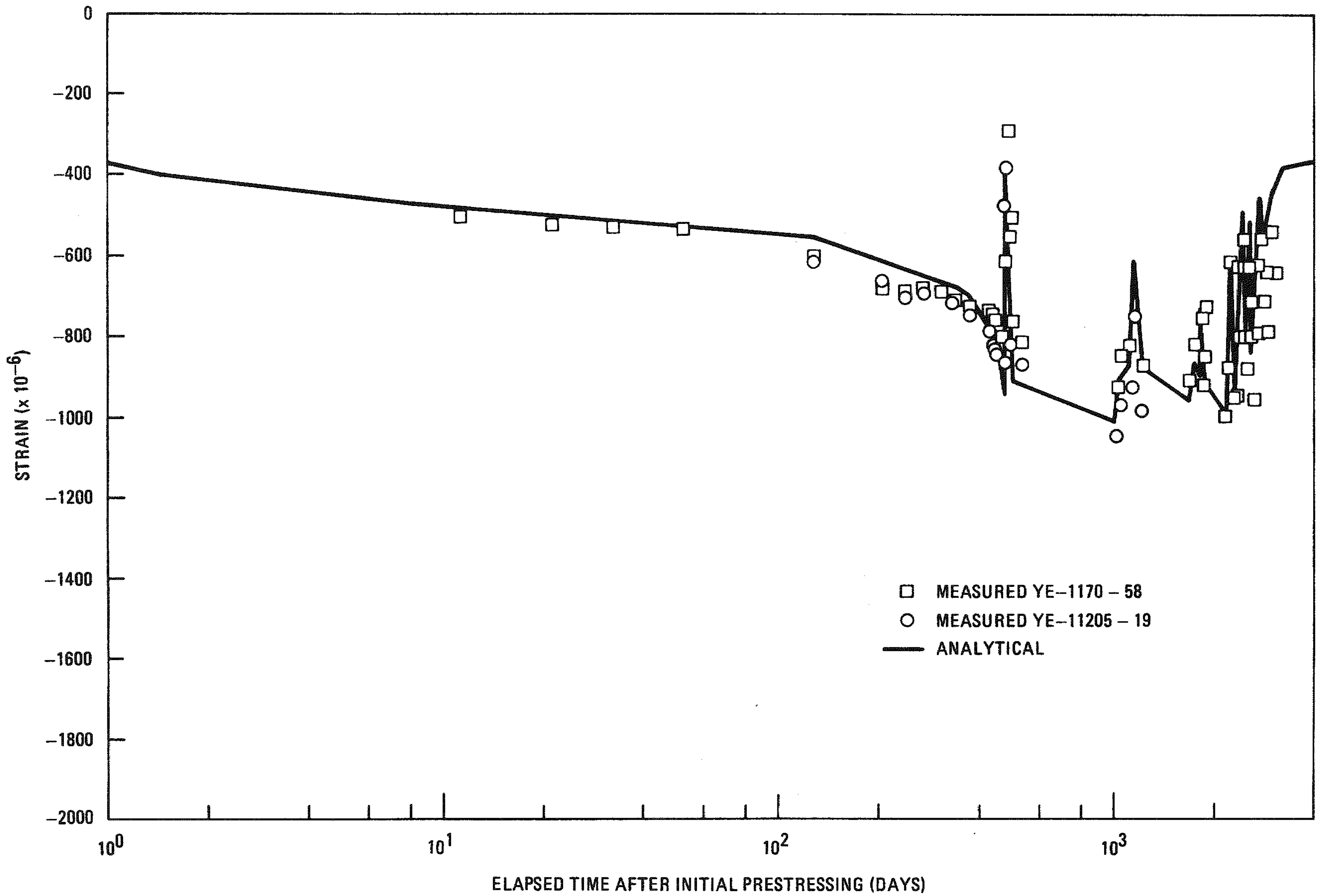

Fig. 22. Strain versus log time for circumferential concrete gages at PCRV inner midplane

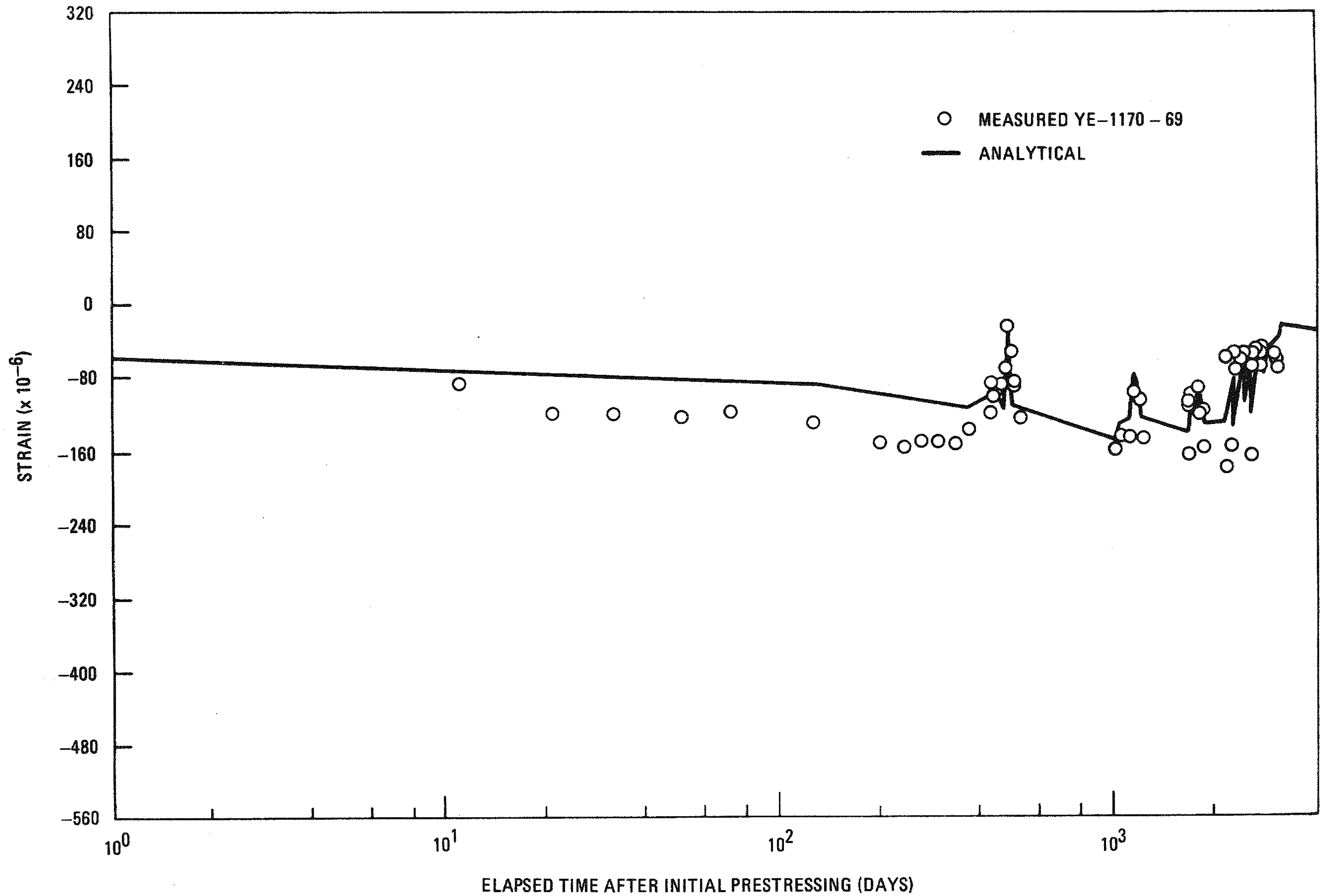

Fig. 23. Strain versus log time for a vertical concrete gage at PCRV outer midplane

4. CONCLUSION AND RECOMMENDATION

Based on analyses of the PCRV sensor data and deflection measurements obtained during the start-up tests, the PCRV generally responded as anticipated in design. The overall PCRV structural response to pressure changes was essentially linear, and the test results were in general agreement with those predicted by the elastic finite element analysis. Judging from the levels of pressure reached during the reactor rise to 70% power, the trend of PCRV response demonstrated would be indicative of the PCRV behavior at full power. The consistency exhibited in the concrete strains and deflection measurements obtained from IPTP and startup tests indicates no significant change in the PCRV structural stiffness. The long-term tendon loads have been conservatively estimated in the FSV PCRV design and the observed prestress losses are well within the design limits.

Despite the overestimate of creep recovery from pressurization, the time-dependent PCRV response as predicted by an axisymmetric creep analysis agrees reasonably well with the measured data. Since the PCRV is assumed axisymmetric in the analyses, better correlation of analytical results is expected in regions where axisymmetric response is anticipated. The many cycles of pressurizations and temperature fluctuations experienced by the vessel during the start-up tests are not fully accounted for by the material parameters necessary to define the constitutive model. The present correlation between analytical results and measured data should be examined with these limitations in mind.

The two-dimensional solution provided by the SAFE-CRACK code used to predict the time-dependent response of the FSV PCRV would not be adequate for the multicavity PCRV configuration. The complex geometry of the multicavity PCRV of recent HTGR designs requires three-dimensional treatments. A realistic three-dimensional analytical model requires the solution of a large system of algebraic equations. An efficient solution algorithm is provided by the 3-D finite element computer program THREED developed at General Atomic. There is a need to validate the THREED code for PCRV design, and the FSV PCRV provides the unique vehicle to obtain the necessary experimental data. It is therefore recommended that data acquisition be continued at FSV to verify time-dependent PCRV behavior prediction.

REFERENCES

1. Ople, F. S., Jr., and H. L. Gotschall, "Fort St. Vrain Unit 1, PCRV Pressure Test Report for the Public Service Company of Colorado," USAEC Report GA-A10839, General Atomic Company, December 1971.

2. Lu, S. C., and C. M. Charman, "SAFE-CRACK User's Manual," GA-A13035, General Atomic Company, December 1974.

APPENDIX A

SPECIFICATION FOR FORT ST. VRAIN PCRV
DEFLECTION MEASURING SYSTEM

PA52-TS-004

General Atomic Company

GA 777

SPECIFICATION FOR FORT ST. VRAIN PCRV DEFLECTION MEASURING SYSTEM

Proj. No. 3273	Document No. PA52-TS-004	Issue B	Date MAR 17 1978

QAL II

ISSUE SUMMARY

Issue	Date	Prepared by	Approvals				Purpose of Issue/ Sections Changed
			Engineering	QA	Project	Program	
A	JUN 29 1976	T. C. Liu/ K.C.Cheung	G. S. Chow	P.Stuart DEH for P.S.S.	L.Swanson 6-22-76	T.McLean	For use.
B	MAR 17 1978	K.C. Cheung R.D. Phelps	G. Chow 3/8/78	D.Pettycord 3/10/78	L. Swanson 3-6-78	P. Steward 3/14/78	Section 2 Revised

RELEASED JUN 29 1976

RELEASED

Do not write in space below. Continue Issue Summary on GA Form 778.

Notations in this column indicate where changes have been made.

SPECIFICATION FOR FORT ST. VRAIN PCRV DEFLECTION MEASURING SYSTEM

Proj. No. 3273	Spec. No. PA52-TS-004	Issue B	Date

TABLE OF CONTENTS

Notations in this column indicate where changes have been made.

SPECIFICATION FOR FORT ST. VRAIN PCRV DEFLECTION MEASURING SYSTEM

Proj. No. 3273	Spec. No. PA52-TS-004	Issue B	Date

1. GENERAL INFORMATION AND SCOPE

This document specifies the performance requirements for the measurement of deflections of the Fort St. Vrain prestressed concrete reactor vessel (PCRV).

The PCRV provides primary containment for the nuclear steam supply system of a high temperature gas-cooled reactor. The general arrangement of the Fort St. Vrain PCRV is shown in Figure 1 and the overall dimensions are given in Figure 2. The measurement of vertical deflections at points on the top head and horizontal deflections at points on the walls are required to assess the structural behavior of the vessel.

2. DEFLECTION MEASURING REQUIREMENTS

2.1 LOCATION OF DEFLECTION POINTS: Deflection points shall be established along north and south pilasters (I&IV) and across the top head as shown schematically in Figure 2. The locations of deflection points shall be those established for the Initial Proof Test Pressure (IPTP) test.

2.2 SYSTEM SPECIFICATION: The deflection measuring system shall be designed to obtain deflections relative to control points at the corners of the vessel (see Figure 2). It shall be capable of measuring the displacement of intermediate points to an accuracy within ± 0.005 in. (± 0.127 mm). The maximum anticipated displacement is 0.050 in. (1.27 mm). The measuring system shall have a minimum range of twice the maximum anticipated deflection or 0.100 in. (2.54 mm).

2.3 FREQUENCY OF MEASUREMENTS: The frequency of measurements shall be as follows:

2.3.1 Start-Up Test

*(1) A reference set of deflection measurements shall be made prior to vessel pressurization or at cavity pressure not greater than 100 psia (0.59 N/mm^2).

*(2) During the pressurization of the vessel, two sets of deflection measurements shall be made at approximately 200 psia (1.28 N/mm^2) and 300 psia (1.97 N/mm^2) pressure level.

(3) During start-up to full power pressure, three sets of deflection measurements shall be made at approximately 100 psia (0.59 N/mm^2), 400 psia (2.66 N/mm^2) and at full power pressure of 700 psia (4.73 N/mm^2), or at as high a PCRV pressure attainable consistent with plant operations.

*The specified performance requirements are not mandatory for the deflection measurements in para. (1) and (2) above.

Notations in this column indicate where changes have been made.

2.3.2 Start-Up From Refueling Status

Deflection measurements shall be performed upon pressurization of the vessel during a normal plant startup from refueling status.

(1) A reference set of deflection measurements shall be made prior to vessel pressurization or at cavity pressure not greater than 50 psia (0.24 N/mm^2).

(2) During the pressurization of the vessel, deflection measurements shall be made at approximately 200 psia (1.28 N/mm^2), 400 psia (2.66 N/mm^2) and at 100% rated pressure (700 psia, 4.73 N/mm^2)

A set of deflection measurements is defined as the measurements of vertical deflection at the top head and horizontal deflections at the side walls.

The deflection measurements may be made at each point without interrupting the vessel pressurization. The vessel pressure shall be recorded at the time when the measurement at each deflection point is made.

3. SITE CONDITIONS

The PCRV is within the reactor building and is subject only to the temperature fluctuations and air turbulence induced by the building heating and ventilation system. Since the effect of the temperature variation over the height of the vessel on the relative displacement of the vessel wall during the startup test and startup from refueling status is insignificant, the temperature distribution may be assumed uniform for the purpose of deflection measurements. Temperature correction shall be made for deflection measurements on the top head.

4. QUALITY ASSURANCE REQUIREMENTS

The requirements given in Appendix I shall be met.

5. REPORT

A final report, listing the required measurements and describing in detail the instrumentation and procedure used to obtain the measurements, shall be submitted to General Atomic Company. It shall include an assessment of the accuracy of the measurements obtained.

Notations in this column indicate where changes have been made.

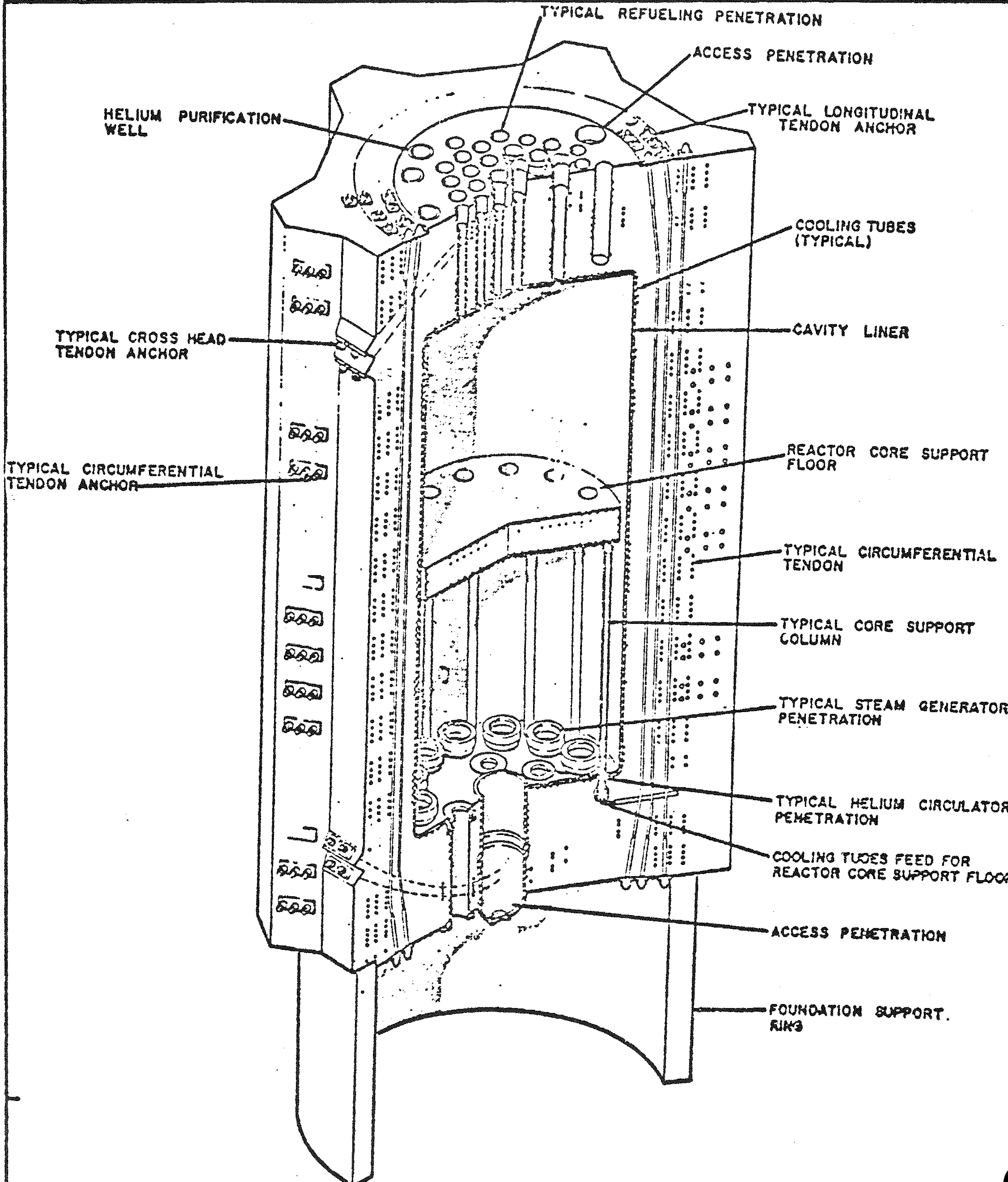

FIG. 1 - PCRV GENERAL ARRANGEMENT

Notations in this column indicate where changes have been made.

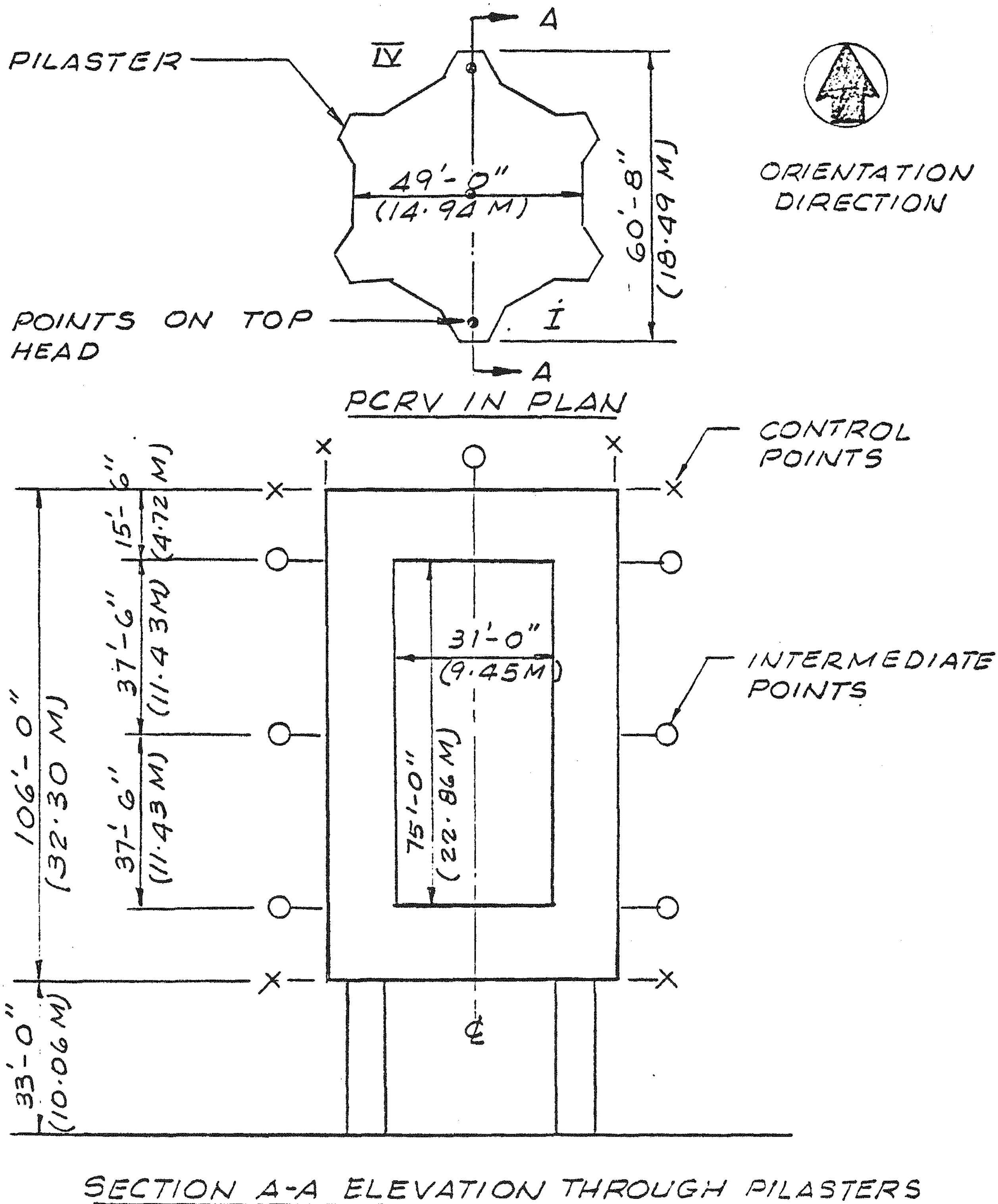

FIG. 2 LOCATION OF DEFLECTION POINTS

GA 317 (Rev 5/74) **GENERAL ATOMIC COMPANY**

SPECIFICATION FOR FORT ST. VRAIN PCRV DEFLECTION MEASURING SYSTEM

Proj. No. 3273	Spec. No. PA52-TS-004	Issue B	Date

Notations in this column indicate where changes have been made.

APPENDIX I - QUALITY ASSURANCE REQUIREMENTS

The following paragraphs comprise the quality requirements for GA Specification titled: Fort St. Vrain PCRV Deflection Measuring System.

1. Mandatory Hold Points

   Mandatory Hold Points are as a minimum:

   1. Start-Up Deflection Measurements
   2. Start-Up Deflection Measurements from Refueling

   Additional Hold Points may be established after review of the Seller's inspection and test plan. They require witnessing by the Buyer, or his designee. Work shall not proceed beyond a Mandatory Hold Point without the written agreement of the Buyer. Mandatory Hold Points require at least 24 hours notification.

2. Buyer drawings and specifications shall not be used to perform work unless the following Release Stamp appears on the document:

   4 RELEASED

   *Number herein is not significant to Seller.

3. Control of Measuring and Test Equipment

   Measuring devices used for test shall be calibrated to limits within specified tolerances for the measurements being made. Standards used for calibration shall have an uncertainty requirement of no more than one-tenth of the equipment being calibrated, unless limited by the state of the art, and shall be traceable to the National Bureau of Standards.

APPENDIX B

COMPUTER PLOTS OF REPRESENTATIVE
PCRV SENSOR DATA

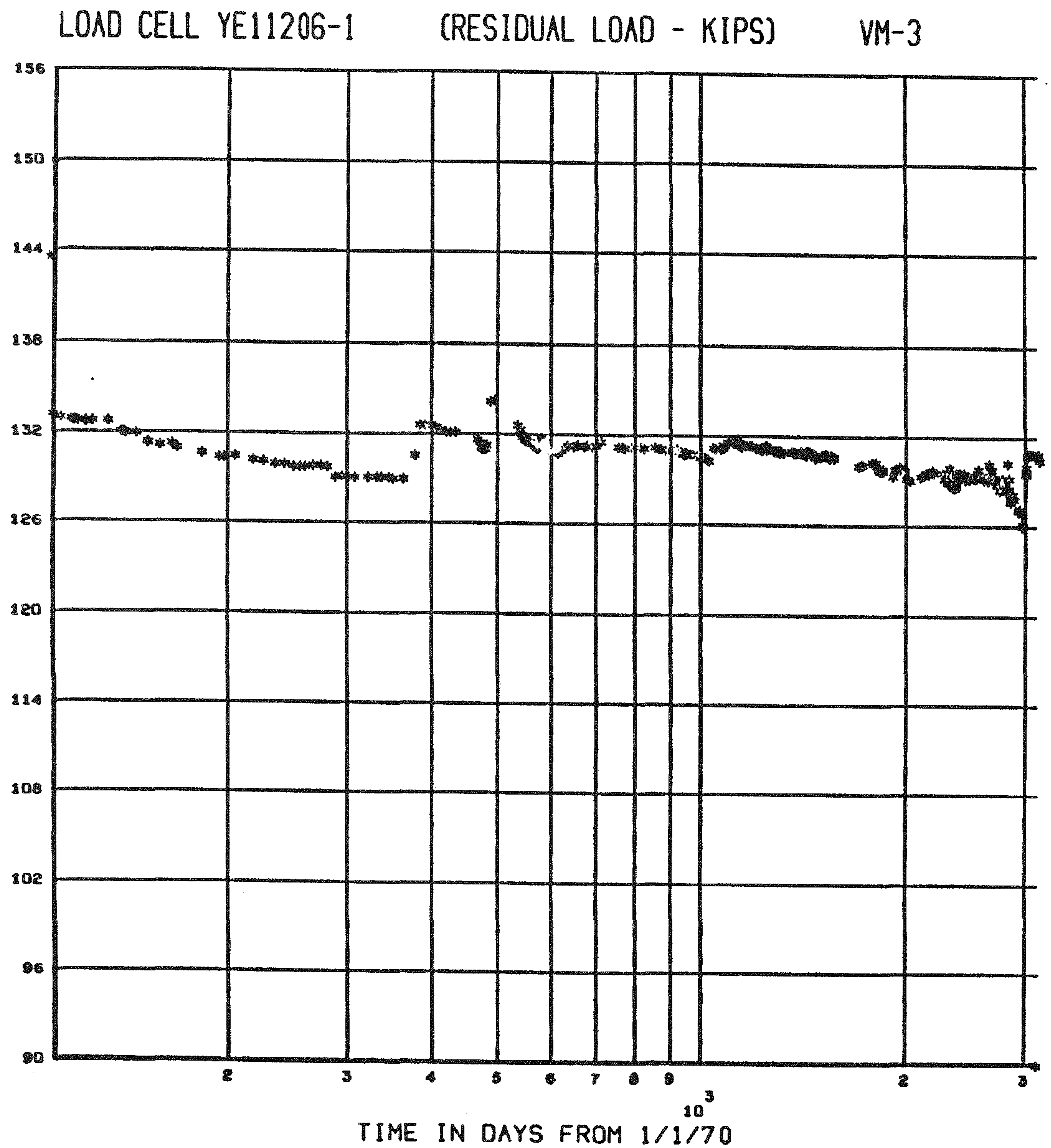

RUN 10742 29 AUG 78 12.18.59

LOAD CELL YE11206-2 (RESIDUAL LOAD - KIPS) VI-10

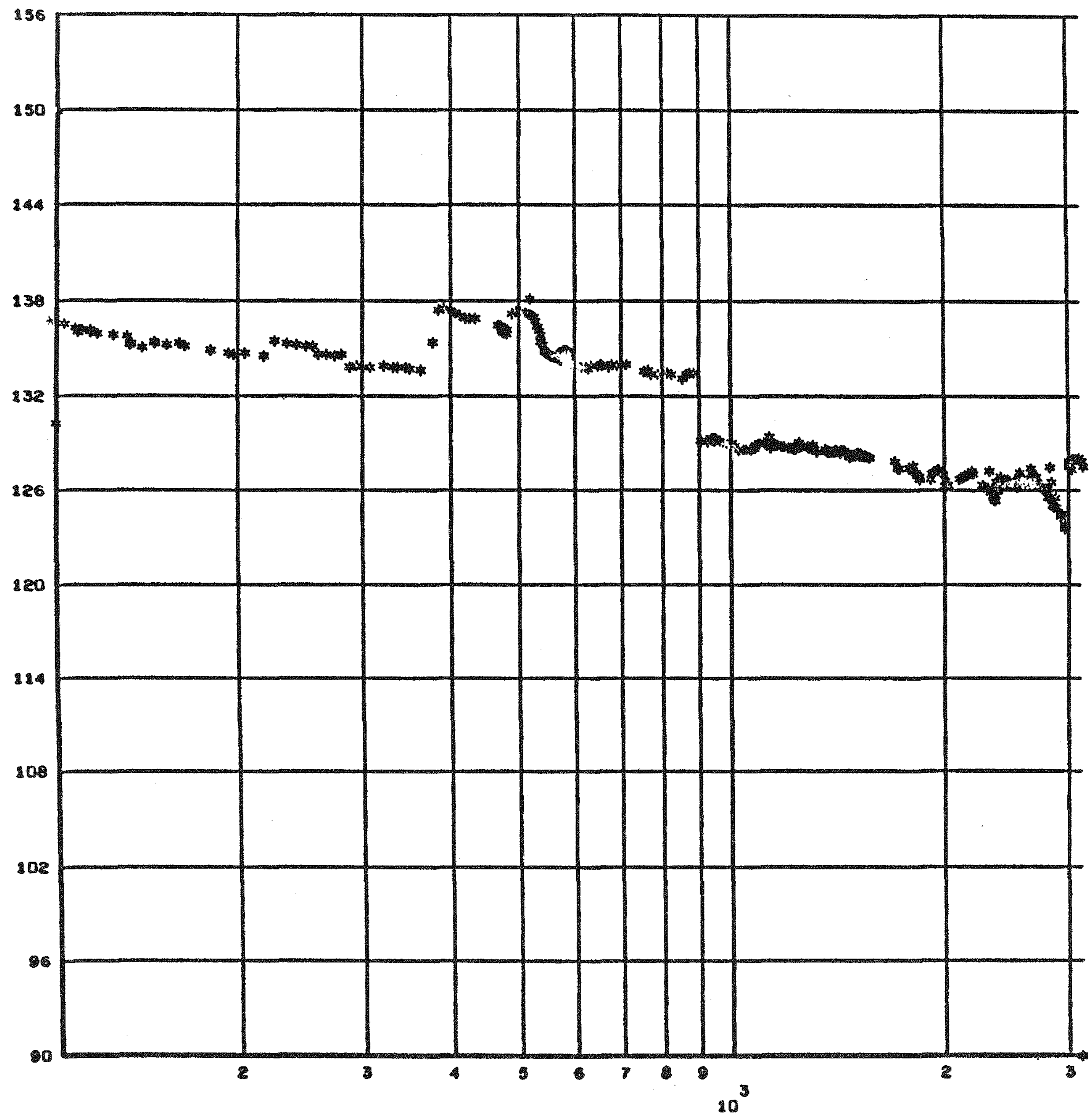

RUN 10742 29 AUG 78 12.19.01

LOAD CELL YE11206-3 (RESIDUAL LOAD - KIPS) VM-17

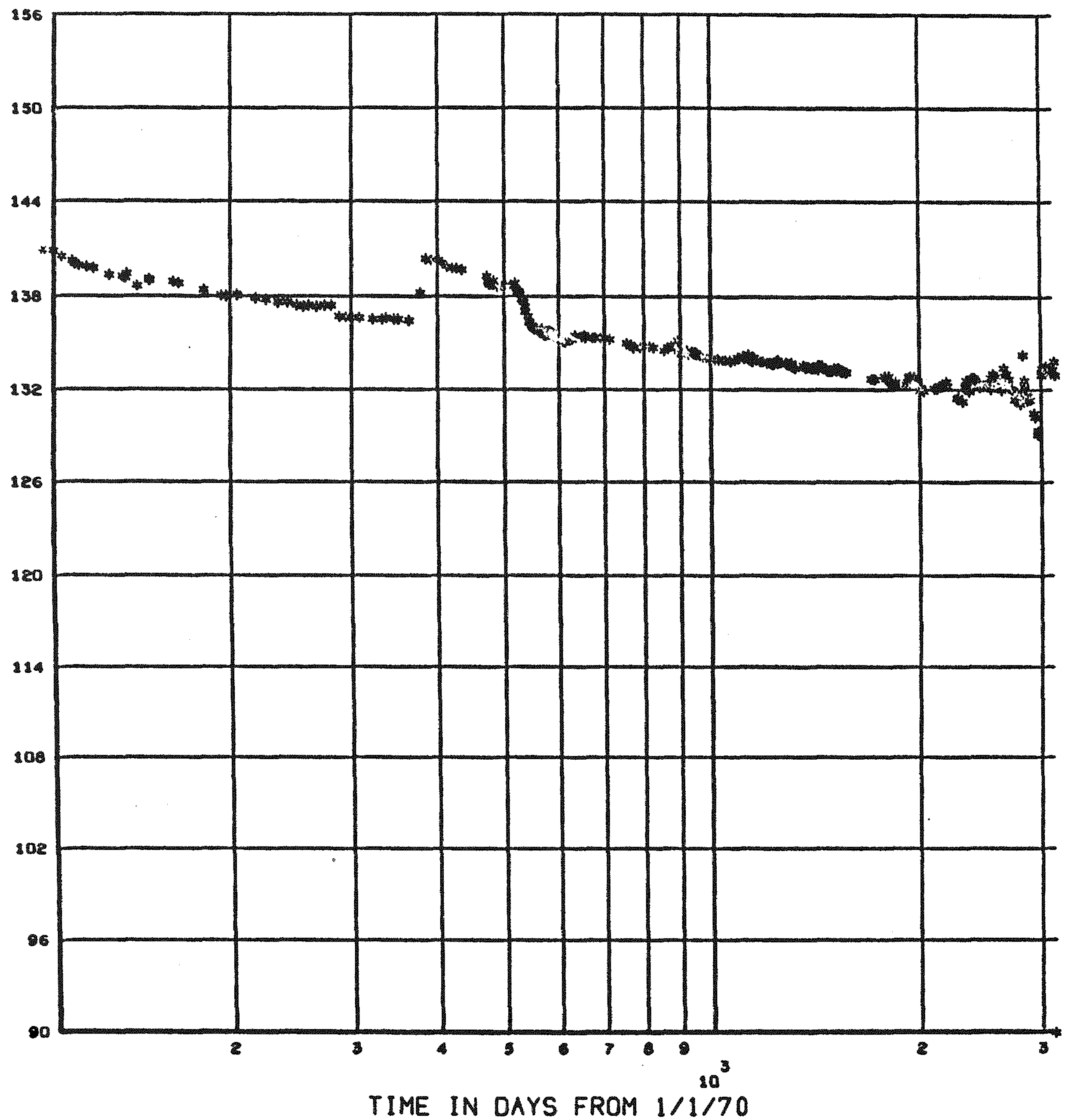

RUN 10742 29 AUG 78 12.19.04

B-3

802

...10

LOAD CELL YE11206-4 (RESIDUAL LOAD - KIPS) VI-24

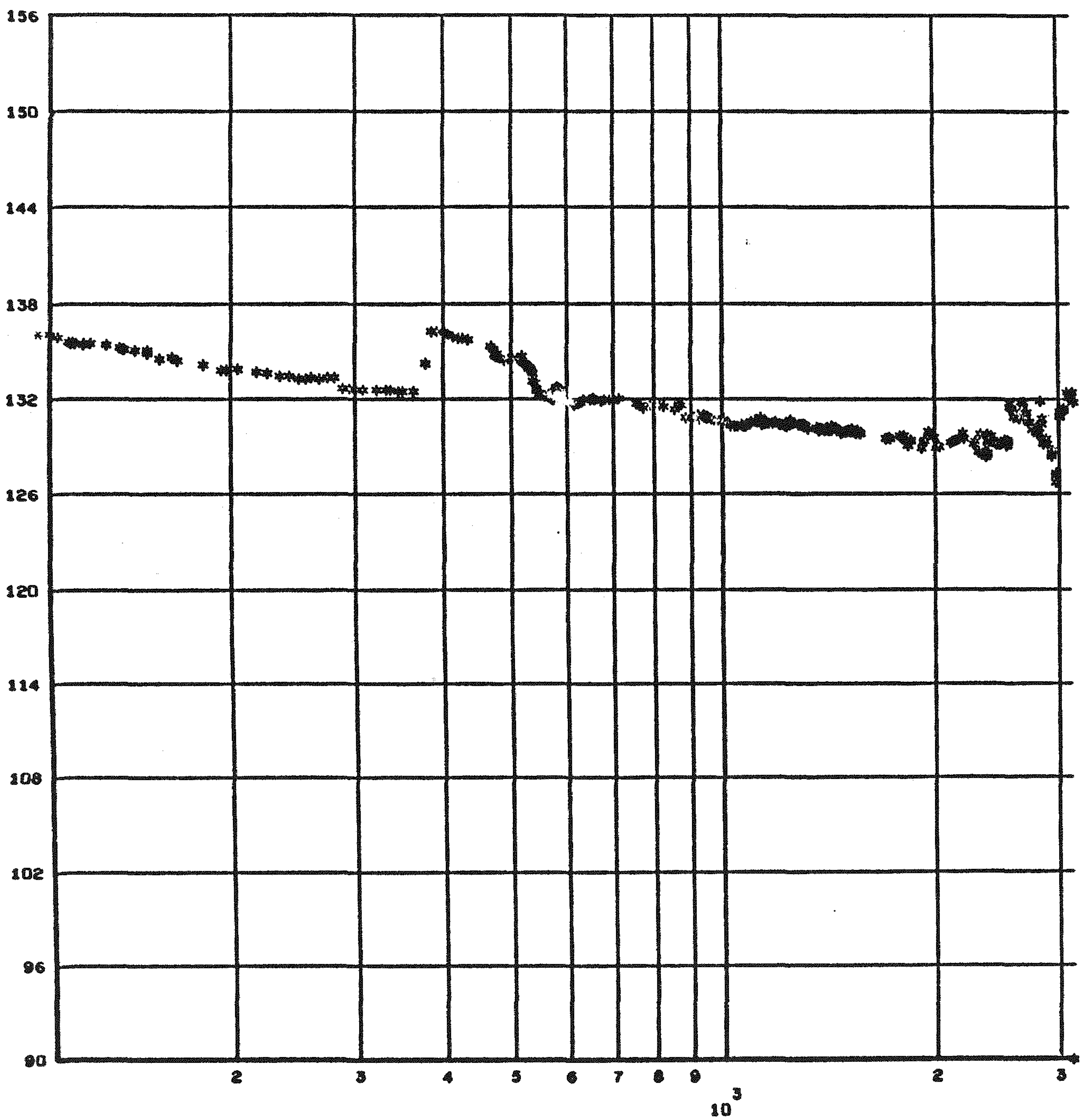

RUN 10742 29 AUG 78 12.19.07

B-4

...10

803

LOAD CELL YE11206-5 (RESIDUAL LOAD - KIPS) VM-31

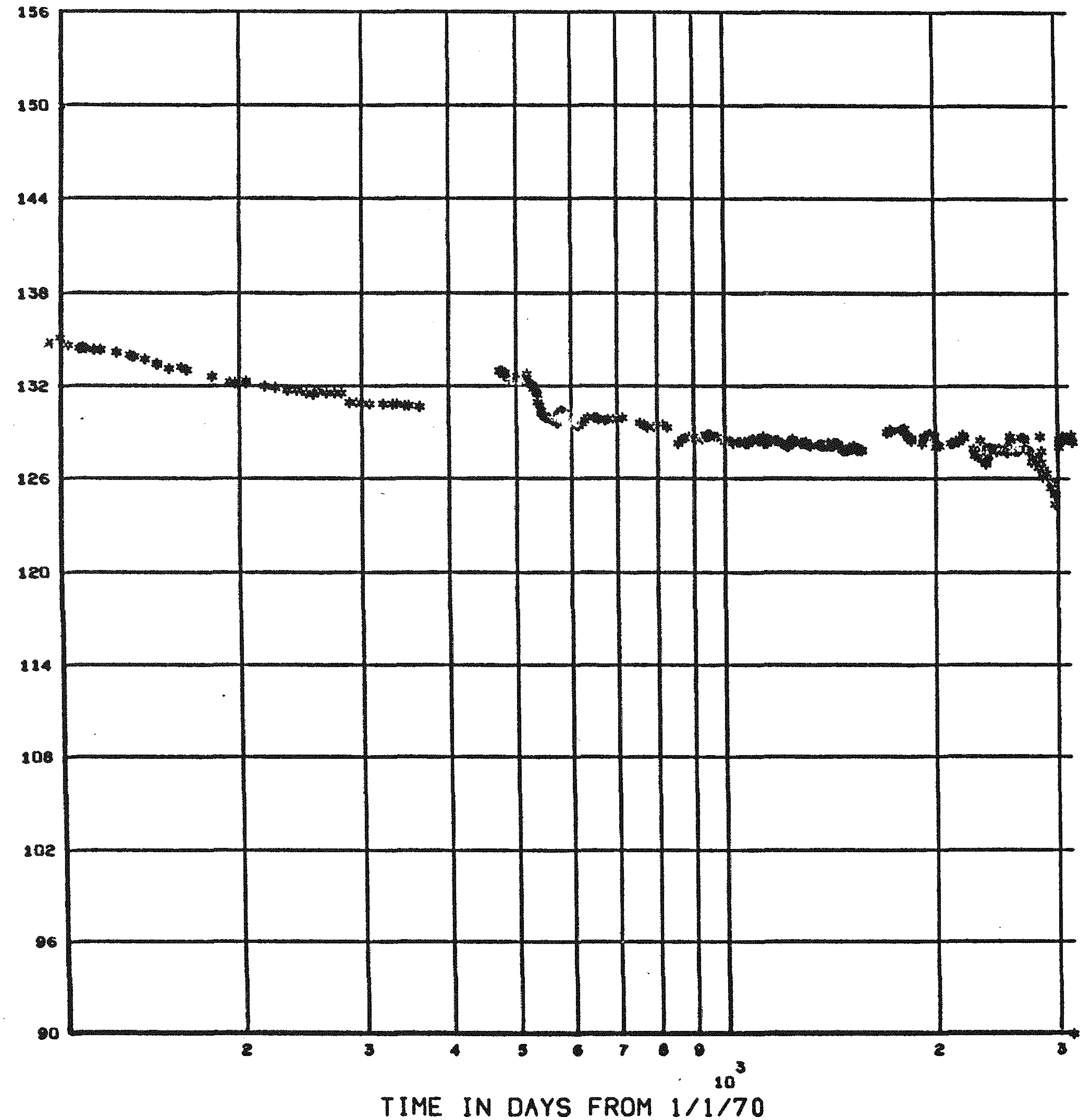

RUN 10742 29 AUG 78 12.19.10

B-5

804

LOAD CELL YE11206-6 (RESIDUAL LOAD - KIPS) VI-38

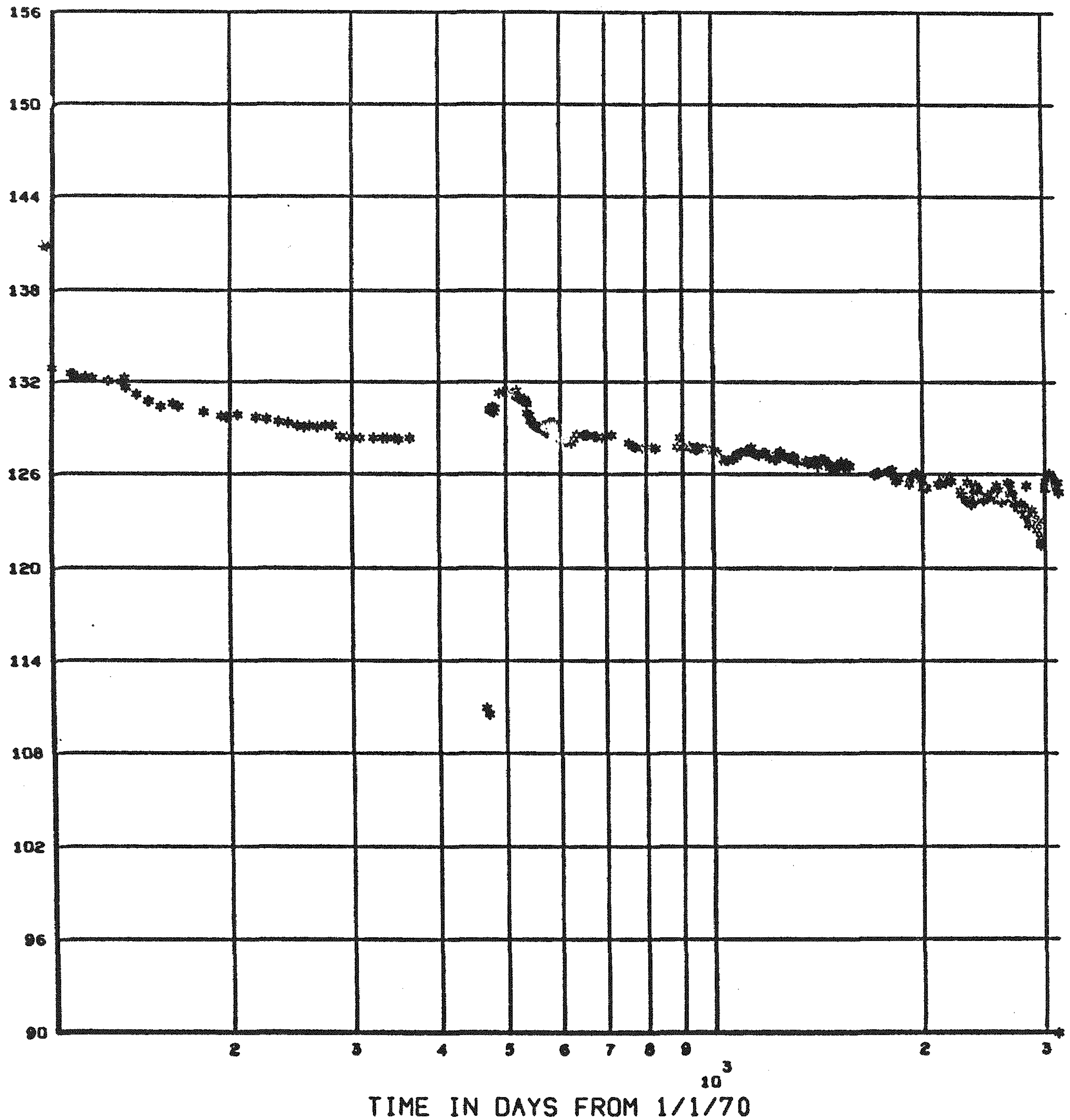

RUN 10742 29 AUG 78 12.19.13

805

LOAD CELL YE11206-7 (RESIDUAL LOAD - KIPS) TOR-U2

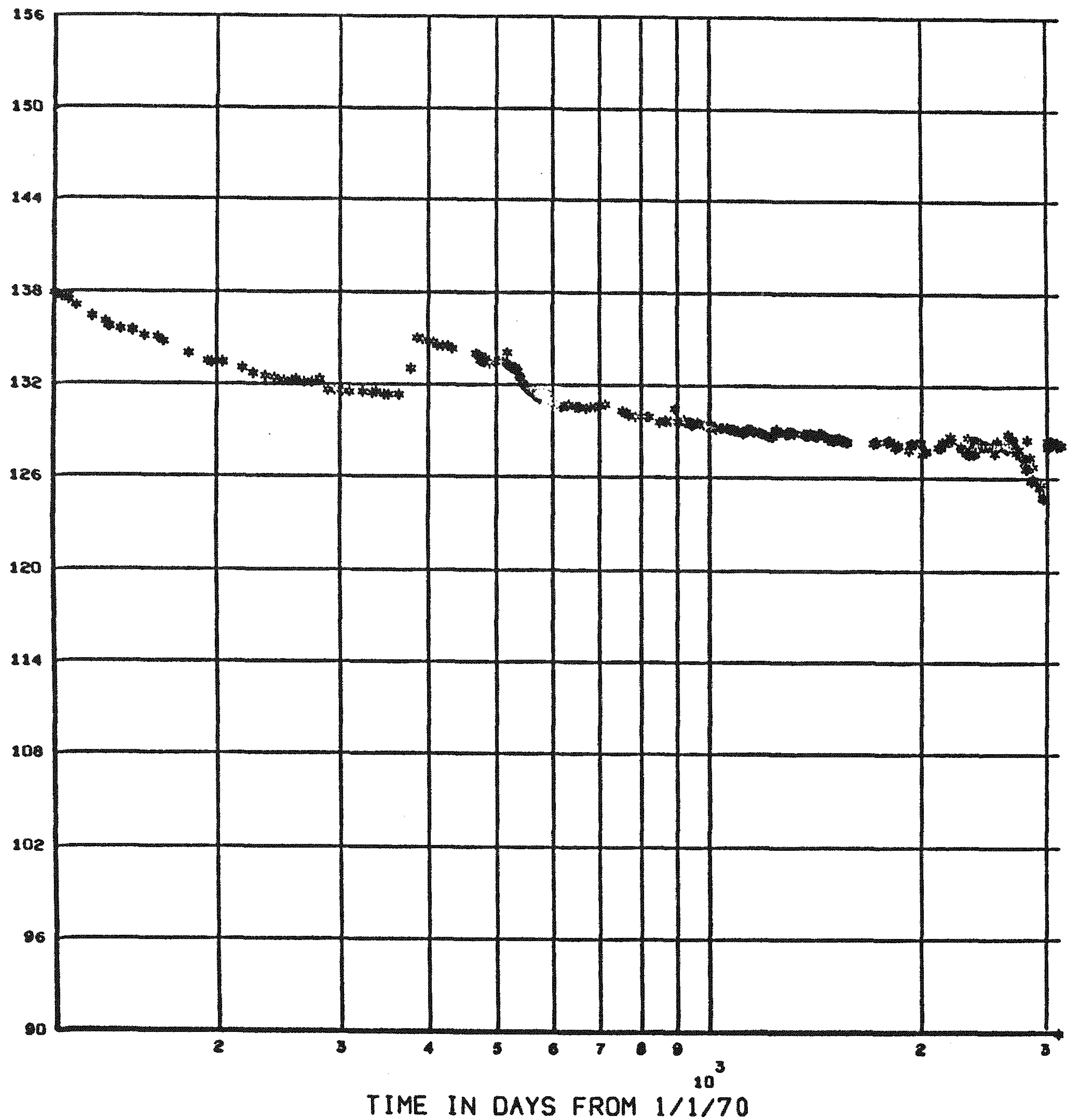

RUN 10742 29 AUG 78 12.19.15

LOAD CELL YE11206-8 (RESIDUAL LOAD - KIPS) TIR-M1

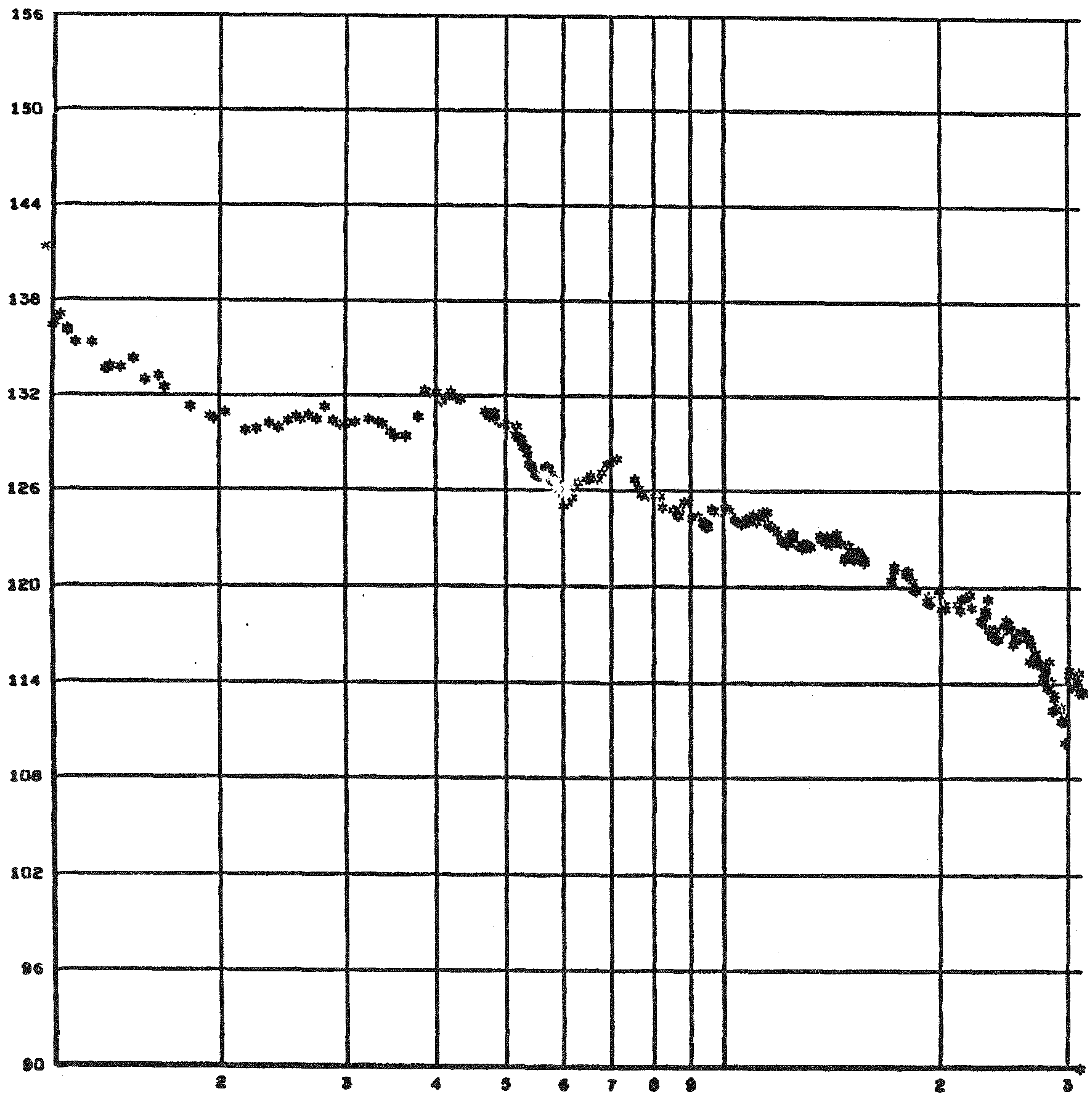

TIME IN DAYS FROM 1/1/70

RUN 10742 29 AUG 78 12.19.18

807

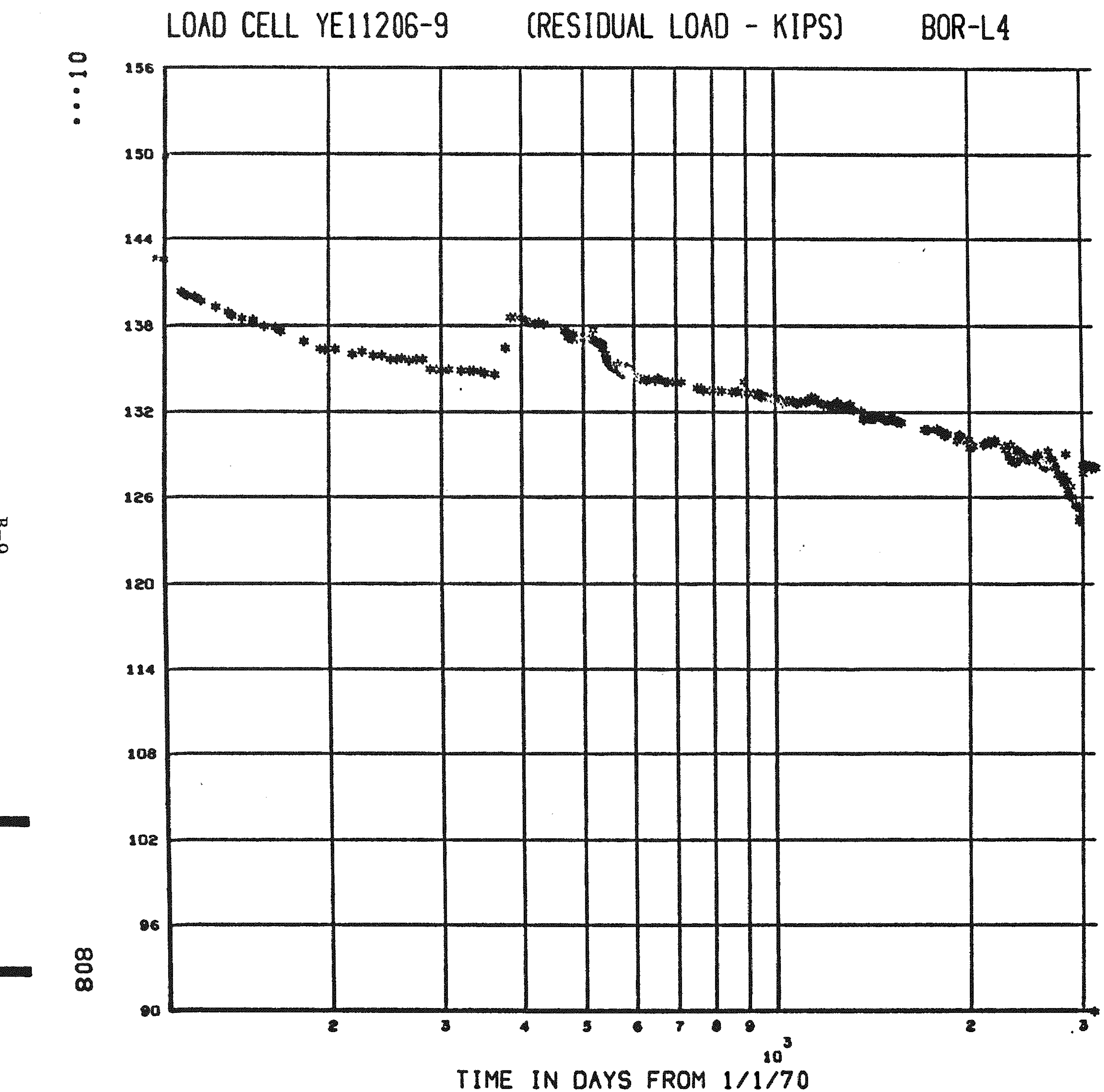

RUN 10742 29 AUG 78 12.19.20

LOAD CELL YE11206-10 (RESIDUAL LOAD - KIPS) BIR-M4

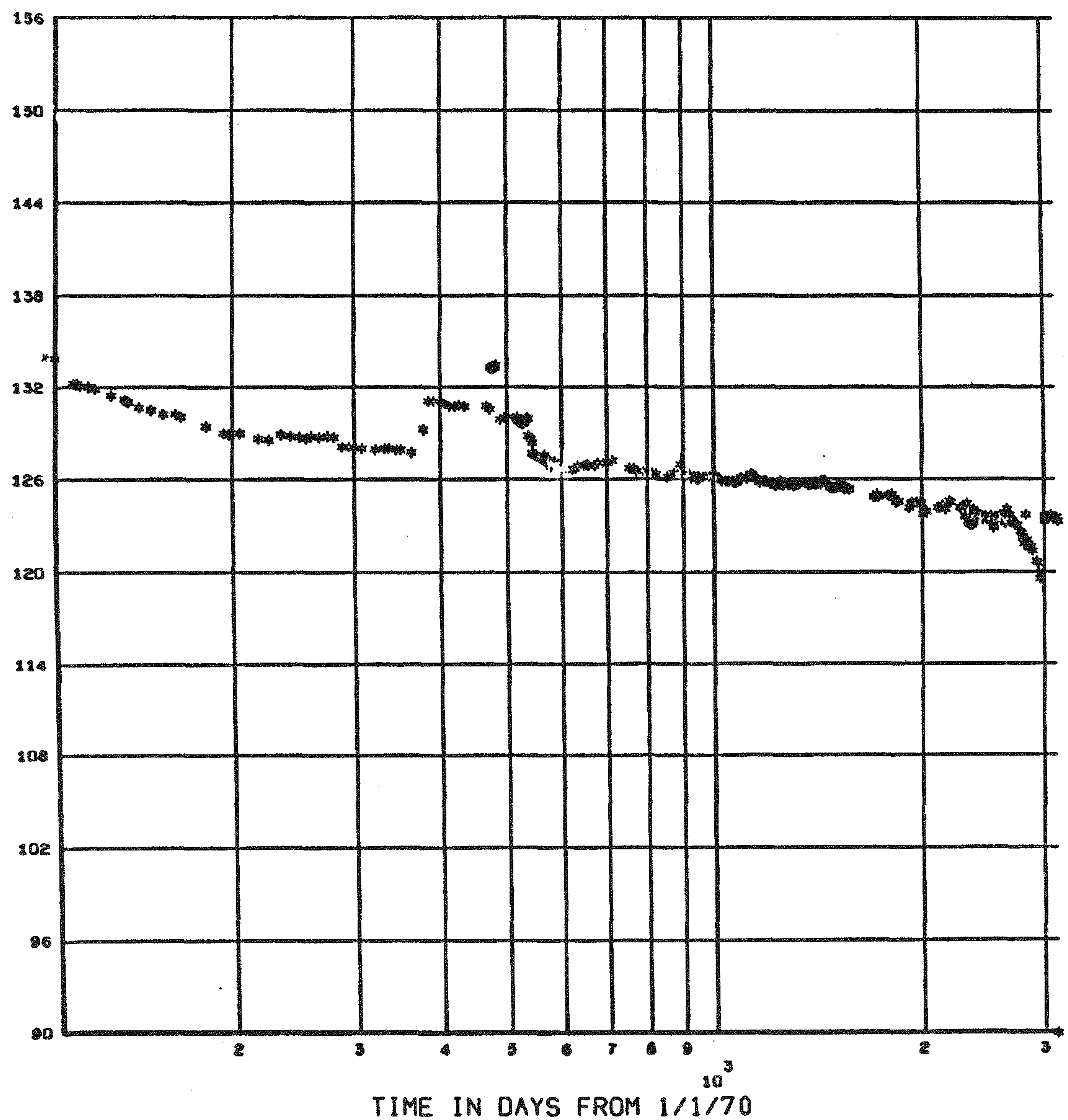

10742 29 AUG 78 12.19.23

LOAD CELL YE11206-11 (RESIDUAL LOAD - KIPS) CO-1.6

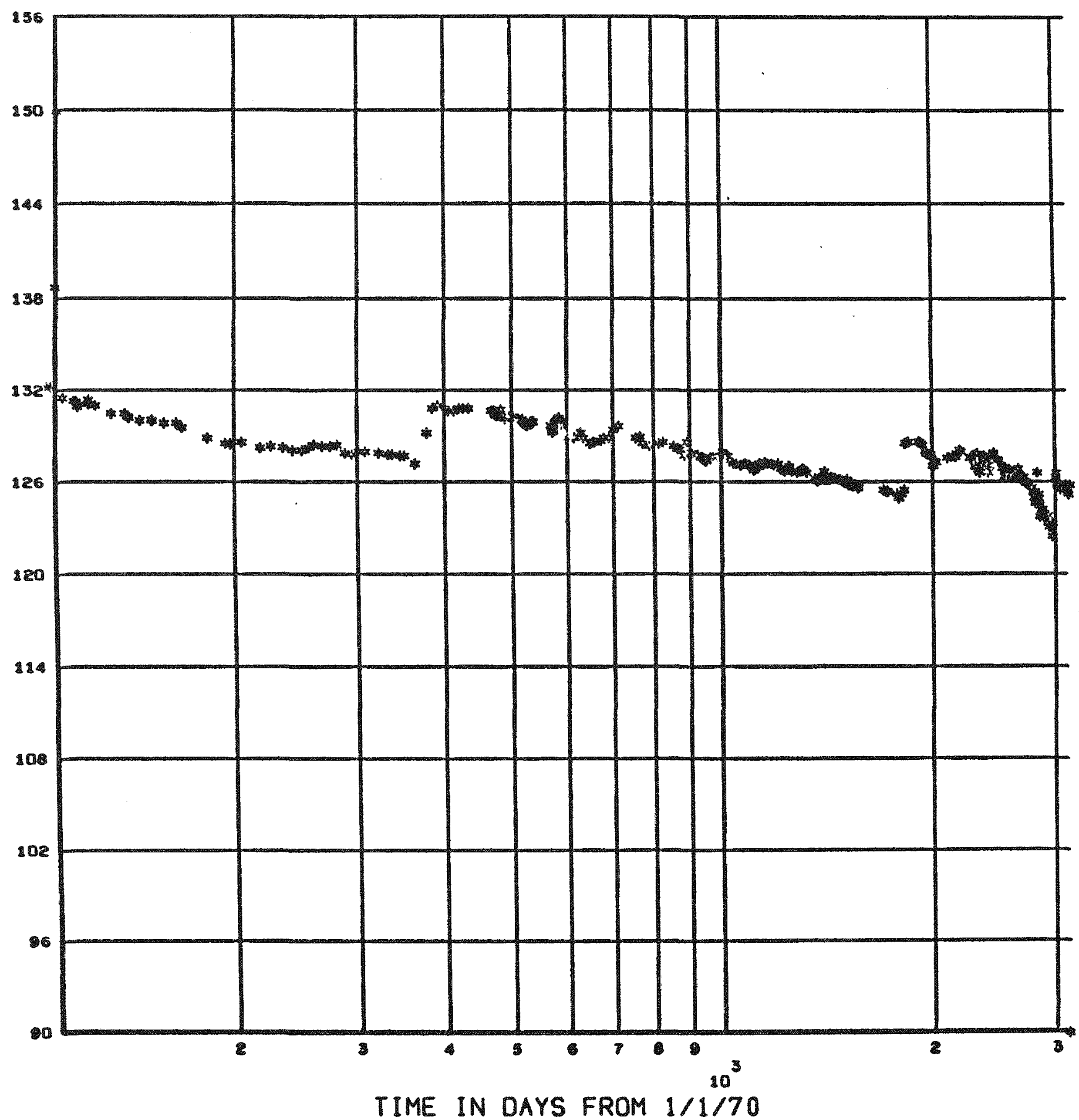

B-11

RUN 10742 29 AUG 78 12.19.25

010...

810

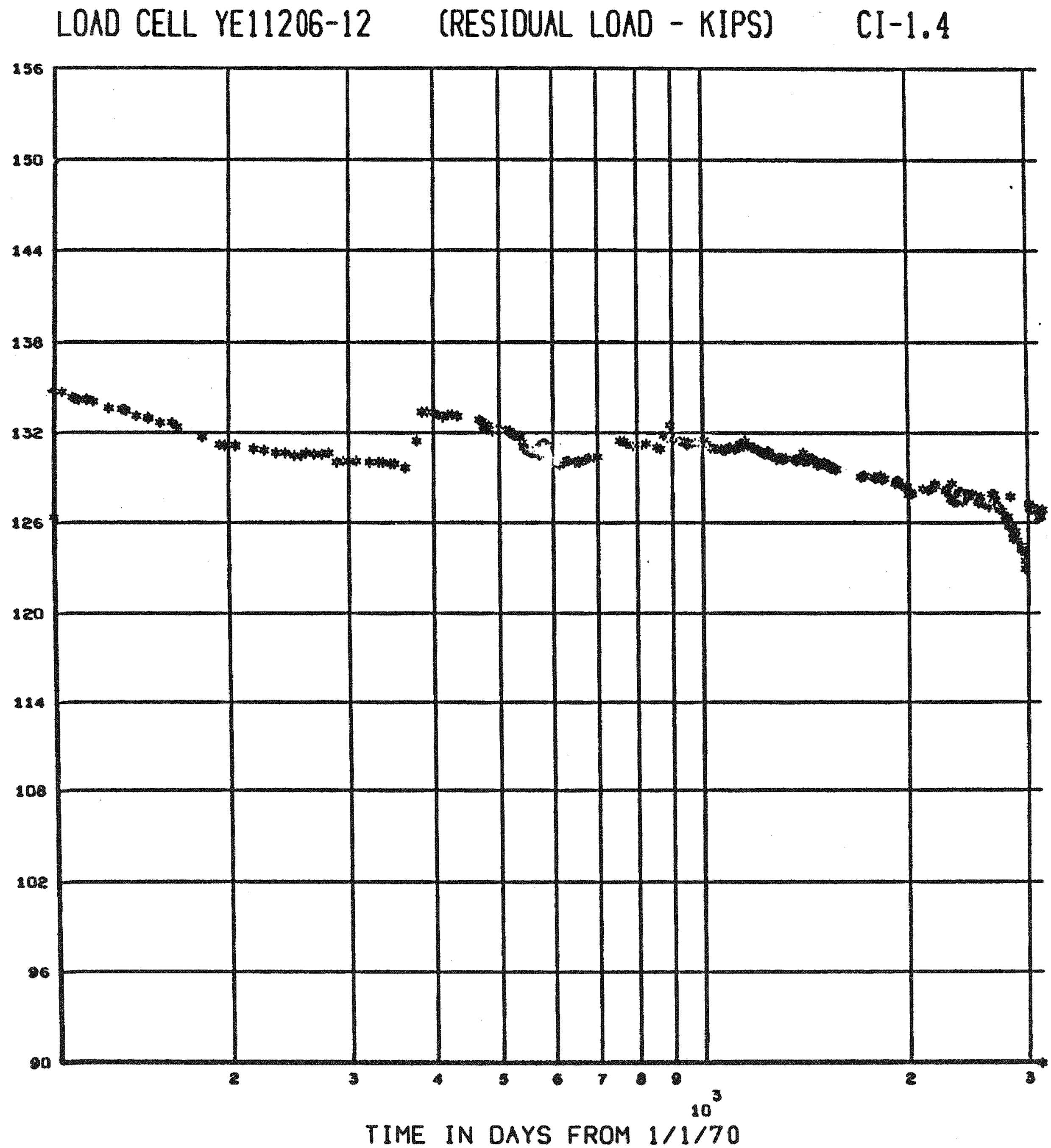

RUN 10742 29 AUG 78 12.19.28

B-12

...10

LOAD CELL YE11206-13 (RESIDUAL LOAD - KIPS) CO-2.2

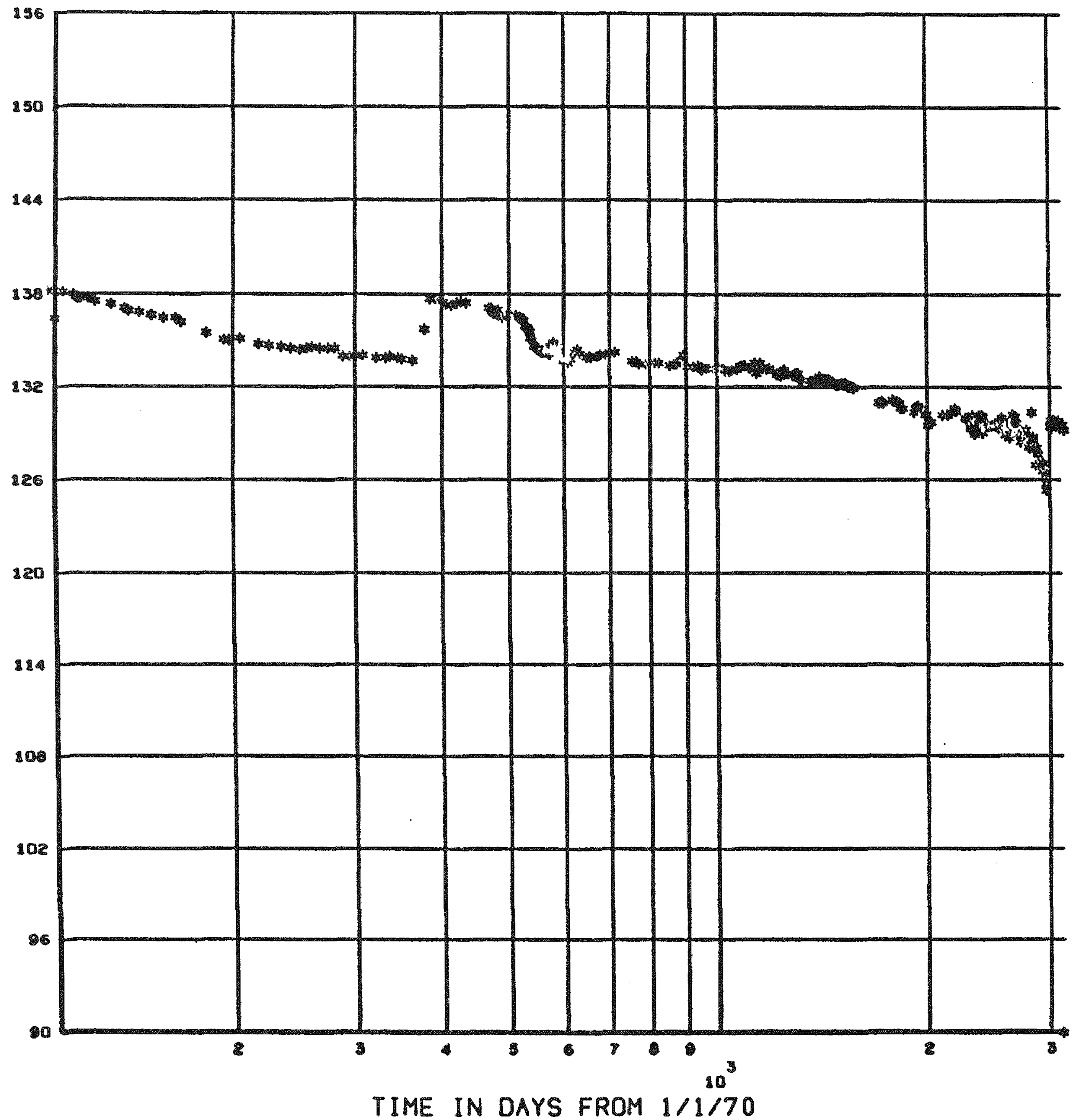

RUN 10742 29 AUG 78 12.21.31

812

LOAD CELL YE11206-14 (RESIDUAL LOAD - KIPS) CO-2.1

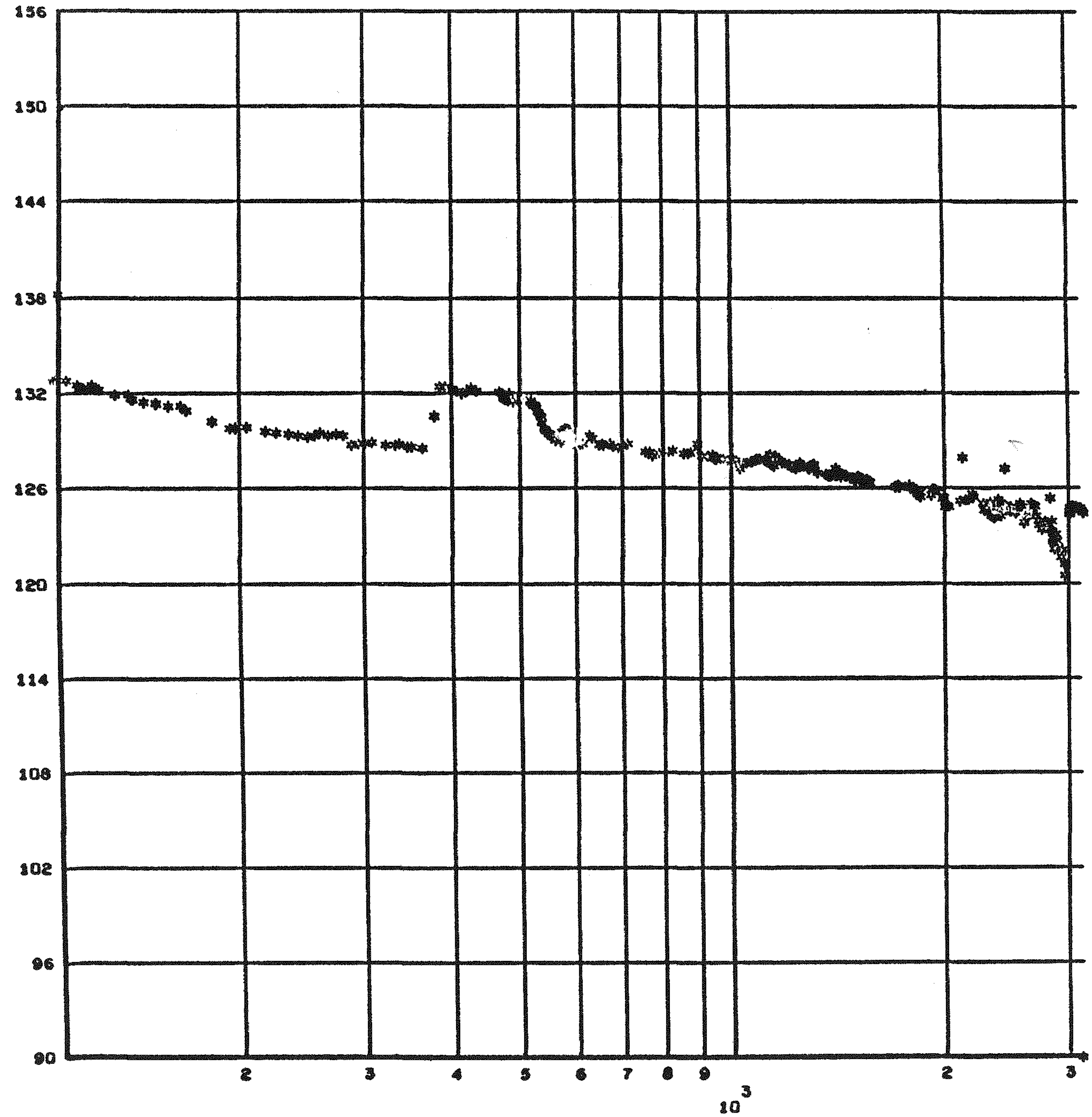

RUN 10742 29 AUG 78 12.21.33

...10

B-14

813

LOAD CELL YE11206-15 (RESIDUAL LOAD - KIPS) CO-3.2

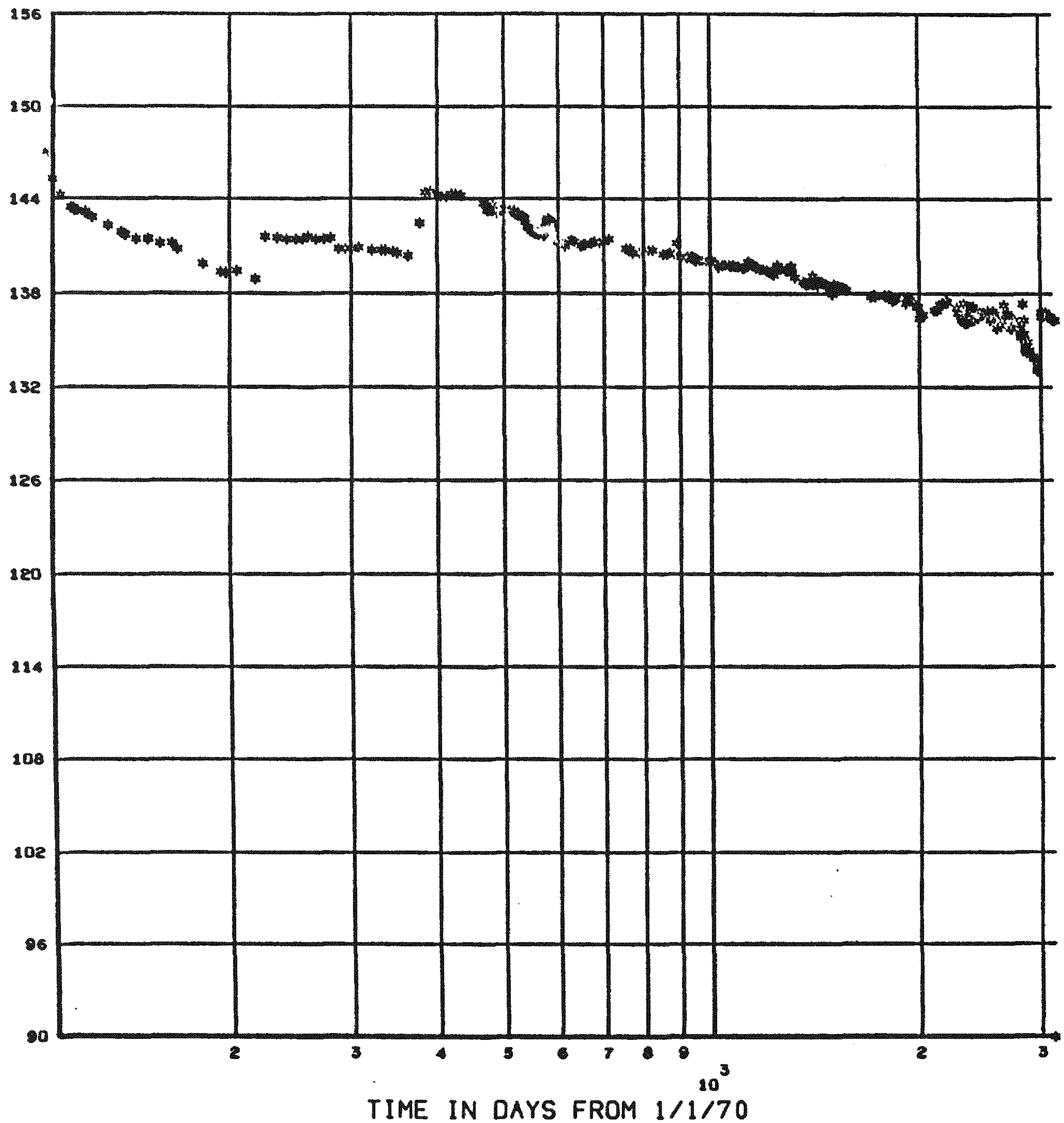

RUN 10742 29 AUG 78 12.21.35

814

LOAD CELL YE11206-16 (RESIDUAL LOAD - KIPS) CO-3.1

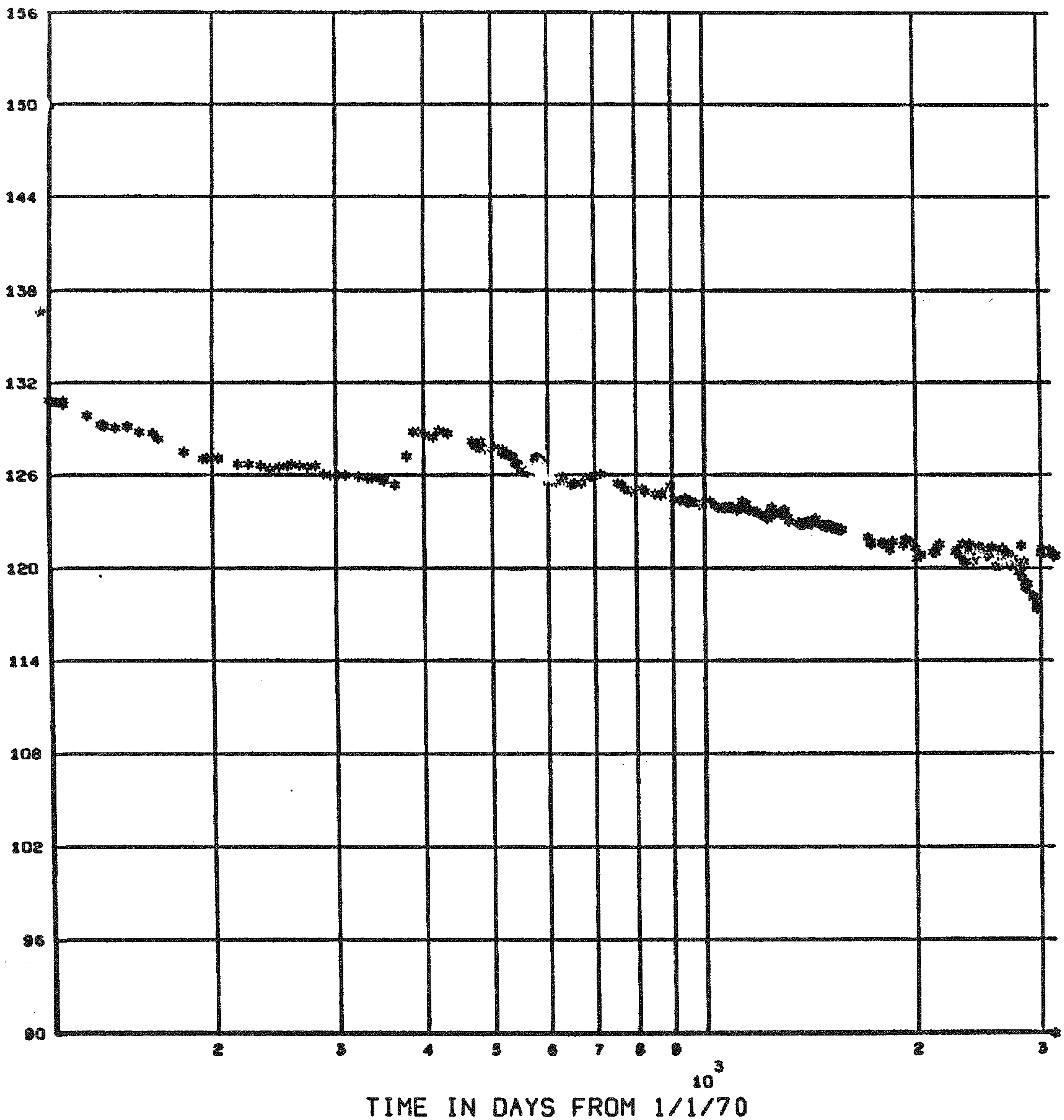

RUN 10742 29 AUG 78 12.21.37

815

LOAD CELL YE11206-17 (RESIDUAL LOAD - KIPS) CI-7.4

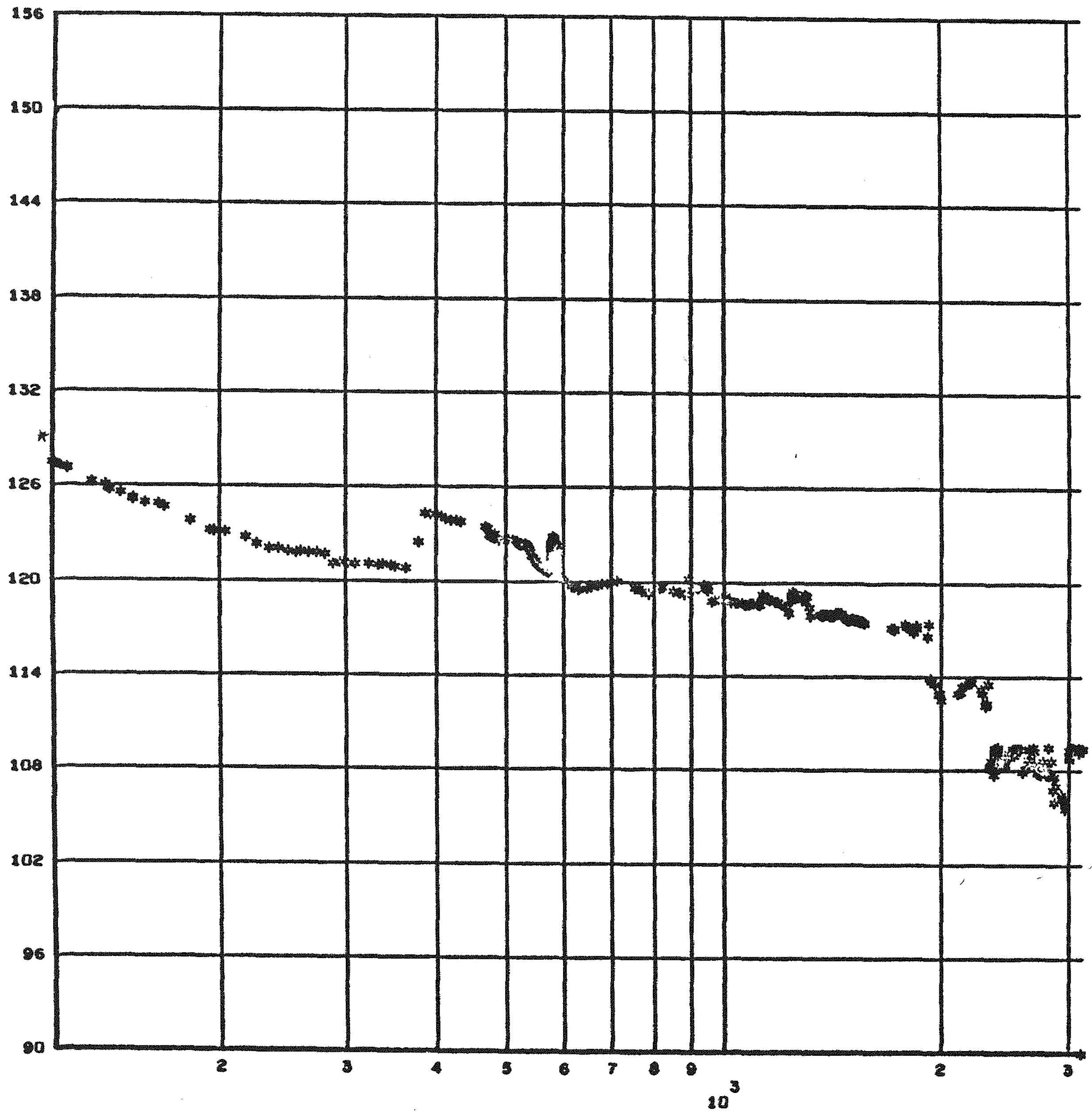

RUN 10742 29 AUG 78 12.21.39

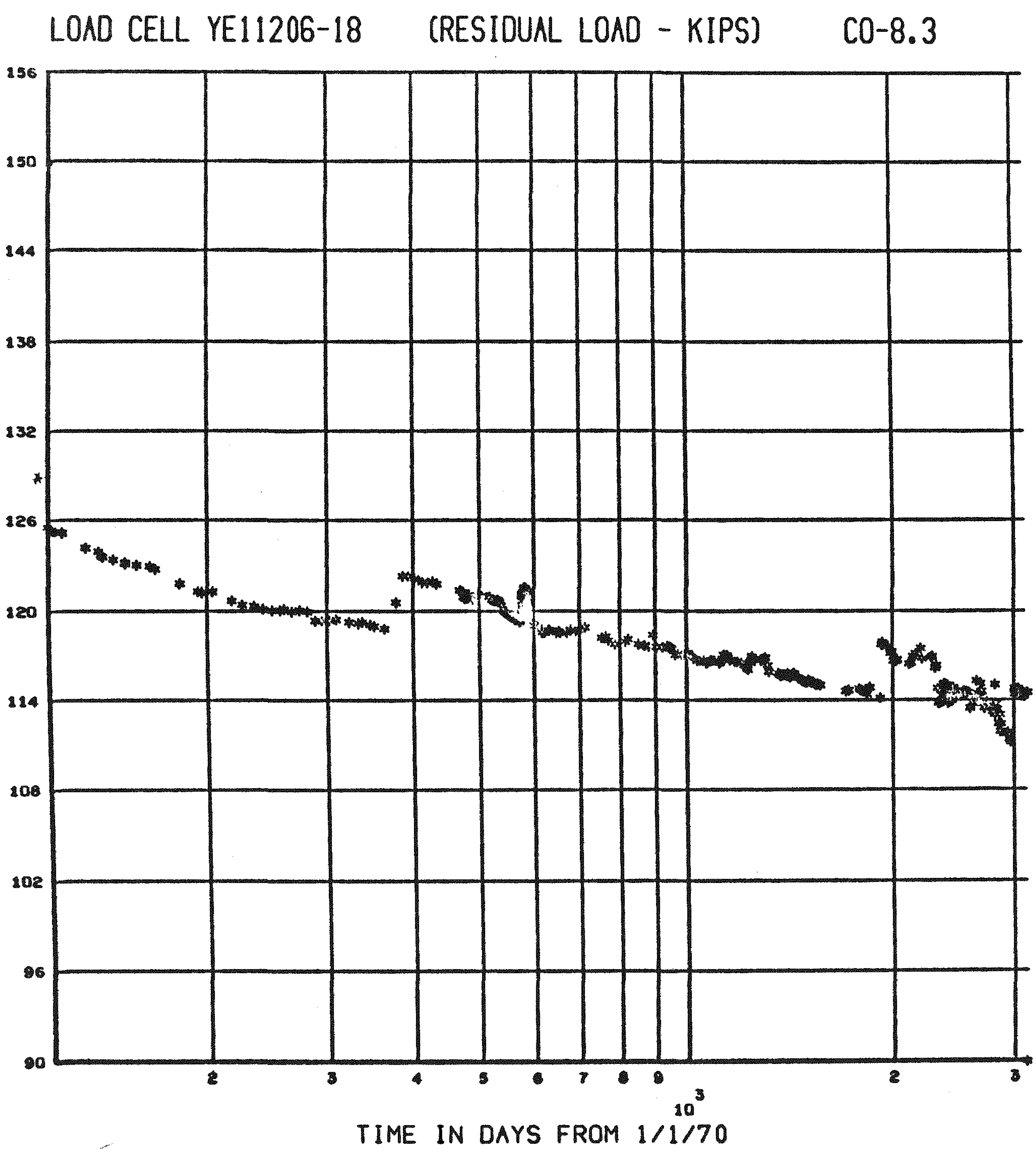

RU..D742 29 AUG 78 12.21.42

B-18

817

...10

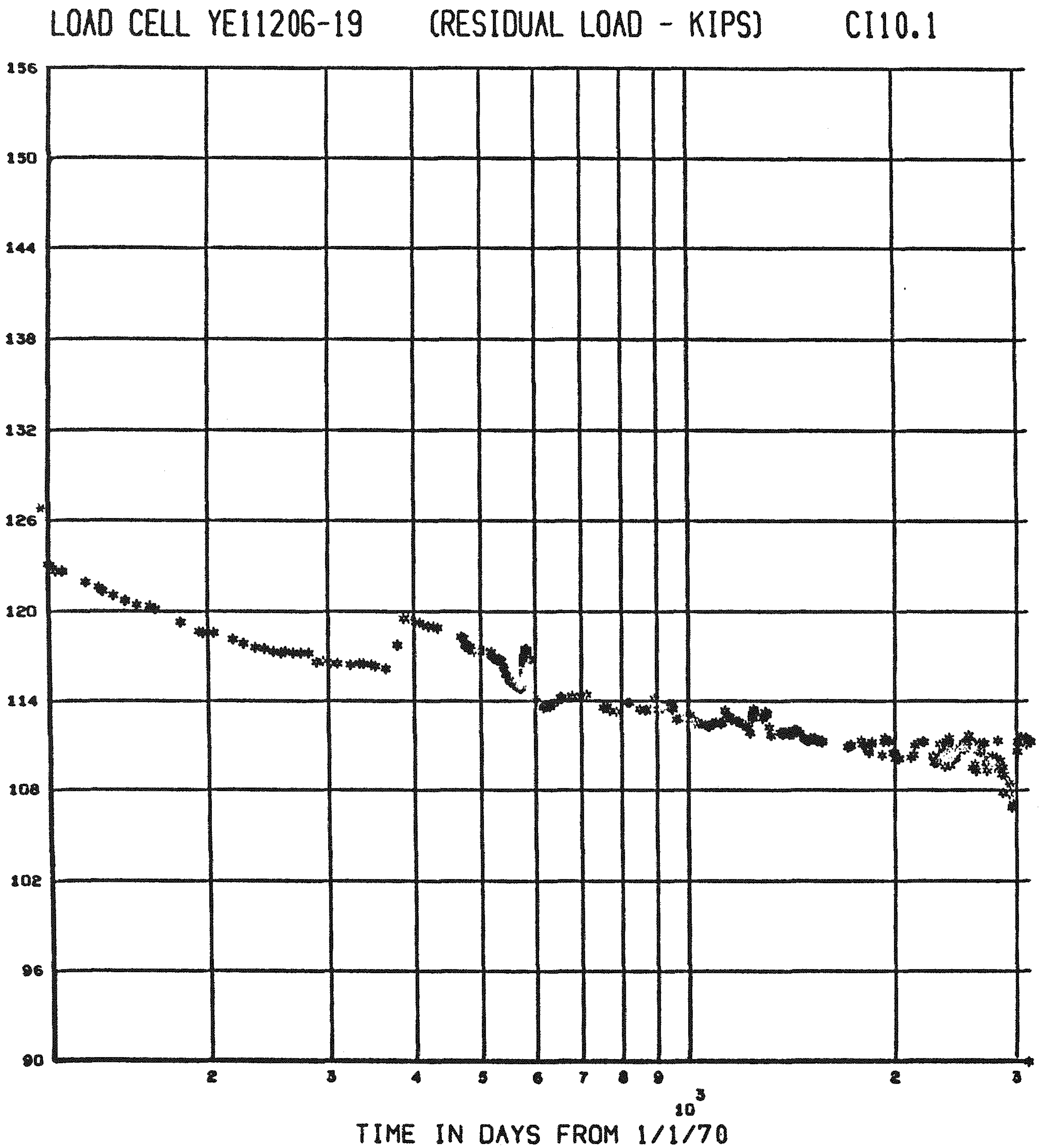

RUN 10742 29 AUG 78 12.21.44

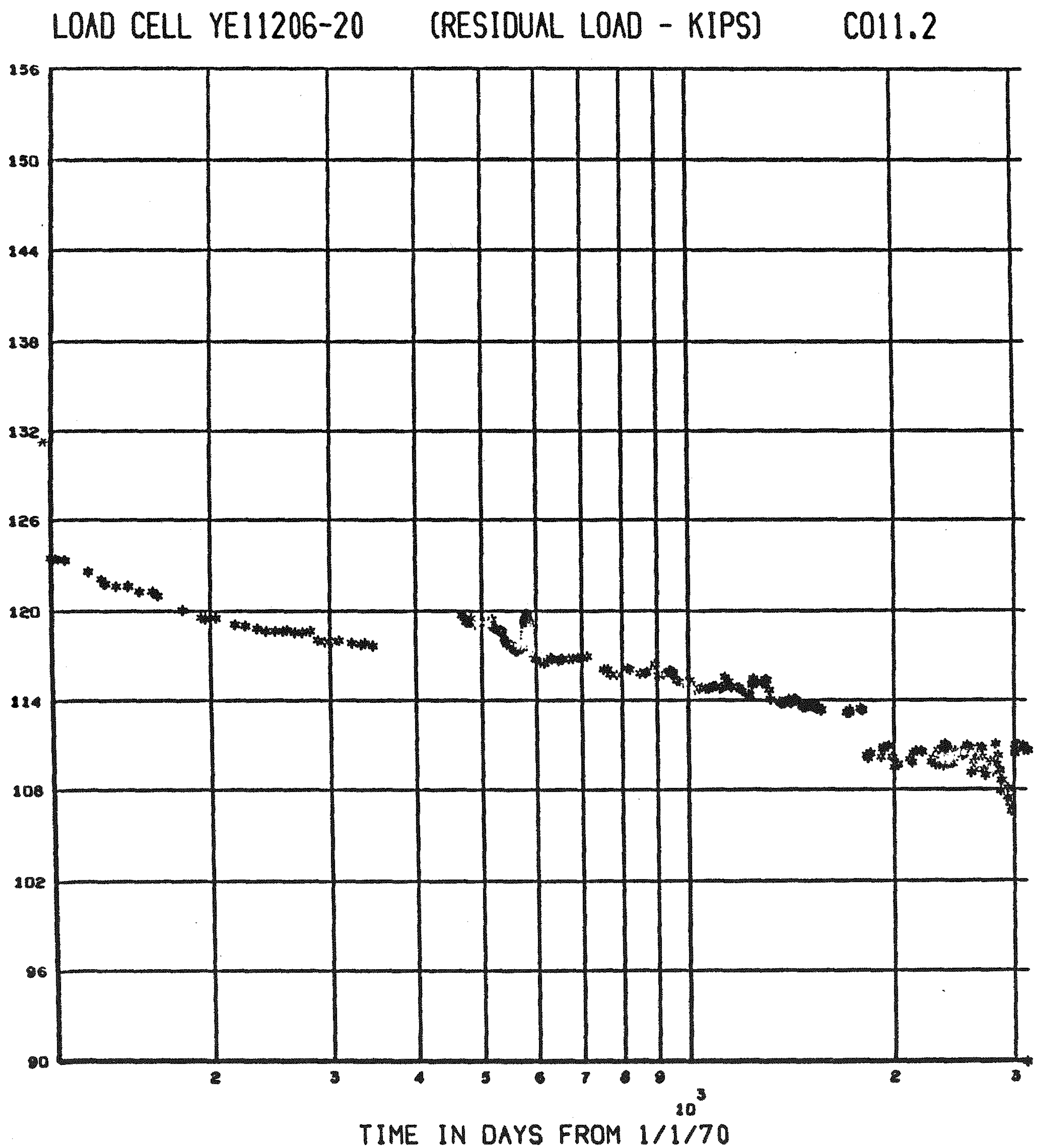

RUN 10742 29 AUG 78 12.21.47

B-20

819

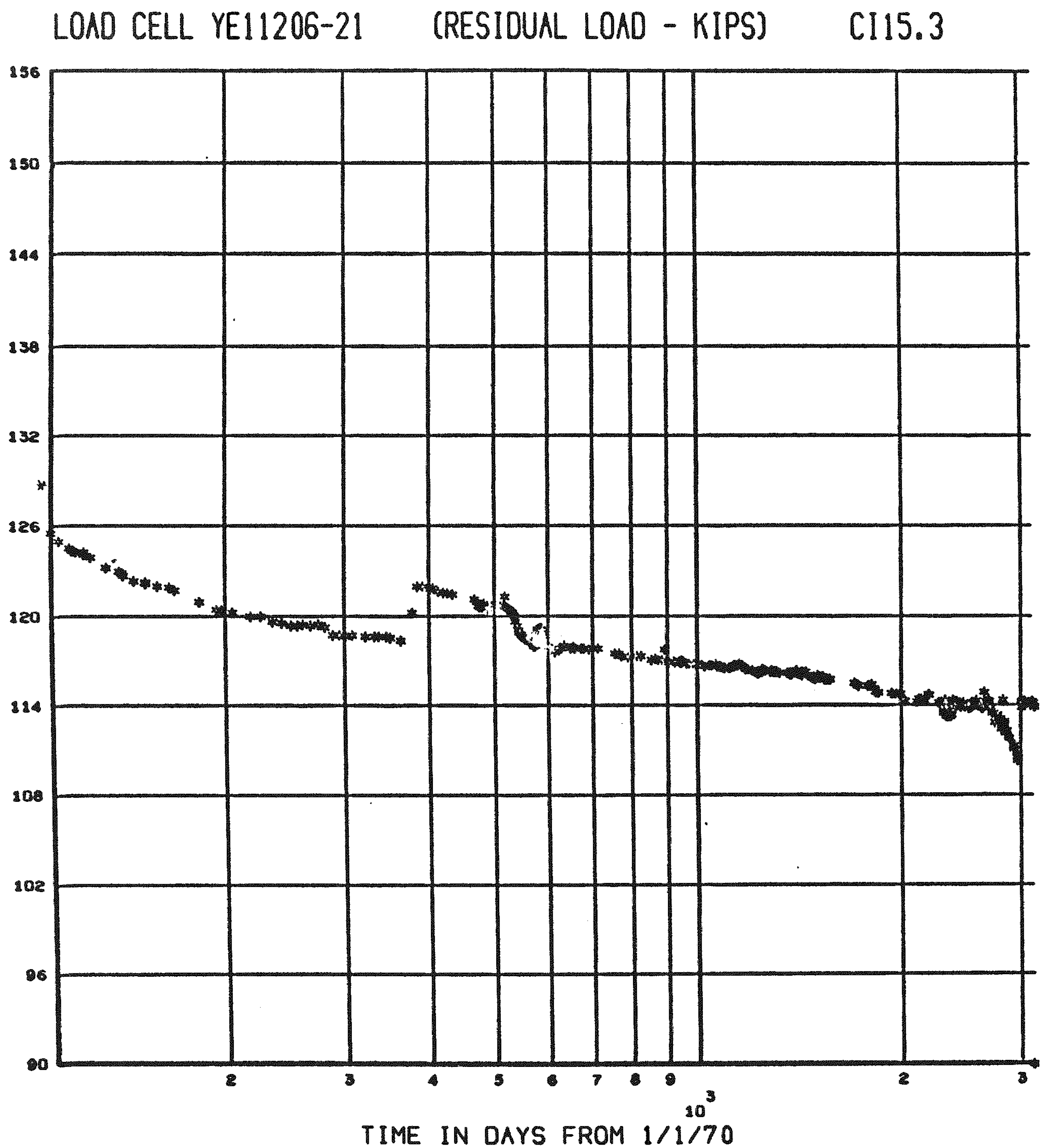

RUN 10742 29 AUG 78 12.21.49

B-21

...10

820

LOAD CELL YE11206-22 (RESIDUAL LOAD - KIPS) C017.6

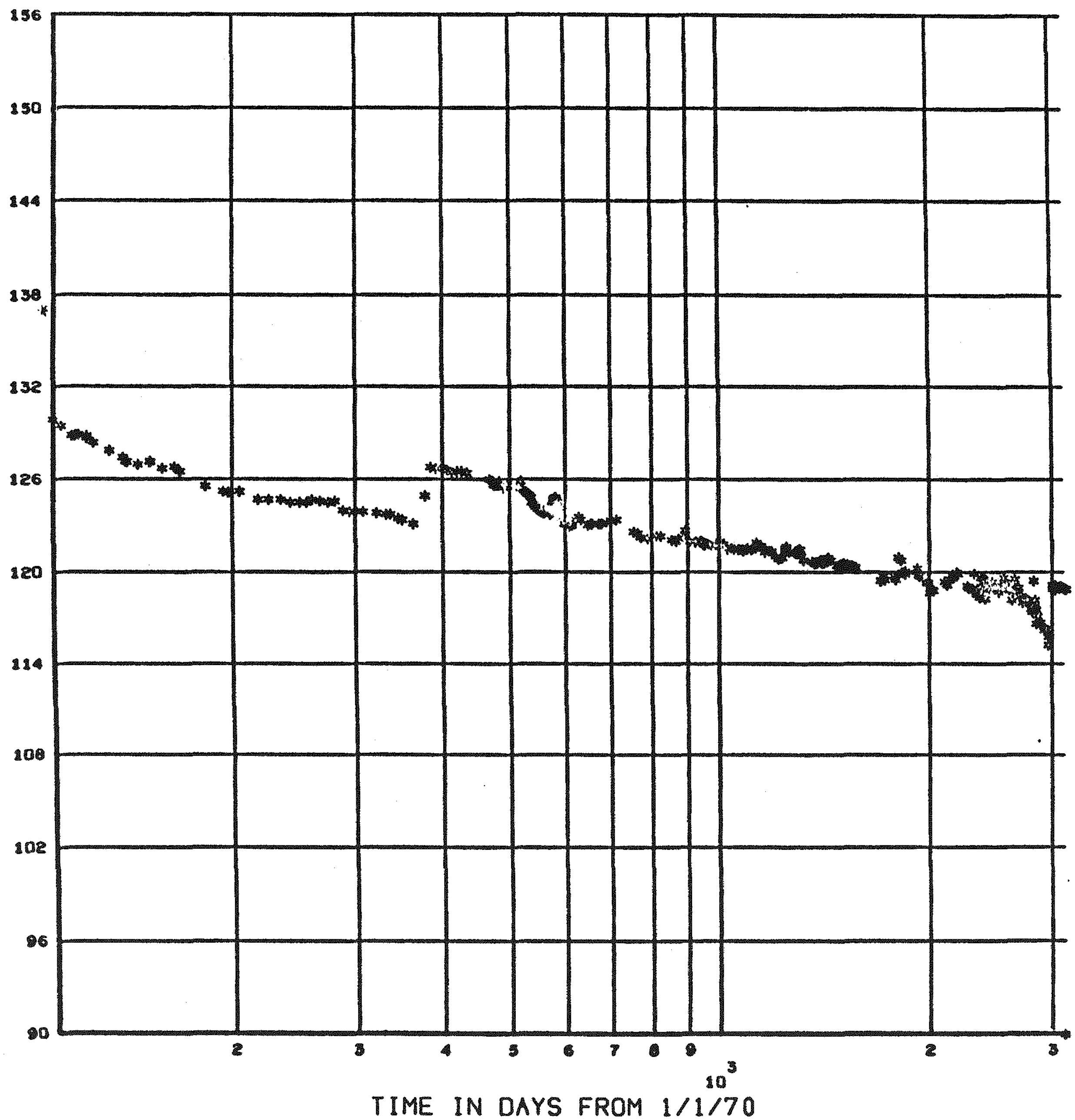

RUN 10742 29 AUG 78 12.21.52

...10

B-22

821

LOAD CELL YE11206-23 (RESIDUAL LOAD - KIPS) C017.5

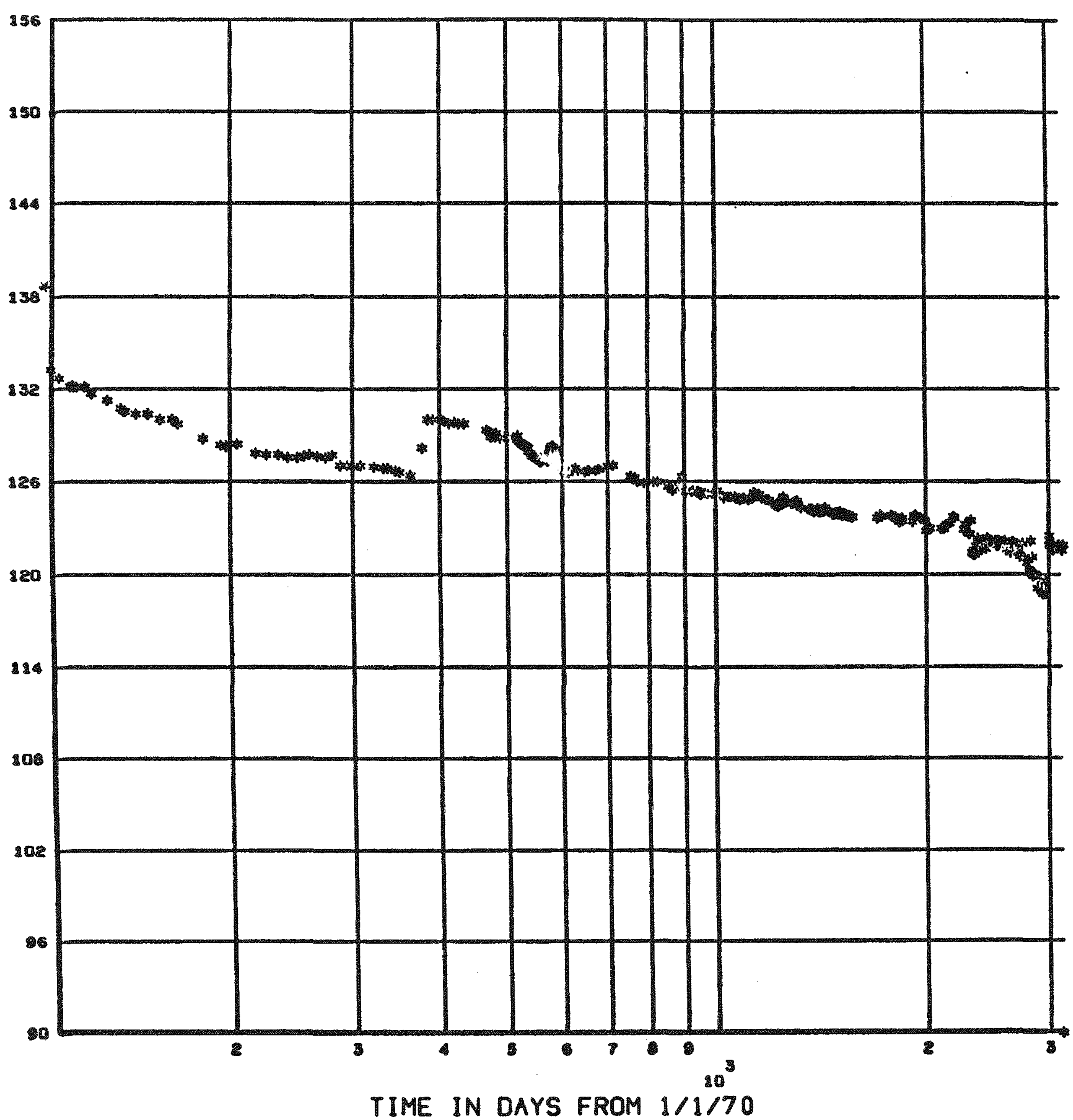

RUN 10742 29 AUG 78 12.21.54

B-23

822

LOAD CELL YE11206-24 (RESIDUAL LOAD - KIPS) C017.4

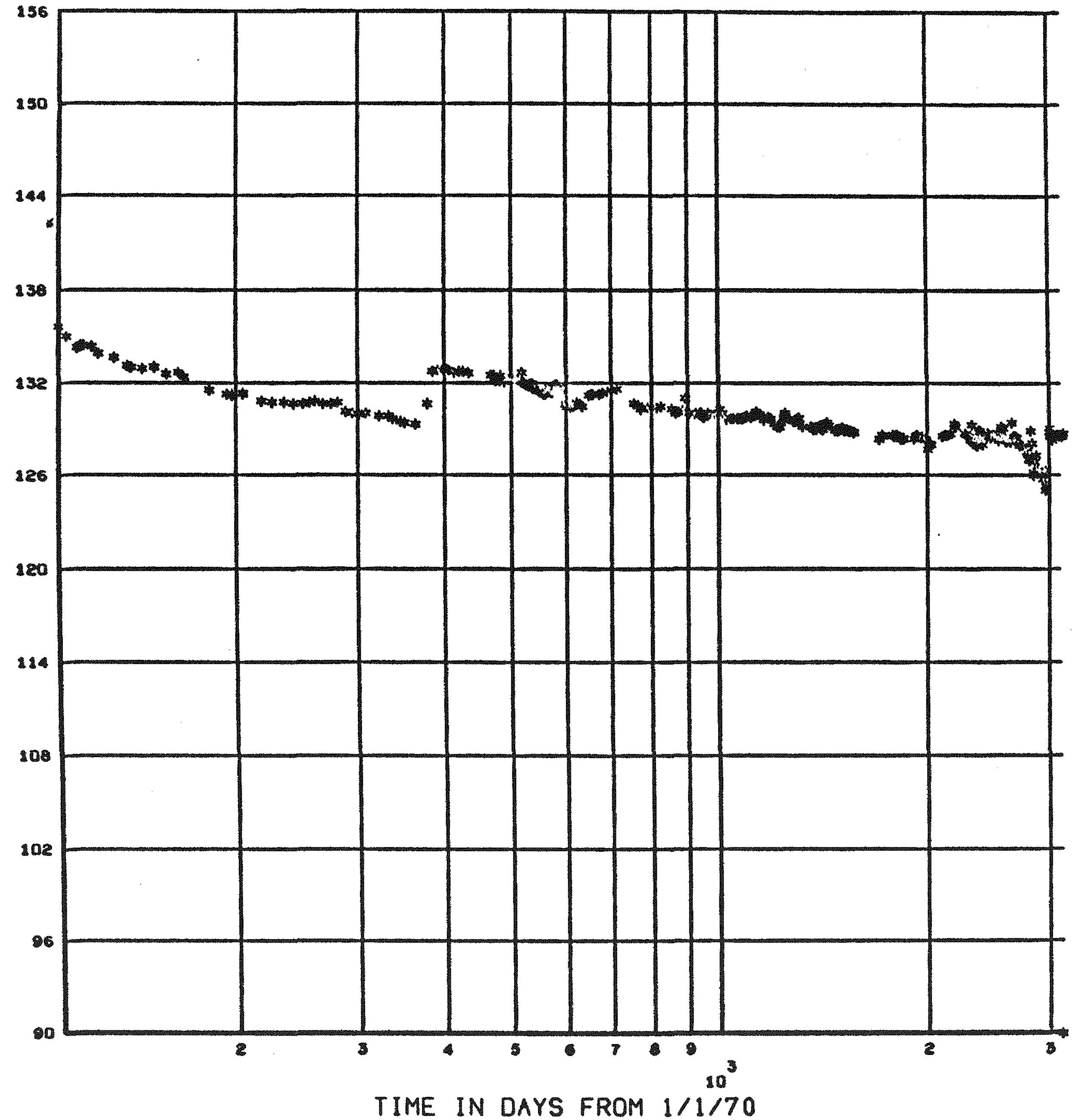

RUN 10742 29 AUG 78 12.21.56

...10

B-24

823

...10

LOAD CELL YE11206-25 (RESIDUAL LOAD - KIPS) C017.3

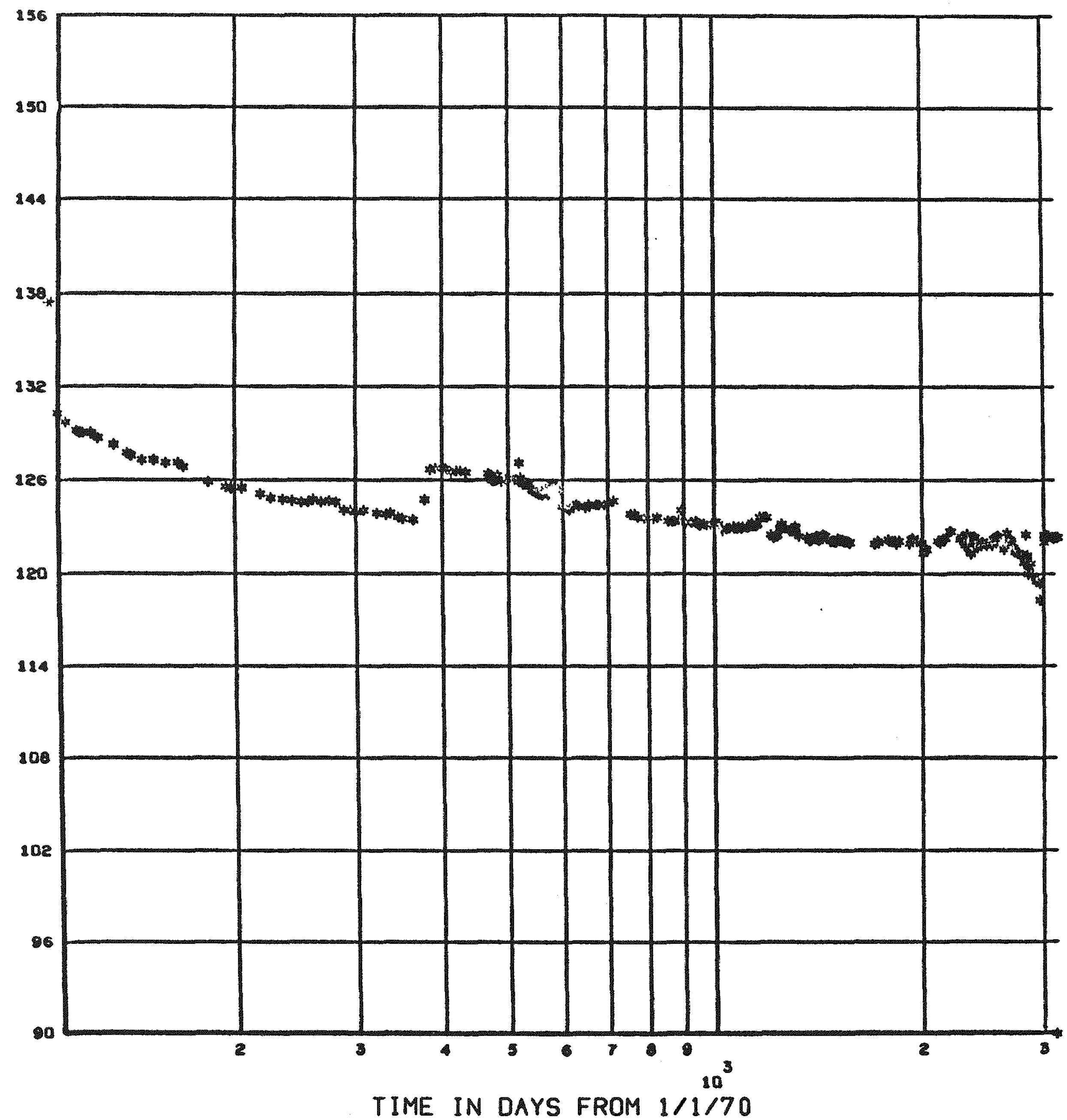

B-25

824

RUN 10742 29 AUG 78 12.24.03

LOAD CELL YE11206-26 (RESIDUAL LOAD - KIPS) CI18.5

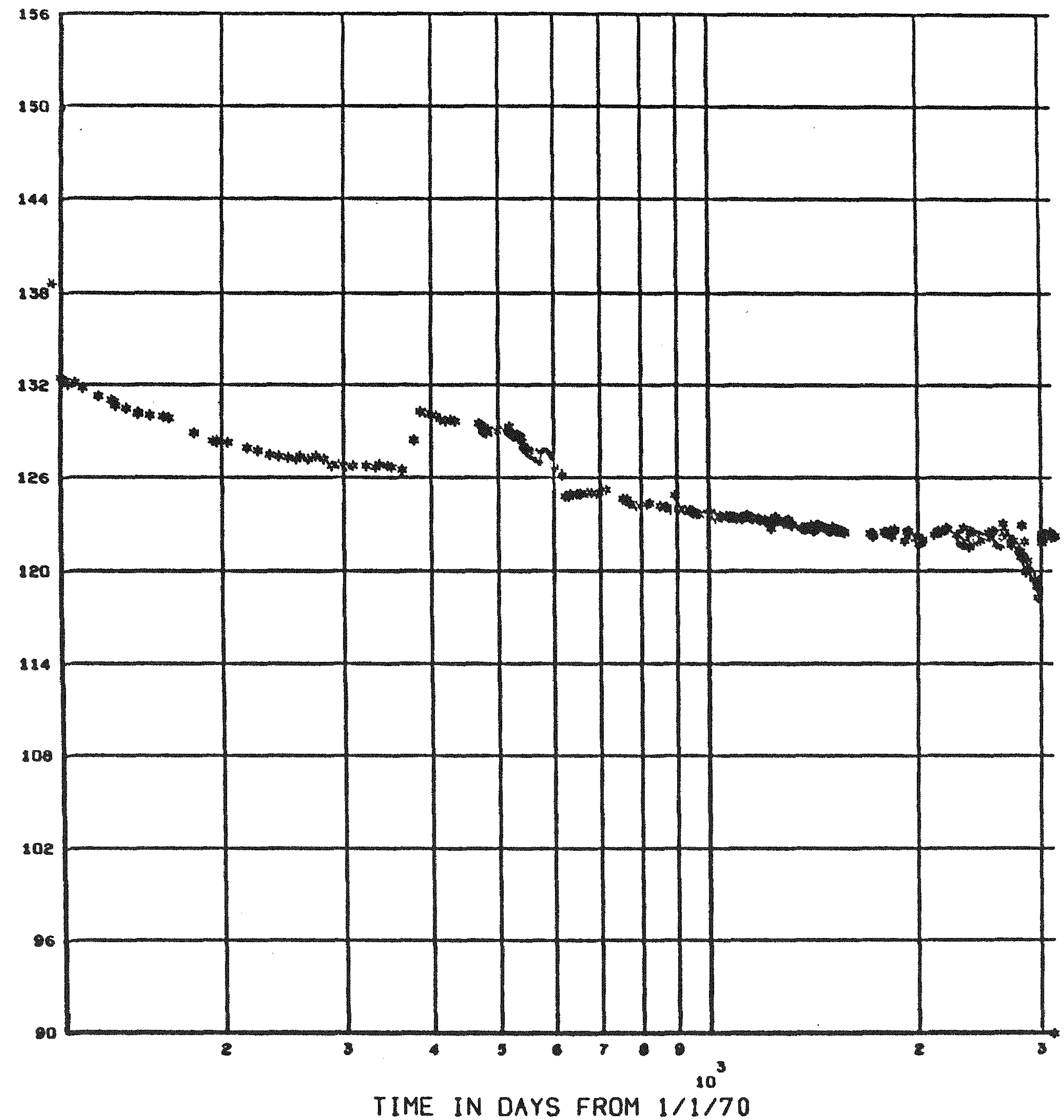

RUN 10742 29 AUG 78 12.24.07

...10

B-26

825

LOAD CELL YE11206-27 (RESIDUAL LOAD - KIPS) C019.6

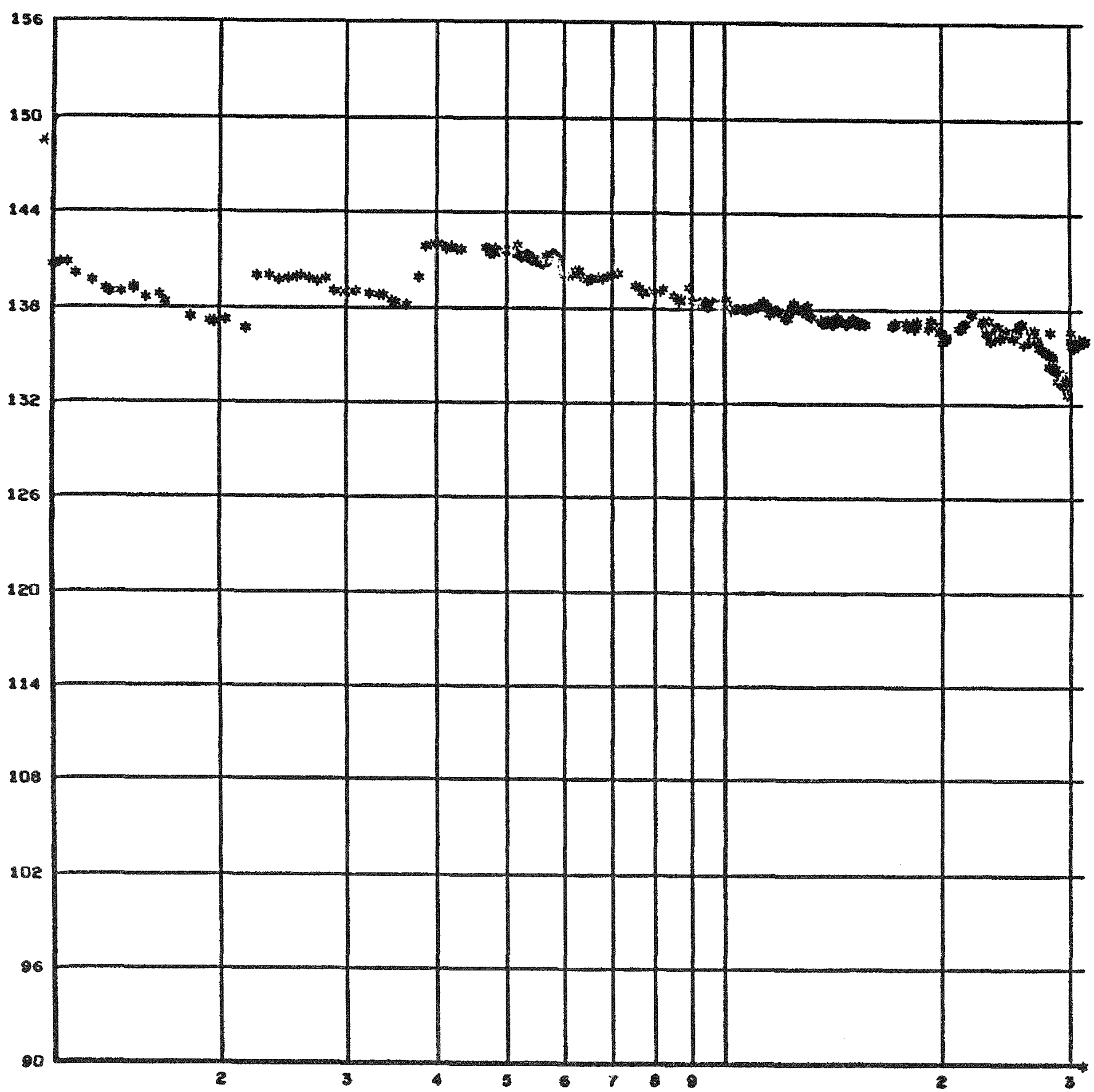

RUN 10742 29 AUG 78 12.24.10

...10

826

VIBRATING WIRE GAGE YE-1170-123 (STRAIN)

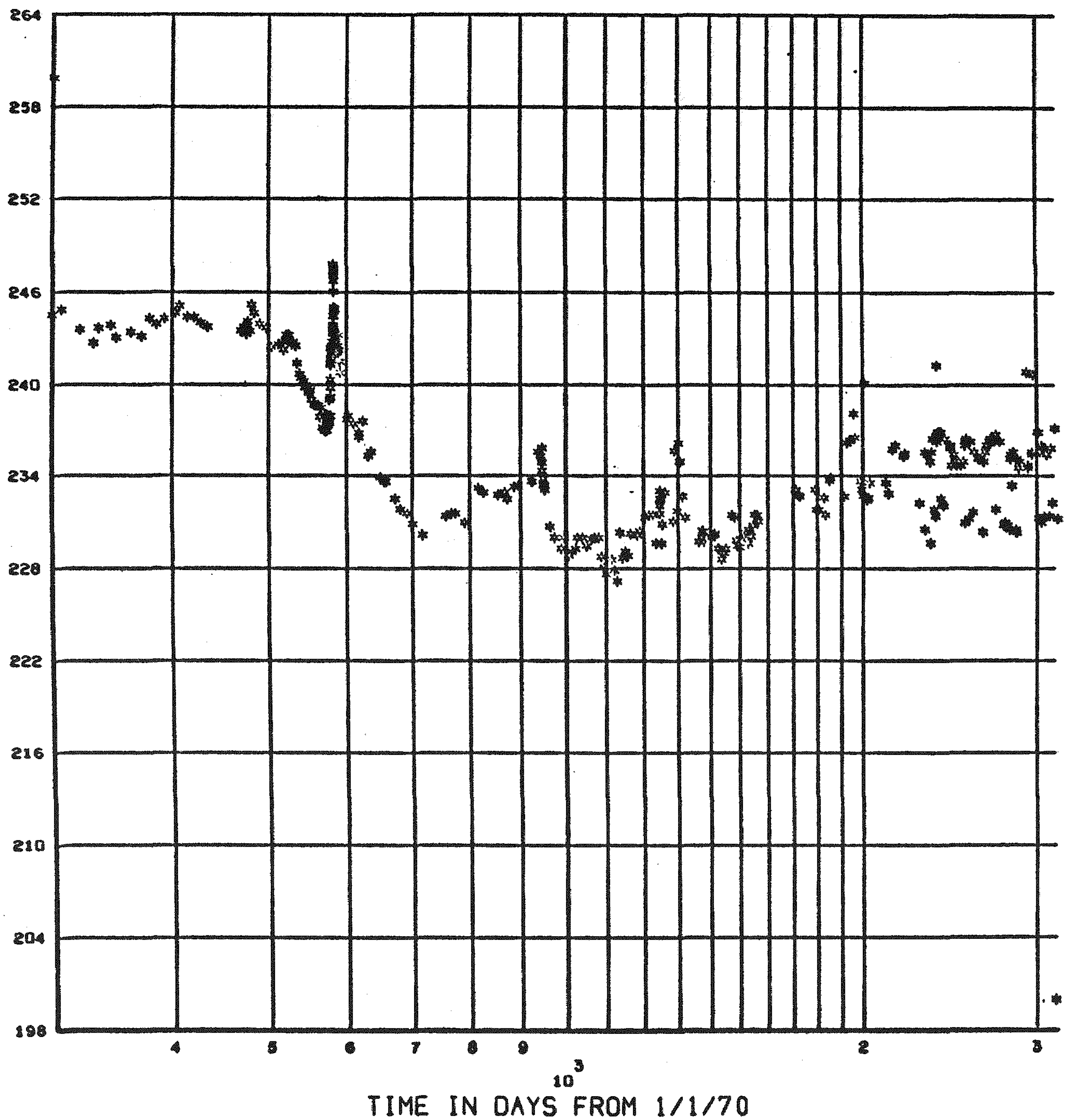

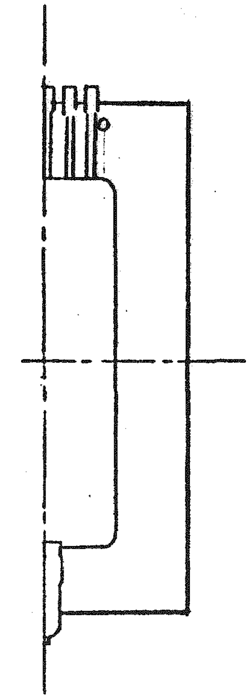

PLANE 3

B-28

614

RUN 17146 30 AUG 78 03.26.48

VIBRATING WIRE GAGE YE-1170-128 (STRAIN)

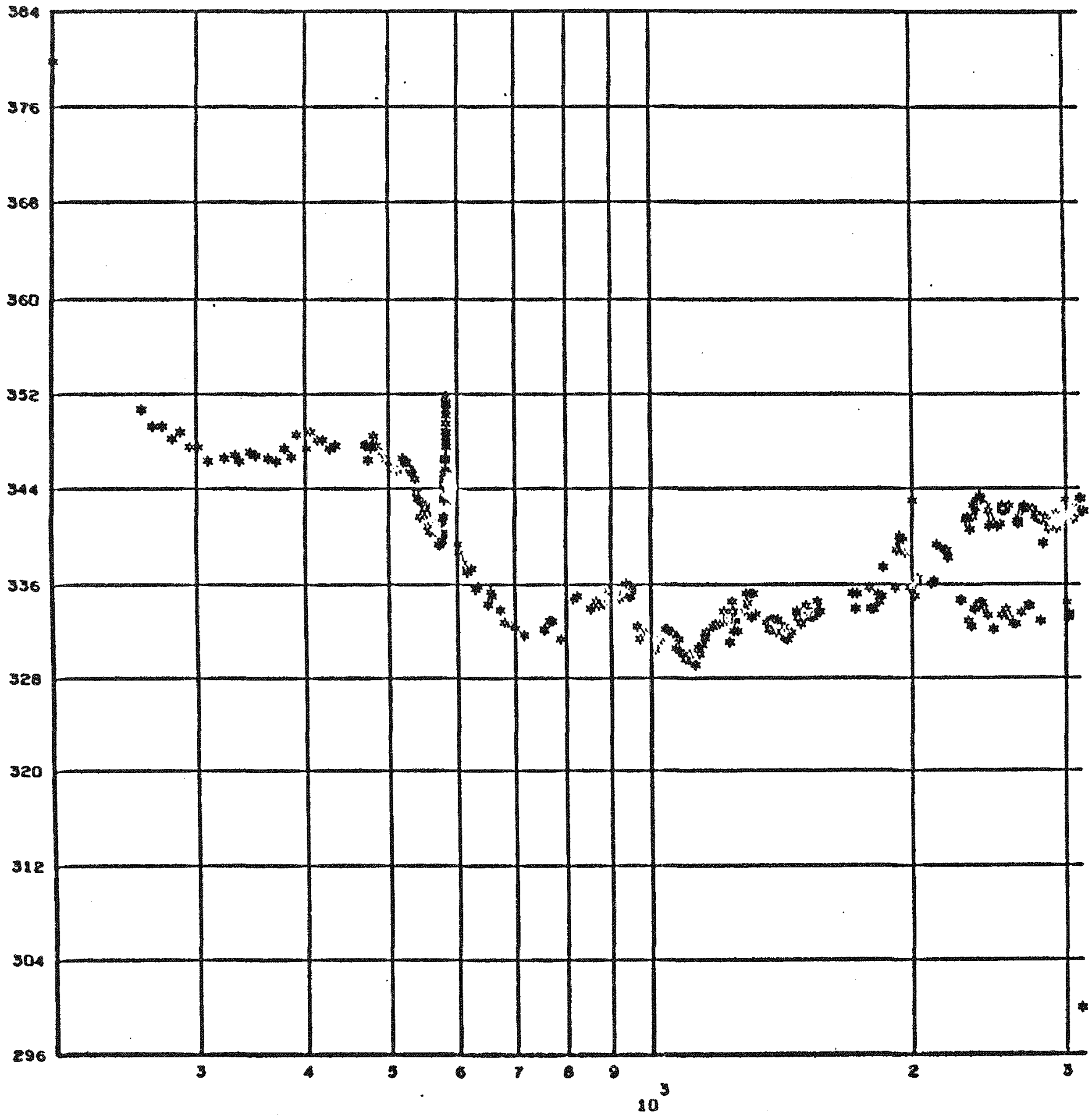

TIME IN DAYS FROM 1/1/70

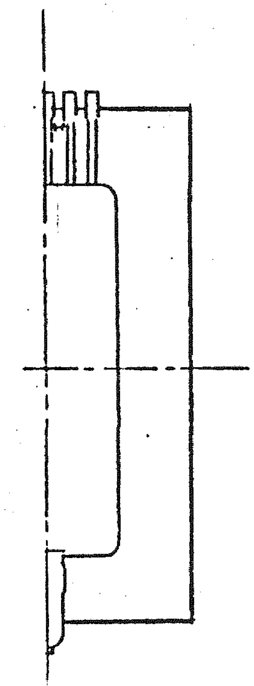

PLANE 3

RUN 17146 30 AUG 78 03.26.56

VIBRATING WIRE GAGE YE-1170-99 (STRAIN)

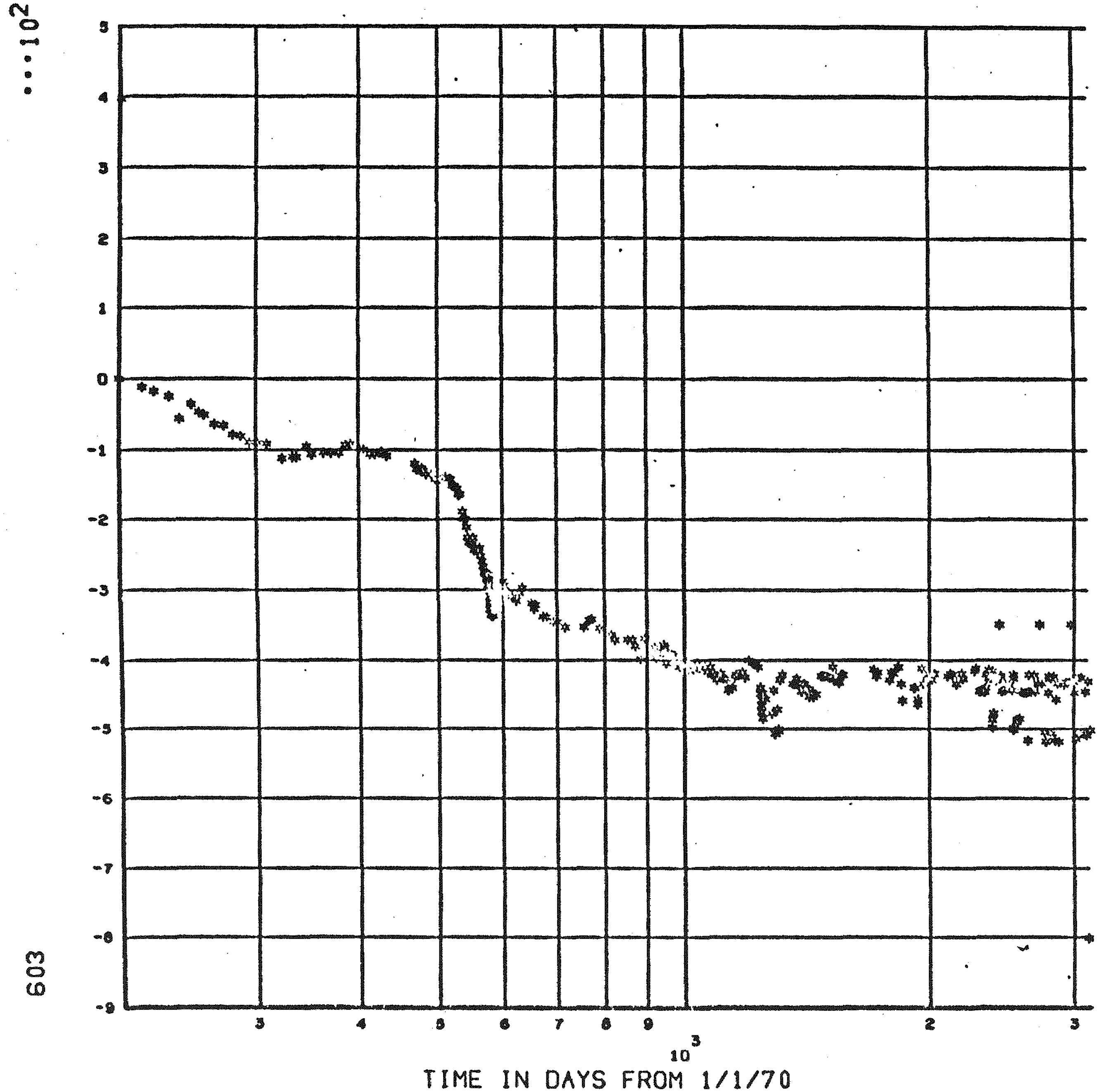

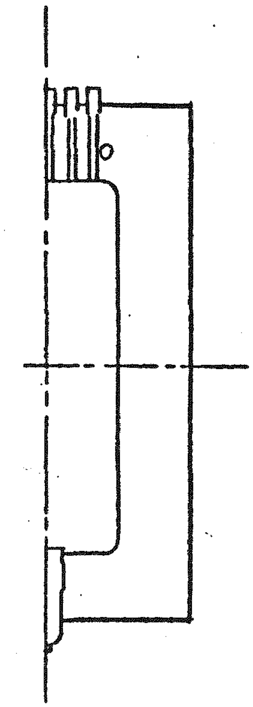

PLANE 3

B-30

603

RUN 17146, 30 AUG 78 03.22.20

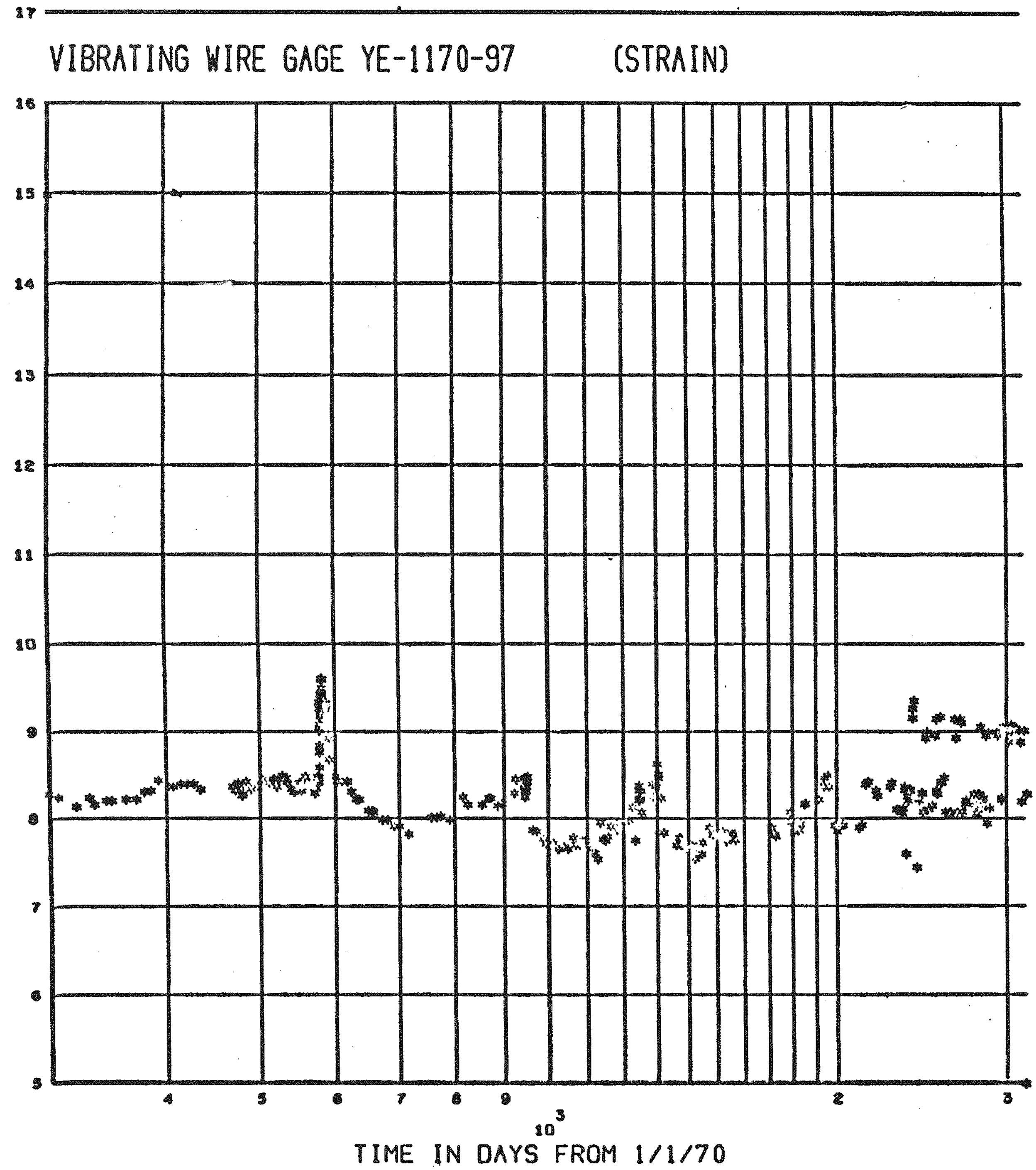

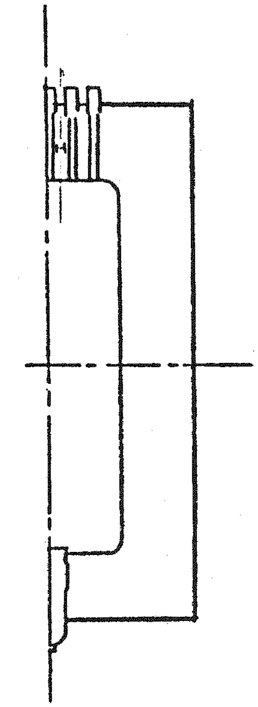

PLANE 3

RUN 17146 30 AUG 78 03.22.24

601·

VIBRATING WIRE GAGE YE-1170-114 (STRAIN)

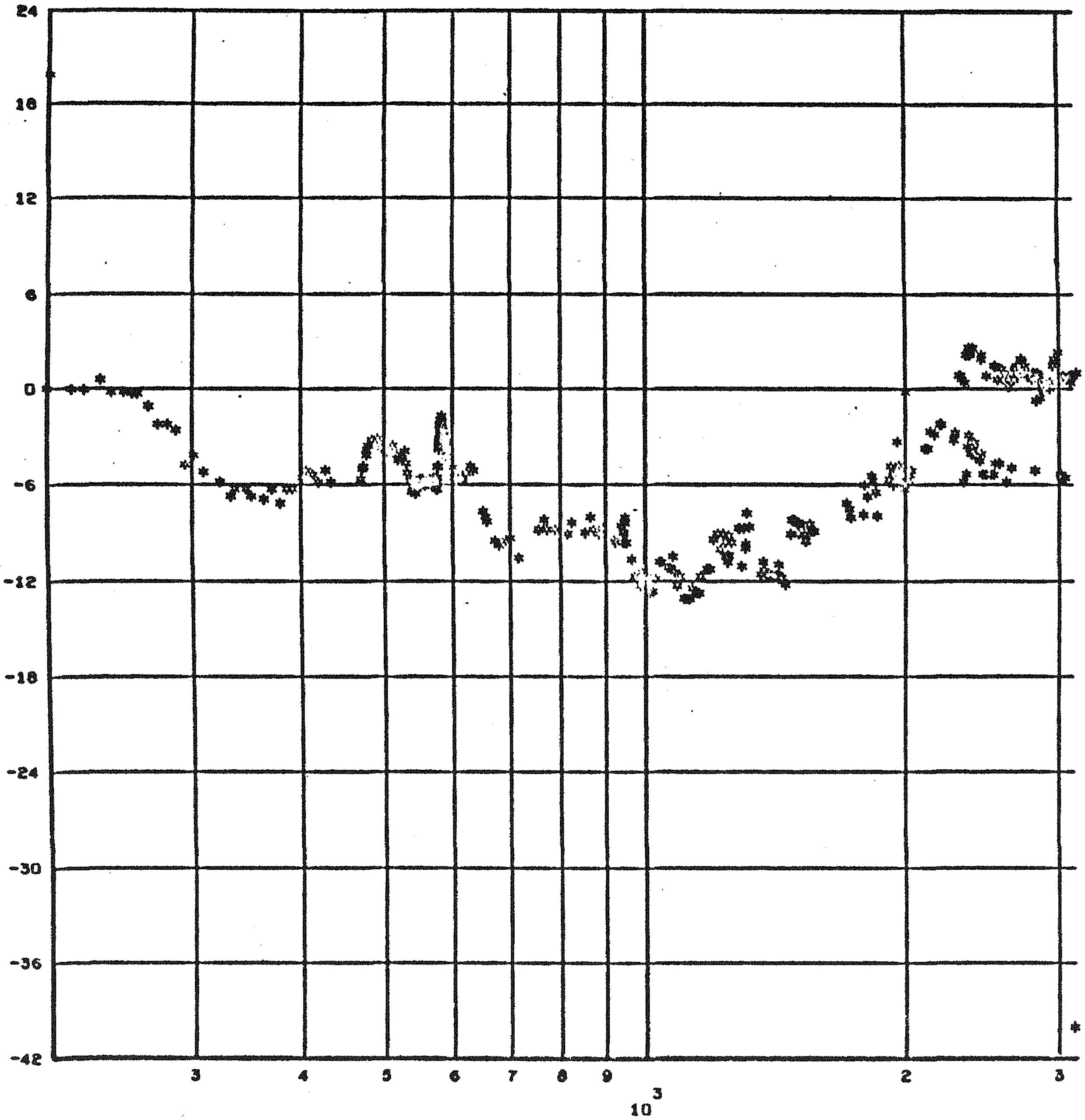

TIME IN DAYS FROM 1/1/70

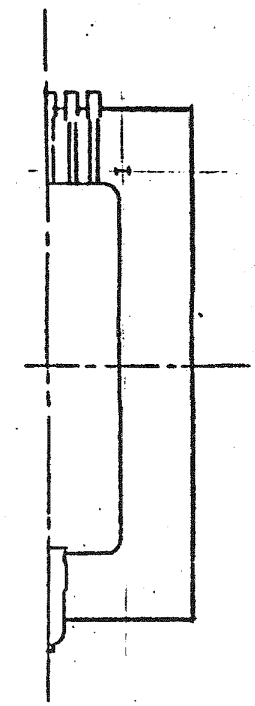

PLANE 1

...10

B-32

592

RUN 17146 30 AUG 78 03.24.49

VIBRATING WIRE GAGE YE-1170-90 (STRAIN)

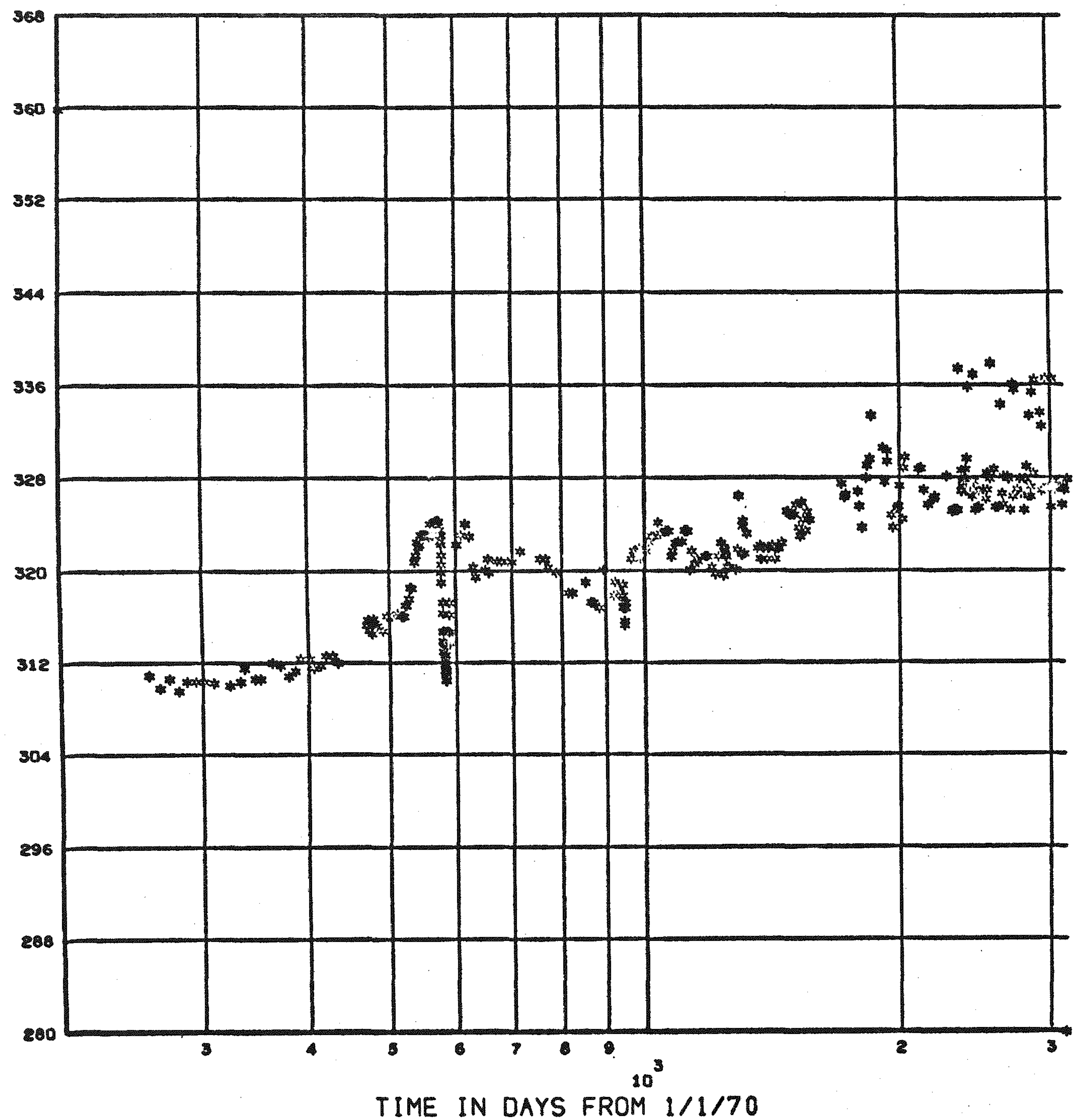

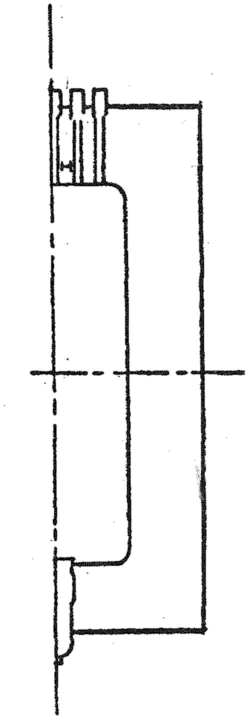

PLANE 3

B-33

594

VIBRATING WIRE GAGE YE-1170-87 (STRAIN)

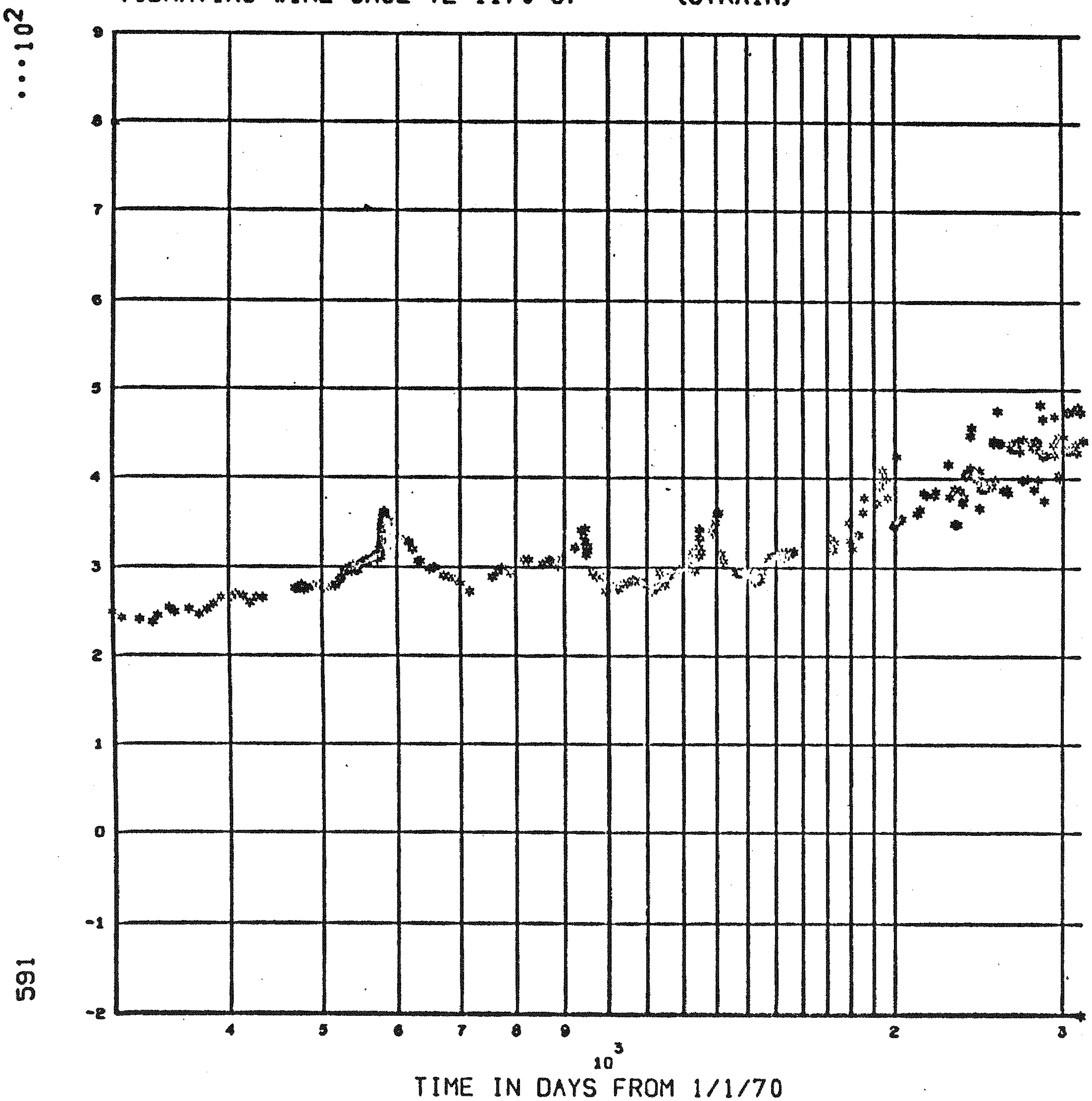

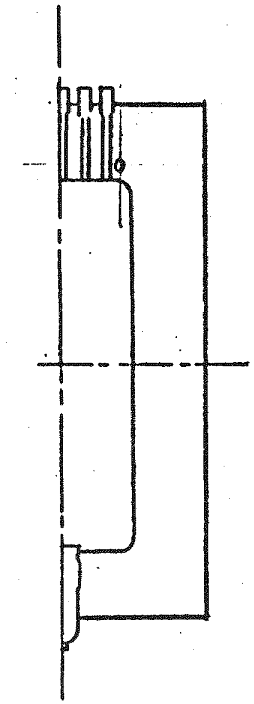

PLANE 1

RUN 17146 30 AUG 78 03.22.12

VIBRATING WIRE GAGE YE-1170-101 (STRAIN)

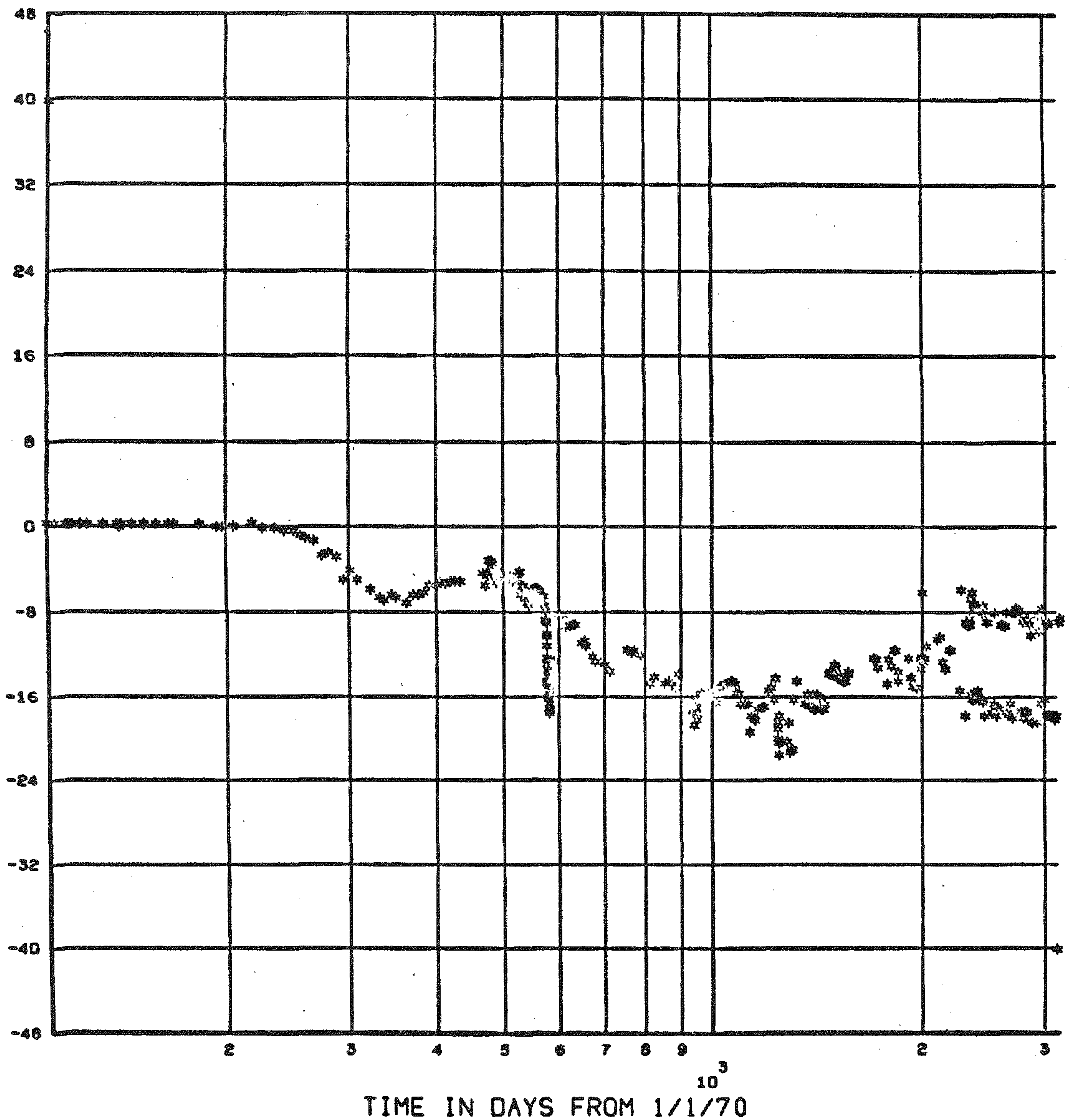

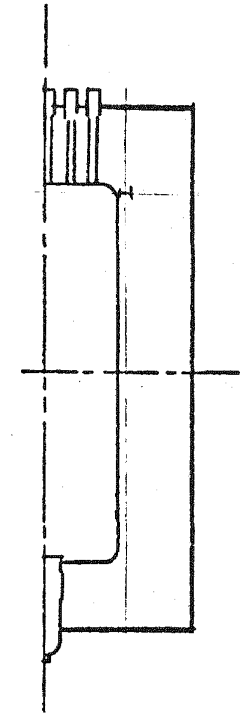

PLANE 1

581

VIBRATING WIRE GAGE YE-1170-103 (STRAIN)

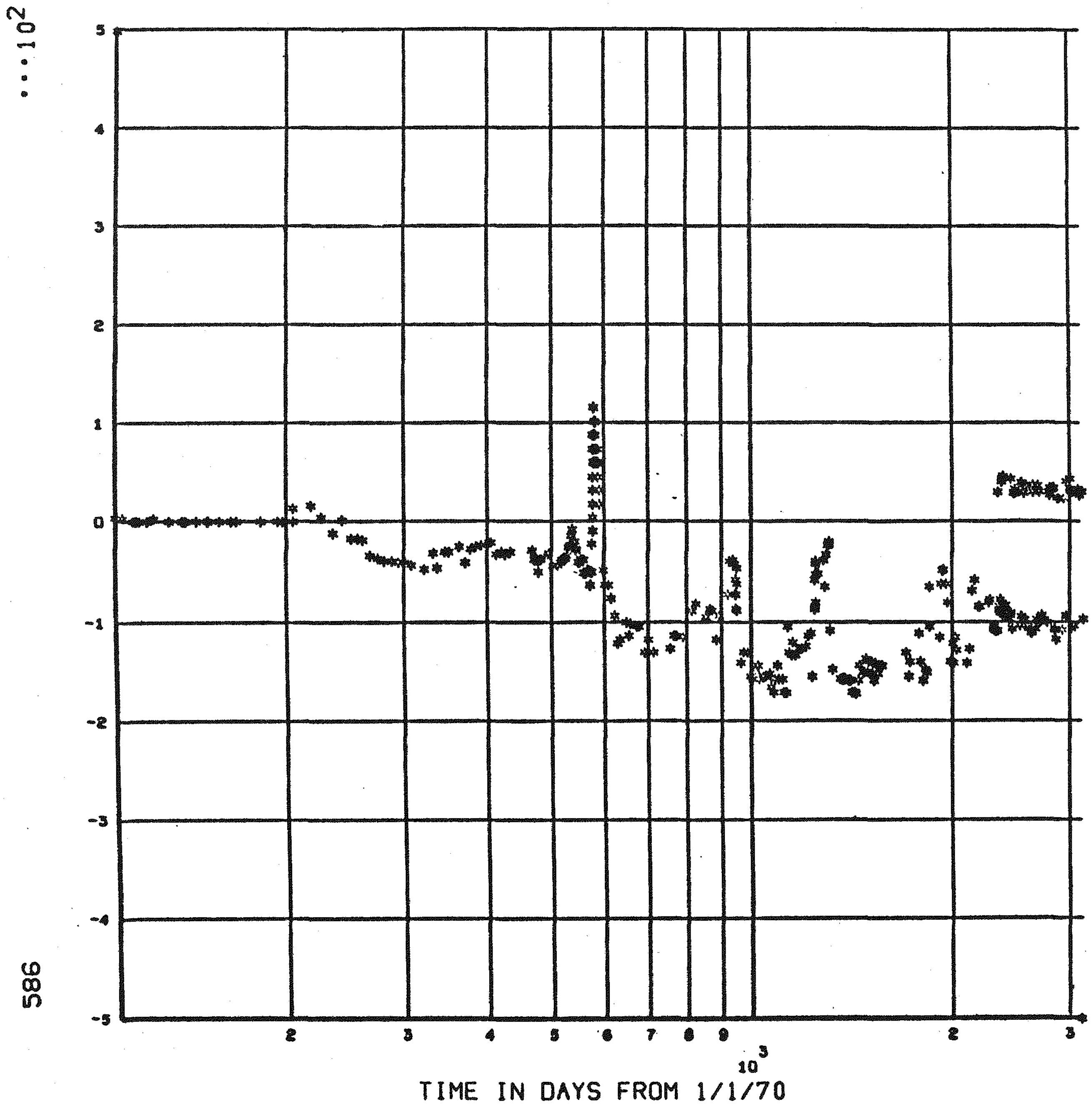

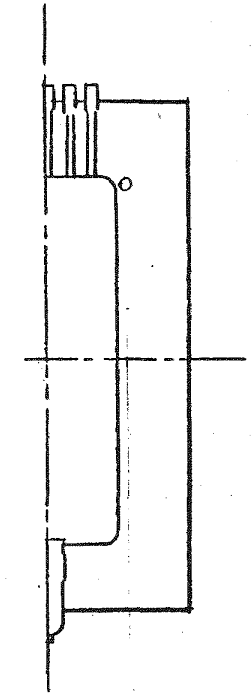

B-36

586

RUN 17146 30 AUG 78 03.24.25

VIBRATING WIRE GAGE YE-1170-104 (STRAIN)

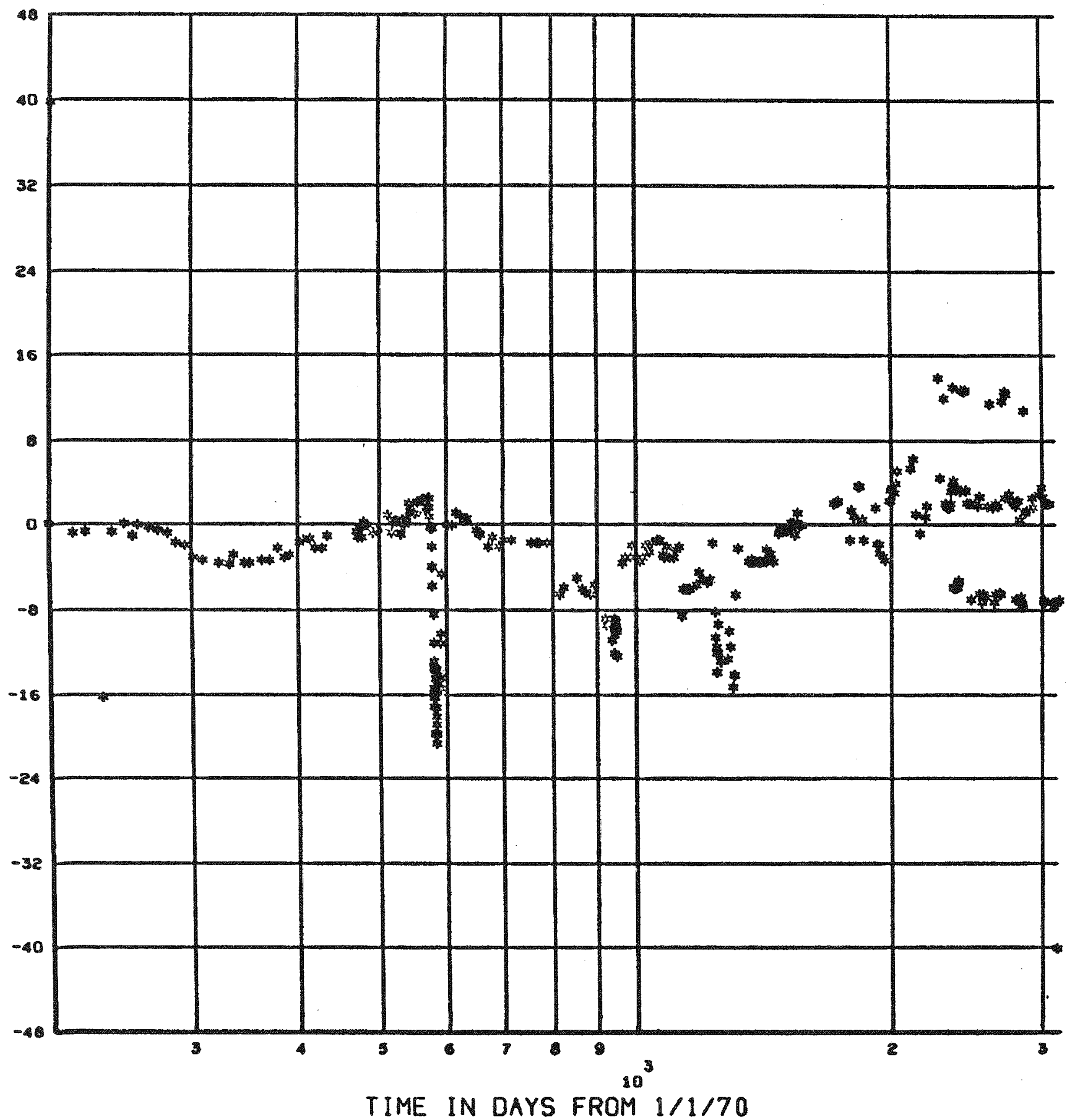

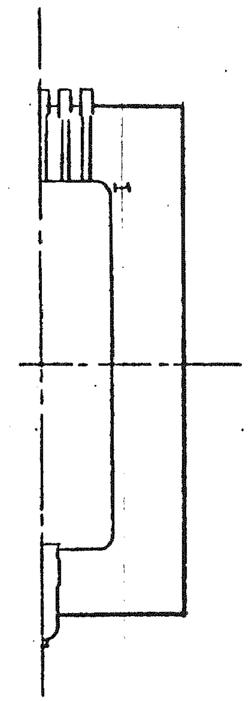

RUN 17146 30 AUG 78 03.24.27

•••10

587

VIBRATING WIRE GAGE YE-1170-112 (STRAIN)

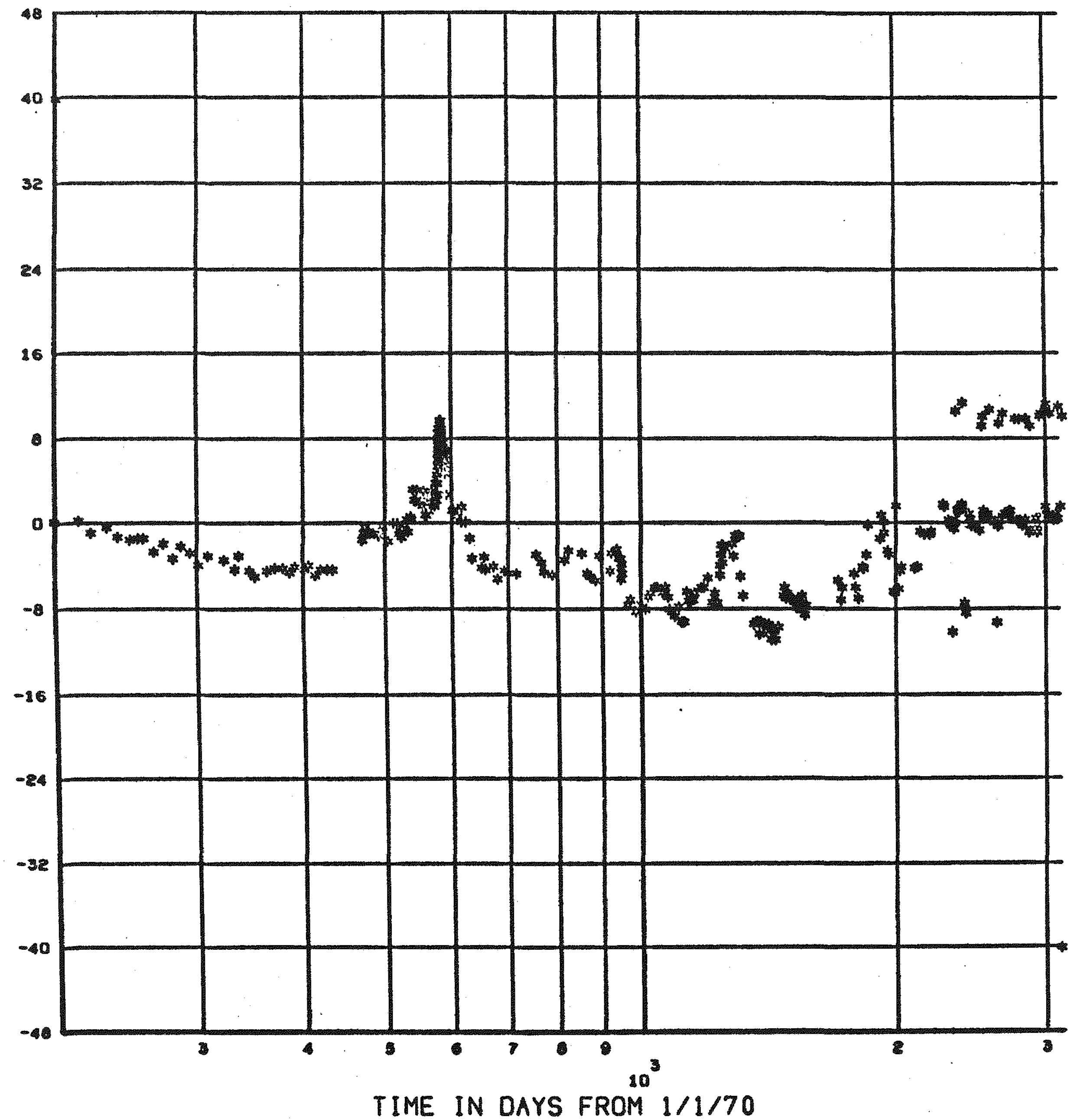

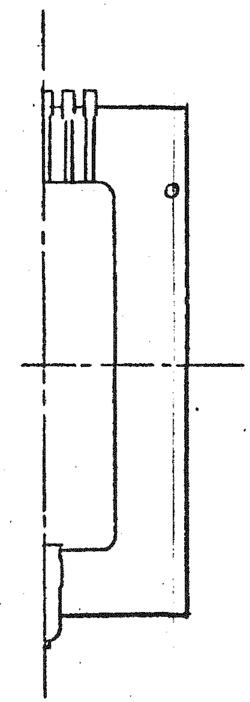

PLANE 1

B-38

585

RUN 17146 30 AUG 78 03.24.44

•••10

VIBRATING WIRE GAGE YE-1170-106 (STRAIN)

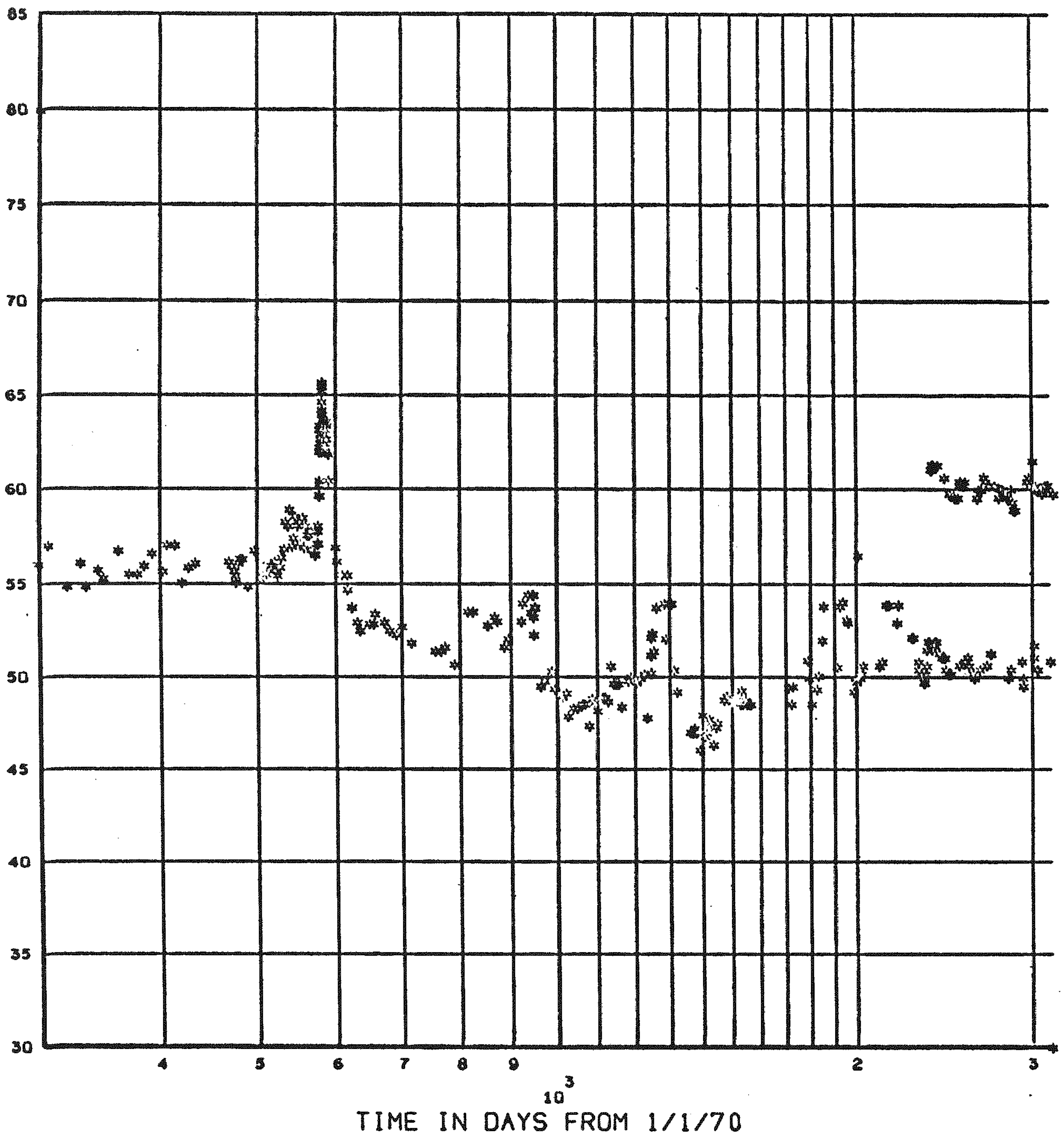

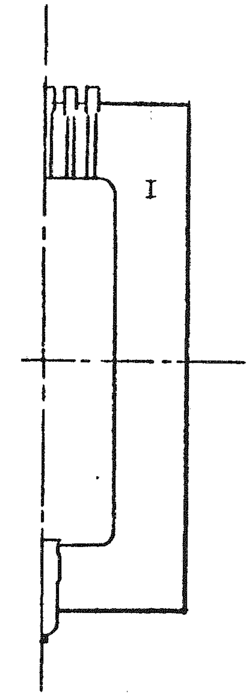

PLANE 1

B-39

584

RUN 10742 19 SEP 78 18.09.44

VIBRATING WIRE GAGE YE-1170-105 (STRAIN)

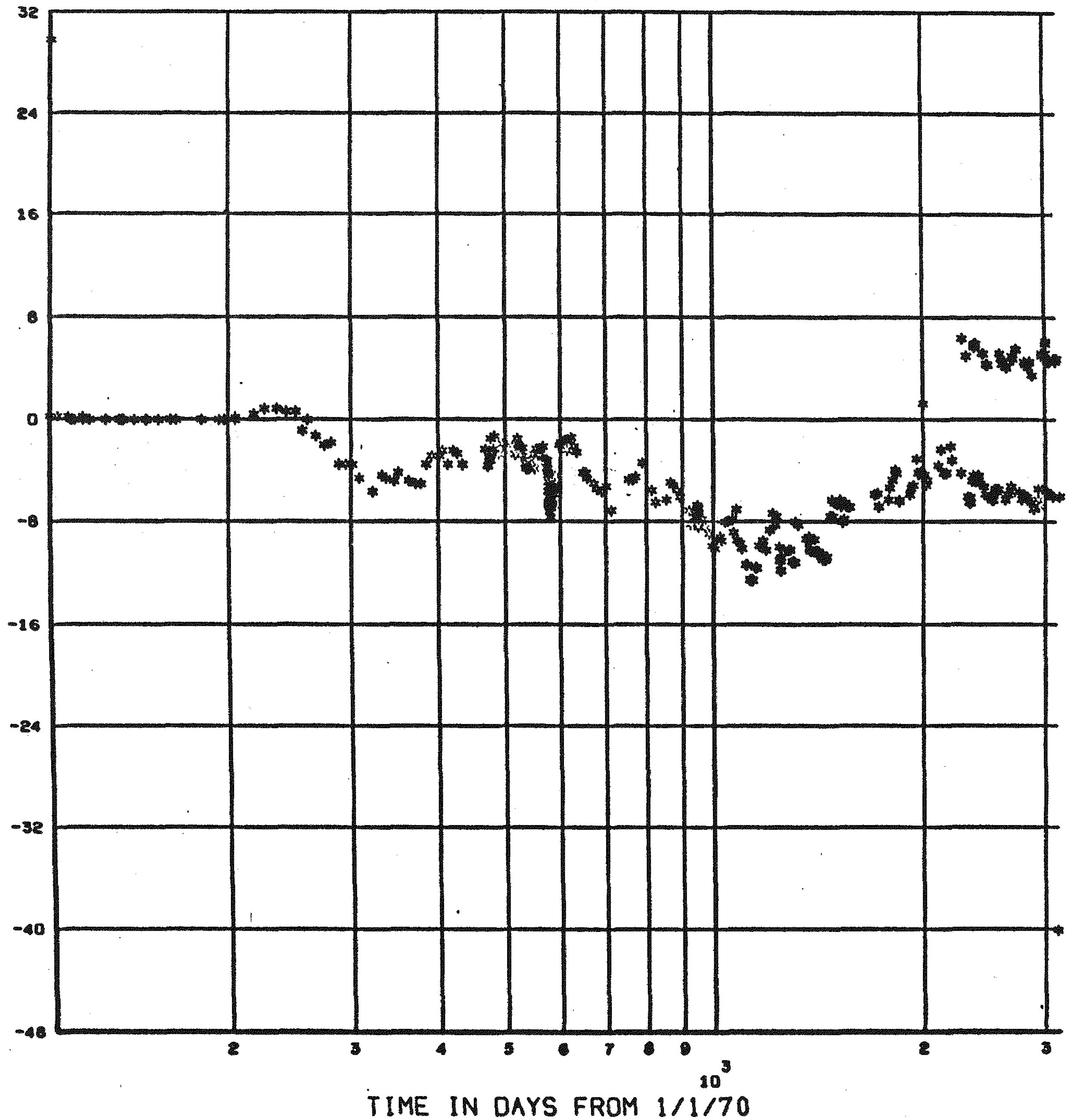

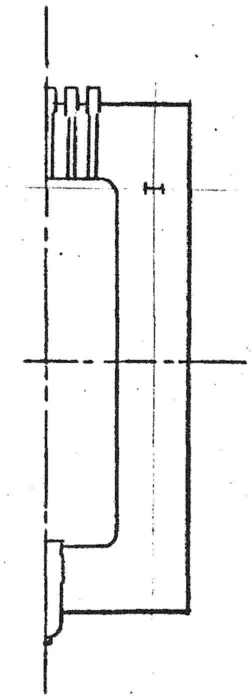

PLANE 1

RUN 17146 30 AUG 78 03.24.31

...10

583

VIBRATING WIRE GAGE YE-1170-74 (STRAIN)

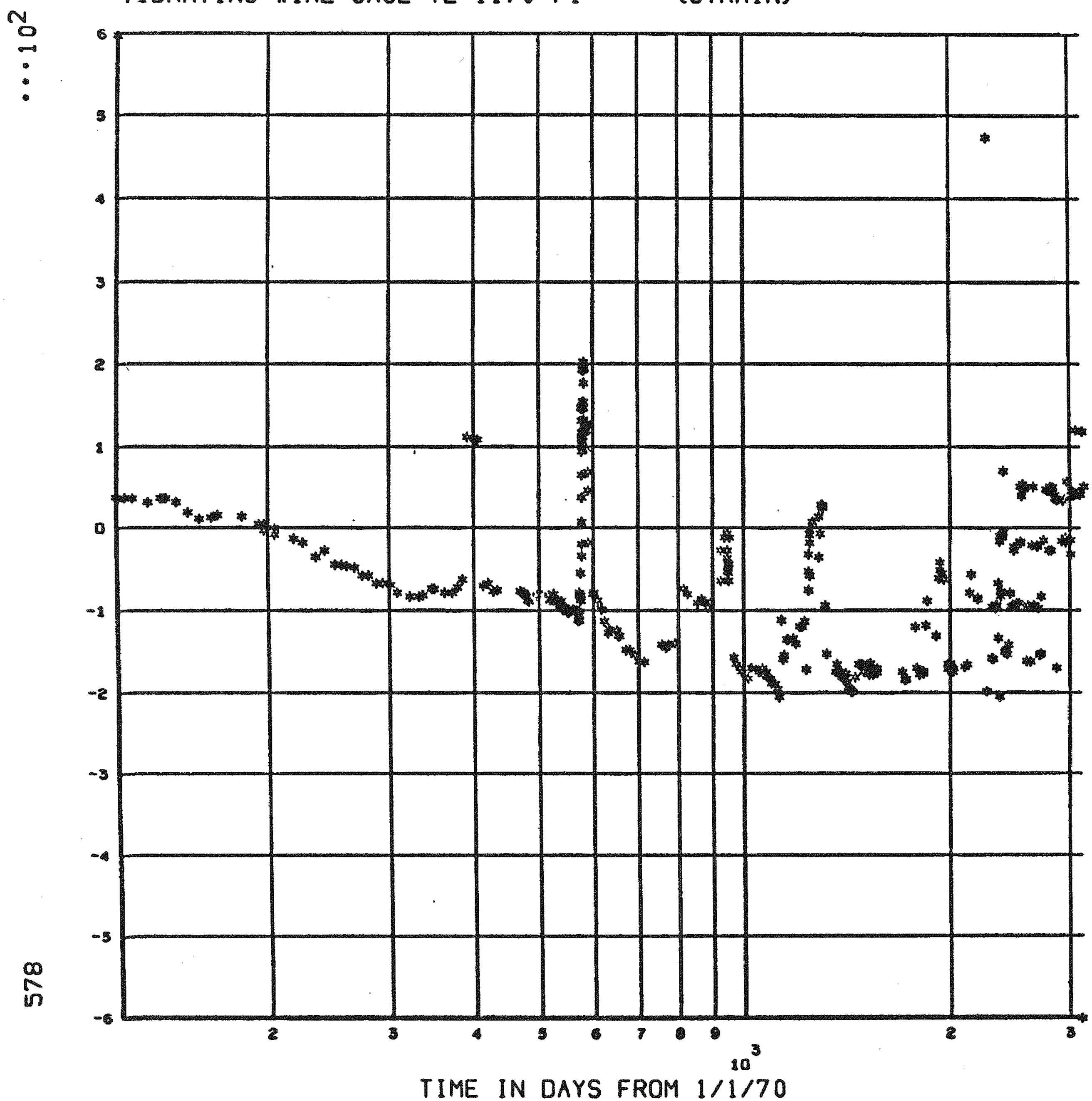

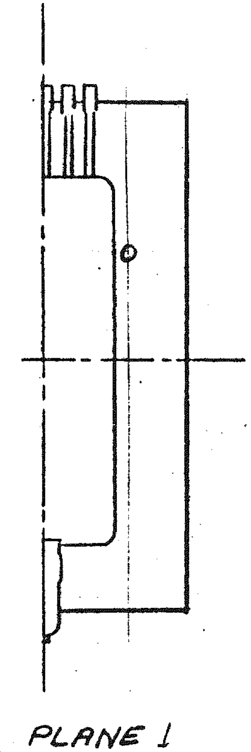

RUN 17146 30 AUG 78 03.22.04

578

VIBRATING WIRE GAGE YE-1170-70 (STRAIN)

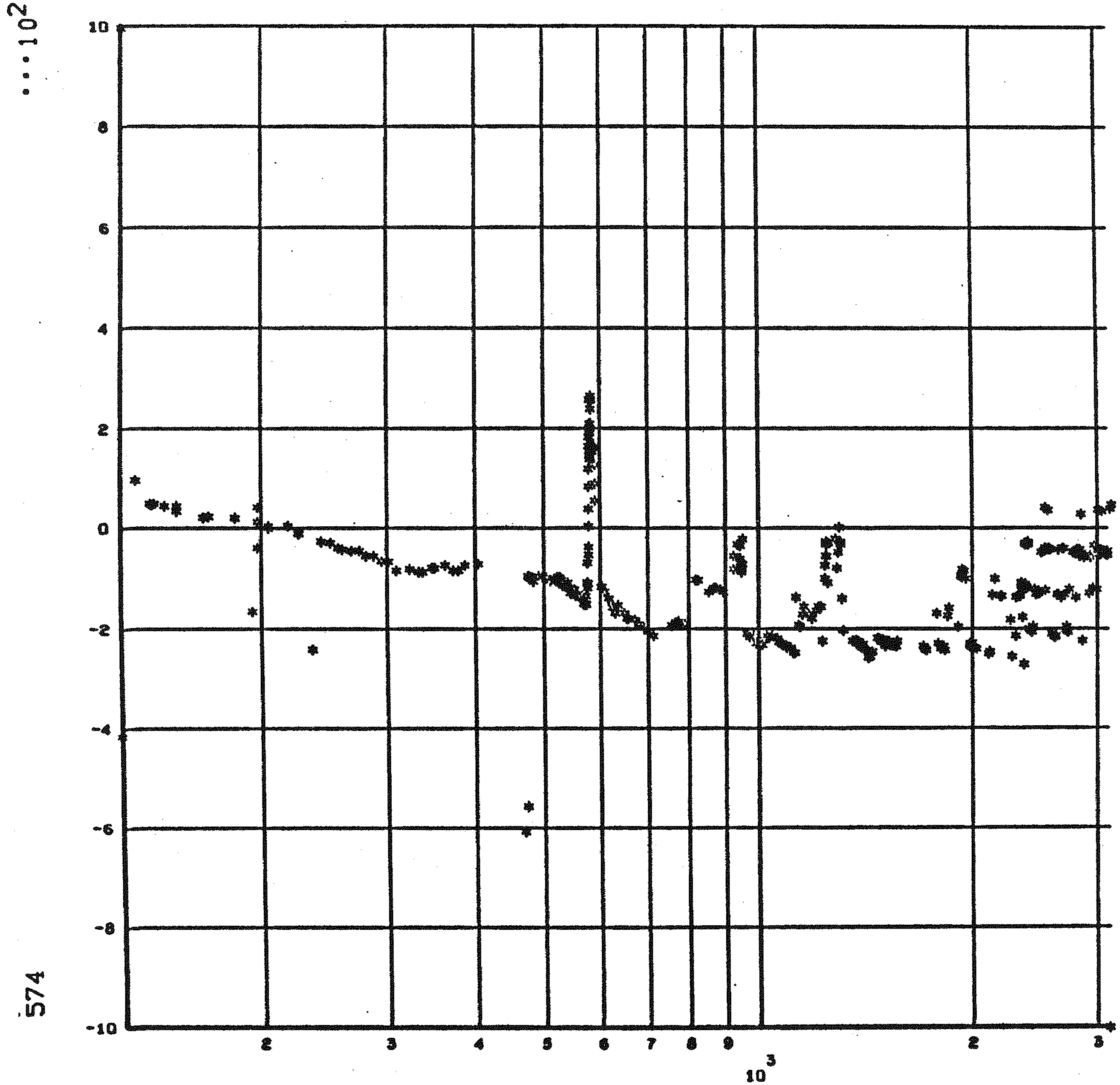

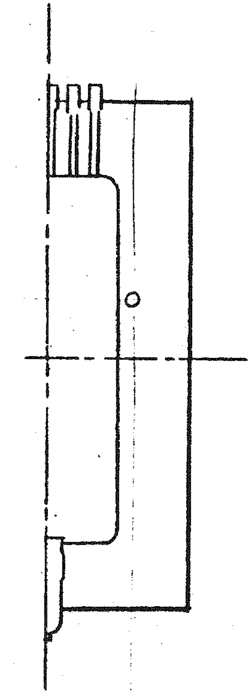

PLANE 1

574

RUN 17146 30 AUG 78 03.20.06

VIBRATING WIRE GAGE YE-1170-72 (STRAIN)

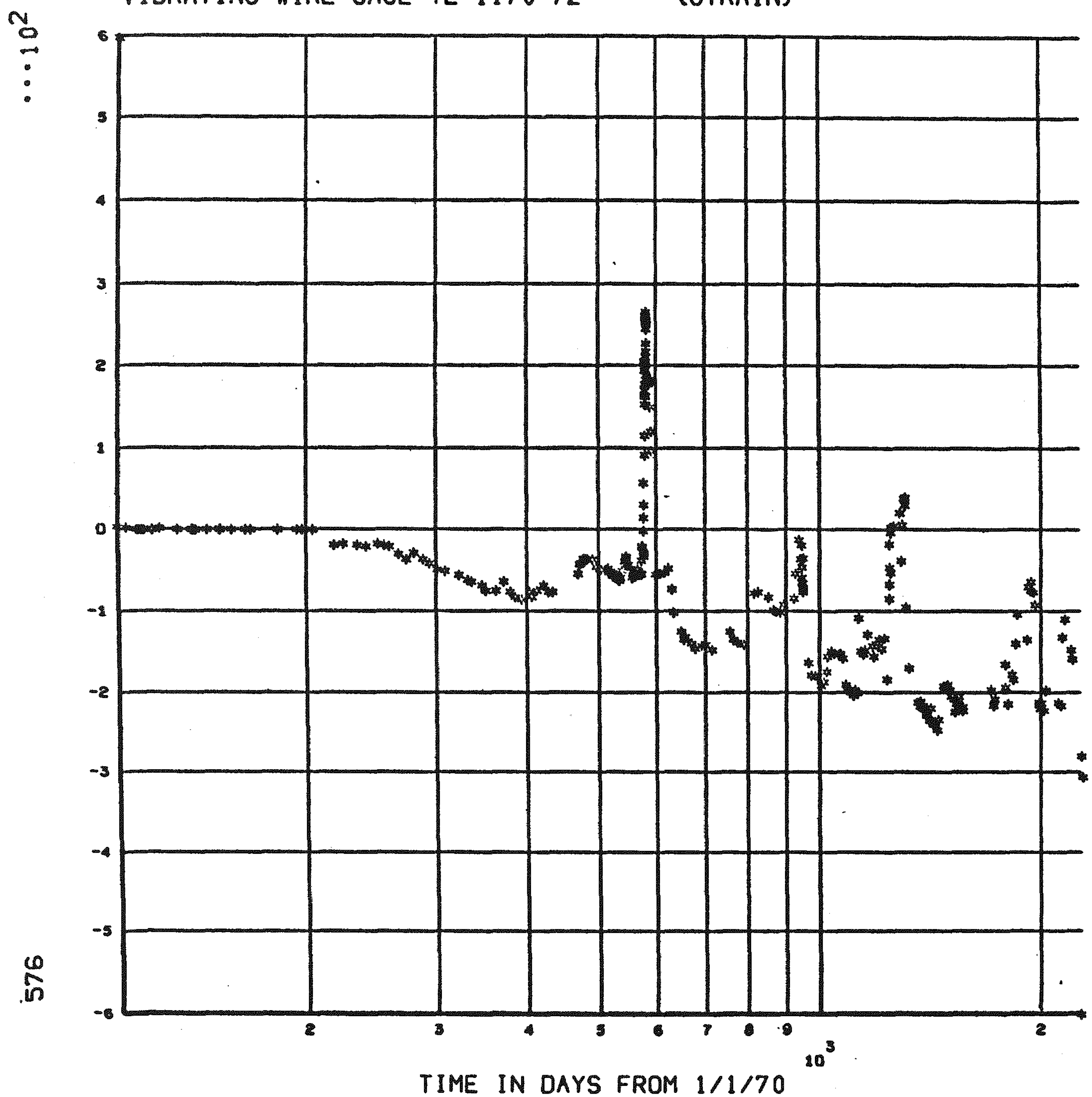

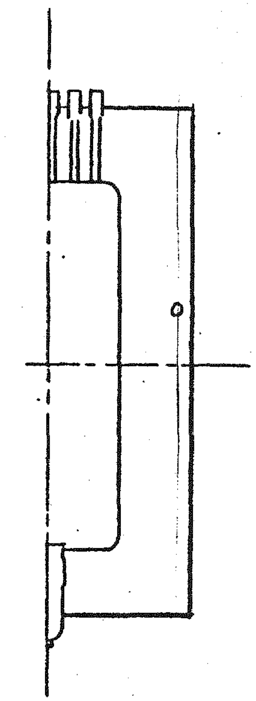

PLANE 1

B-43

576

RUN 17146 30 AUG 78 03.20.08

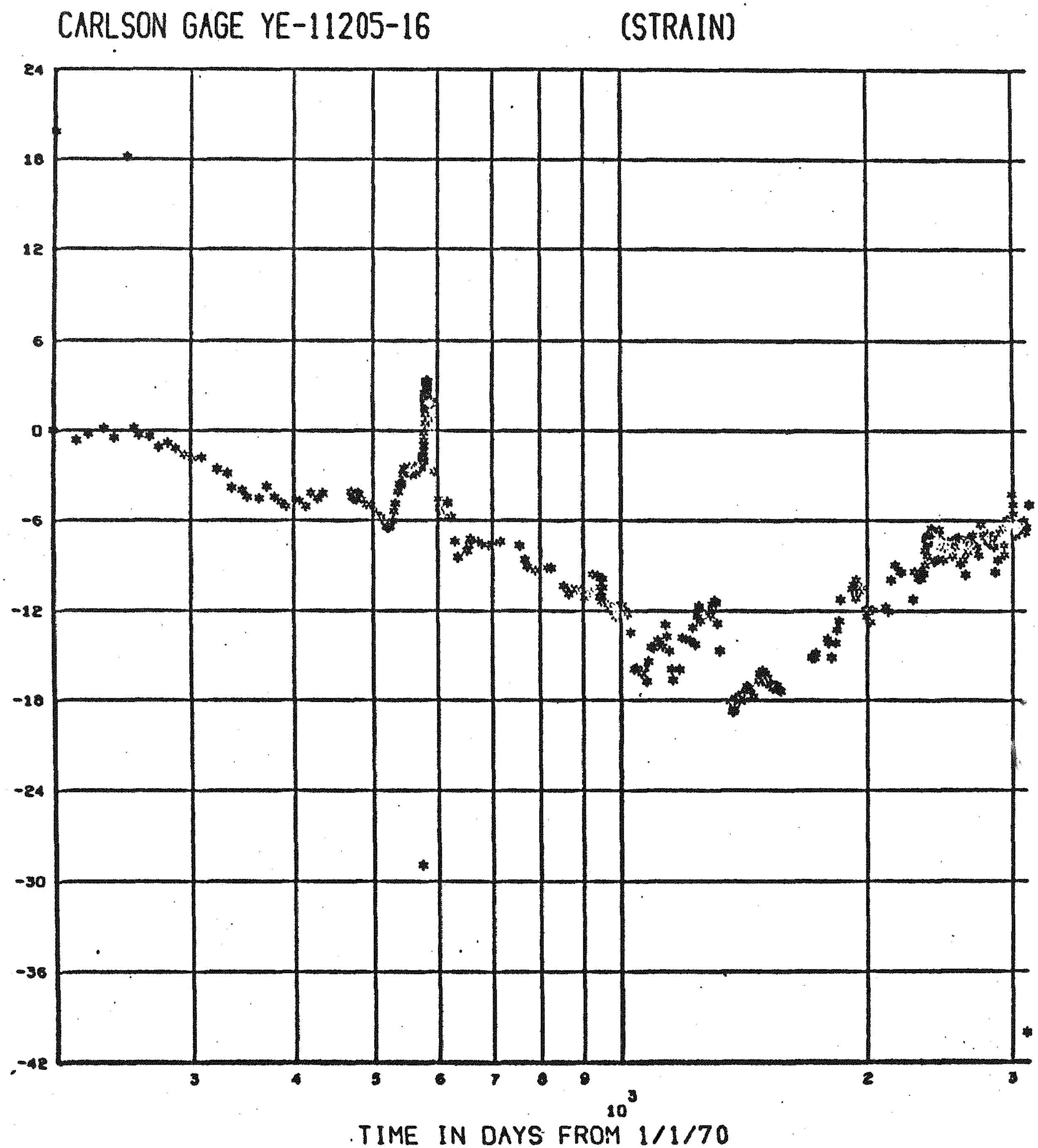

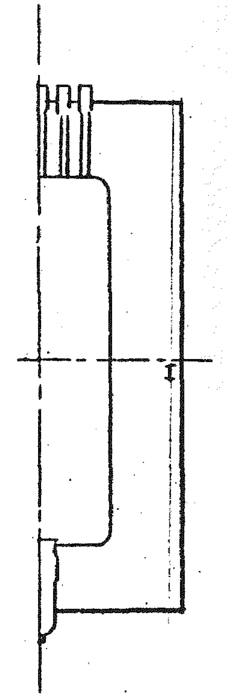

RUN 10741 29 AUG 78 23.08.23

...10

490

CARLSON GAGE YE-11205-18 (STRAIN)

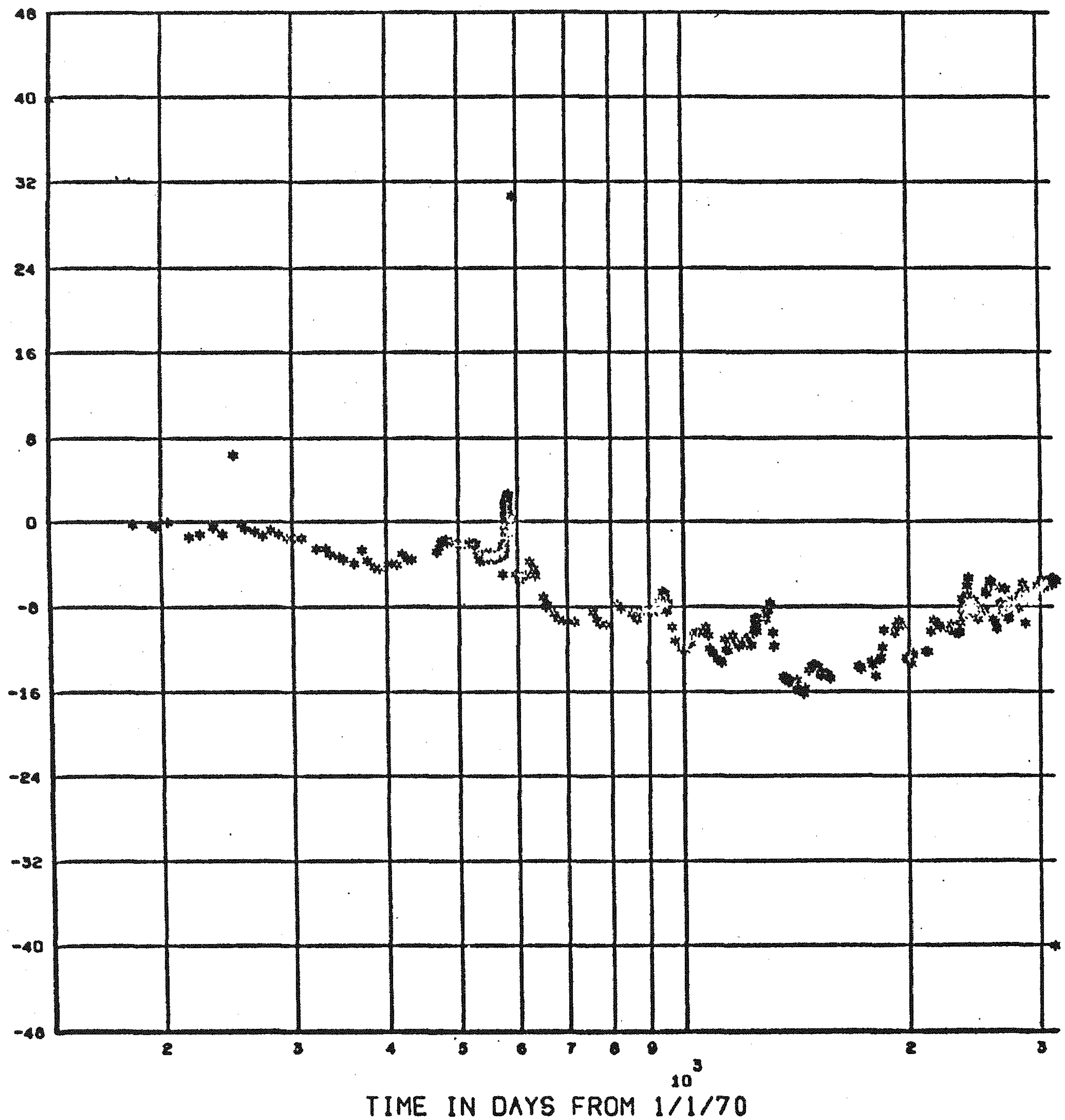

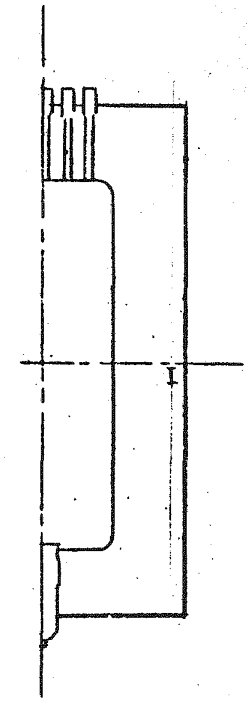

PLANE 2

RUN 10741 29 AUG 78 23.10.52

...10

492

CARLSON GAGE YE-11205-15 (STRAIN)

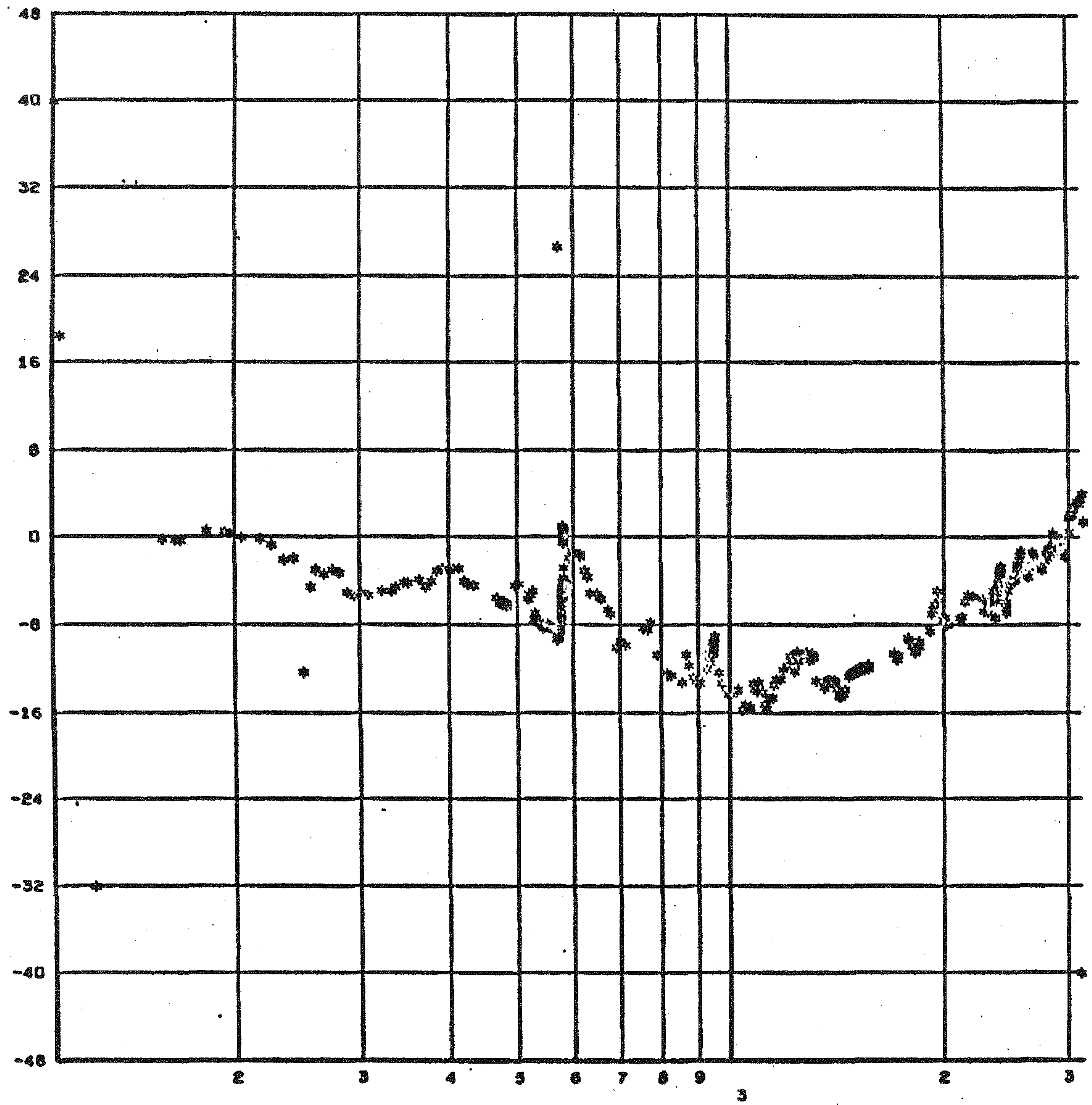

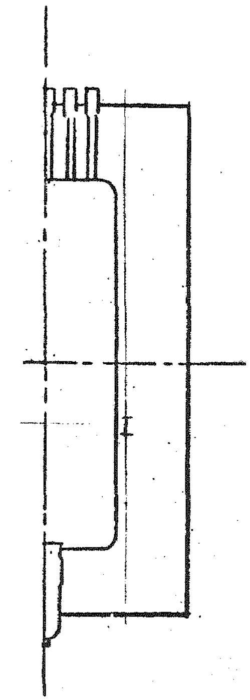

RUN 10741 29 AUG 78 23.08.19

489

VIBRATING WIRE GAGE YE-1170-65 (STRAIN)

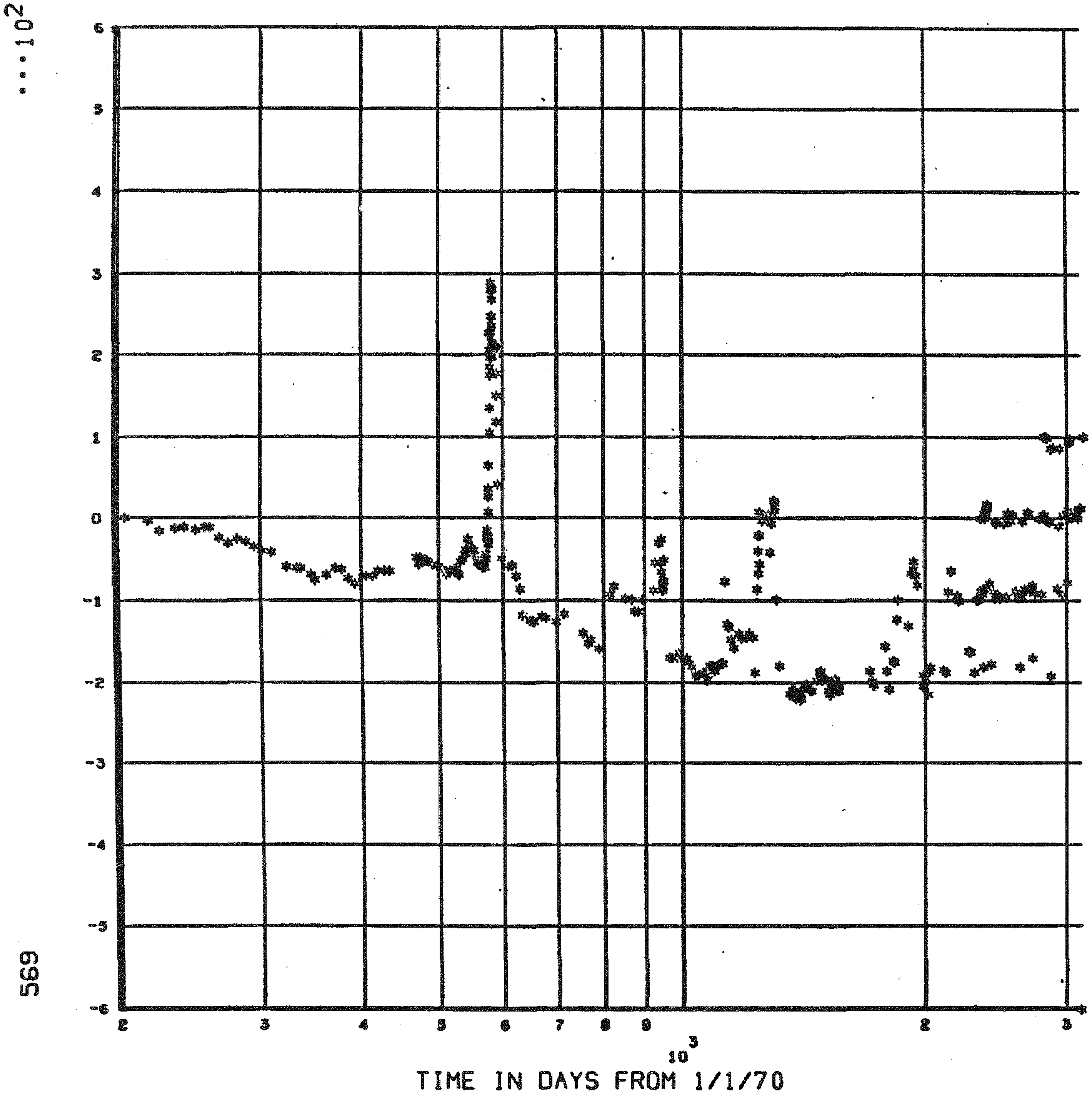

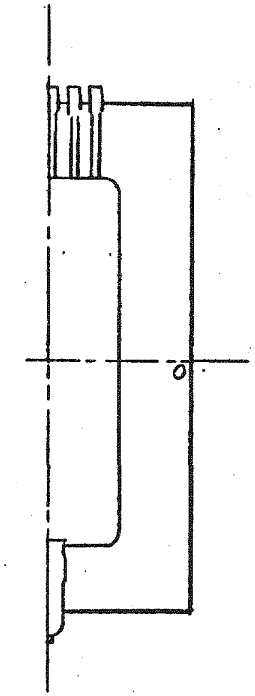

RUN 17146 30 AUG 78 03.18.13

569

VIBRATING WIRE GAGE YE-1170-58 (STRAIN)

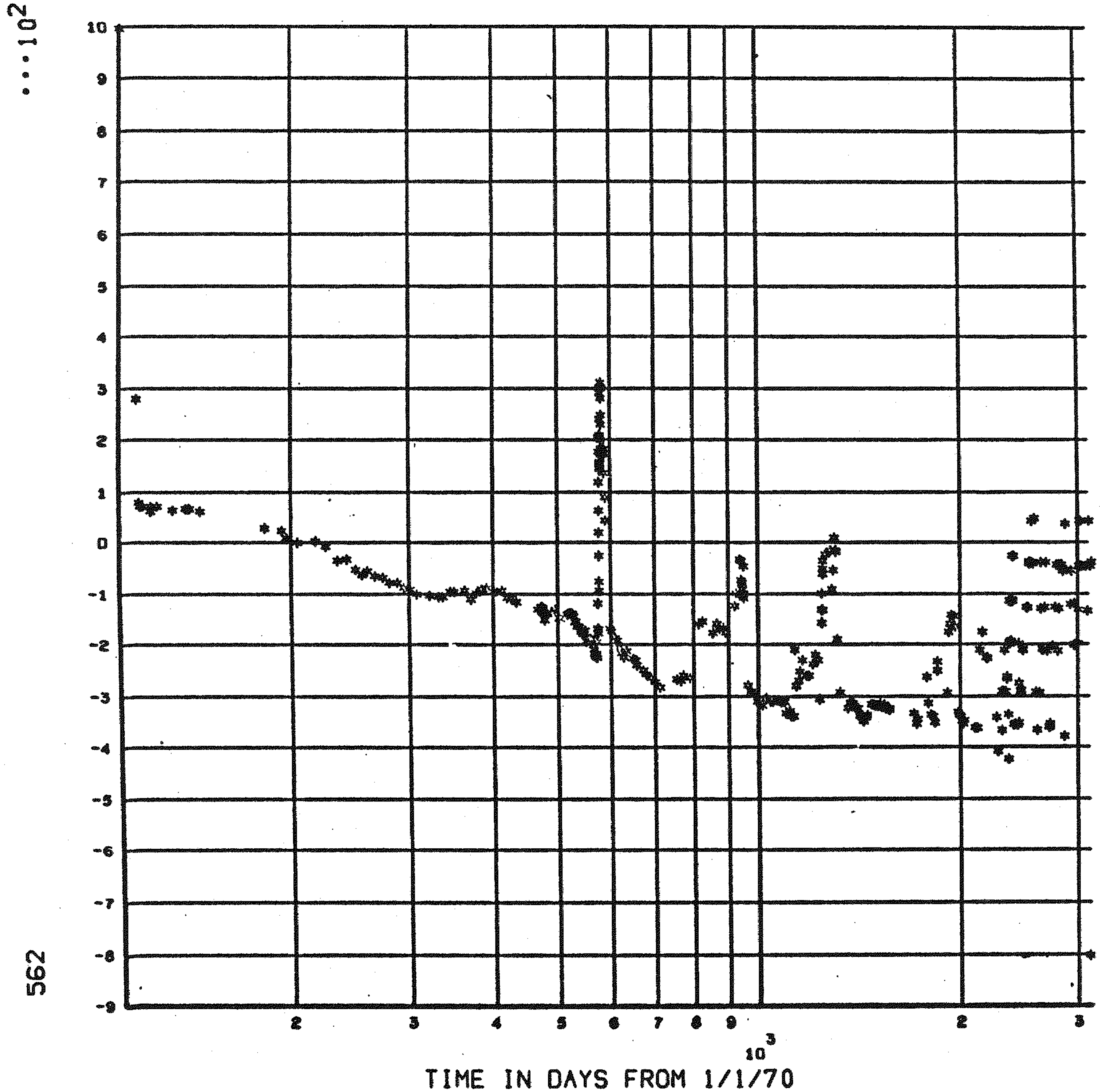

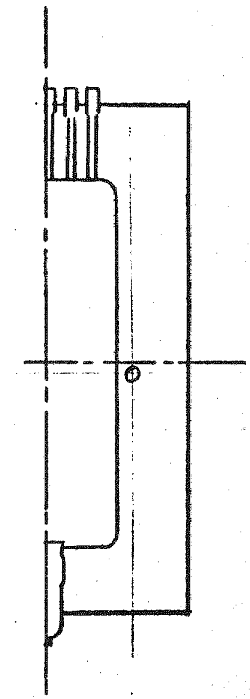

B-48

562

RUN 17146 30 AUG 78 03.14.27

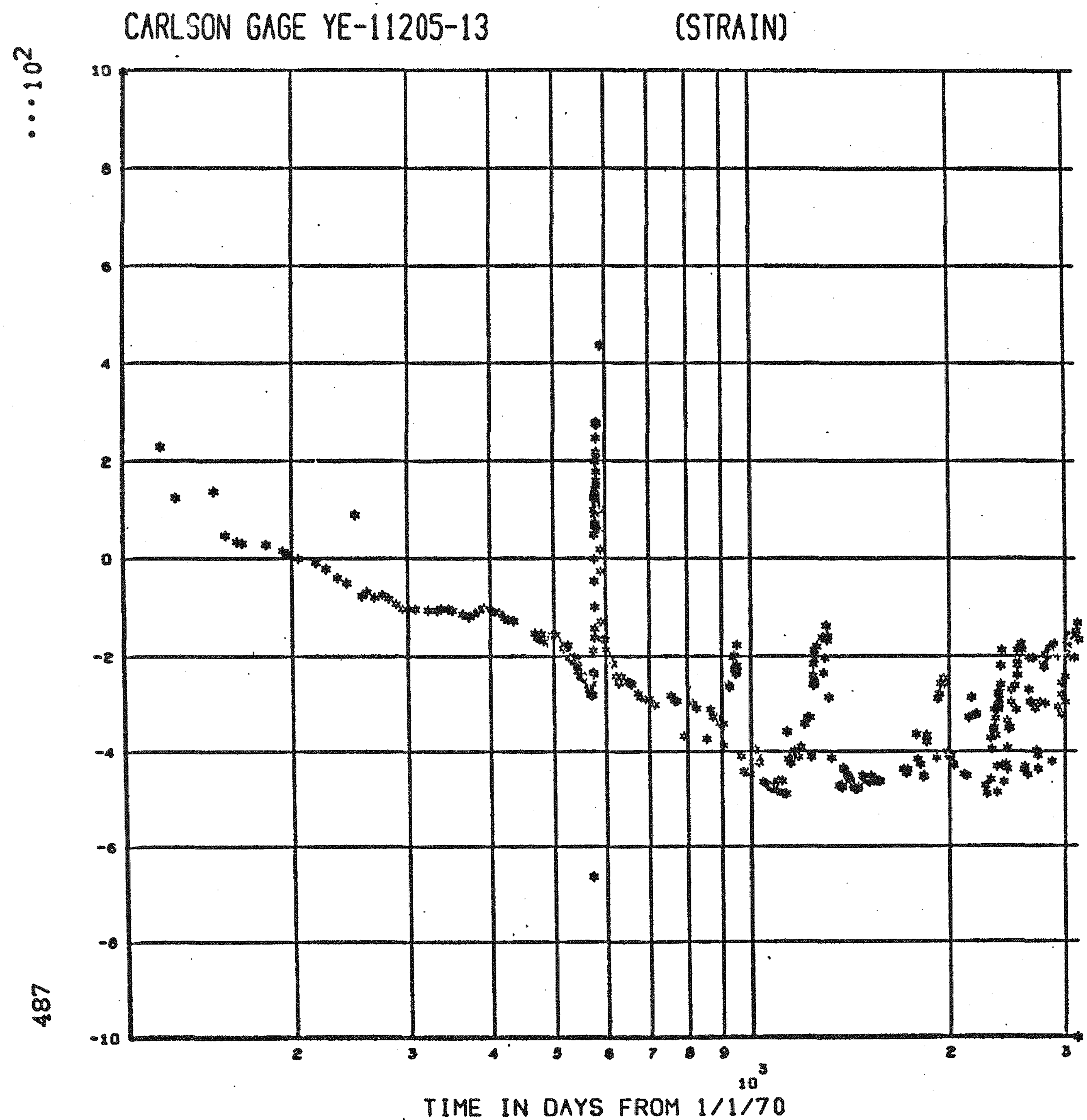

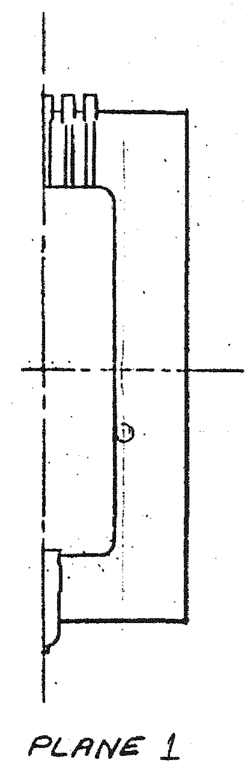

B-49

487

RUN 10741 29 AUG 78 23.07.49

CARLSON GAGE YE-11205-10 (STRAIN)

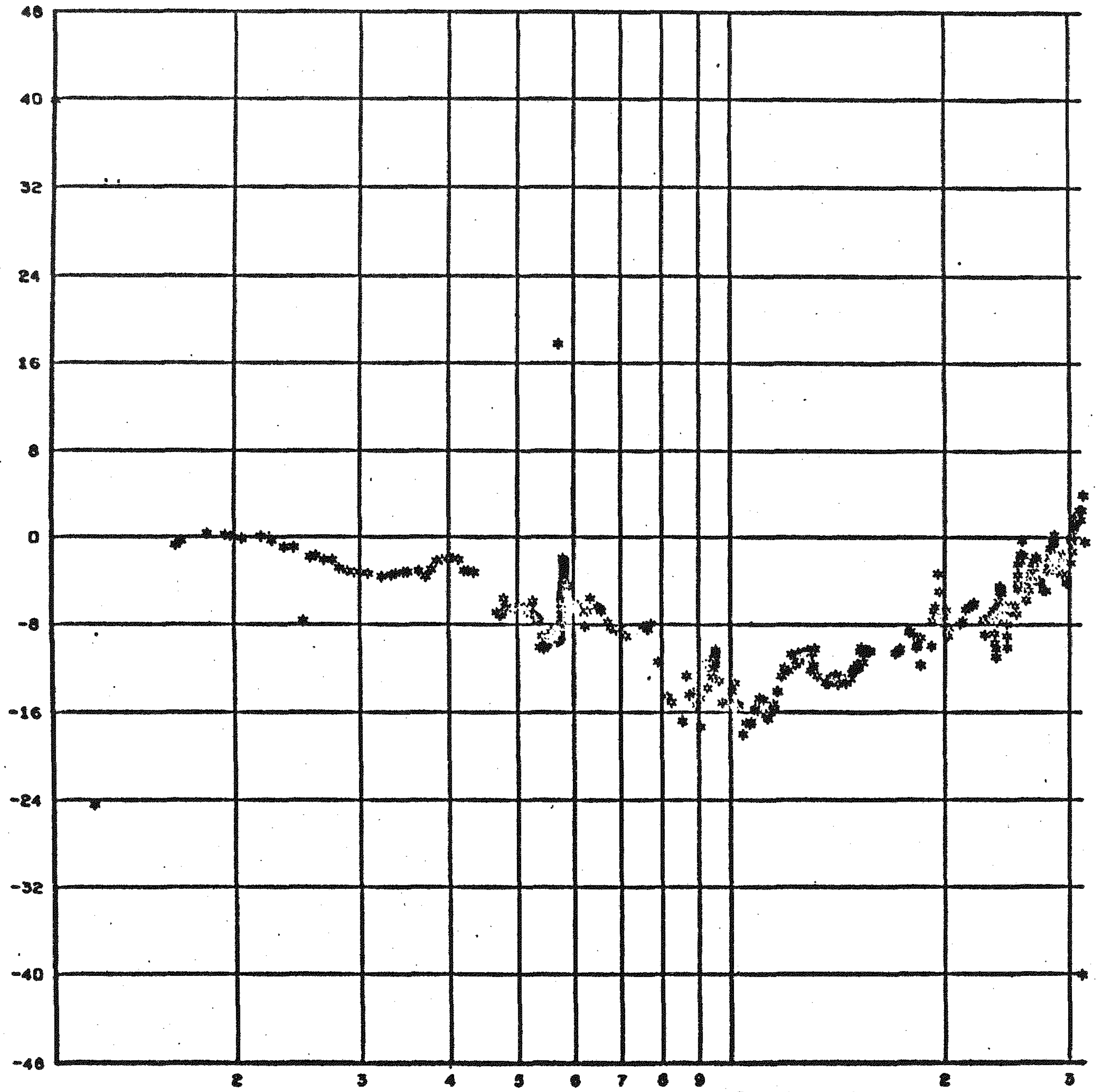

TIME IN DAYS FROM 1/1/70

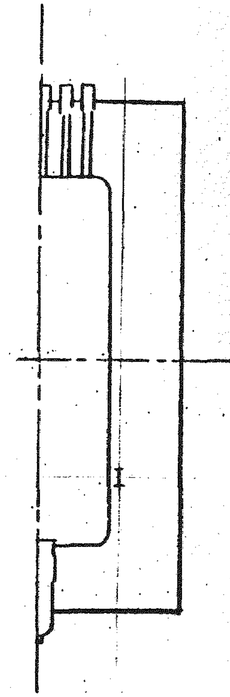

PLANE 1

RUN 10741 29 AUG 78 23.07.25

...10

484

CARLSON GAGE YE-11205-12 (STRAIN)

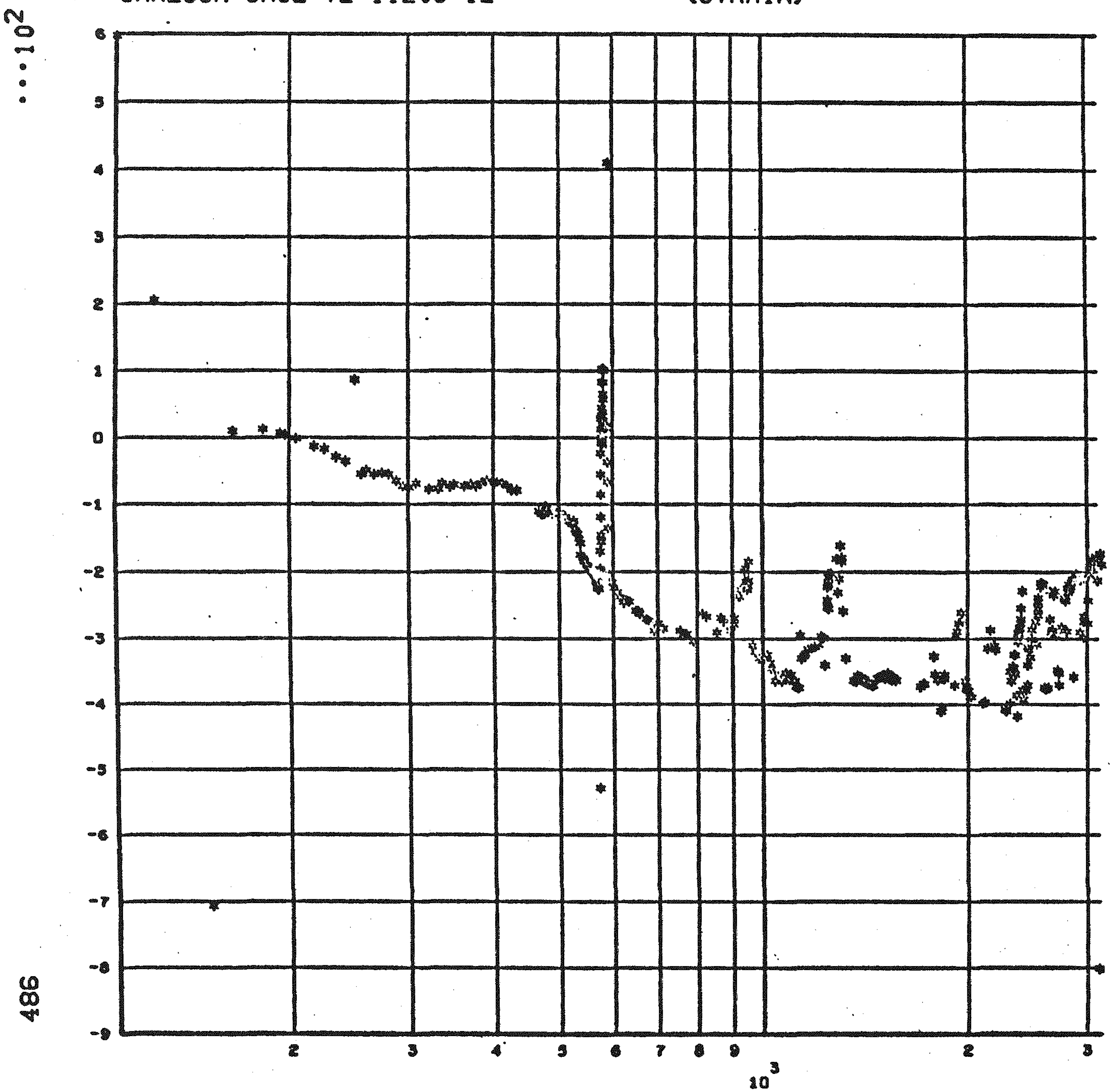

TIME IN DAYS FROM 1/1/70

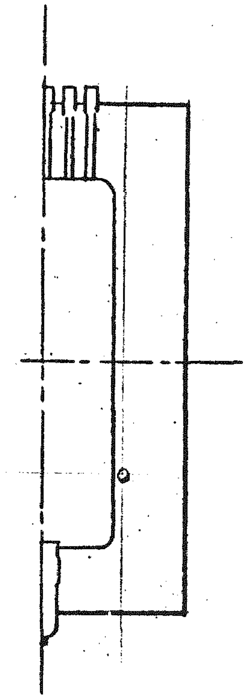

PLANE 3

RUN 10741 29 AUG 78 23.07.40

486

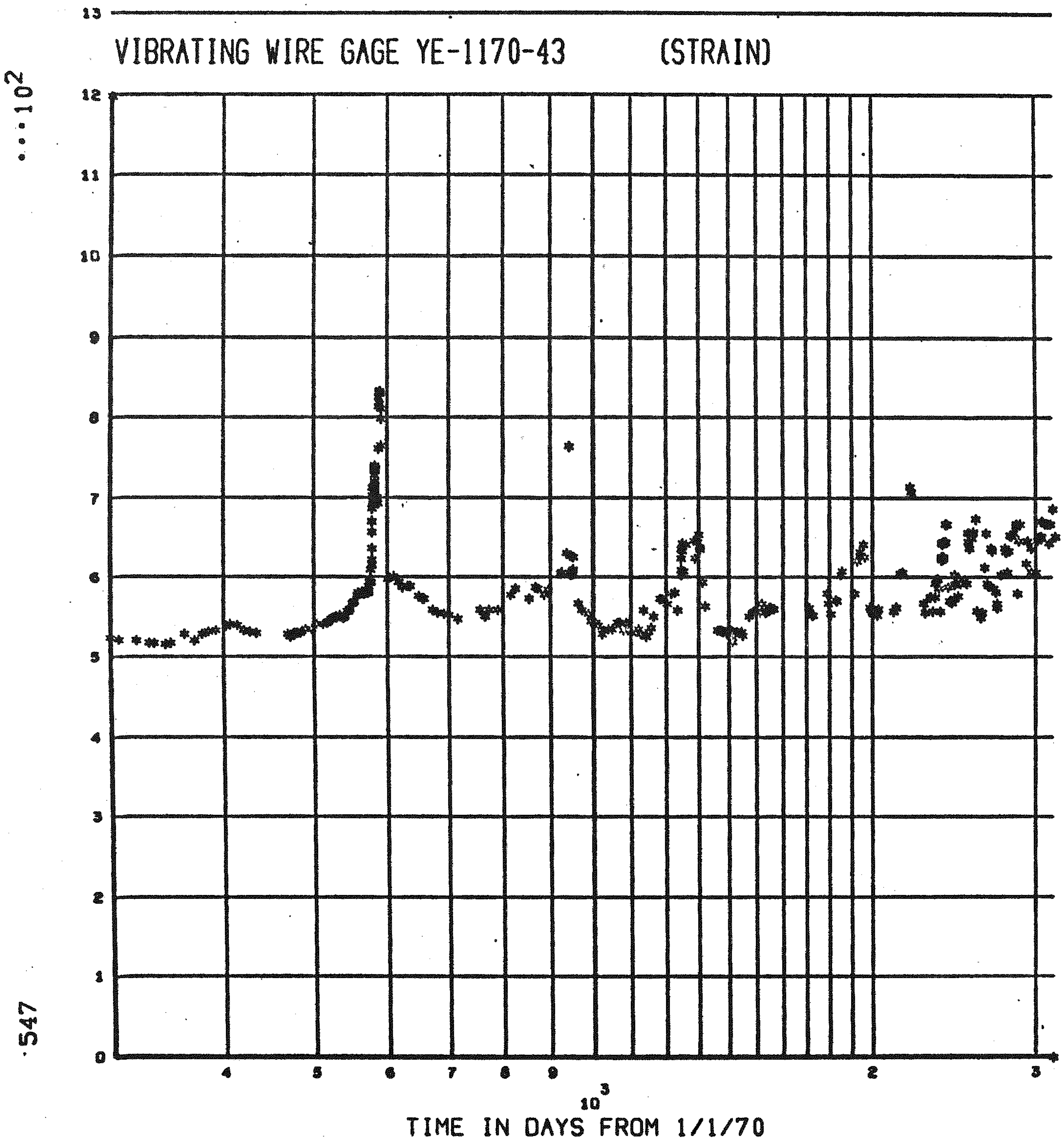

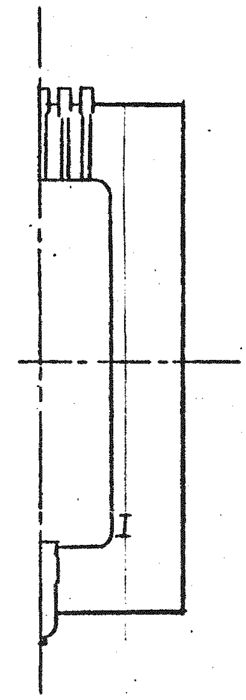

PLANE 1

B-52

RUN 17146 30 AUG 78 03.13.40

VIBRATING WIRE GAGE YE-1170-37 (STRAIN)

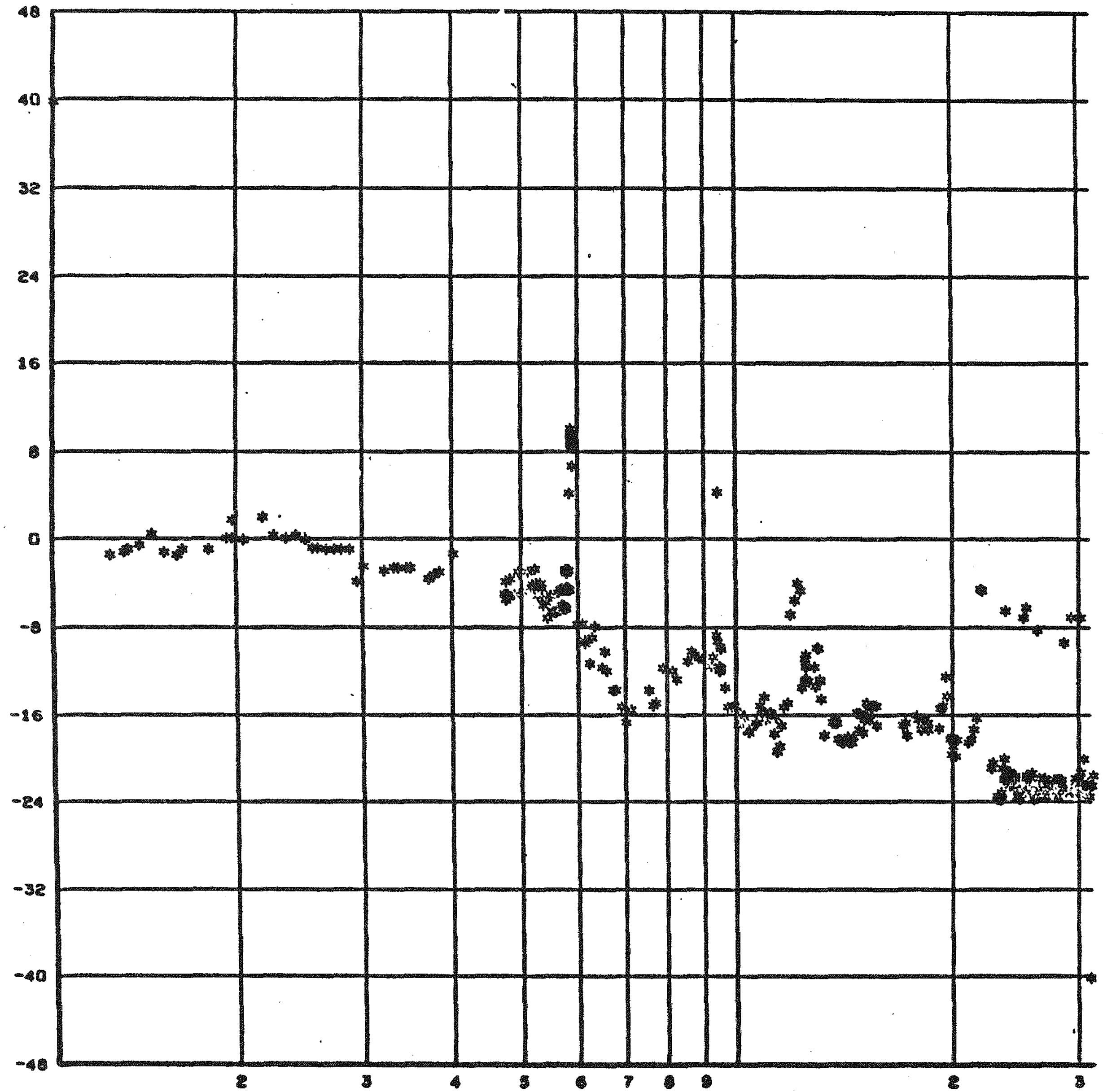

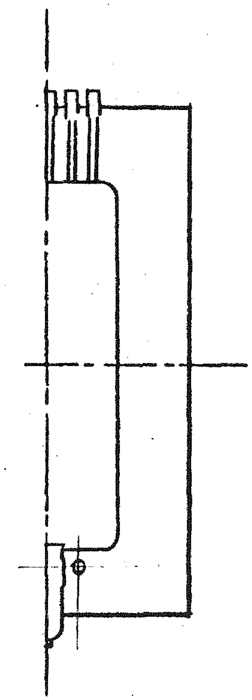

PLANE 3

B-53

...10

541

RUN 17146 30 AUG 78 03.11.31

VIBRATING WIRE GAGE YE-1170-41 (STRAIN)

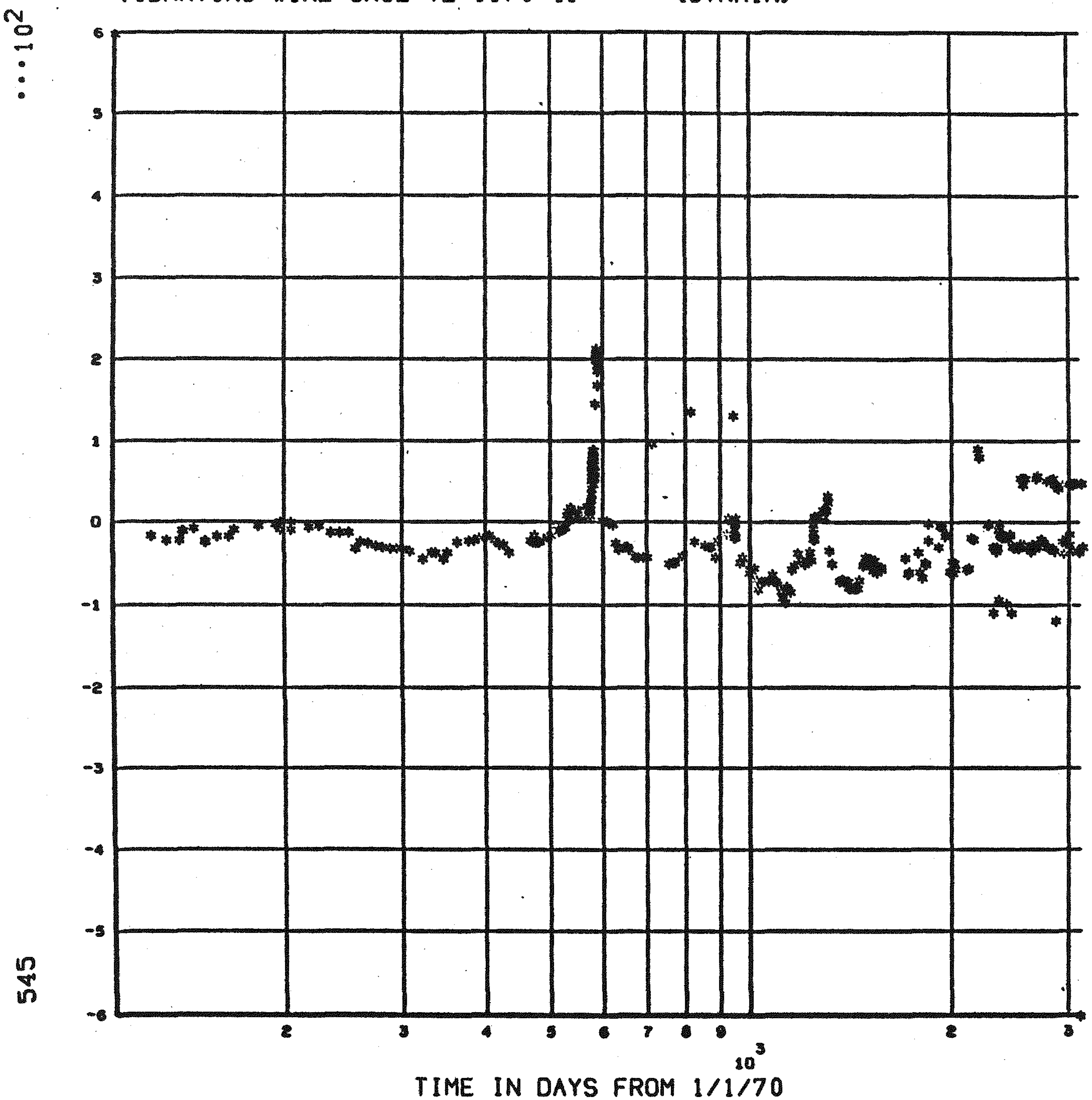

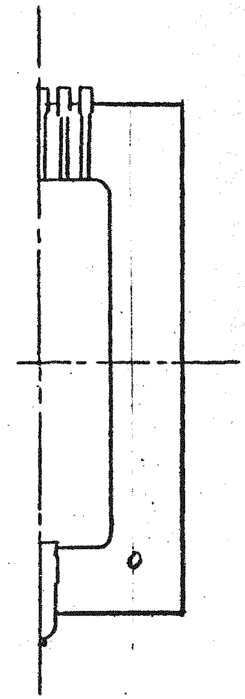

PLANE 3

RUN 17146 30 AUG 78 03.13.33

VIBRATING WIRE GAGE YE-1170-15 (STRAIN)

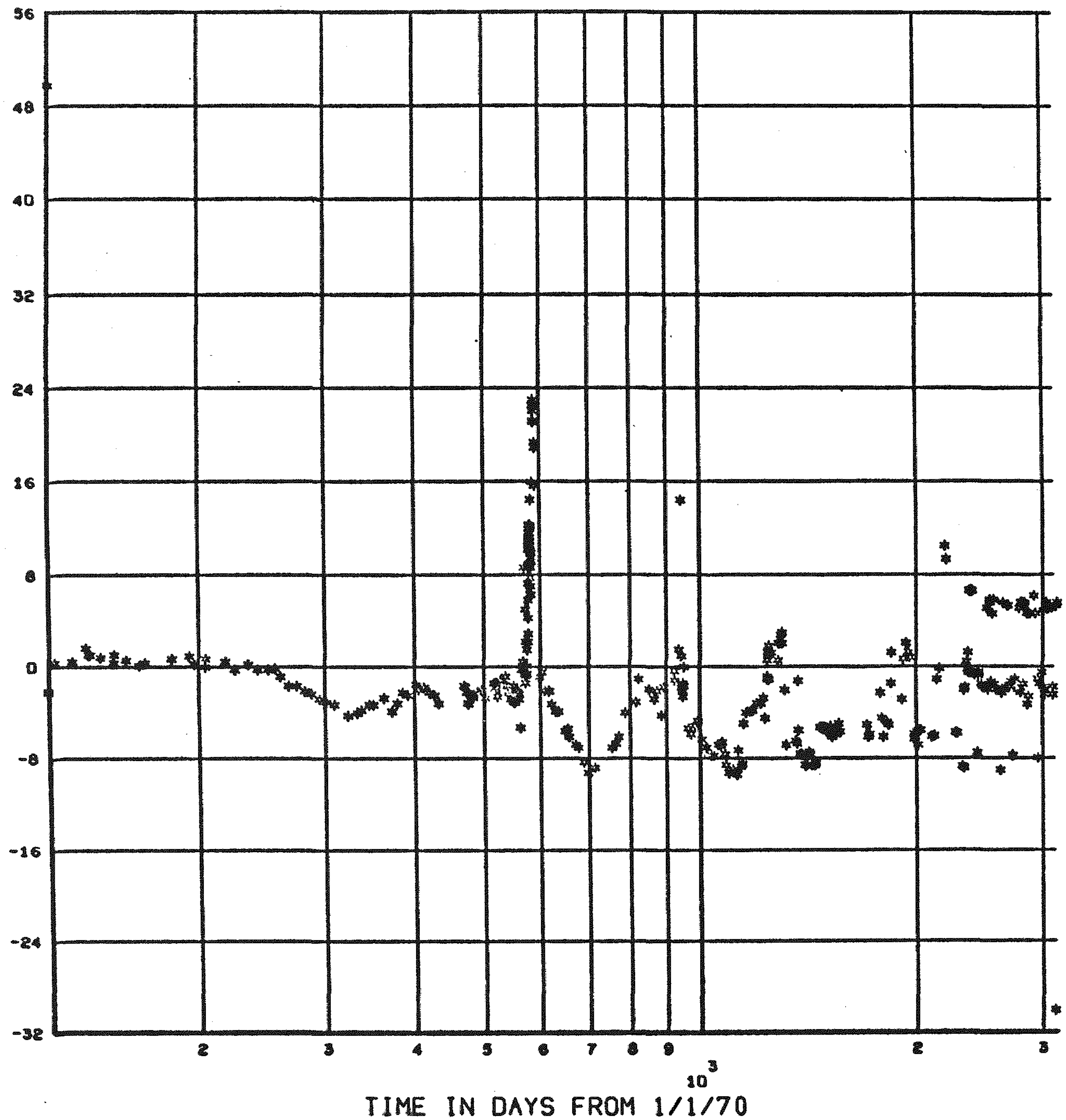

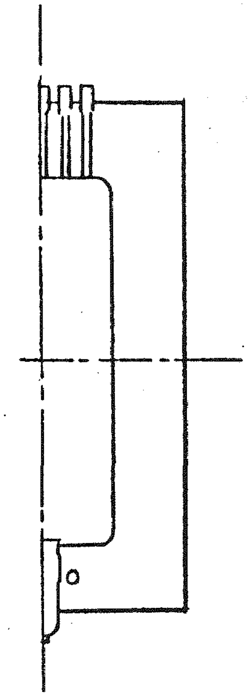

PLANE 1

RUN 17146 30 AUG 78 03.08.42

519

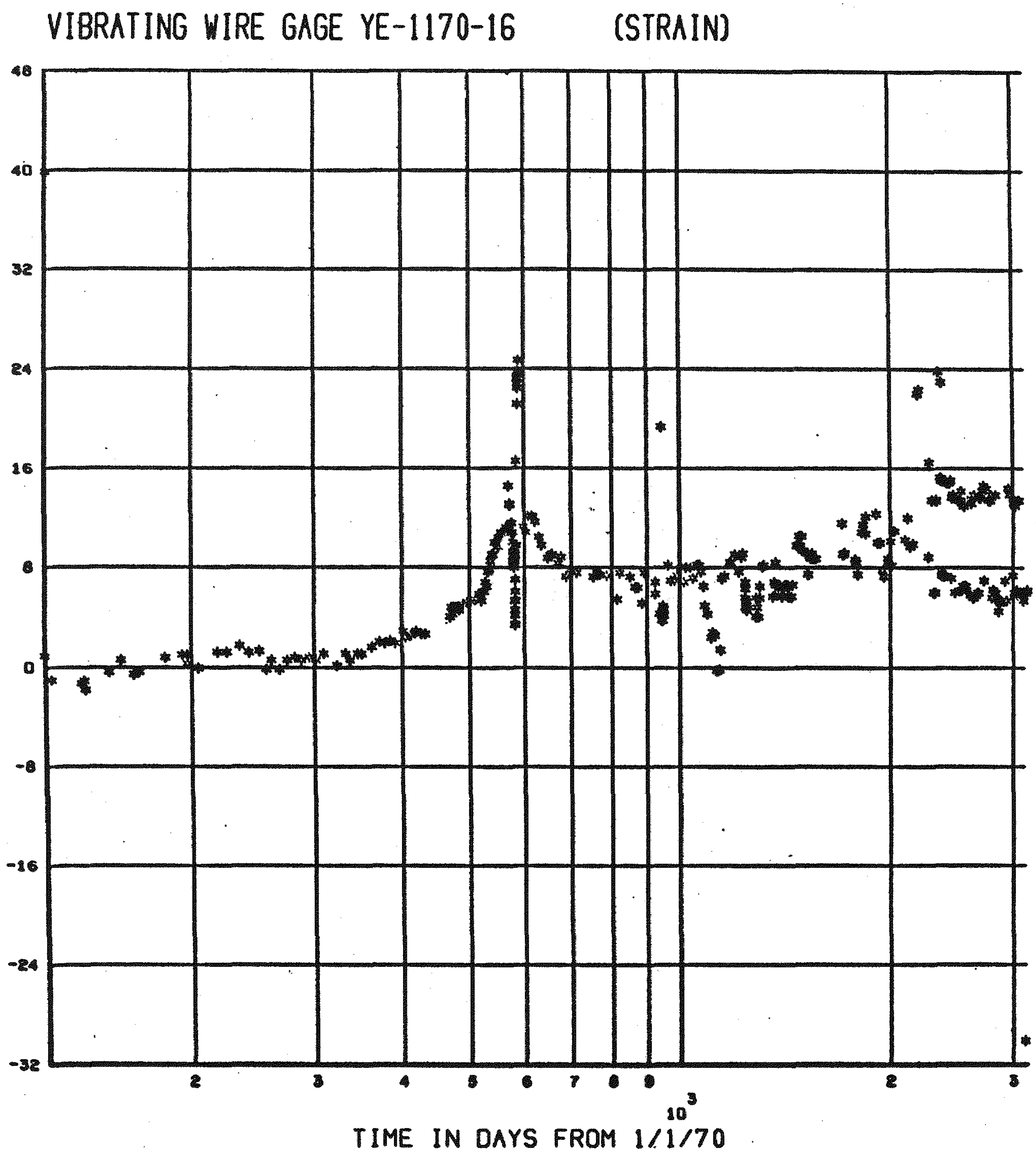

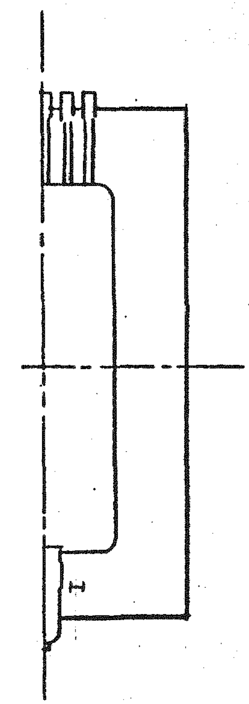

PLANE 1

RUN 17146 30 AUG 78 03.08.48

...10

520

CARLSON GAGE YE-11205-4 (STRAIN)

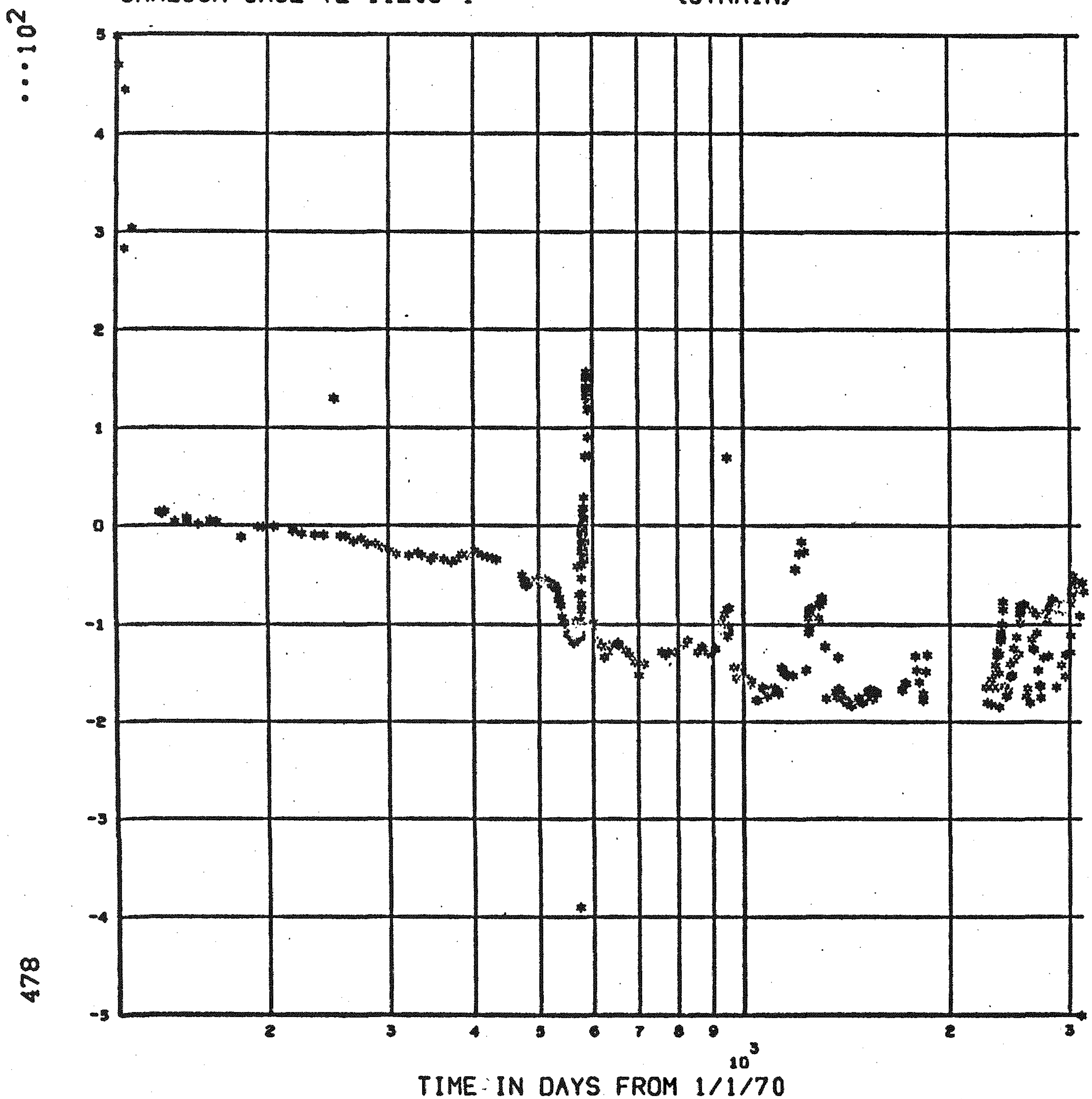

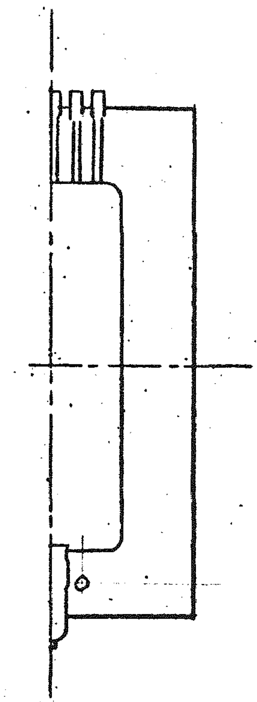

PLANE 3

B-57

478

RUN 10741 29 AUG 78 23.07.01

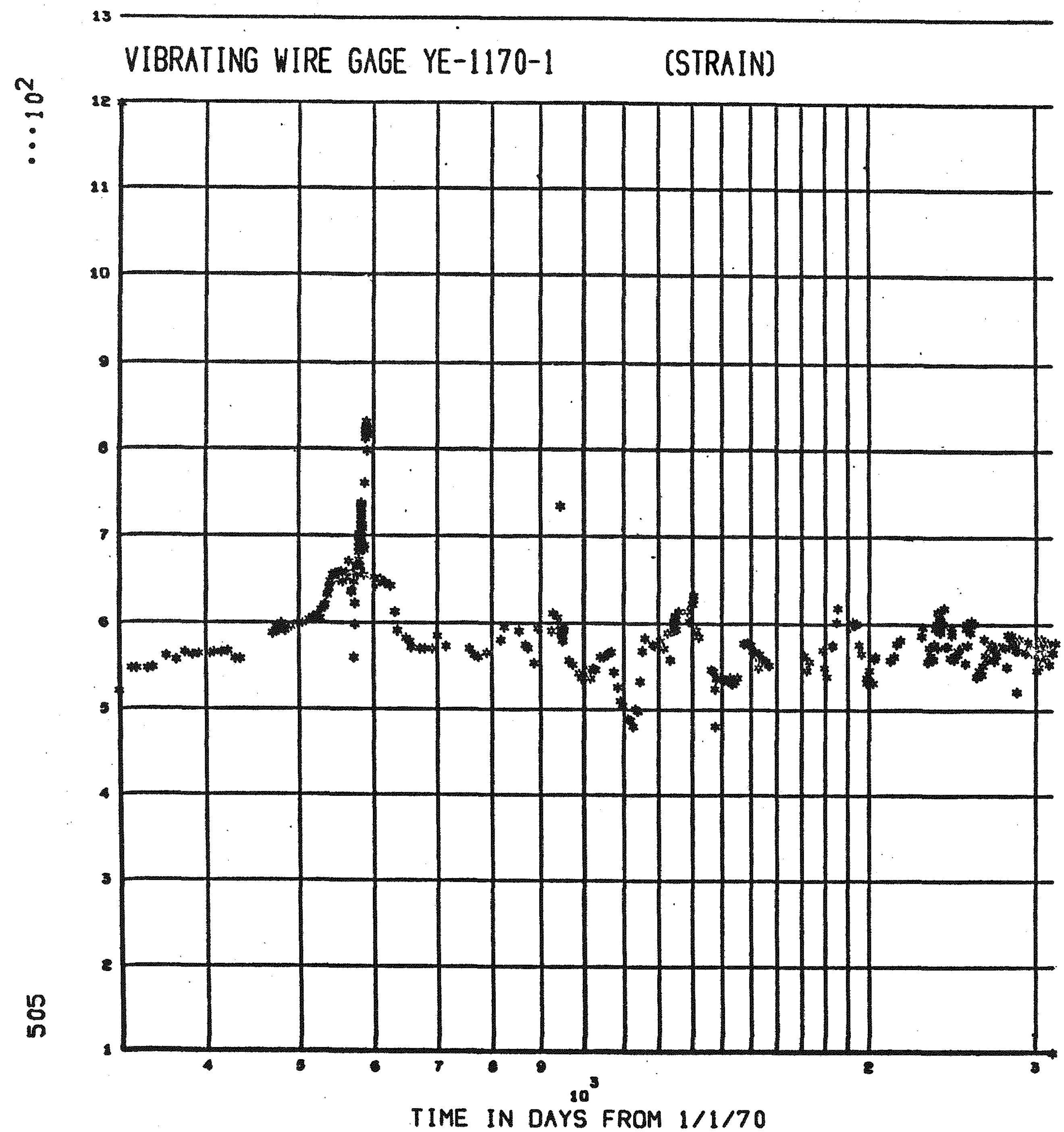

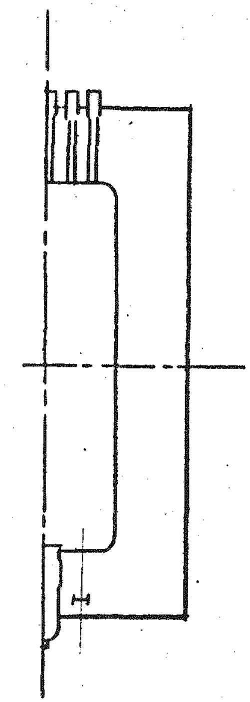

PLANE 1

RUN 17146 30 AUG 78 03.07.56

505

VIBRATING WIRE GAGE YE-1170-2 (STRAIN)

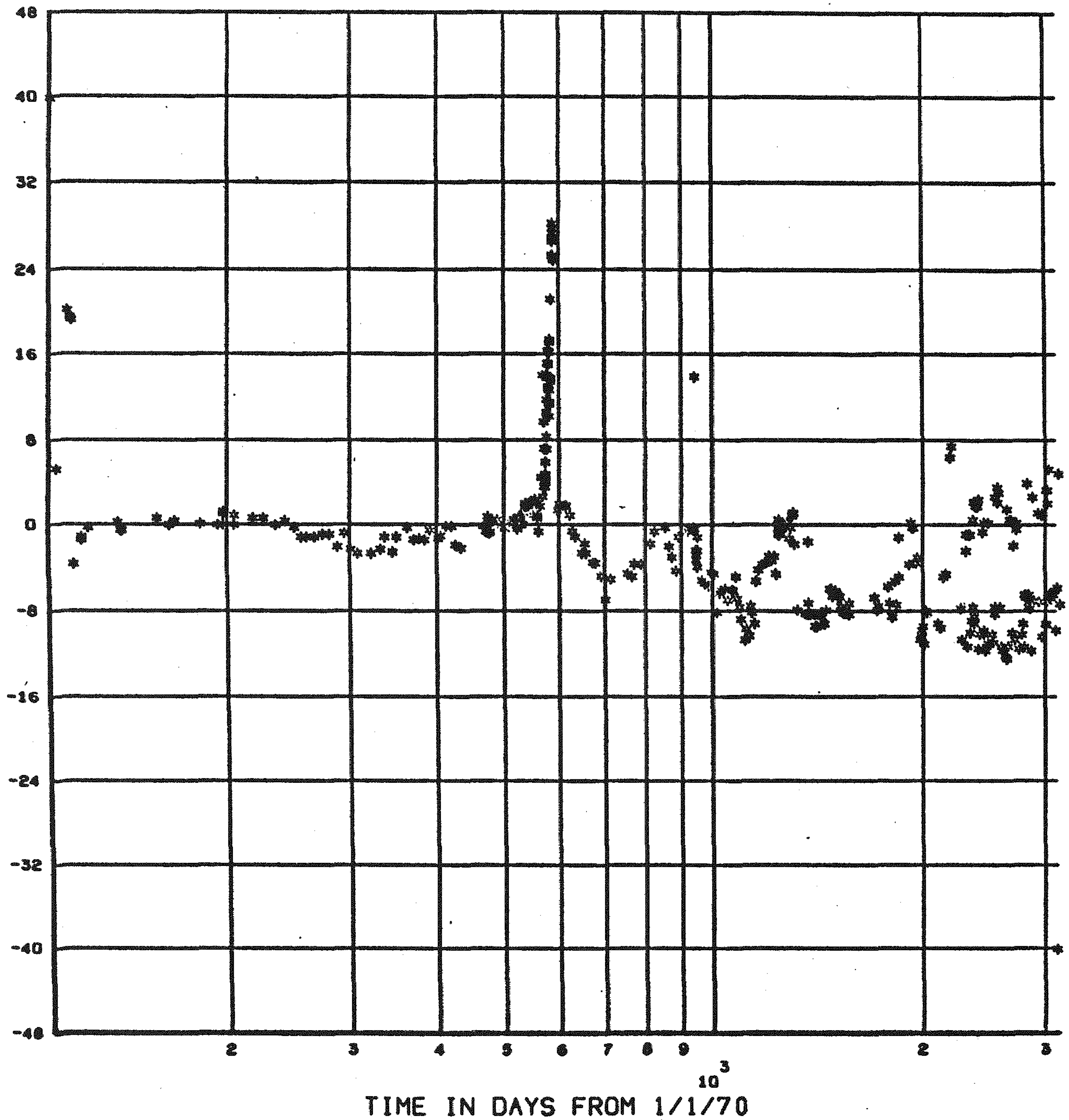

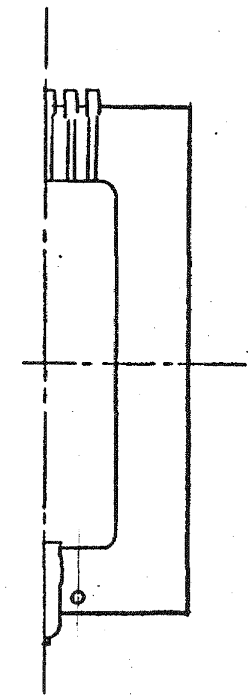

PLANE 1

RUN 17146 30 AUG 78 03.08.01

506

VIBRATING WIRE GAGE YE-1170-9 (STRAIN)

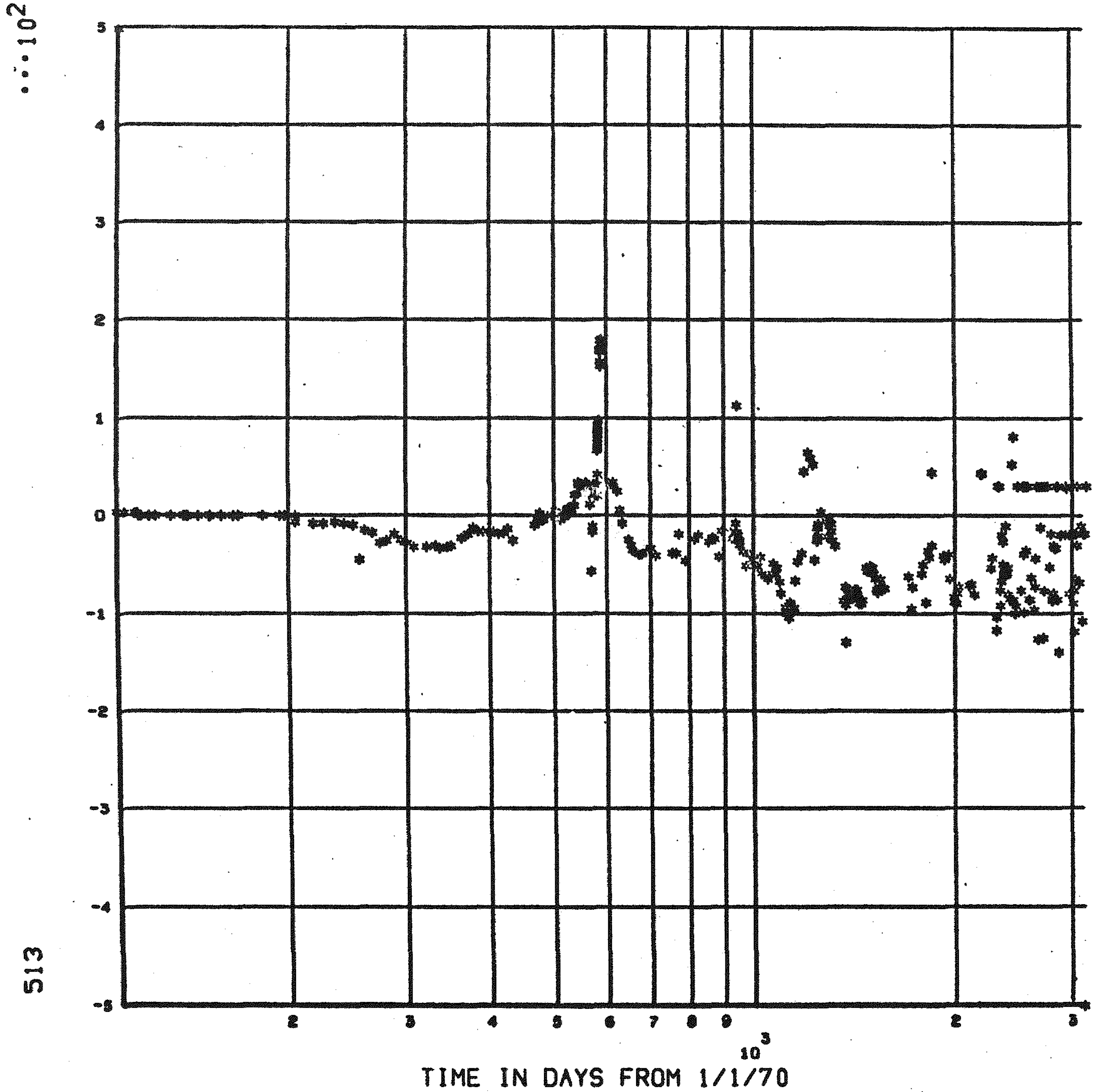

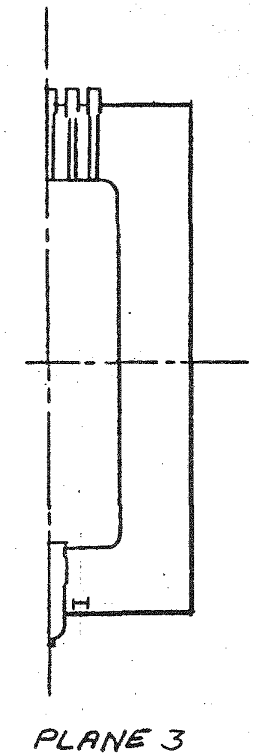

RUN 17146 30 AUG 78 03.08.18

513

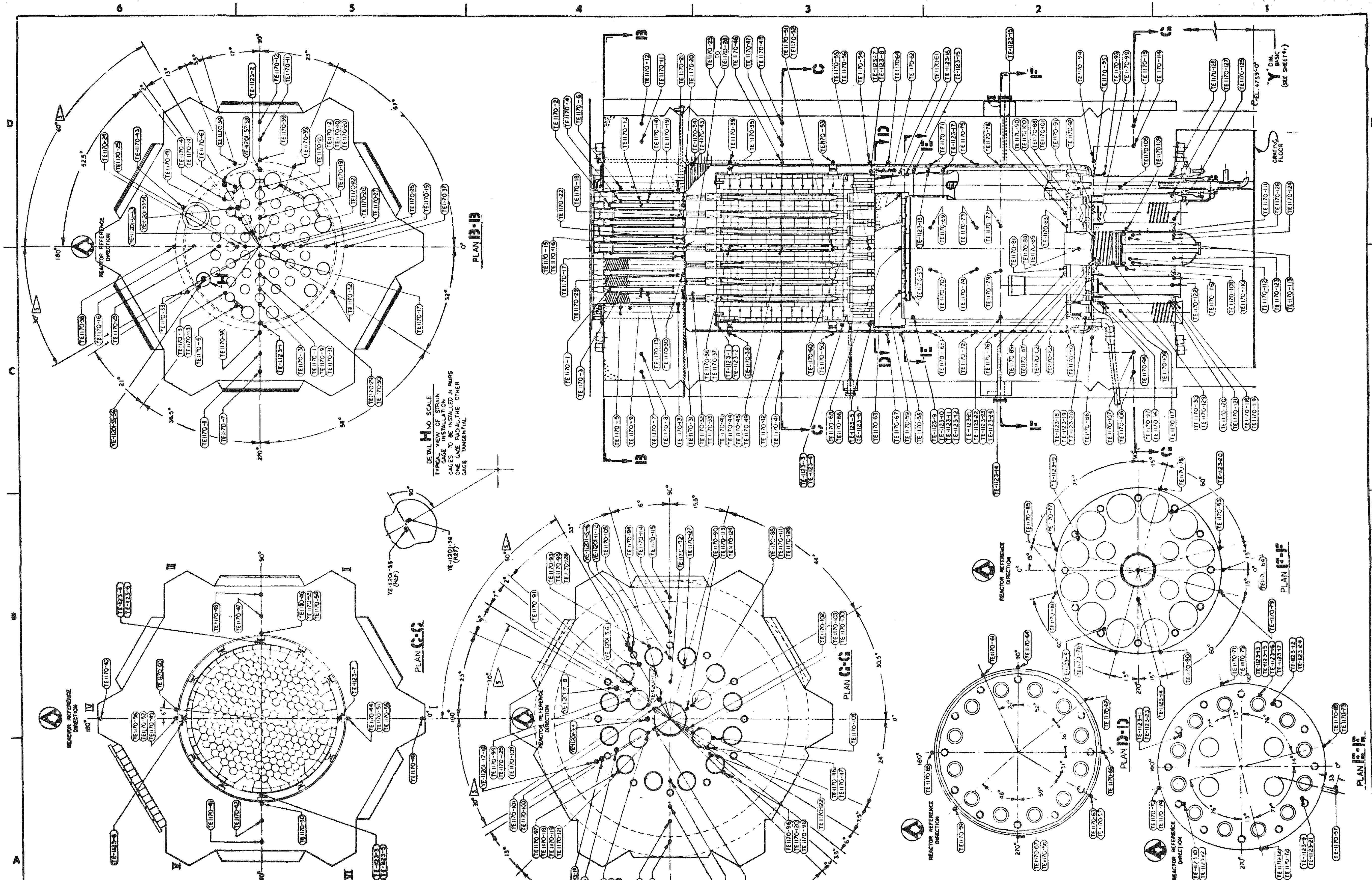

REQUIRED	ITEM	PART NO.	DESCRIPTION	MATL	MATL SPEC

LIST OF MATERIAL

LTR	DATE	ISSUE DESCRIPTION	DR	CHKD	DES	APPD	APPD
C		GENERAL REVISION	LK	PCA			
B		FOR CONSTRUCTION	PCA				
A		FOR INQUIRY					

UNLESS OTHERWISE SPECIFIED DIMENSIONS ARE IN INCHES
TOLERANCES
ALL MACHINED SURFACES ✓

NEXT ASSEMBLY 90-R1100-100

SCALE 3/16" = 1'0"

PCRV LINER PENETRATIONS & CONCRETE THERMOCOUPLES & LINER STRAIN GAGES

Gulf General Atomic Incorporated

PROJ NO 90 | DRAWING NUMBER R1100-104 | ISSUE C

SHEET 2

THERMOCOUPLE TE-1170-1 (TEMPERATURE) TOP HEAD

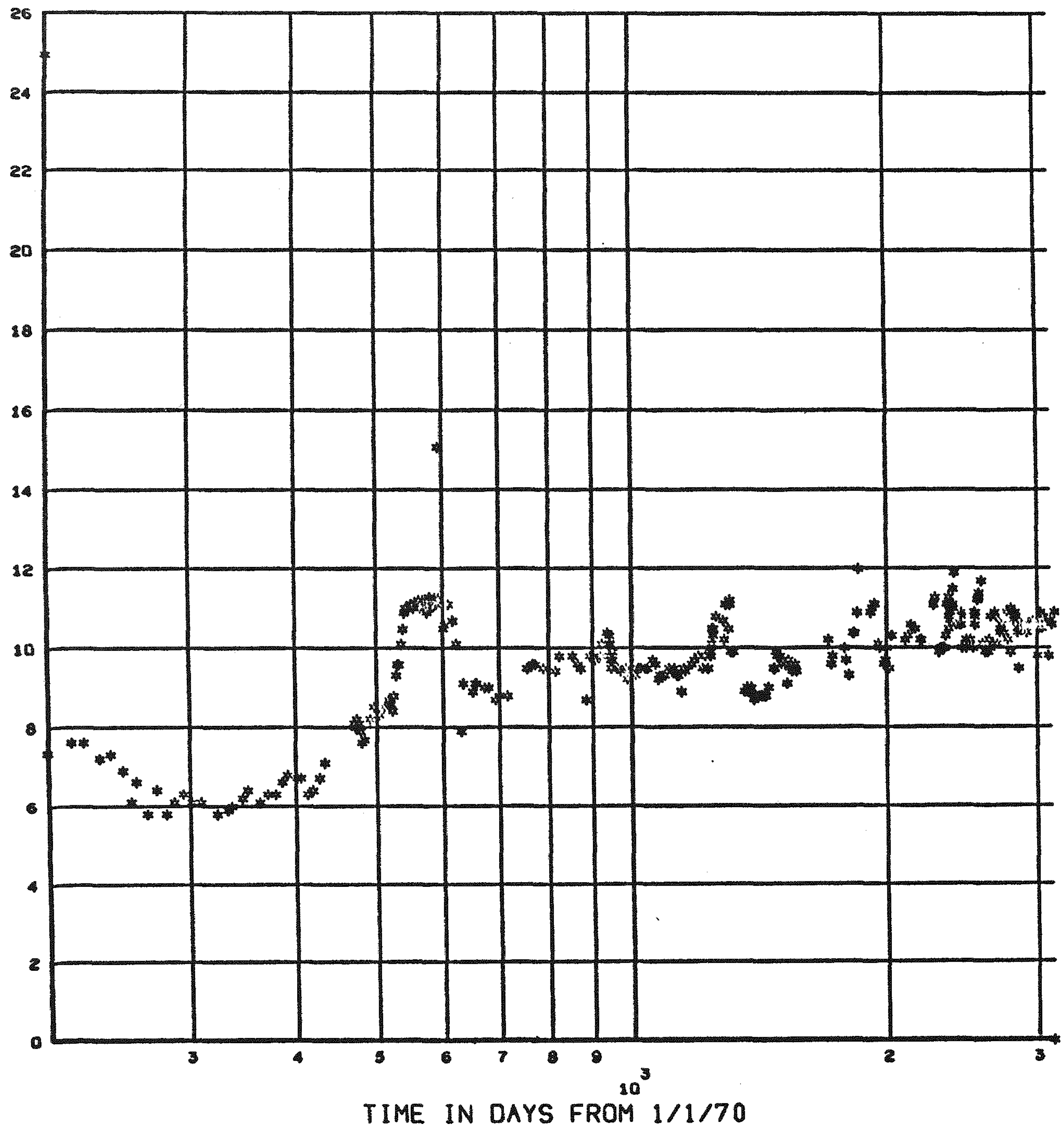

RUN 17146 14 SEP 78 21.37.25

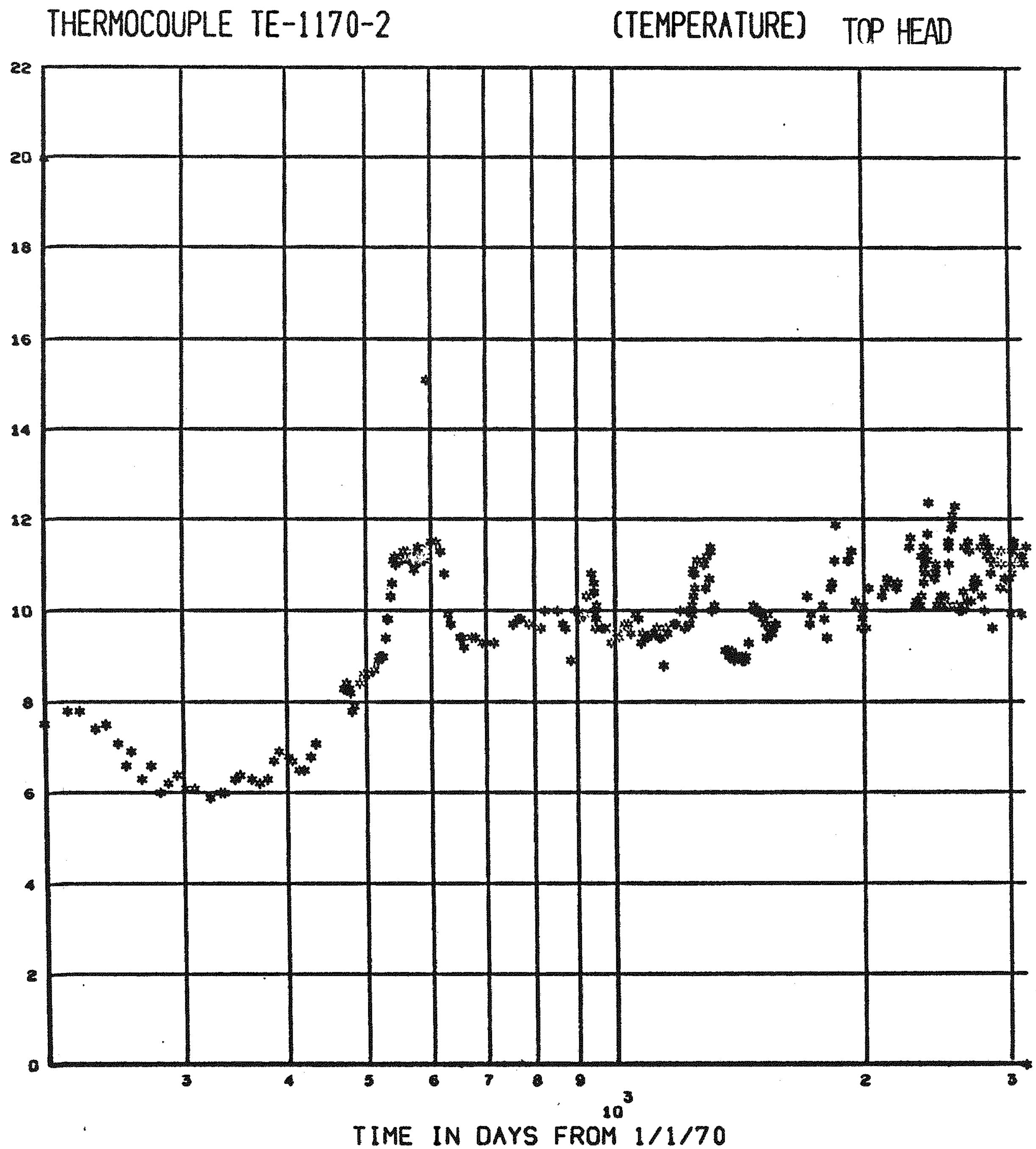

RUN 17146 14 SEP 78 21.37.29

B-64

56

...10

THERMOCOUPLE TE-1170-9 (TEMPERATURE) TOP HEAD

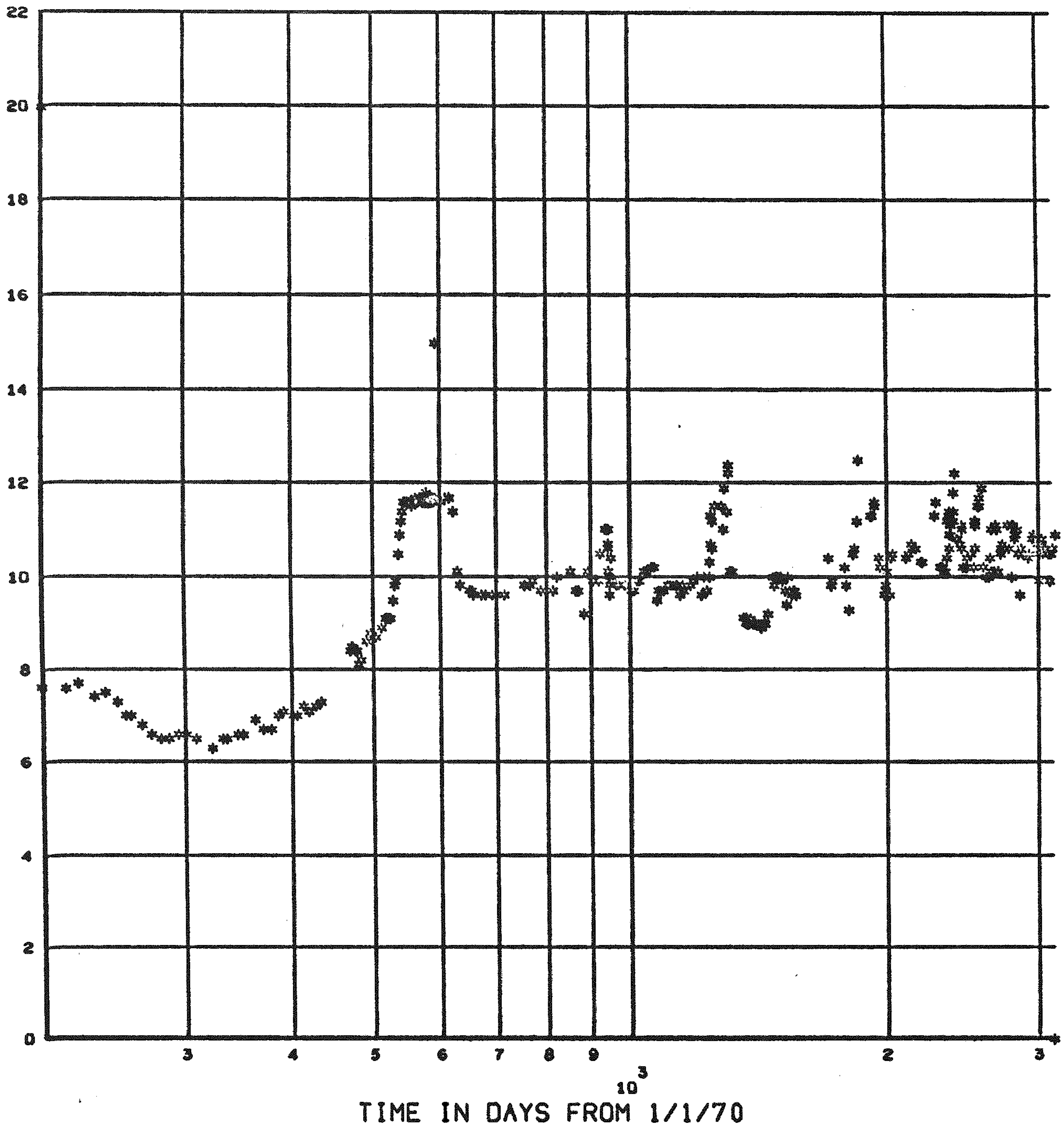

RUN 17146 14 SEP 78 21.37.57

63

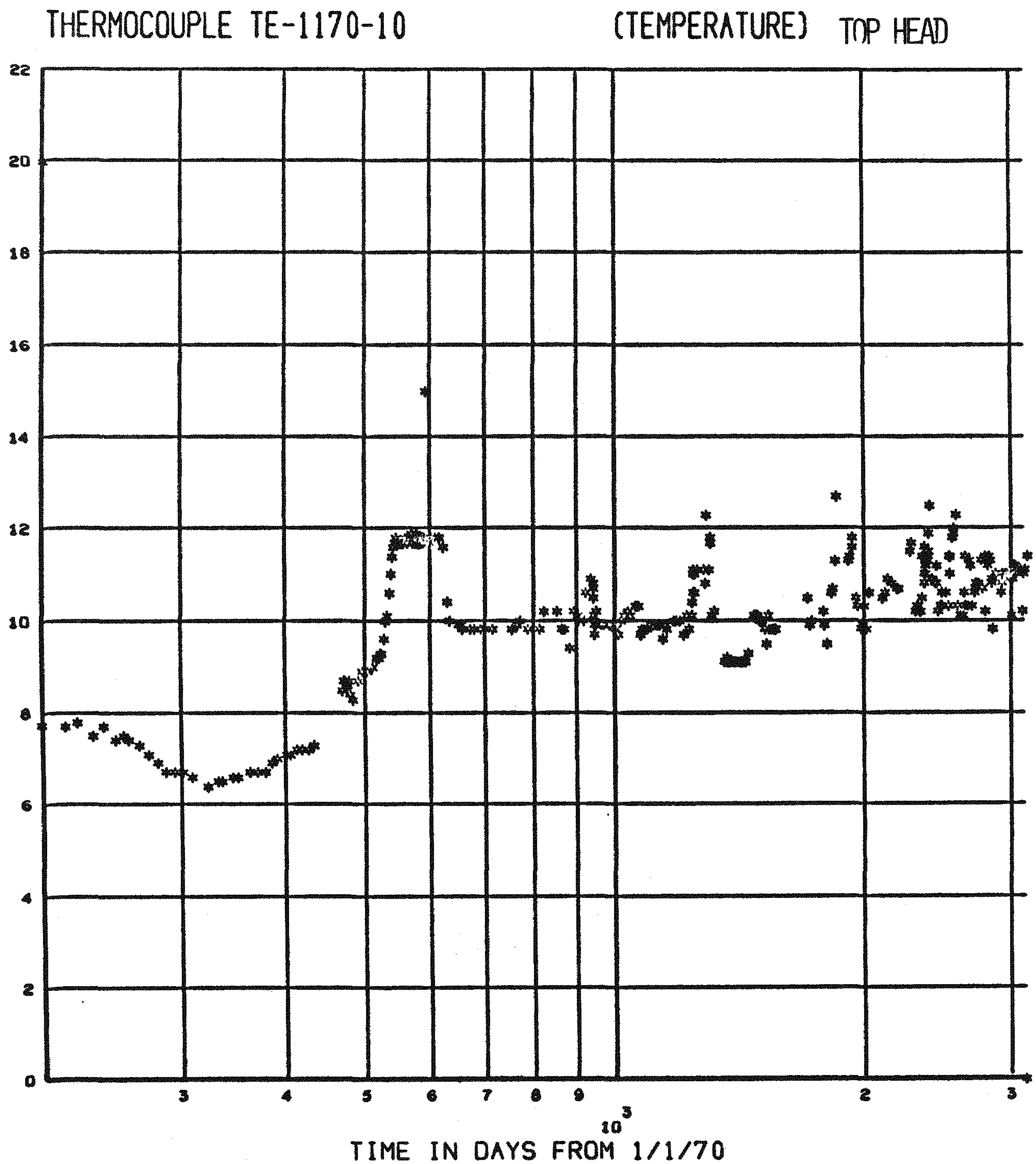

RUN 17146 14 SEP 78 21.38.01

...10

64

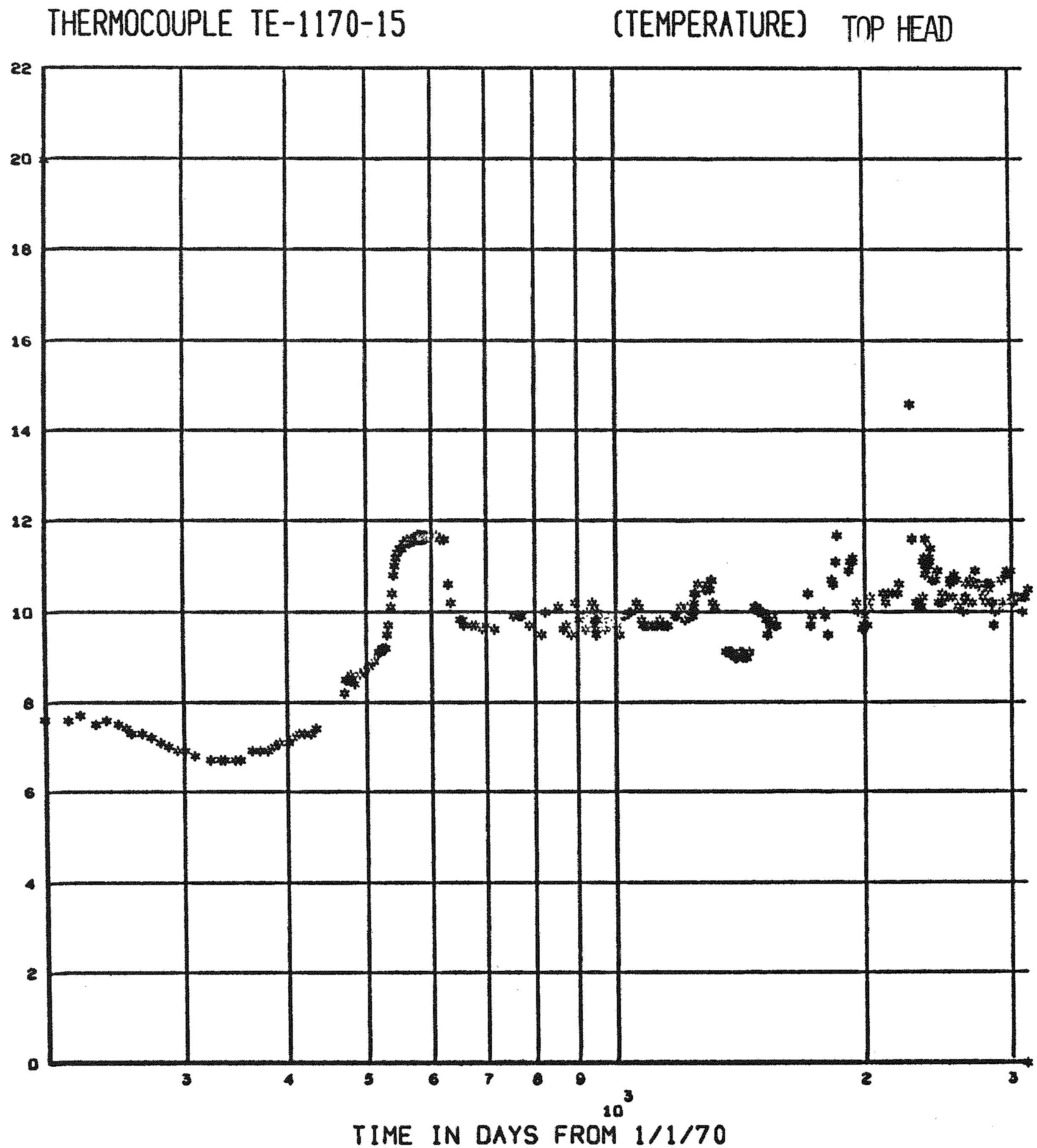

RUN 17146 14 SEP 78 21.40.49

69

THERMOCOUPLE TE-1170-16 (TEMPERATURE) TOP HEAD

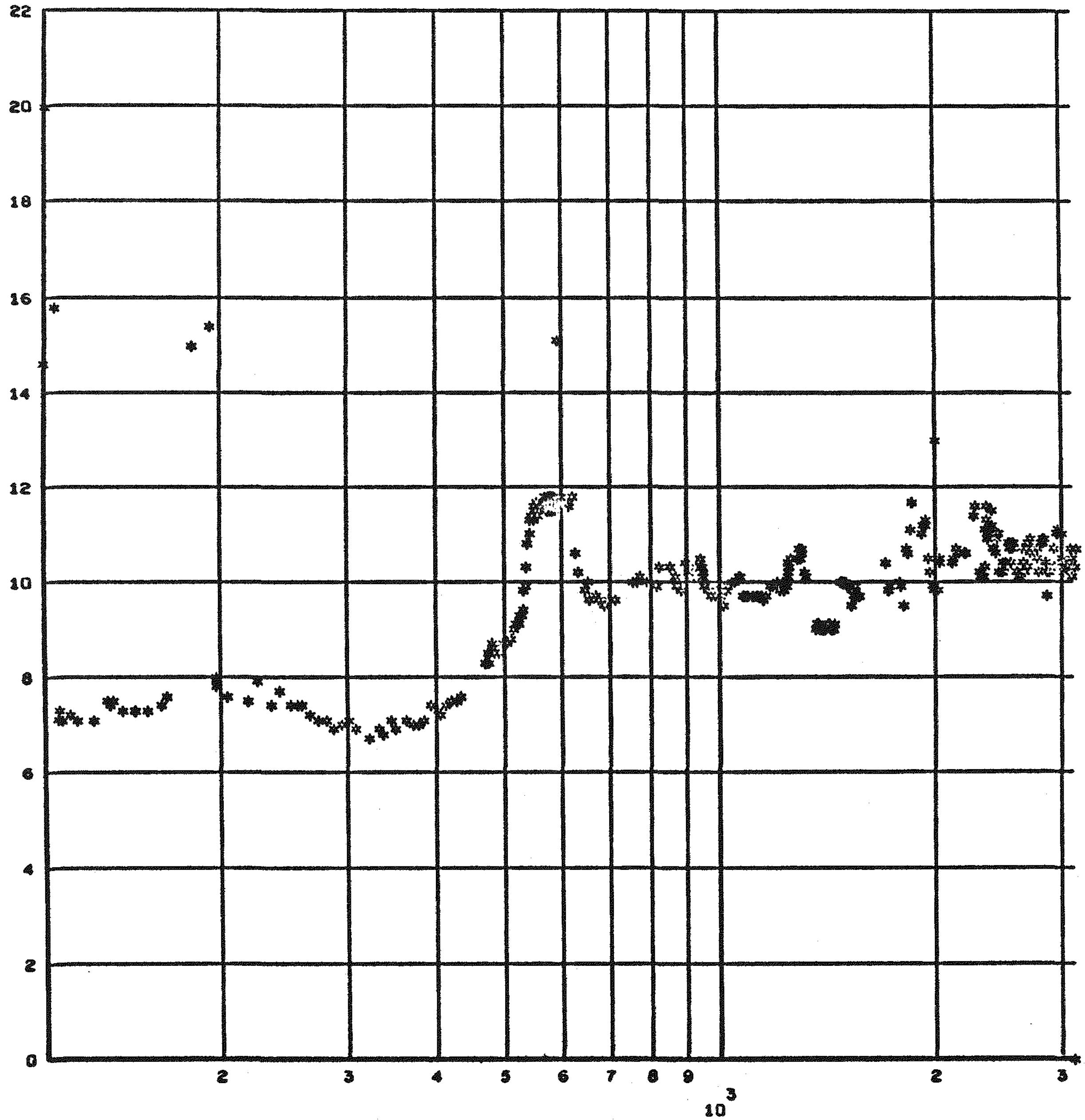

RUN 17146 14 SEP 78 21.40.53

THERMOCOUPLE TE-1170-17 (TEMPERATURE) TOP HEAD

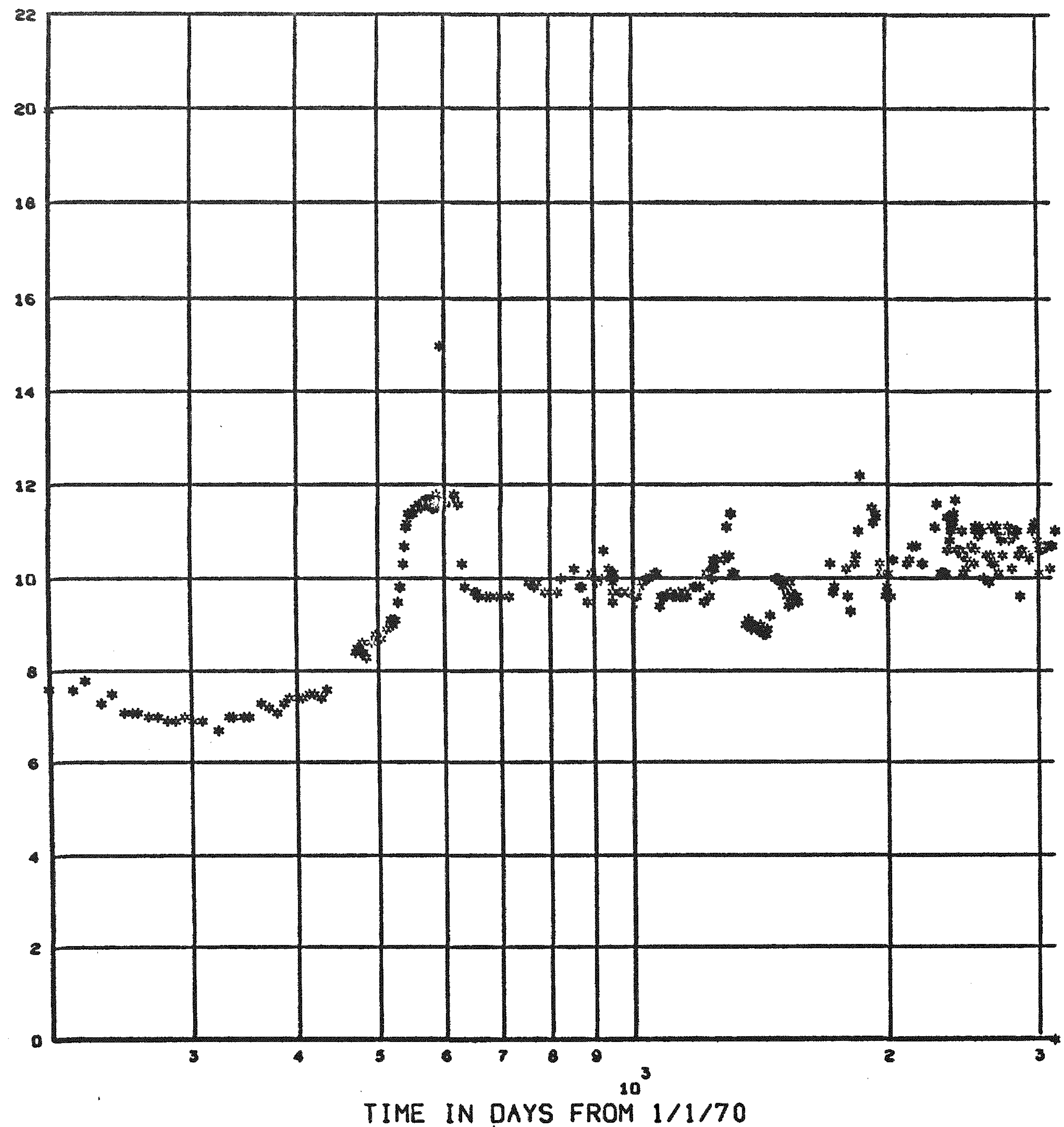

RUN 17146 14 SEP 78 21.40.57

THERMOCOUPLE TE-1170-19 (TEMPERATURE) TOP HEAD

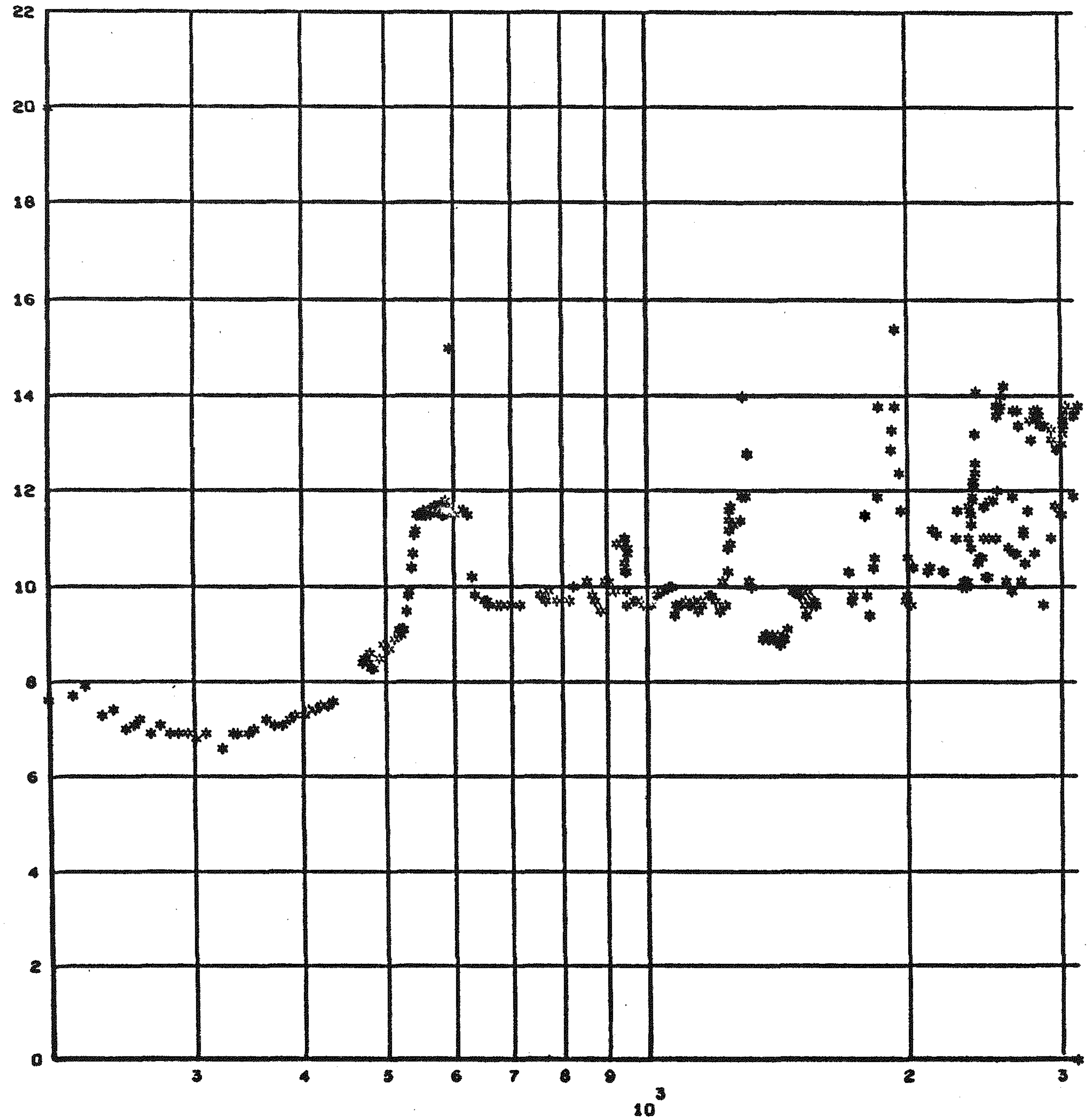

RUN 17146 14 SEP 78 21.41.03

...10

B-70

73

...10

B-71

76

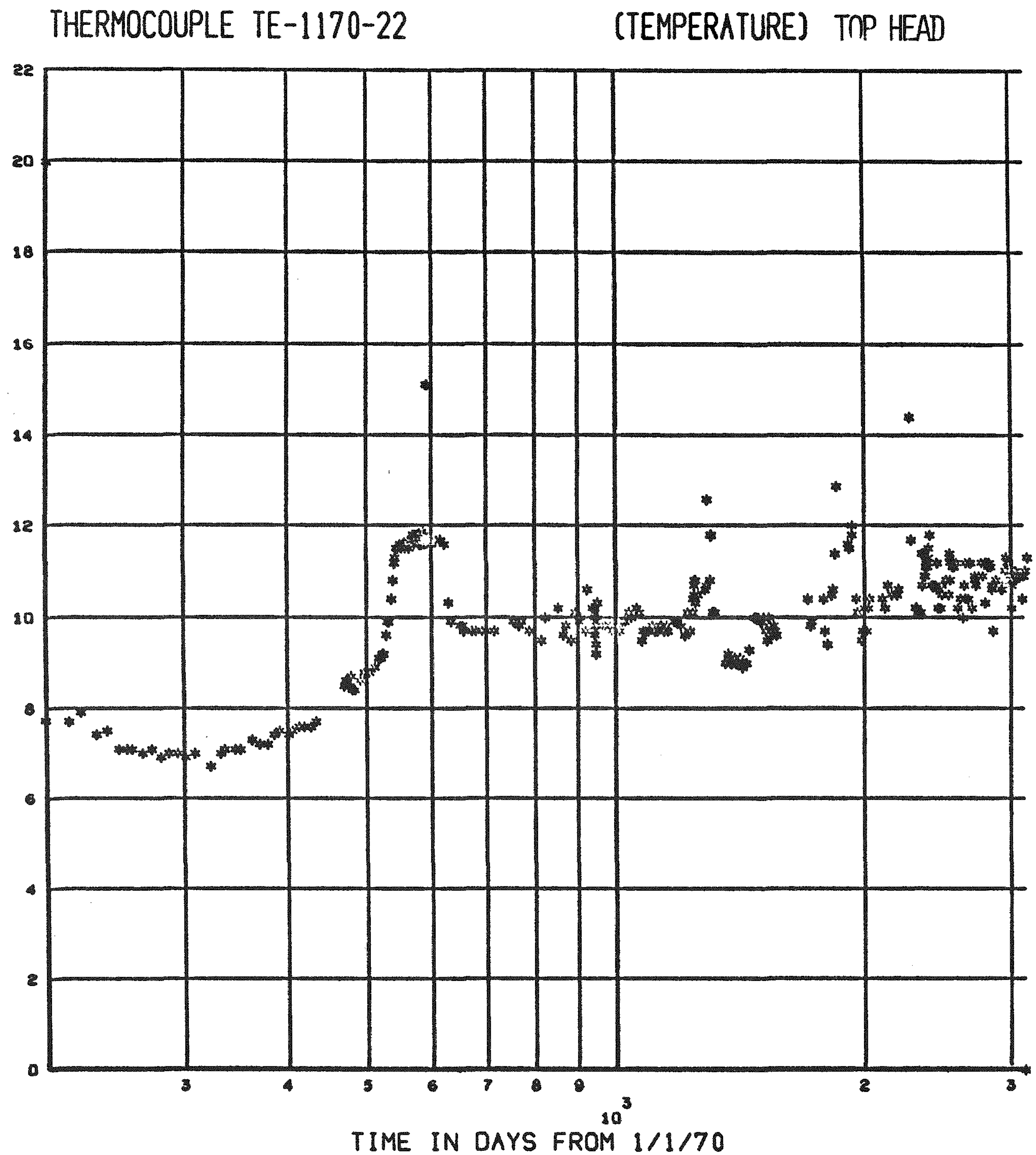

RUN 17146 14 SEP 78 21.41.09

THERMOCOUPLE TE-1170-23 (TEMPERATURE) TOP HEAD

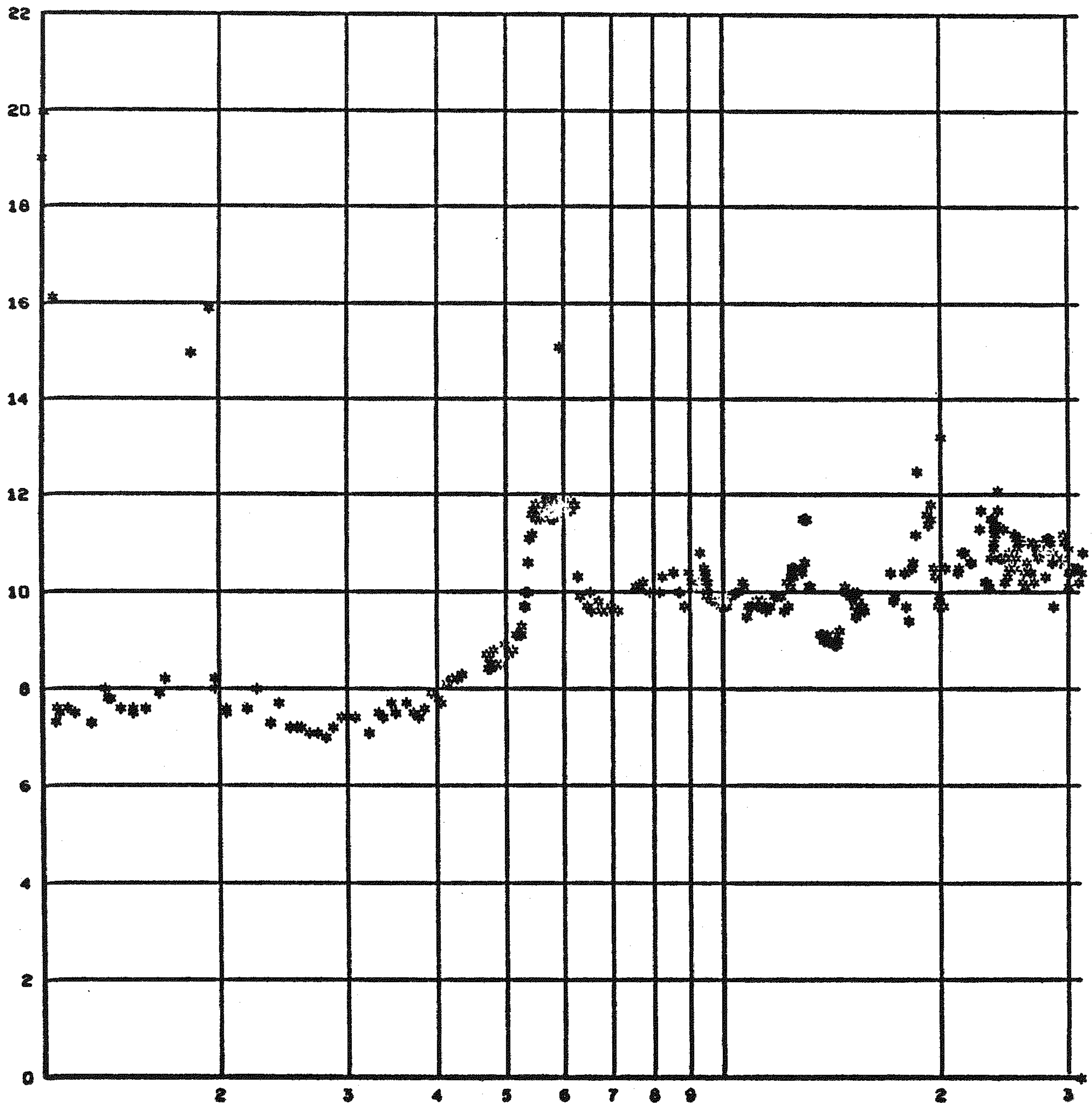

TIME IN DAYS FROM 1/1/70

RUN 17146 14 SEP 78 21.41.12

B-72

77

...10

THERMOCOUPLE TE-1170-24 (TEMPERATURE) TOP HEAD

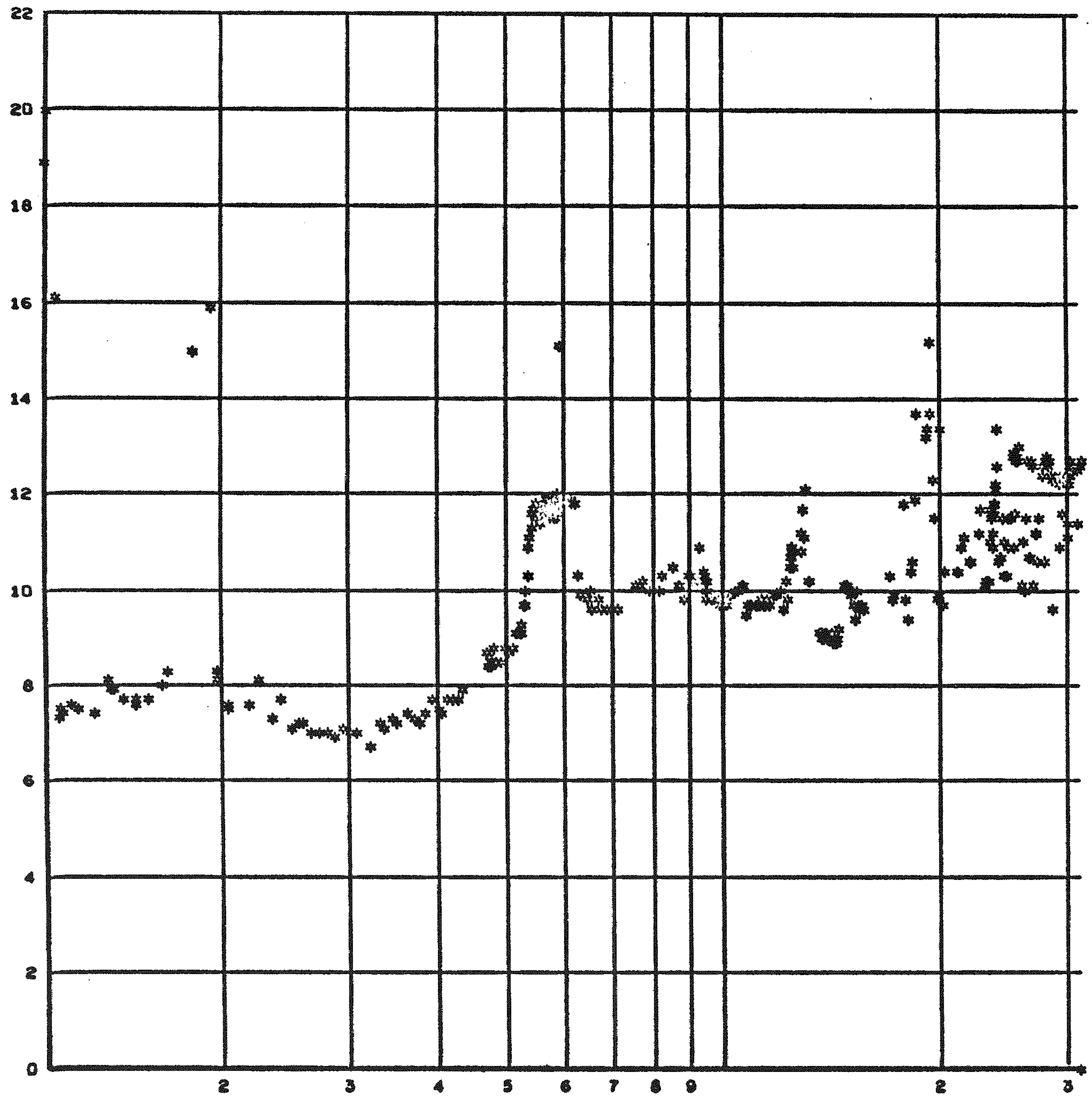

RUN 17146 14 SEP 78 21.43.49

...10

78

THERMOCOUPLE TE-1170-25 (TEMPERATURE) TOP HEAD

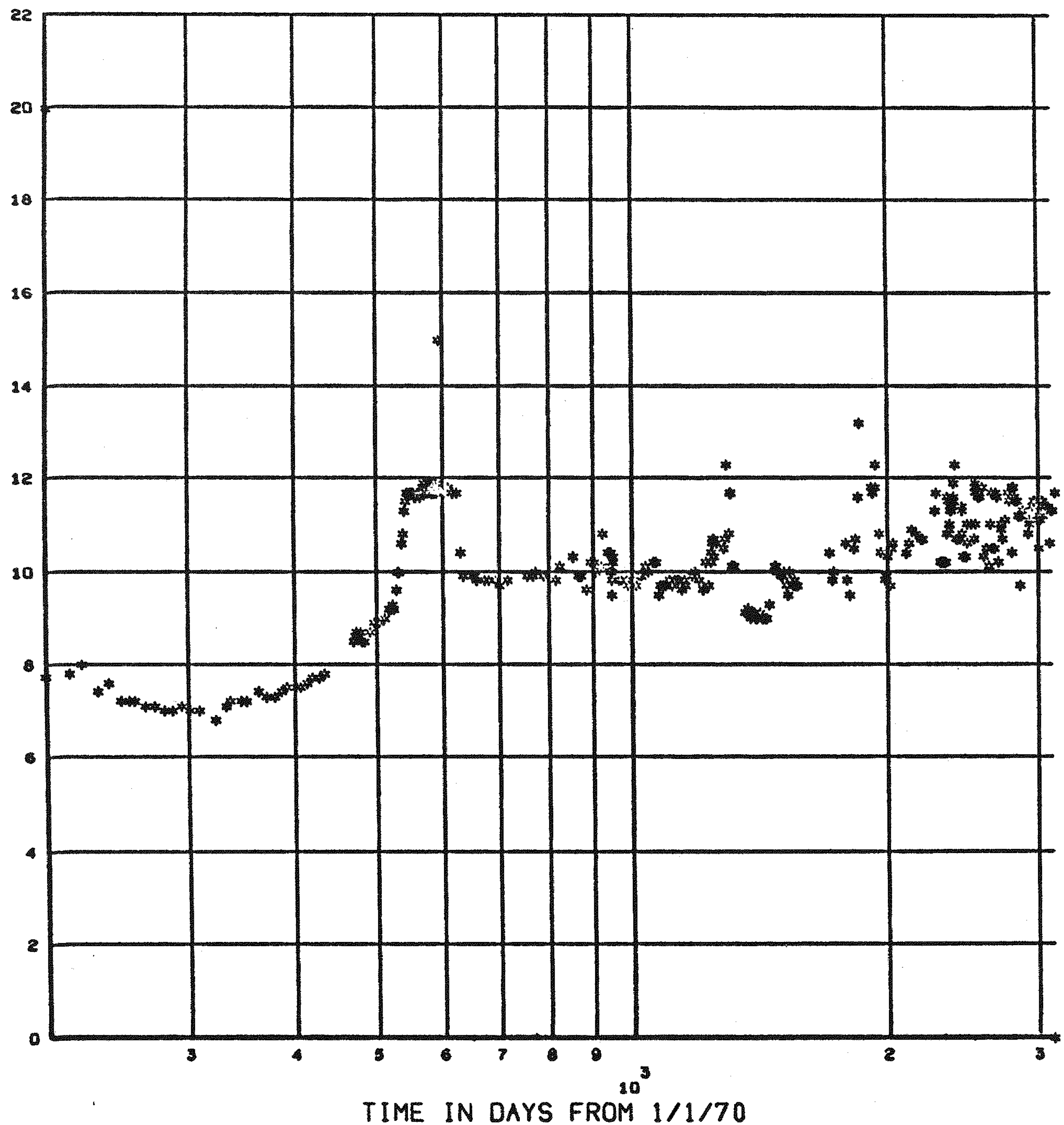

RUN 17146 14 SEP 78 21.44.07

...10

79

THERMOCOUPLE TE-1170-27 (TEMPERATURE) TOP HEAD

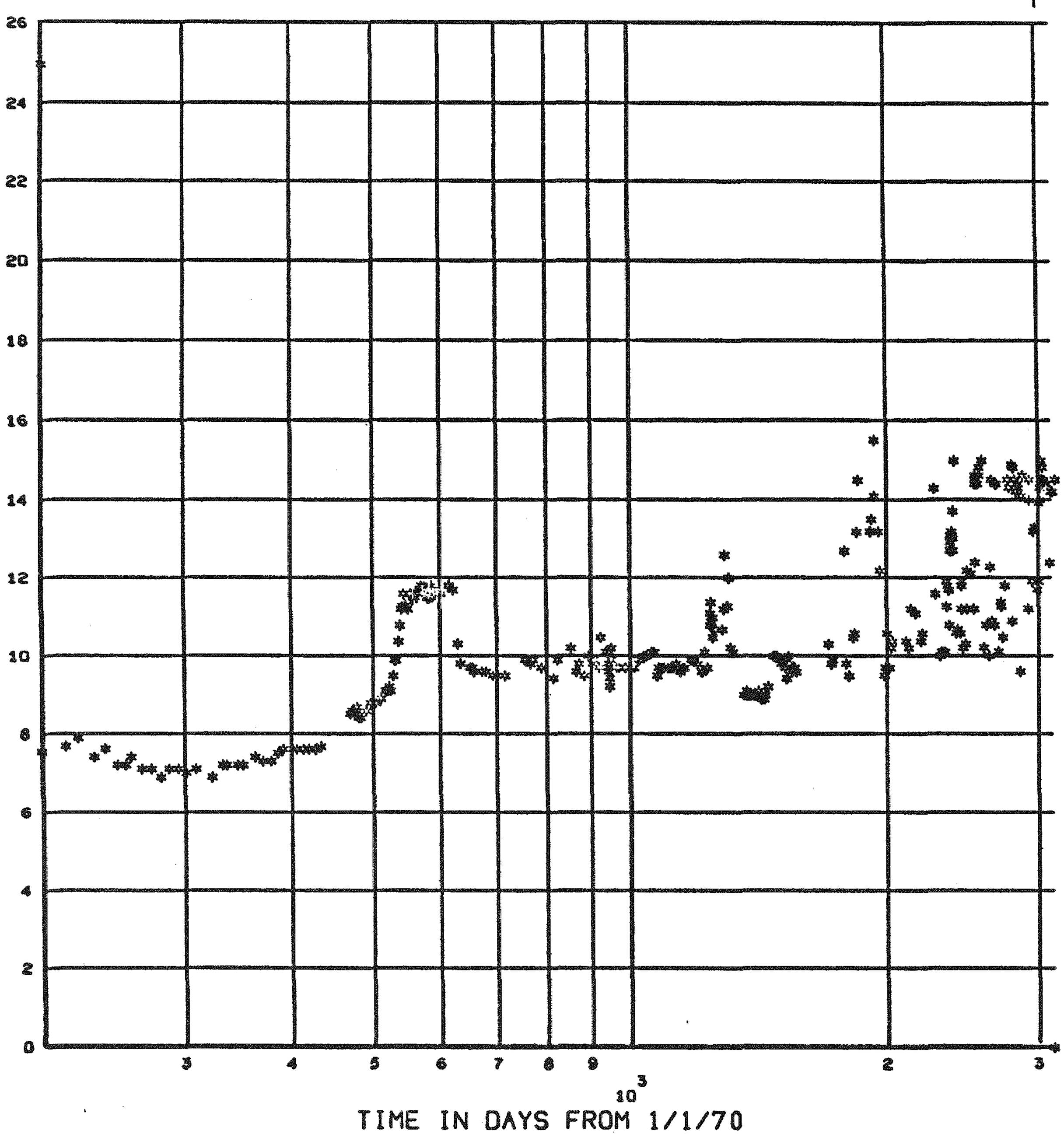

RUN 17146 14 SEP 78 21.44.19

THERMOCOUPLE TE-1170-28 (TEMPERATURE) TOP HEAD

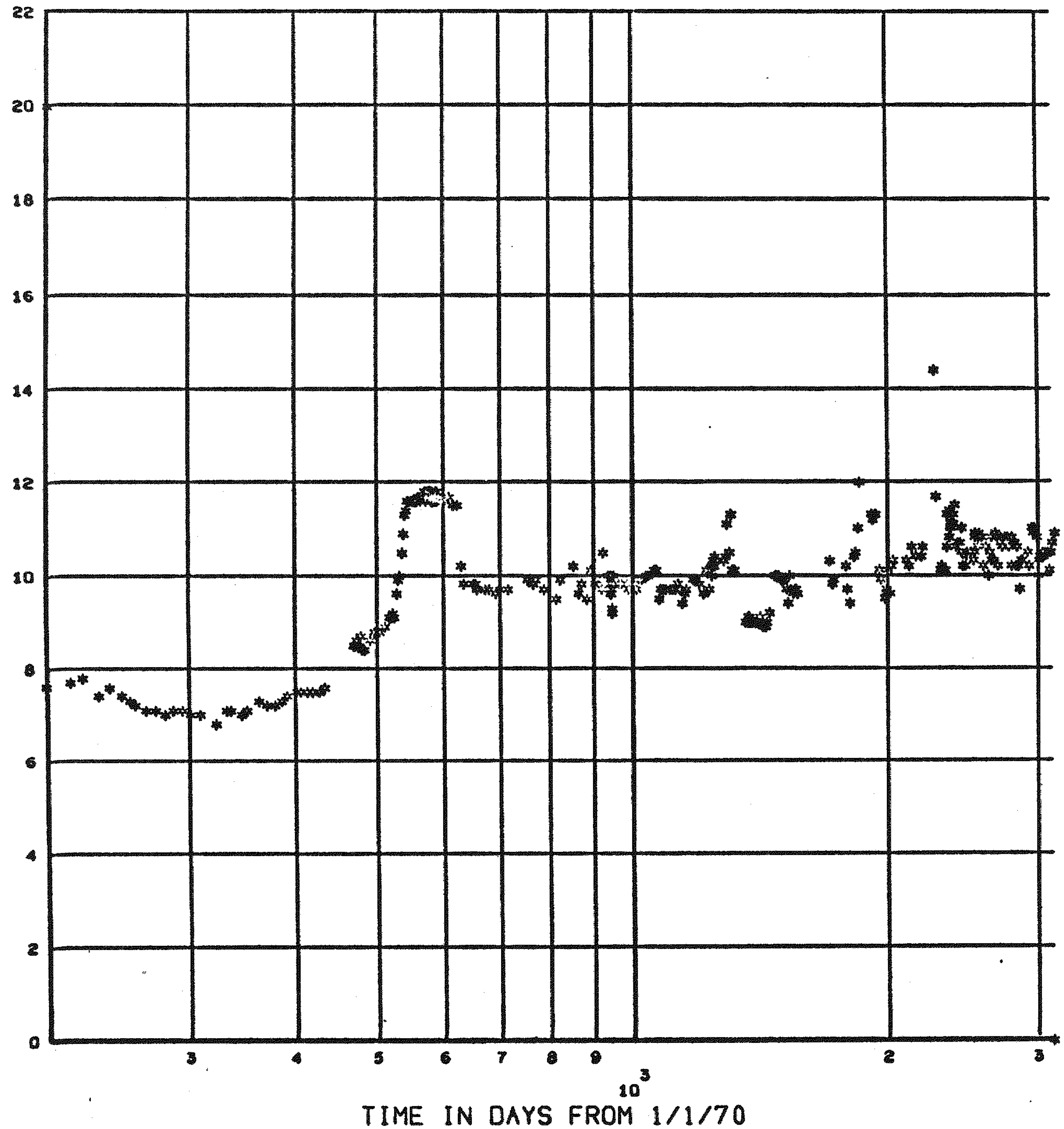

RUN 17146 14 SEP 78 21.44.25

B-76

•••10

82

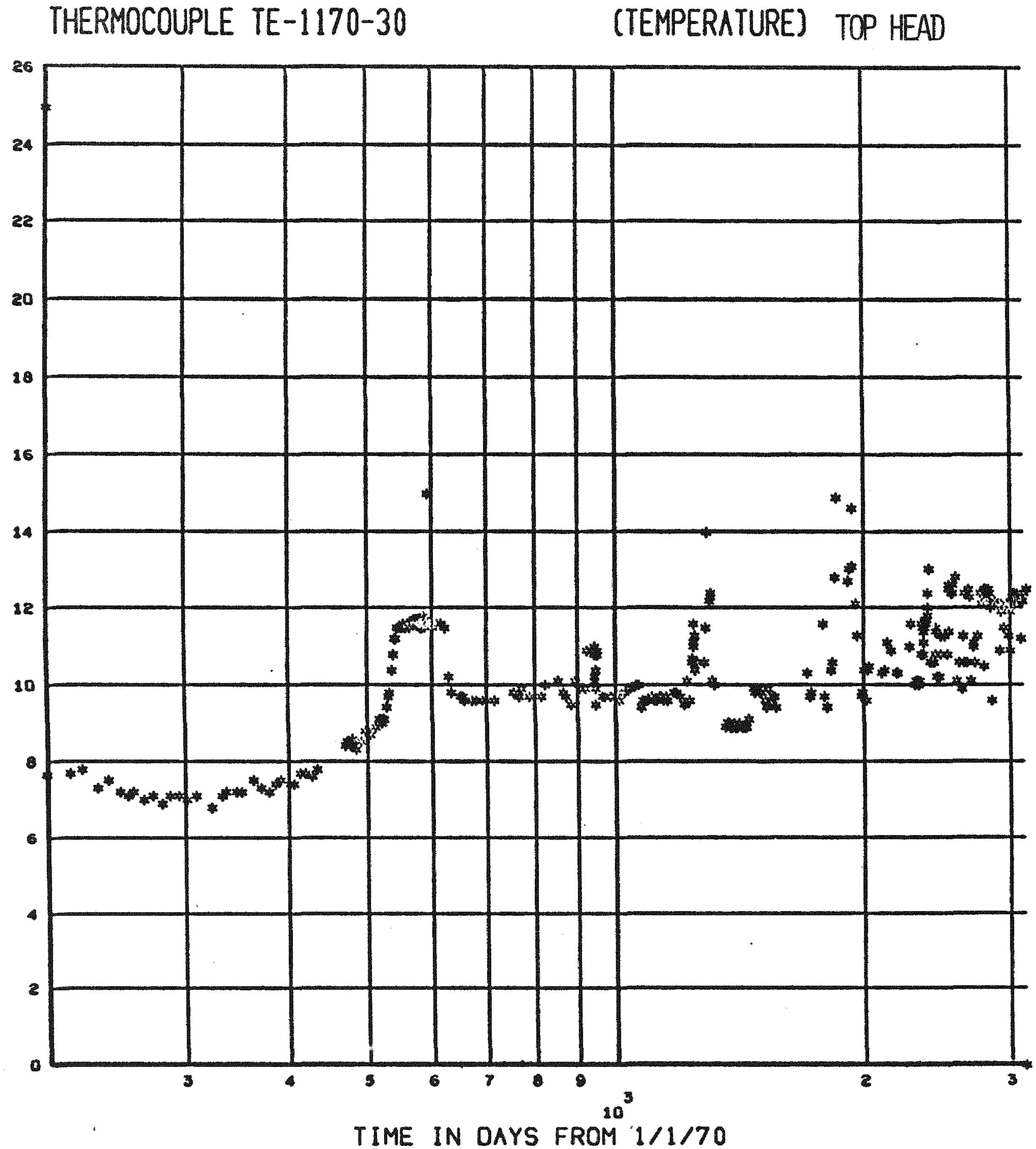

RUN 17146 14 SEP 78 21.44.42

THERMOCOUPLE TE-1170-31 (TEMPERATURE) TOP HEAD

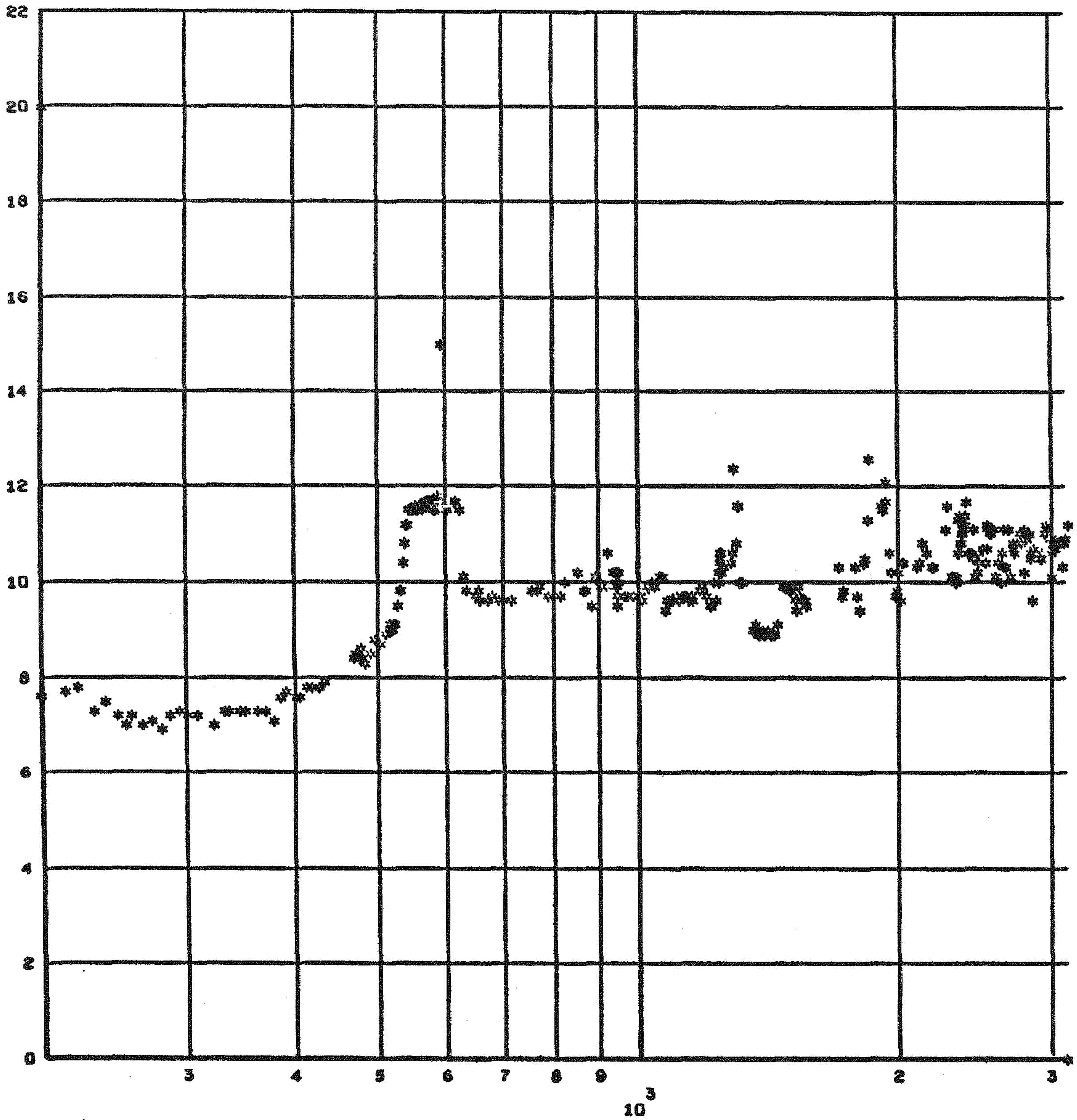

RUN 17146 14 SEP 78 21.44.55

B-78

...10

85

THERMOCOUPLE TE-1170-131 (TEMPERATURE) TOP HEAD

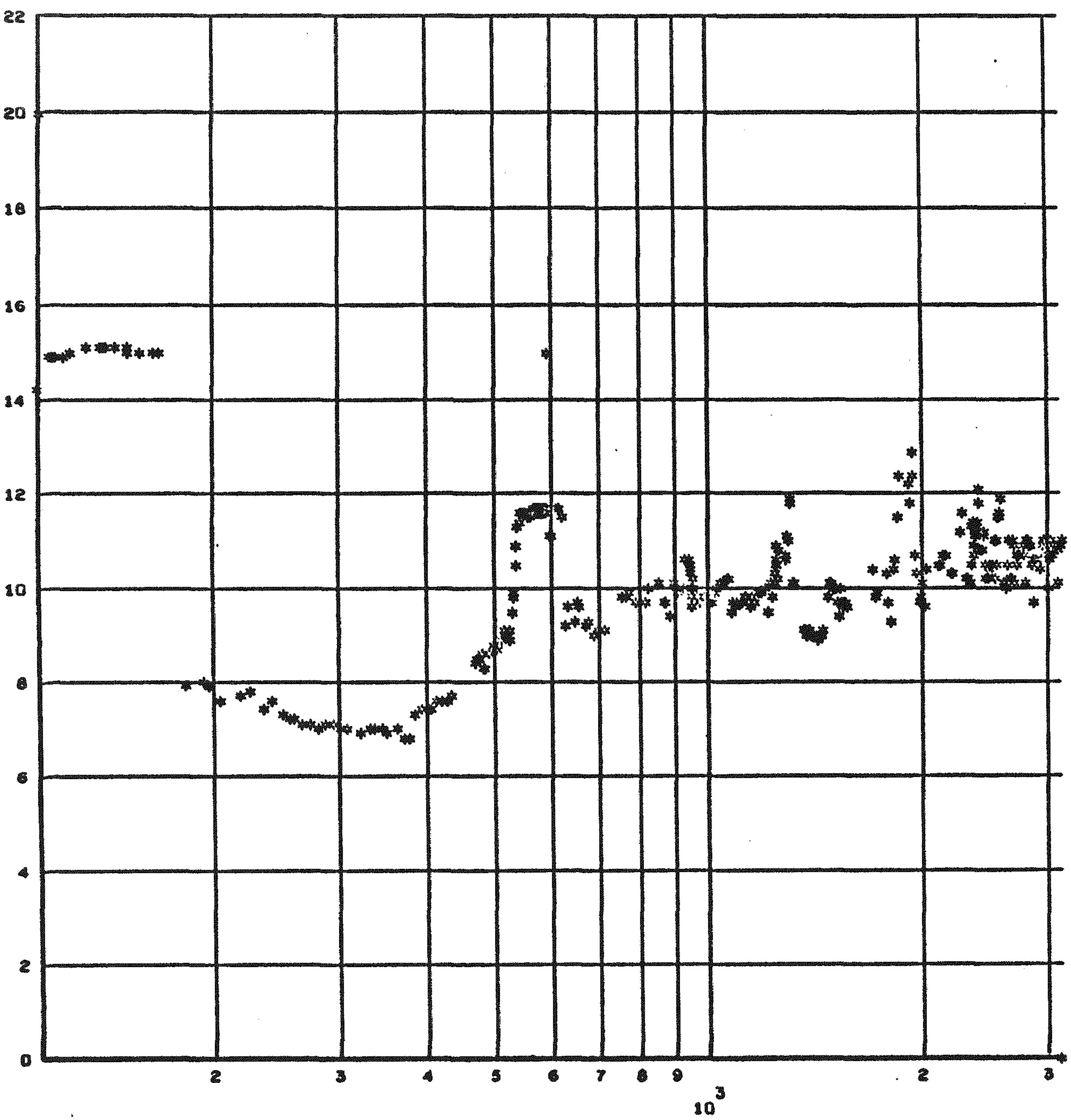

RUN 17146 16 SEP 78 06.38.30

185

THERMOCOUPLE TE-1170-46 (TEMPERATURE) BARREL

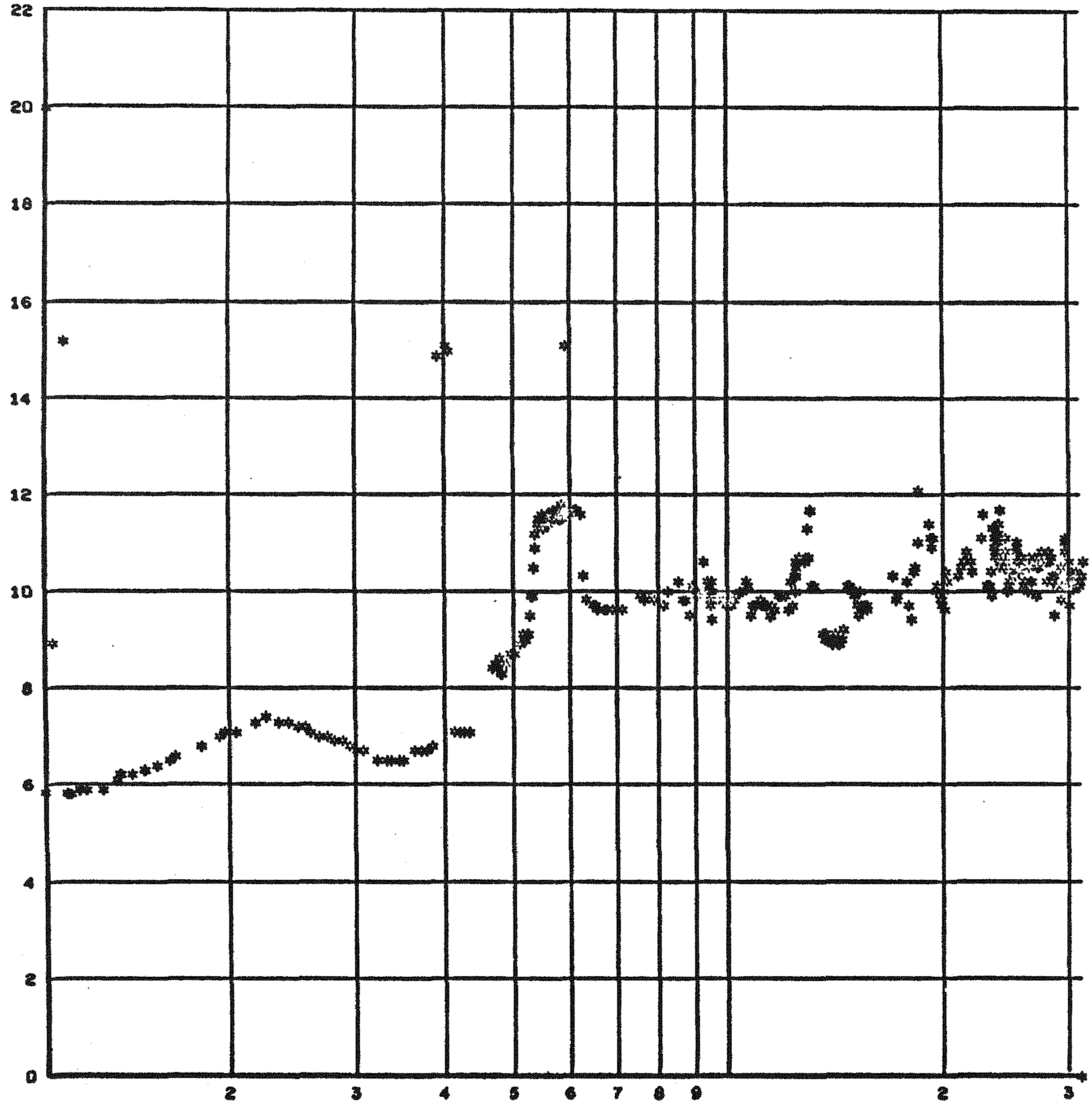

RUN 17146 14 SEP 78 21.48.28

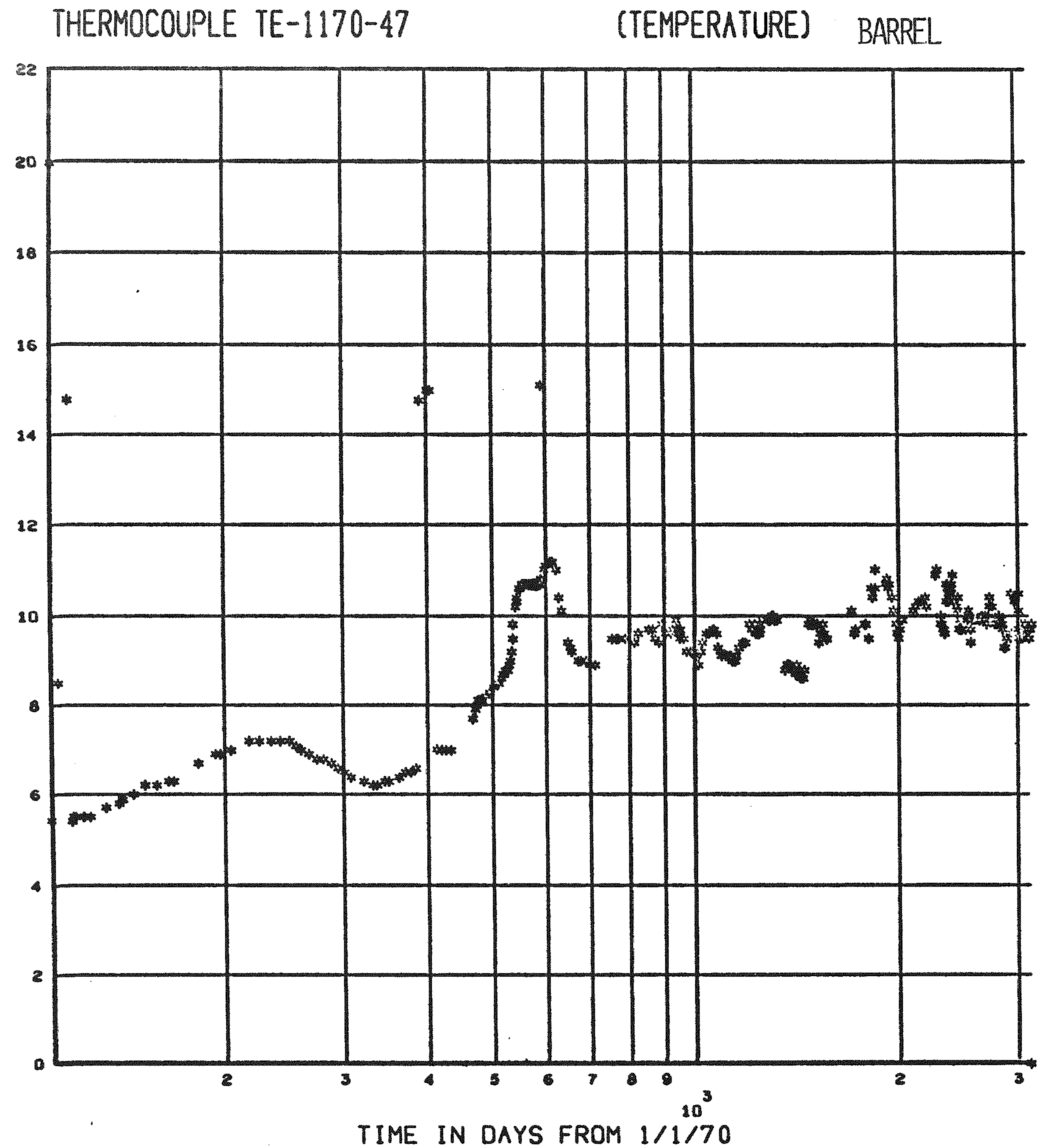

RUN 17146 14 SEP 78 21.48.32

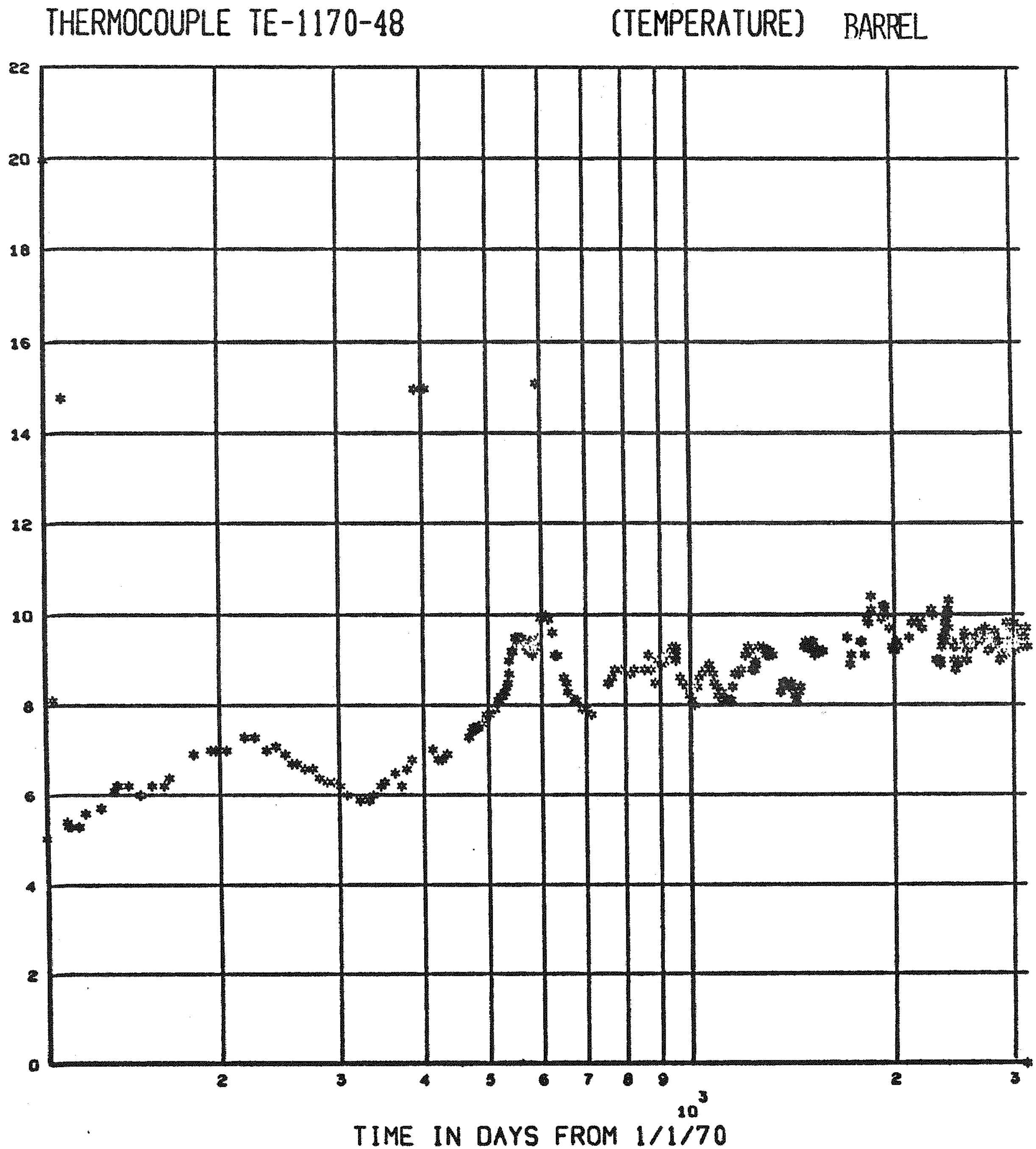

RUN 17146 14 SEP 78 21.51.03

B-82

...10

102

THERMOCOUPLE TE-1170-54 (TEMPERATURE) BARREL

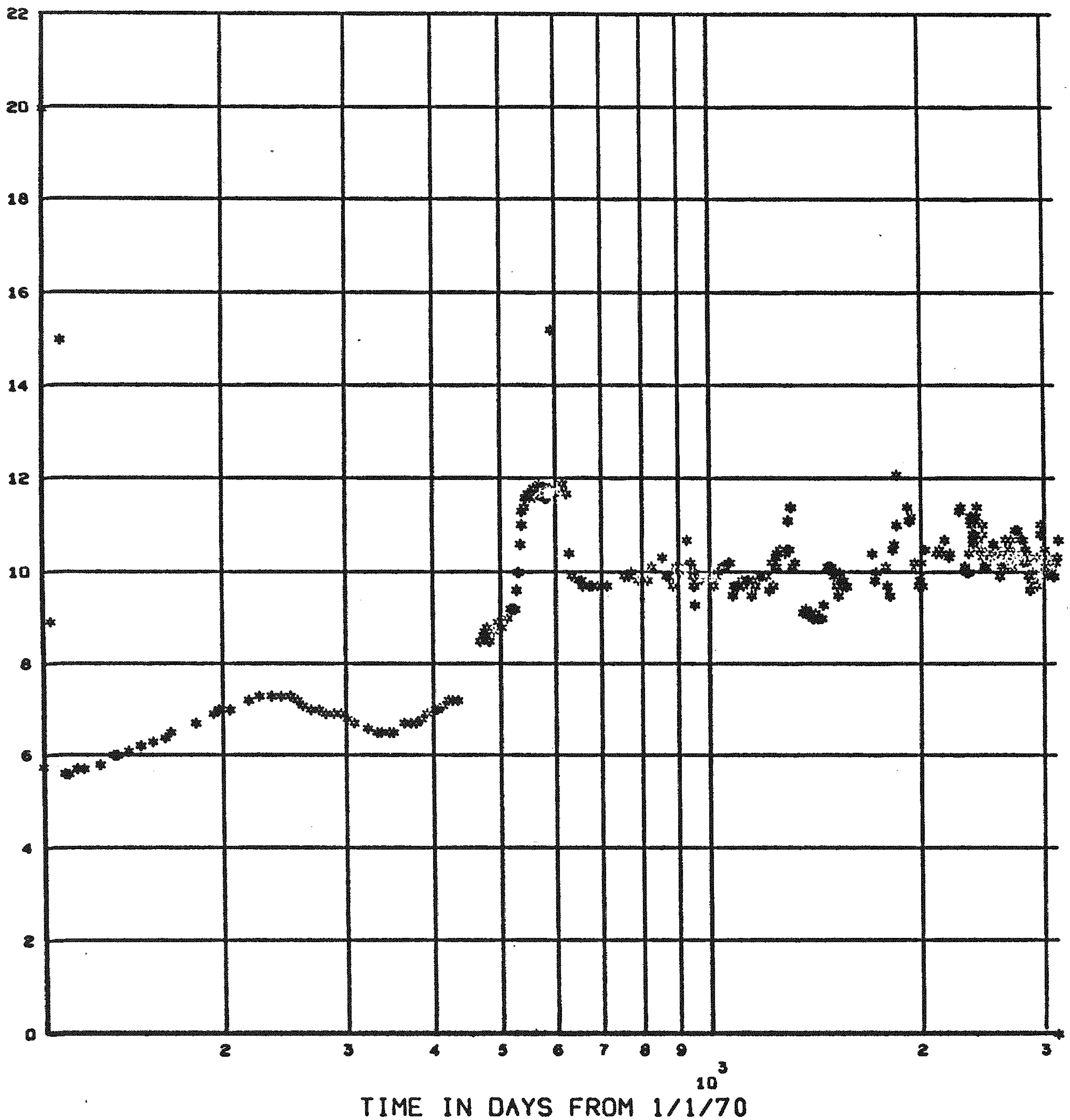

RUN 17146 14 SEP 78 21.51.29

108

THERMOCOUPLE TE-1170-56 (TEMPERATURE) BARREL

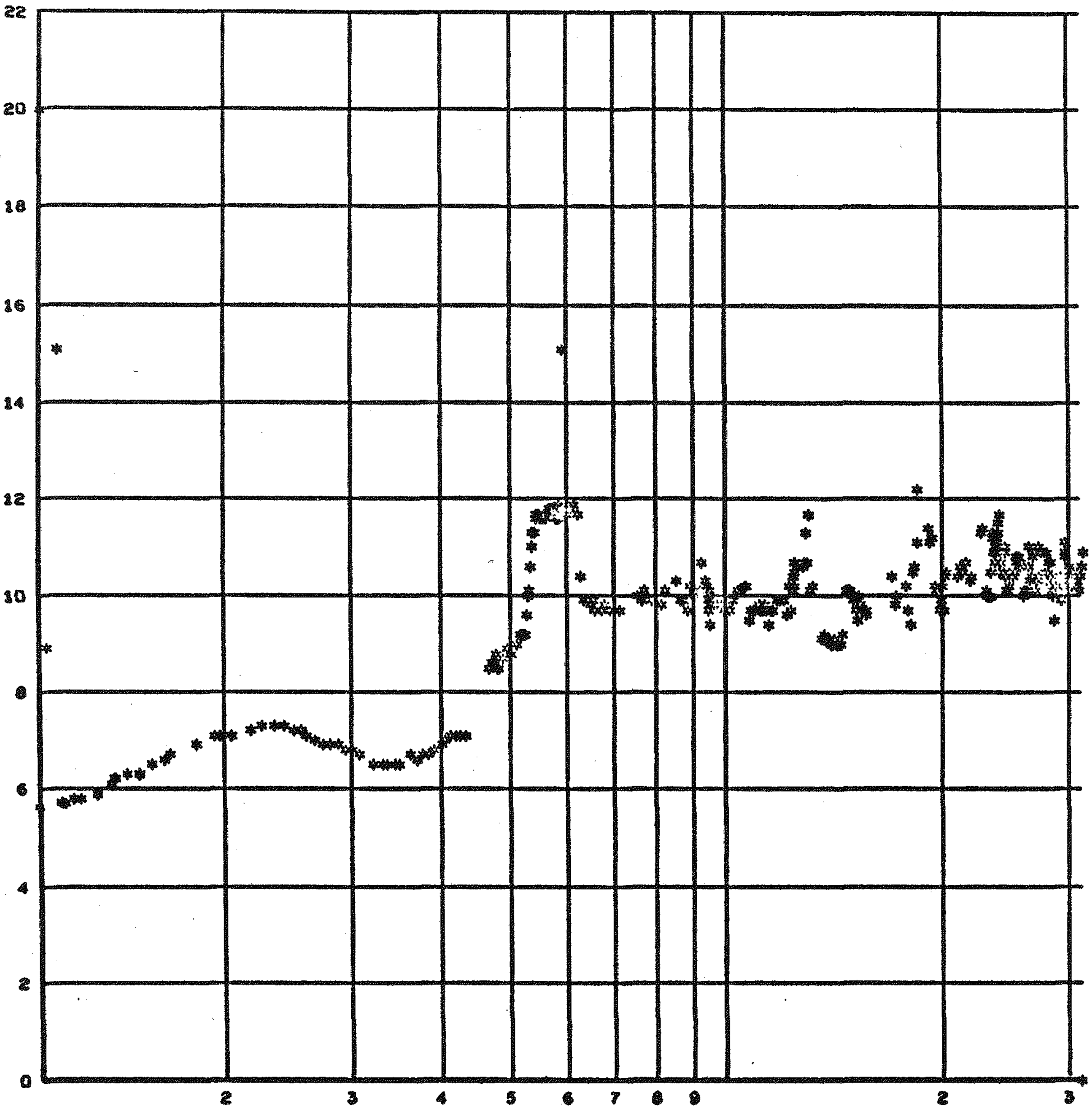

RUN 17146 14 SEP 78 21.51.34

THERMOCOUPLE TE-1170-65 (TEMPERATURE) BARREL

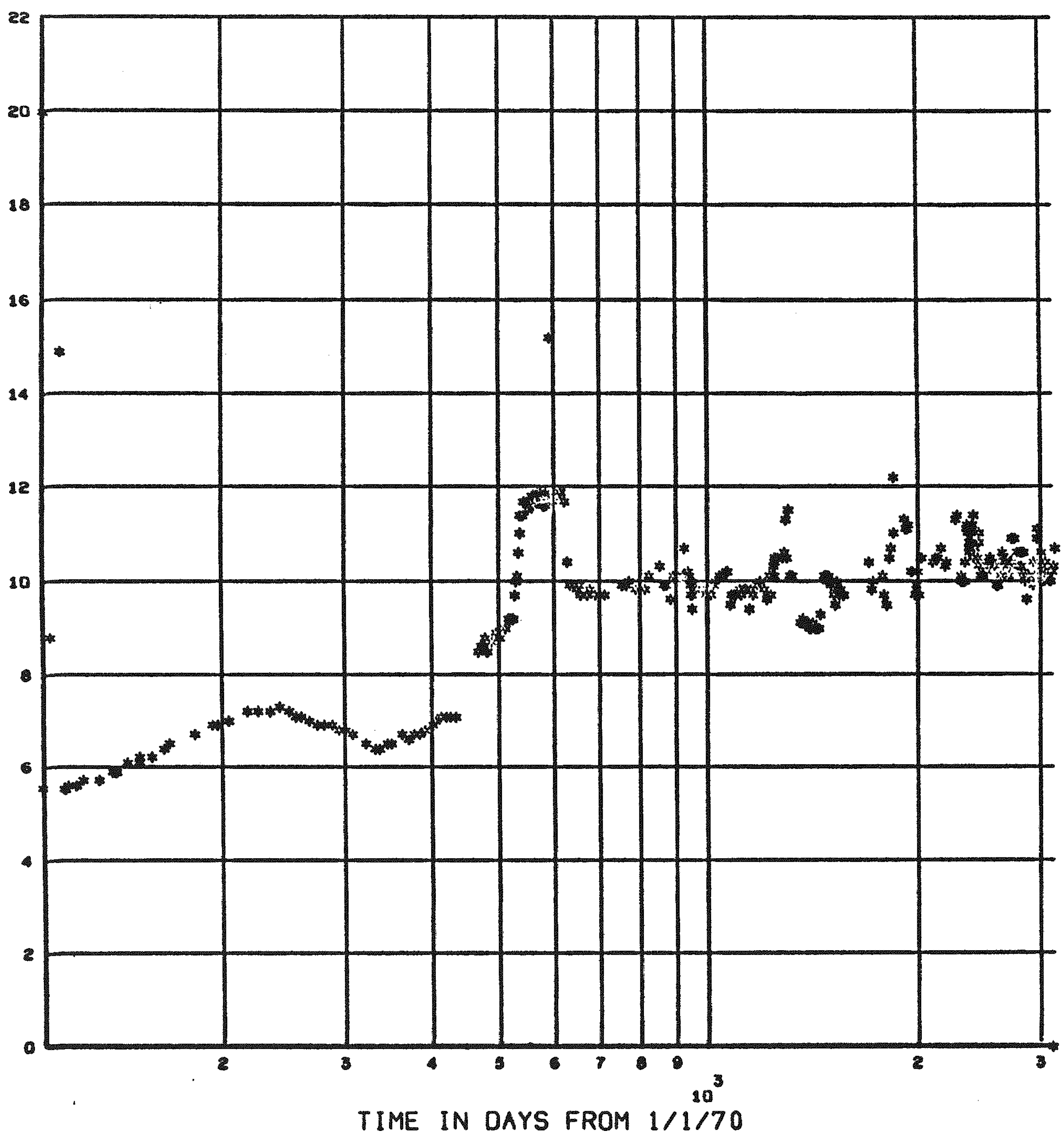

RUN 17146 16 SEP 78 06.24.55

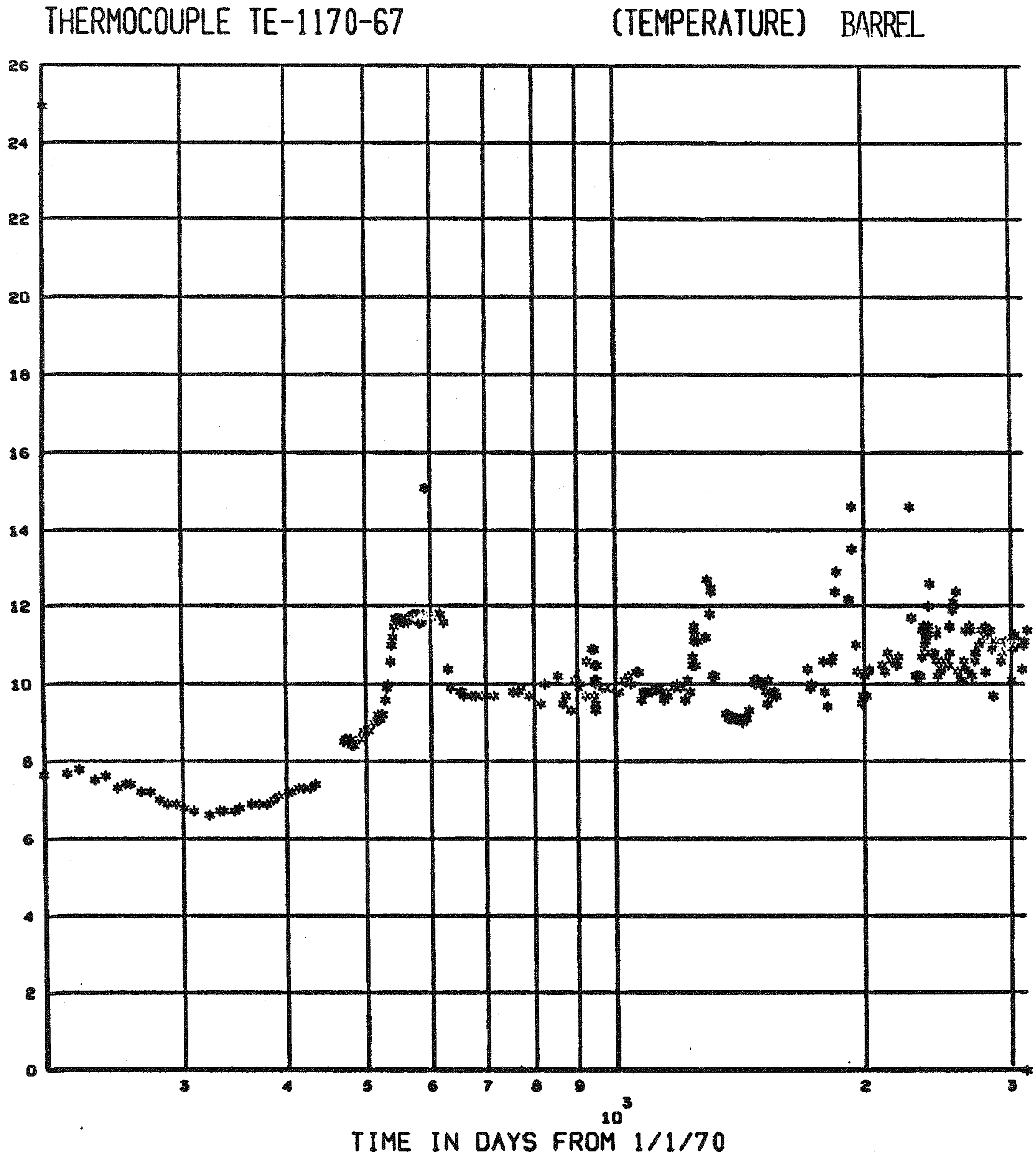

RUN 17146 14 SEP 78 21.41.06

...10

75

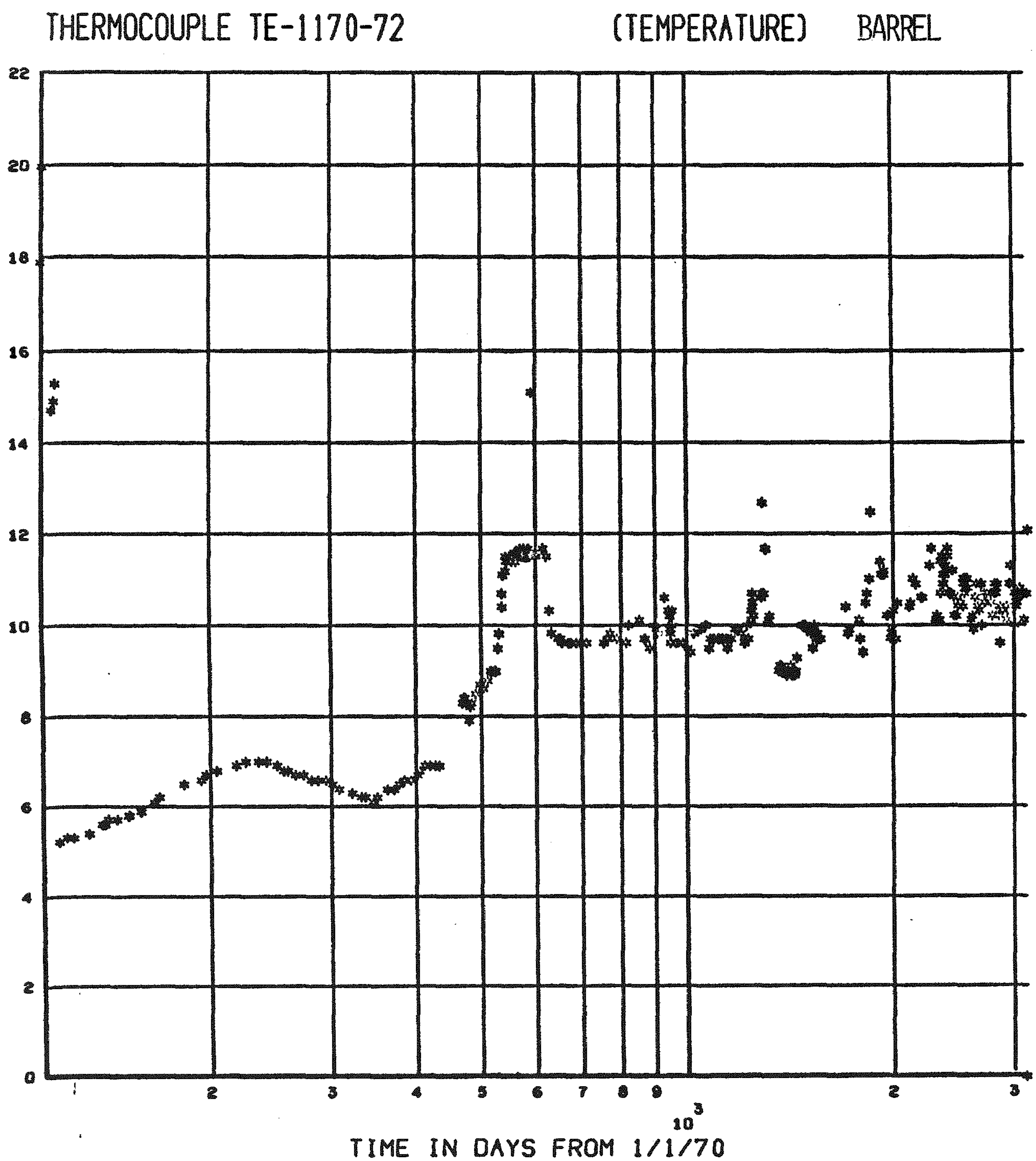

B-87

126

RUN 17146 16 SEP 78 06.27.08

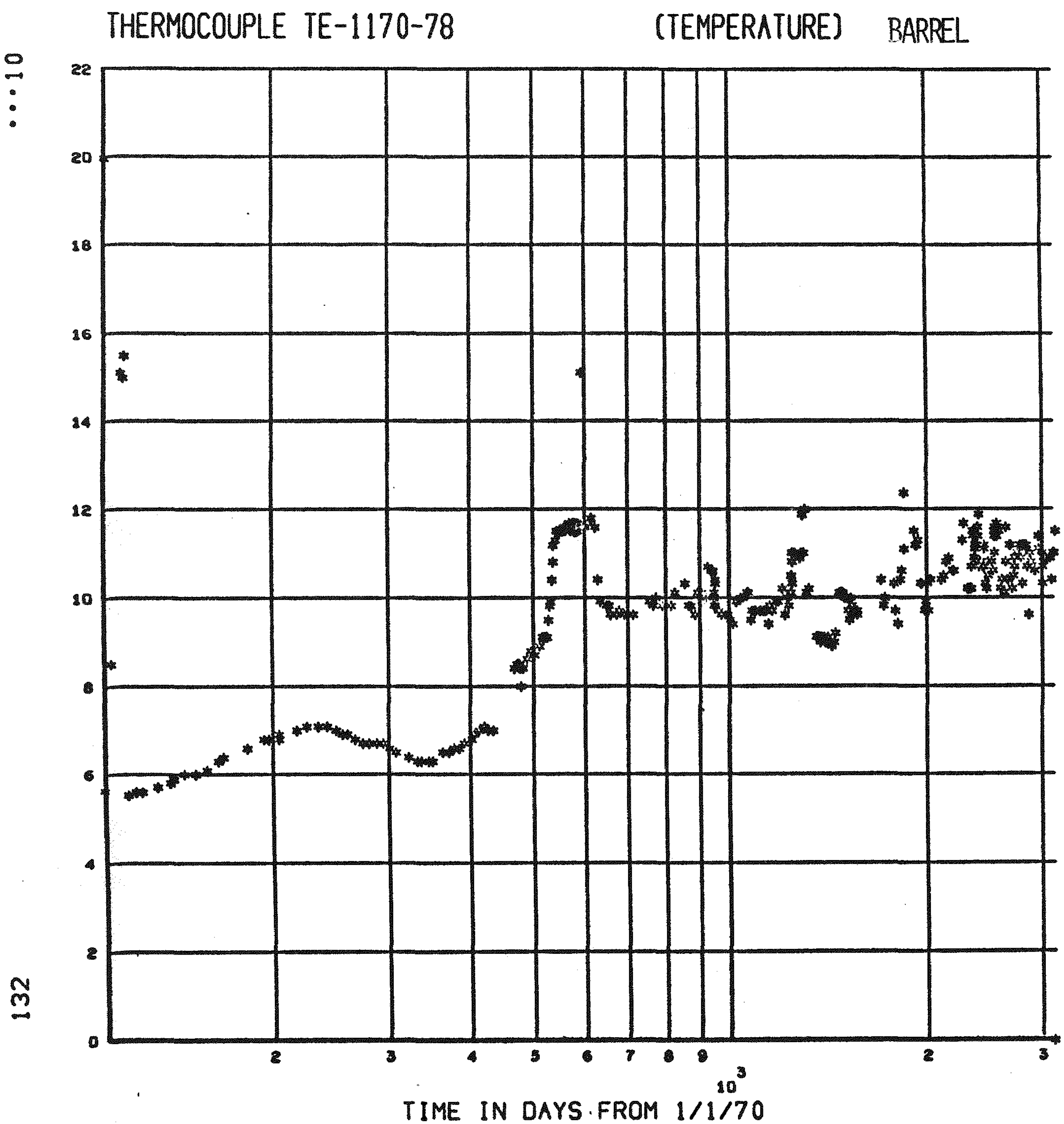

RUN 17146 16 SEP 78 06.27.26

132

THERMOCOUPLE TE-1170-96 (TEMPERATURE) BOTTOM HEAD

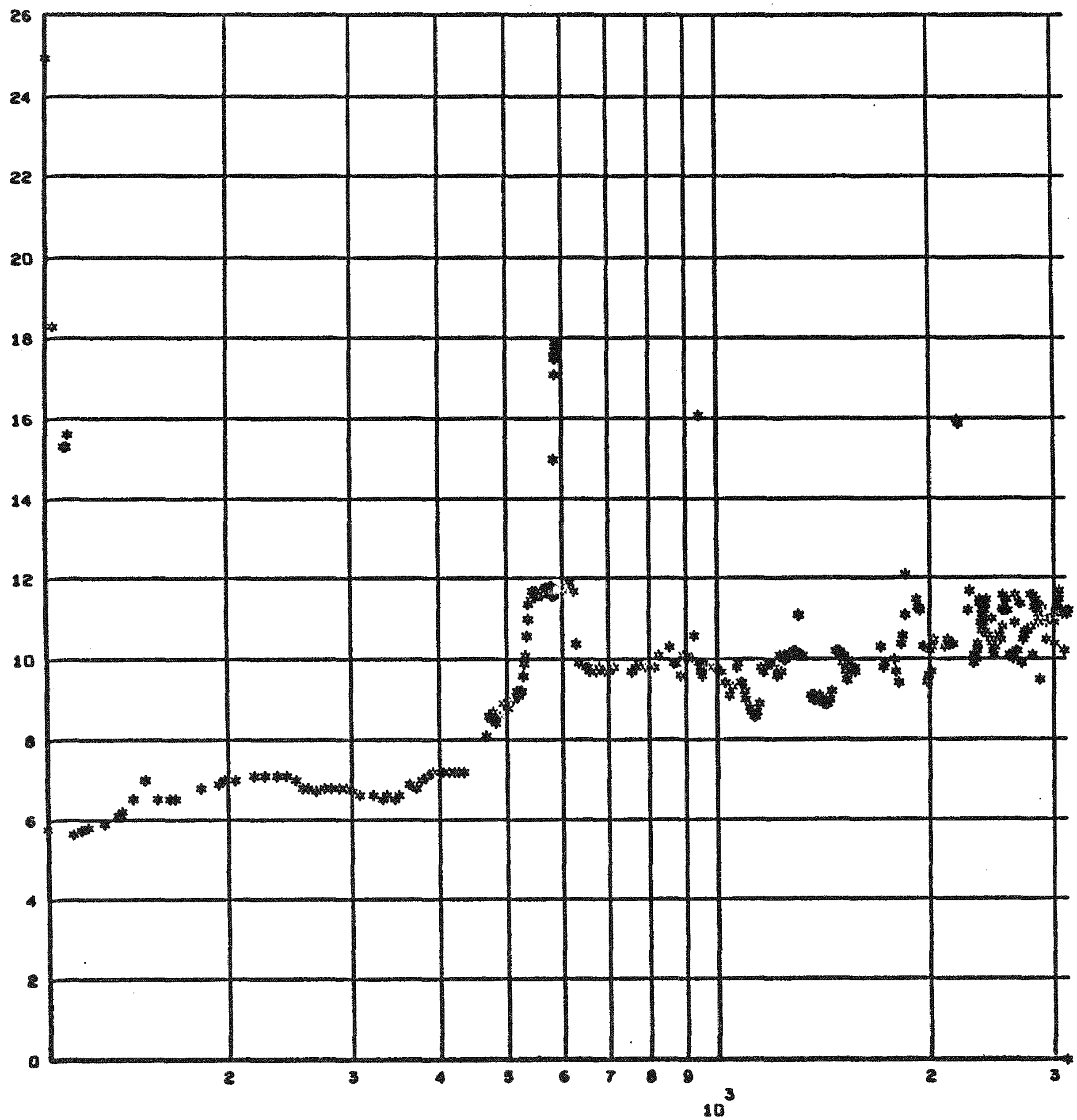

RUN 17146 16 SEP 78 06.32.42

THERMOCOUPLE TE-1170-107 (TEMPERATURE) BOTTOM HEAD

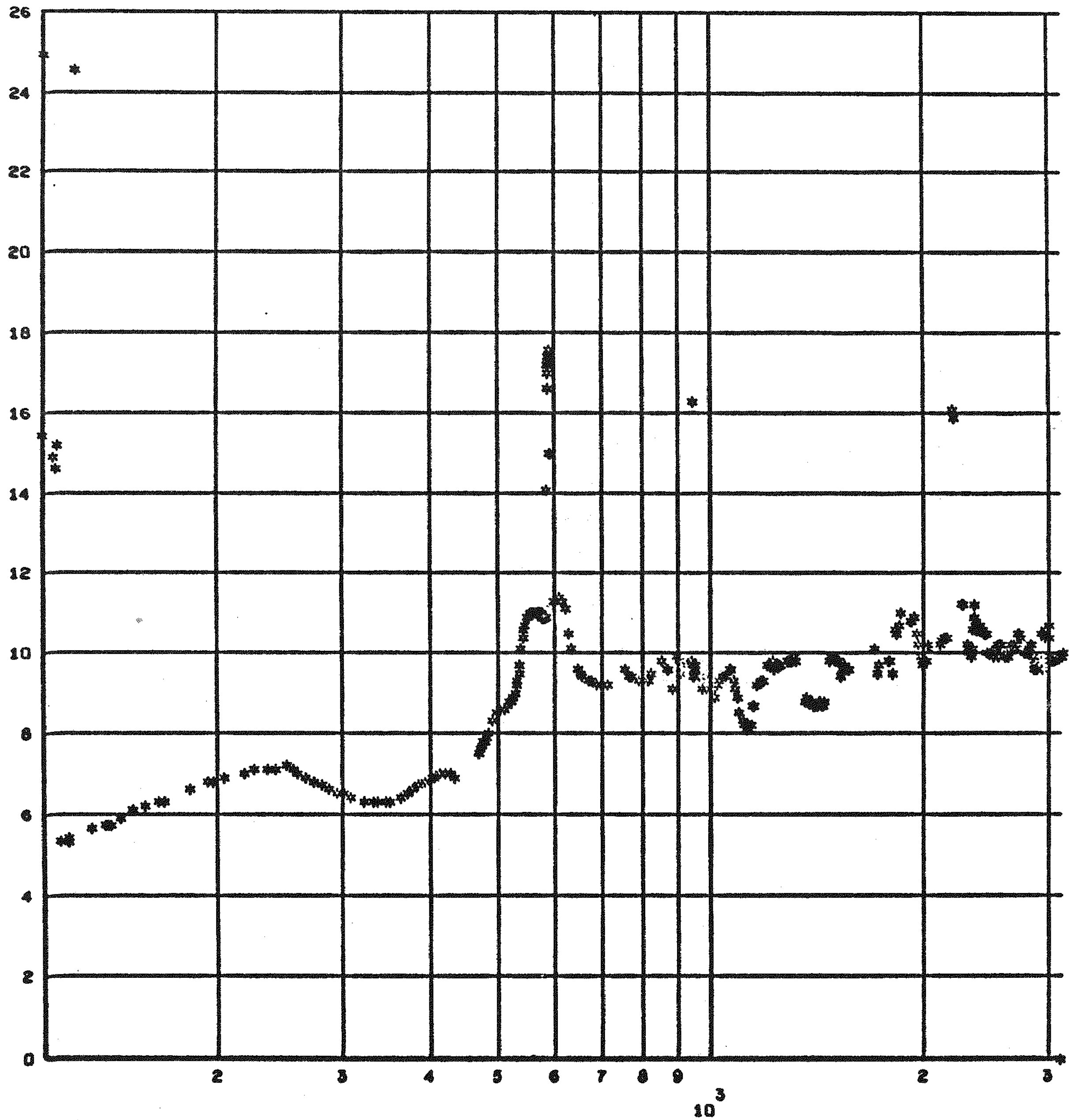

RUN 17146 16 SEP 78 06.35.00

161

...10

THERMOCOUPLE TE-1170-109 (TEMPERATURE) BOTTOM HEAD

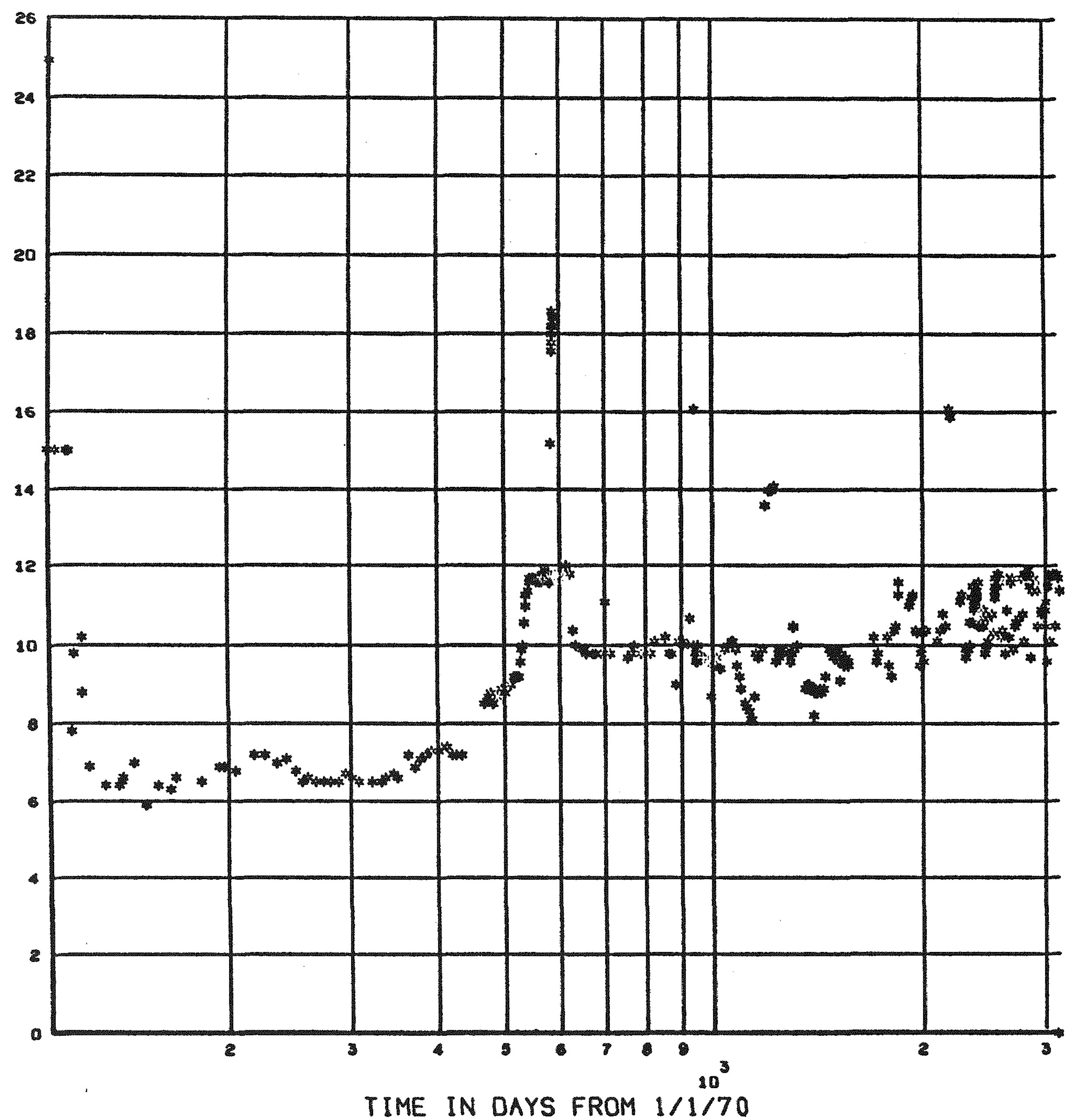

RUN 17146 16 SEP 78 06.35.05

B-91

163

•••10

THERMOCOUPLE TE-1170-110 (TEMPERATURE) BOTTOM HEAD

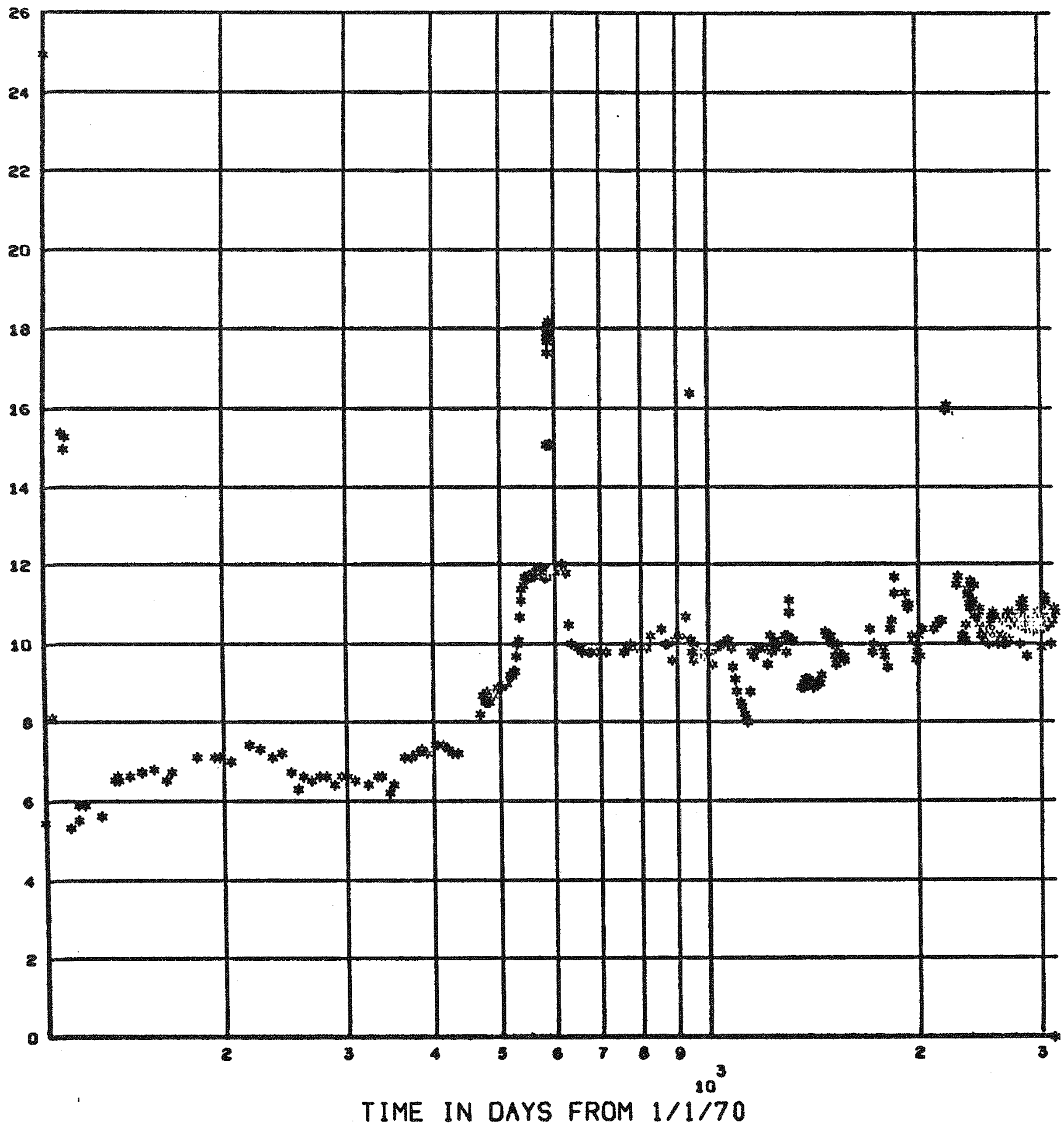

RUN 17146 16 SEP 78 06.35.07

...10

164

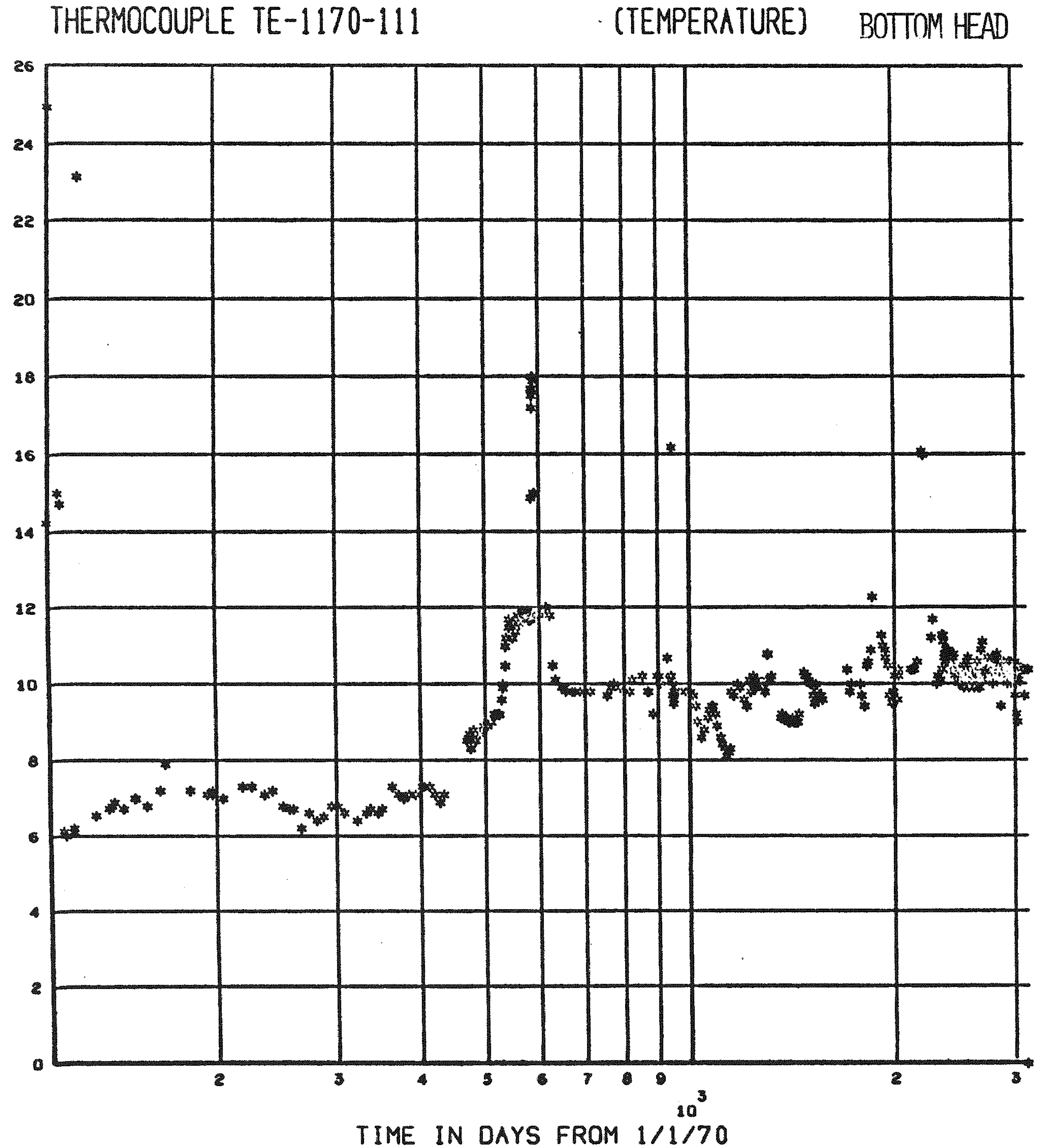

RUN 17146 16 SEP 78 06.35.11

B-93

165

...10

THERMOCOUPLE TE-1170-114 (TEMPERATURE) BOTTOM HEAD

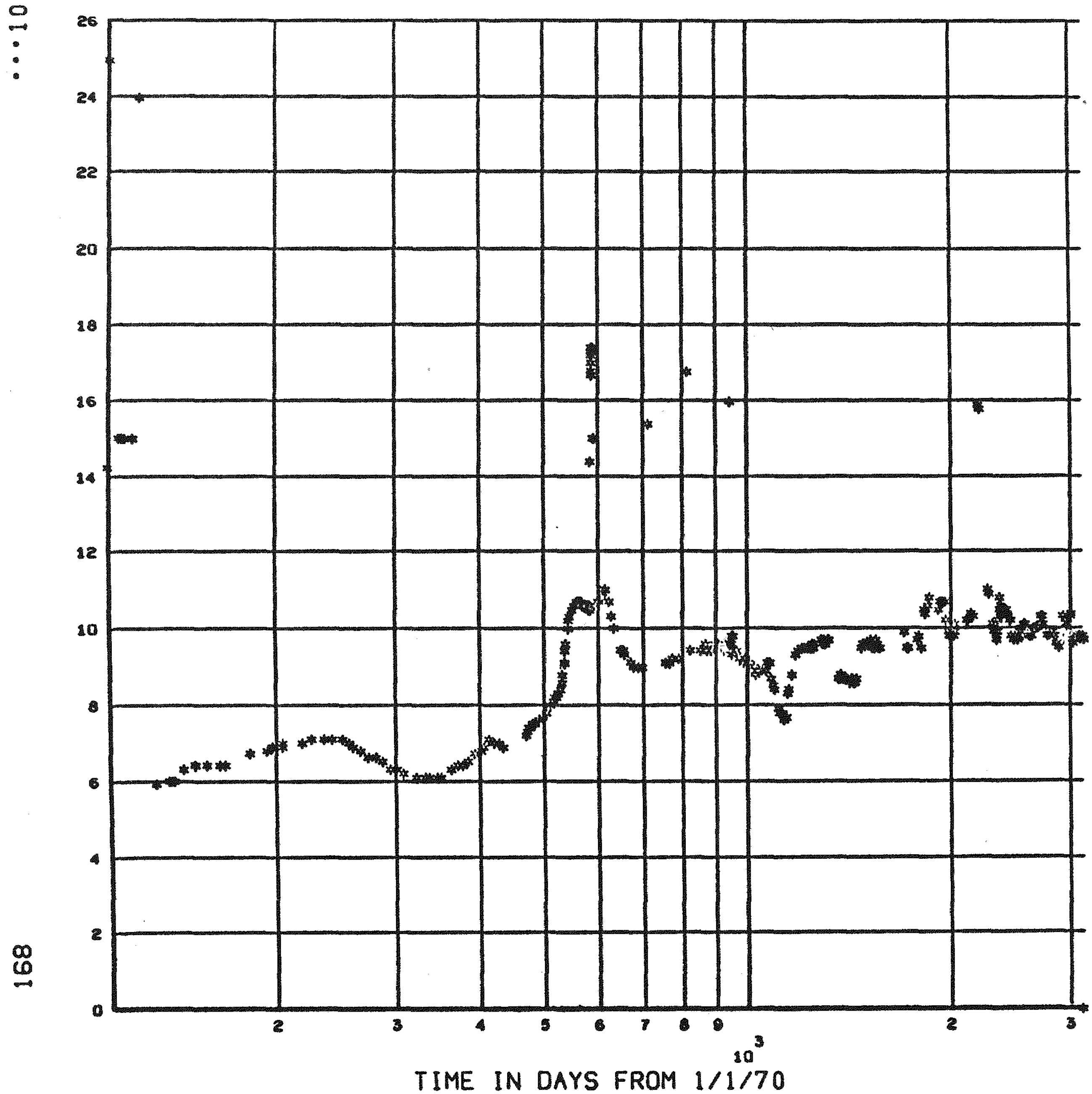

RUN 17146 16 SEP 78 06.35.18

168

THERMOCOUPLE TE-1170-127 (TEMPERATURE) BOTTOM HEAD

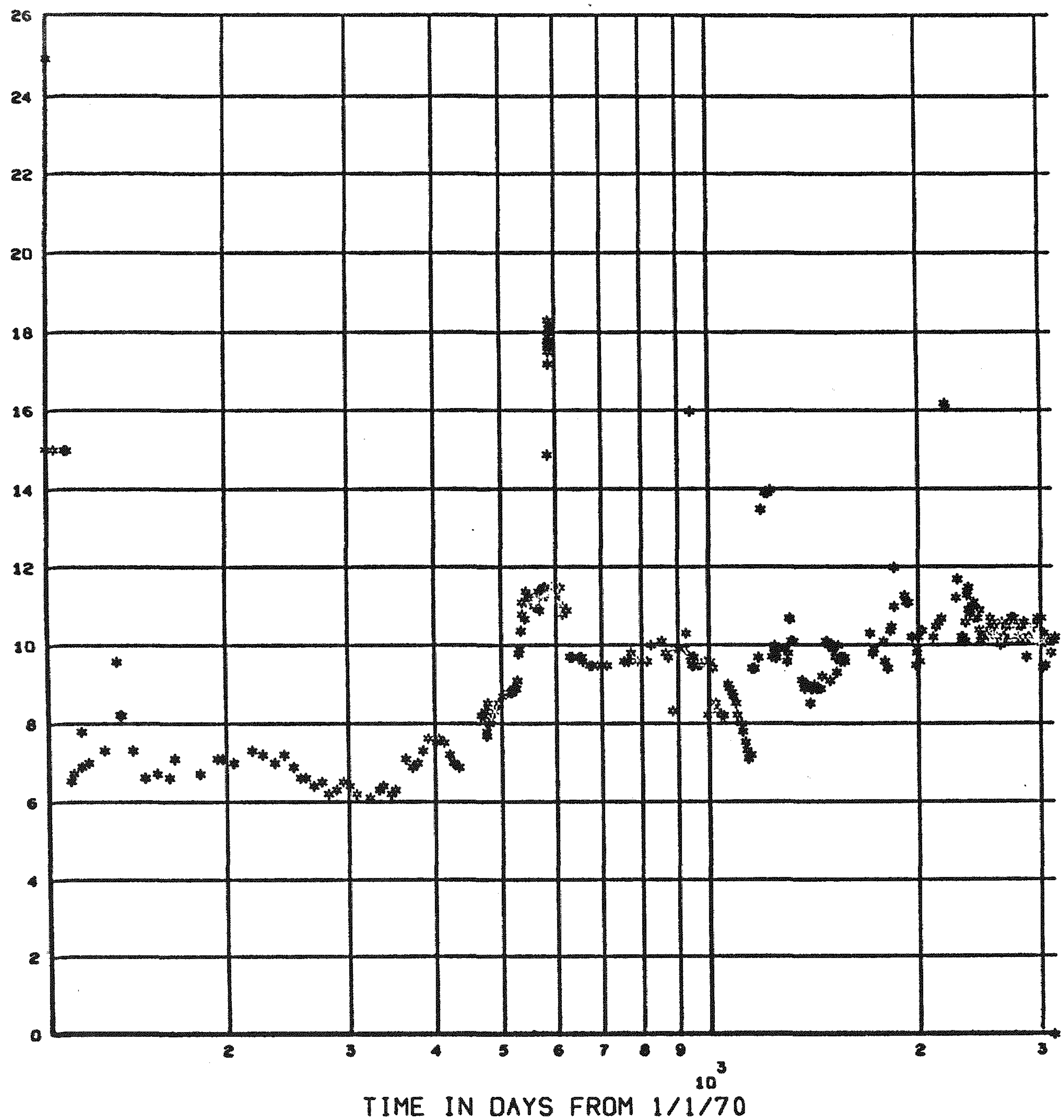

RUN 17146 16 SEP 78 06.38.15

RUN 17146 16 SEP 78 06.38.27

181

THERMOCOUPLE TE-1170-130 (TEMPERATURE)

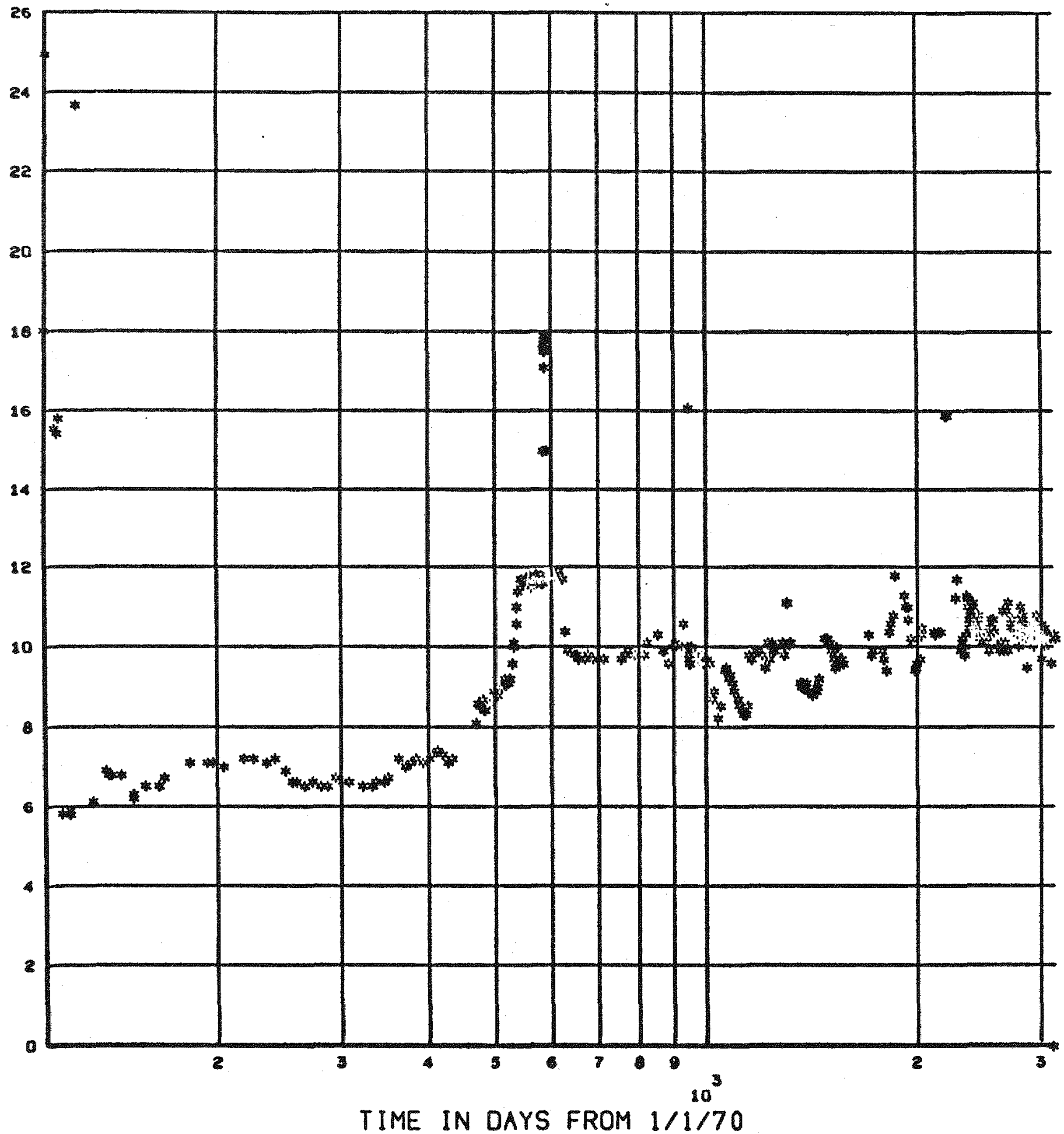

RUN 17146 16 SEP 78 06.38.27

...10

184